

Formula SAE Interchangeable Independent Rear Suspension Design

Sponsored by the Cal Poly Formula SAE team



A Final Report for Reid Olsen, FSAE Technical Director

By:



Suspension Solutions Design team

Mike McCune - mmcun2002@yahoo.com
Daniel Nunes - dbnunes1087@gmail.com
Mike Patton - mpatton@mpatton.org
Courtney Richardson - cnrichar@gmail.com
Evan Sparer - esparer650@gmail.com

2009
ME 428/481/470



Table of Contents

Abstract.....	6
Chapter 1: Introduction.....	7
<i>FSAE Team History and Opportunity.....</i>	<i>8</i>
<i>Formal Problem Definition.....</i>	<i>10</i>
<i>Objectives/Specification Development.....</i>	<i>11</i>
Chapter 2: Background.....	13
<i>Solid Rear Axle Design.....</i>	<i>14</i>
<i>Tire Research.....</i>	<i>15</i>
<i>Steady State Cornering Model.....</i>	<i>16</i>
Chapter 3: Design Development.....	19
<i>Suspension Geometry.....</i>	<i>20</i>
<i>Loading Conditions and Forces.....</i>	<i>22</i>
<i>Space Frame Adaption.....</i>	<i>23</i>
<i>Differential.....</i>	<i>27</i>
<i>CV Joints and Half Shafts.....</i>	<i>28</i>
<i>Uprights.....</i>	<i>30</i>
Chapter 4: Final Design.....	33
<i>Summary and model.....</i>	<i>34</i>
<i>Detailed Design Description and Analysis.....</i>	<i>36</i>
Rear A-Arms.....	36
Rear Rockers.....	39
Shocks and the Anti-Roll Bar (ARB).....	40
Front Suspension Analysis and Redesign.....	41
Rear Frame Adaptation.....	43



Differential Choice and Mounting.....	47
CV Joints, Half Shafts, Splines, and Axles	52
Spline Analysis.....	52
Half Shaft Fatigue.....	54
Spindle Fatigue Sizing.....	55
Uprights.....	57
<i>Cost Analysis</i>	58
<i>Manufacturing Plan</i>	60
Chapter 5: Manufacturing Process	61
<i>Suspension:</i>	62
A-Arms.....	62
Rockers.....	63
Push-rod's/Tie-rods:.....	64
<i>Chassis</i>	65
<i>Drivetrain:</i>	67
Differential Inserts	67
Differential Axle Stubs.....	68
Differential Uprights	68
Differential Half Shafts.....	69
Differential Drilling.....	69
Drive train Assembly	69
<i>Uprights:</i>	70
Wheel Uprights	70
Upright Suspension Tabs.....	71
Spindles.....	71



Hubs	72
Chapter 6: Design Verification	73
<i>Weight Results</i>	74
<i>Dynamic Test Plan and Equipment</i>	75
Strain Gages	77
Transducer Calibration.....	78
Accelerometer.....	79
DAQ.....	80
<i>Initial Installation Testing</i>	82
Axle Stubs.....	82
Upright Thrust Bearing.....	84
<i>Dynamic Testing Results</i>	85
Stopwatch	85
Data Acquisition System	88
.....	88
<i>Discussion</i>	90
<i>Future Testing</i>	91
Acceleration Test	91
Autocross Test.....	91
Chapter 8: Conclusion	92
<i>Conclusion and Recommendations</i>	93
Rear Suspension Members and Geometry	93
Differential choice.....	94
Uprights.....	94
Rear Frame.....	94



Final Thoughts.....	95
Appendix A: Gantt Chart.....	Error! Bookmark not defined.
Appendix B: QFD.....	Error! Bookmark not defined.
Appendix C: Selection of Detailed Analysis.....	Error! Bookmark not defined.
Appendix D: Decision Matrices.....	Error! Bookmark not defined.
Appendix E: Suspension Forces Matlab Code.....	Error! Bookmark not defined.
Appendix F: Detailed Engineering Part Drawings.....	Error! Bookmark not defined.
Appendix G: Bill of Materials.....	Error! Bookmark not defined.
Appendix H: Testing Summary.....	Error! Bookmark not defined.



Abstract

The Suspension Solutions design team has completely designed built and tested an independent rear suspension system for the 2008 FSAE car. The car currently features a solid rear axle, and the task of converting it to incorporate an interchangeable rear suspension has been undertaken in order to quantify the advantages and disadvantages of each design philosophy. The car has been properly tested with both the solid axle and independent rear suspension side-by-side, however more testing is suggested. After pushing both setups to their limits on a 50ft diameter skid pad, the test results were quantified, and a final comparison between the two design philosophies was tabulated. From our limited tested we can easily conclude an IRS FSAE car, at minimum, can match the performance of the previous solid axle setup, while being 22lbs heavier. We suspect its performance advantage to become apparent with additional testing however. More subjectively, it was found that the IRS handled more predictably and was easier for novice drivers to control and drive. Our results help quantify the advantages and disadvantages of each system and can be used by future FSAE teams to make more informed design decisions. Our independent rear suspension design includes an unequal length A-Arm configuration, new rear uprights, spindles and hubs, a Torsen differential, and an additional steel space frame to connect all of the listed components to the CP08 chassis. Our initial analysis shows that a performance edge between the two competing systems is dependent on the overall weight of each system and our preliminary testing results help confirm this analysis.



Chapter 1: Introduction

FSAE Team History and Opportunity

Cal Poly's Formula SAE team has been at the university since the early seventies, and has always been a great representation of the university's "Learn by Doing" philosophy. As a division of the Society of Automotive Engineers (SAE), the Formula club on campus designs, builds and competes with a mini-formula style racecar every year. In recent years the Formula SAE team has taken a different approach to their car's design than most other teams. In an effort to reduce weight, the team converted to a solid rear axle instead of a traditional independent rear suspension.

Three generations of cars have used a solid rear axle. The first was in 2006 (CP06), which had 10" wheels, a relatively light WR-450 single cylinder engine, and weighted 319lbs. CP06 competed and



Figure 1.1: 2008 FSAE car with solid rear axle.

performed well in the FSAE West competition, placing 3rd in the skid pad event. The axle and engine were then carried over to the 2008 car (CP08), which also had larger 13" wheels, an aero package, and fuel injection. While CP08's weight was higher at 374lbs, the car's performance capabilities were never properly tested. Brake problems, engine noise, gas tank and oil tank leaks kept the car off the track during competition. The third generation to use a solid

rear axle was manufactured in 2009 (CP09). It had no carry-over parts from CP08 except the engine and shocks. The team expected the car to weigh and perform similarly or better than the CP06 car.

With so few carry over parts from the CP08 to the CP09 car the opportunity is present to analyze the effects of using a solid rear axle as compared to an independent rear suspension, specifically with emphasis on the overall weight of the car. Unfortunately, the team has never been able to accurately quantify the advantages and disadvantages of using a solid rear axle. This project calls for re-designing the 2008 FSAE car, giving it an independent rear suspension with a rear differential to replace the solid rear axle set-up. It is also required that this new rear suspension design be interchangeable with the solid rear axle design. This will allow testing of the two different design approaches for a more



controlled and complete trade study. Testing procedures will be developed to quantify the performance of each design throughout the fall quarter of the project.

The ultimate goal of this design project is to see if a better performing car can be built with an independent rear suspension. The latter is assumed to inherit a weight penalty, but this hasn't been verified. We will determine if the dynamic advantages of an IRS outweigh the additional weight and component complexity. We want to evaluate both analytically and experimentally the assumed increased weight of an IRS with respect to increased dynamic performance on a skid pad track. This needs to be determined in order to better justify the FSAE team's design decisions for upcoming years. More specific goals include designing a rear suspension to be as light as possible and defining how the performance of both rear end designs (independent vs. solid rear) are affected by total weight. Our design team will quantify the advantages of each design with respect to total weight.



Formal Problem Definition

Suspension Solutions defines the problem of this project as follows: the current solid rear axle design being used by the Cal Poly FSAE team is not properly justified. As engineers, we strive for the highest level of proof available to justify our designs. The solid rear axle design that Cal Poly's FSAE team has implemented for three generations works under the assumption that less weight is worth the decrease in cornering agility.

An independent rear suspension is heavier than a solid rear axle due to a greater number of moving parts which include: a rear differential, half shafts, CV joints, rear uprights, additional rear frame tubing, and upper and lower A-Arms. With this added weight, is it even possible to decrease lap times overall? This is a function of the relative tire loading of the two cases, as well as the overall power-to-weight ratio of the car. With that said, we are aiming for an overall added weight of 25 lbs.

While the solid rear axle design will most likely always weigh less than the independent rear suspension, it corners on three tires (like a go-kart), placing dynamic loads on less of a contact patch. The purpose of this project is to justify the use of a live rear axle design, by comparing it head-to-head against a more traditional independent rear suspension. The latter is assumed to perform better due to the increase in traction with four tires in contact with the road.



Objectives/Specification Development

Certain customer requirements must be met. Most importantly, this car should be as light as possible. As mentioned previously, the main downfall of IRS vehicles is the added weight, therefore weight savings is critical. In addition to weight, a competitive IRS vehicle must have proper handling characteristics and be predictable and stable when pushed to its limits. Budget constraints also exist, as well as practical assembly, maintenance, and vehicle life considerations. It is our job at Suspension Solutions to develop a car that meets these design requirements and provide a method to test the pros and cons of each design.

In order to satisfy the stated customer requirements presented to us, Suspension Solutions has developed a list of engineering specifications. This list was formed by carefully examining the customer requirements and transforming them into quantifiable parameters, using the QFD method (refer to Appendix B). In compliance with the stated requirement of a fully functioning independent suspension vehicle, most of the engineering specifications deal with performance, stiffness, and weight. These parameters are chosen to maximize lateral traction, while maintaining neutral and predictable handling.

Because of the experimental nature of this vehicle, several parameters deal with increased adjustability of geometry, including wheel camber, track, toe, and adjustable shock mounting locations. Shock mounting adjustability will be incorporated only to the extent that it will not significantly impact the performance of the vehicle, minimizing changes in ride height, roll center, and so forth. The remaining specifications deal with non-performance variables such as design life, fabrication and assembly cost, which are necessary to create a reliable, enjoyable, and consistent vehicle.

As previously mentioned, one of the main reasons for Cal Poly's SAE team turning to a solid axle is weight savings. The argument stated that the decreased weight, as compared to a similarly designed independent rear axle vehicle, would offset any performance losses incurred by the limitations of solid axle geometry. Our job is to design a functioning IRS prototype at a weight similar to the current solid axle design. This requirement affects many other criteria, including material selection, suspension, frame stiffness, and designed safety factor. Another major design consideration deals with our vehicle's center of mass. Our challenge is to maintain neutral handling during cornering, as well as other handling



characteristics such as roll center, over steer/under steer, and weight transfer. The remaining design criteria are meant to produce a car that is reliable, predictable, intuitive, and affordable.

Additional specifications deal with the ease of vehicle maintenance, as well as the method of assembly, ensuring that this vehicle will be easy to assemble, maintain, and upgrade. The following list of engineering requirements (refer to Appendix B) will produce a vehicle that will illustrate the comparative advantages of both solid-axle and independent suspension designs.

Table 1.1: Design Requirements

Suspension Solutions Formal Design Requirements				
Parameter Description	Requirement or Target (units)	Tolerance	Risk	Compliance
Weight	25 lb (additional)	+2 lb	H	T
Size	62" (wheelbase)	+2"	L	T
Production Cost	\$2,000	\$500	L	I
Suspension Deflection	< 0.01"	0.005"	M	T
Suspension Travel	> 2"		L	T
Ride Height	1"	+0.5"	L	T
Design Life	500 miles +		L	A
Tire Adjustability	Camber/Track		L	I
Steering Feedback	Consistent Steering Force		H	T
Cornering Ability	Neutral Steering		M	T
Shock Mounting Locations	Multiple Locations		L	I
Safety	Safety Factor n=1.5	±0.2	L	A
Maintenance	2" Clearance on Critical Elements	±.5"	L	I
Fabrication Method	CNC / Welding		L	I
Assembly Method	Standard Tools		L	I
Steering Reversal	None		H	T



Chapter 2: Background

Solid Rear Axle Design

When designing CP06, the driving goal was the lightest car possible, aiming for a weight target of 300lbs. The switch to the solid rear axle was made to decrease the weight and complexity of the drive train components altogether, and thus it was selected over an independent rear suspension. The switch to the smaller single cylinder engine and using 10" wheels was also made purely for weight reduction reasons. The FSAE team expected the disadvantages of the solid rear axle but could never fully quantify them.

While the reduced weight and simplified design are definite advantages, the solid axle setup is not without its shortcomings. Having a solid rear axle added more complexity to other chassis and suspension components. This extra complexity is a result of the need to overcome a solid rear axle's inability to corner smoothly. Thus, the FSAE cars were designed to corner by lifting the inside rear tire



Figure 2.1: CP06 lifting inside rear tire

(much like a go-kart), as shown in Figure 2.1. When lifting the inside wheel of the solid rear axle, an entire contact patch of the inside rear tire is lost, along with its ability to transmit tractive and lateral forces. The lack of normal force of the tire directly affects the lateral forces which can be generated by the tire. All the weight of the rear of the car and all the lateral

force in the rear must be produced only by the outside rear tire. Having only three contact patches on the road

is not as effective as four, but the team has felt the car's agility due to its lightweight would make up for this natural disadvantage.

Tire Research

Initial background research consisted of studying the behavior of tires and their ability to create lateral force for various slip angles and normal loads acting on the tire. As long as the tire is outside of the frictional region, available lateral force will always increase with increasing normal load and slip angle as shown in Figure 2.2.

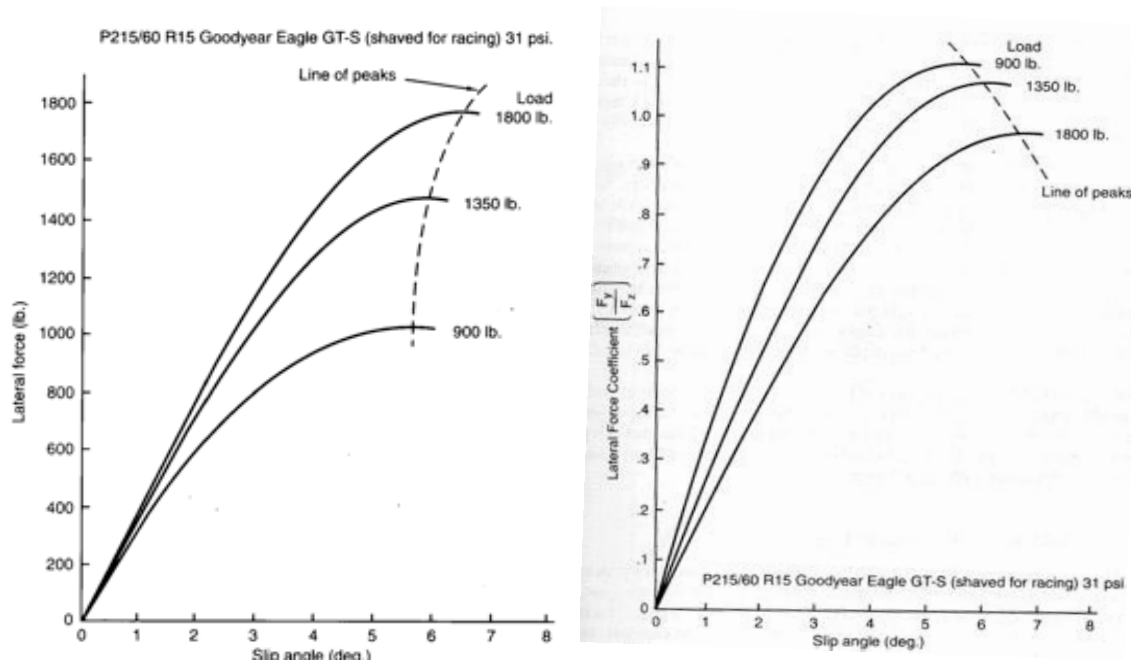


Figure 2.2: Tire data graphs as given in the Race Car Vehicle Dynamics textbook. The left graph is lateral force with respect to increasing slip angle and normal loads. The right graph is lateral force coefficient with increasing slip angle and normal loads.

Also shown in the above figure is another tire relationship; the lateral force coefficients with respect to increasing slip angle and normal loads. The lateral force coefficient given by ($F_{lateral} / F_{normal}$) is a normalized measurement of a tire's efficiency. The Milken figures show the lower normal loads have higher coefficients, meaning a more efficient use of the tire. This is one reason why a lightweight vehicle in racing is always important.

Other tire factors play a role in the generation of lateral forces, such as the camber of the tire. Typically a tire performs best under zero camber; however, for racing applications this can change. It is known that negatively cambered tires perform better than positively cambered tires.

Steady State Cornering Model

Since it is known that having four tires on the ground during a turn (as opposed to three) leads to less normal force on each tire, one can conclude that the lateral coefficients of each tire would increase. Four tires on the ground during cornering would be more efficient than only having three tires on the ground. This is of course assuming that not much weight is added in the process. To accurately represent our performance assumptions that a vehicle with four wheels in contact with the road is more stable than one with three, analysis compared the lateral force coefficients of each tire during a 1.5G steady state turn. A Matlab program owned by the SAE club calculated the difference in lateral force coefficient for the rear right tire (in a left-hand turn), which can be seen below.

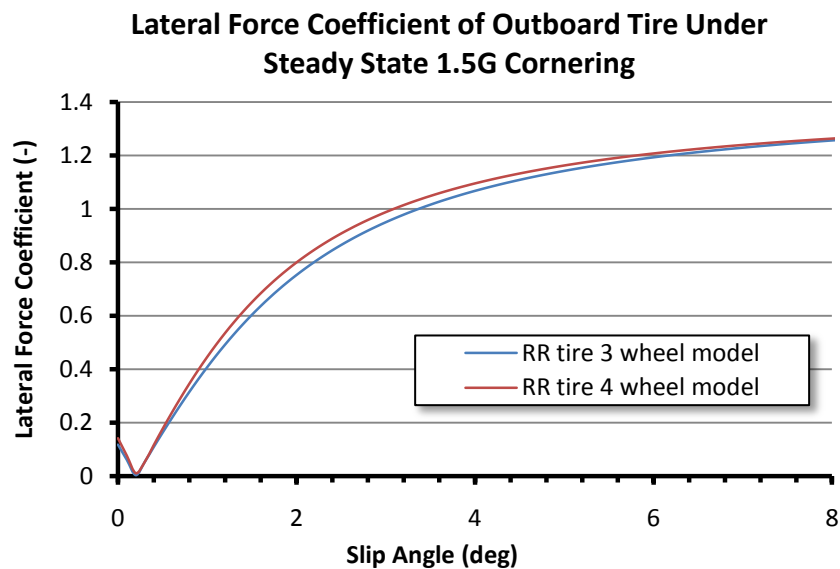


Figure 2.3: Lateral force coefficient with respect to slip angle for a three wheel model and four wheel model cases.

Although this change in the lateral force coefficient seems small (about 5%), this model takes into account certain assumptions. One of these assumptions is that the tires all act at 0° of camber. This is obviously untrue. We know that by lifting the inside rear wheel with a solid rear axle the loaded outside wheel will camber outward. A tire's available lateral force is inversely proportional to camber change, and a tire typically performs at its best between 0 and -1° of camber. The positive camber introduced under cornering with the solid rear axle would further reduce the lateral force coefficient available at the rear. In comparison, the independent rear can be designed to minimize camber change under cornering and keep the tire within the range where it performs best.



Manipulating the above mentioned Matlab code produced a relationship comparing the lateral slip coefficients of the tires of a three and four wheel model with respect to total vehicle weight. Figure 2.4 below shows how much weight is available to add to an independent rear suspension car for a given slip angle while maintaining higher lateral force coefficients of the inboard and outboard tires than a solid rear axle car.

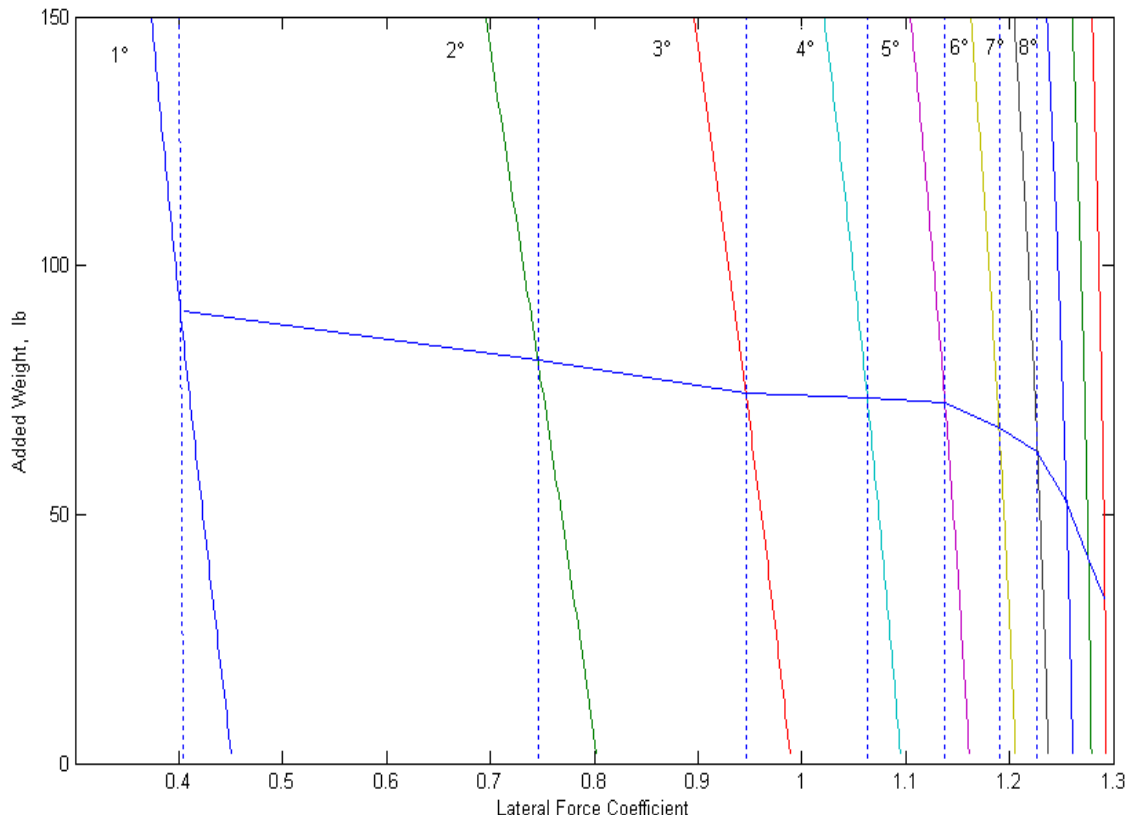


Figure 2.4 Available total weight increases with respect to increase slip angle of outboard and inboard tires

Following the blue line (Figure 2.4) shows how much weight can be added to maintain equal lateral force coefficients for different slip angles. Even at turns pushing the tires up to 7° slip, it can be seen that more than 70lbs of weight can be added to the 2008 car if it corners on all four tires. The data becomes even more relevant at higher slip angles approaching the limits of the tires. As shown in the graph, at 10° slip, 35lbs can be added to an IRS car without losing advantage over the solid axle.

Knowing how much added weight will affect the performance of our independent rear suspension system, an analysis was conducted comparing the CP06 car with the last independent rear



suspension car built at the school, the CP04 car. Estimated weight values were used to gauge how much weight we anticipated adding to the CP08 car with our system.

Table 2.1 Weight Addition Estimation

Additions/Removals to 2008 Car	
Rear Frame	20
Differential	10
CV Joints & 1/2 shafts	12
Uprights	5
A-Arms	5
Shocks	3
(Rear A-Arms)	-10
(Solid Axle)	-15
(Bearing Blocks)	-5
Weight Addition	25

Table 2.1 shows that converting the CP08 car to independent rear suspension will add approximately 25lbs to the overall weight of the car (bringing the total weight to about 400lbs, without a driver). This 25 lbs addition is still within the performance advancement of an IRS (Figure 2.4) even at slip angles approaching 9°.



Chapter 3: Design Development

Suspension Geometry

The first phase of the suspension design began with the development of suitable rear geometry. It was immediately decided that an unequal length double wishbone suspension should be employed. This suspension type was chosen for its ability to meet the most desired performance objections with the minimum amount of compromises. Its use is almost universal in not only FSAE cars but also road racing cars. The unequal length design features shorter upper A-Arms, which put the wheels in negative camber under bump. This is desirable under cornering, where the roll of the body typically increases the positive camber of the outside wheel; with the short long arm design, the outside wheel's camber is kept at a more consistent value under cornering.

Optimum K suspension software was used to place the upper and lower pickup points of the upright and the chassis in order to determine dynamic properties of the suspension. The design of any

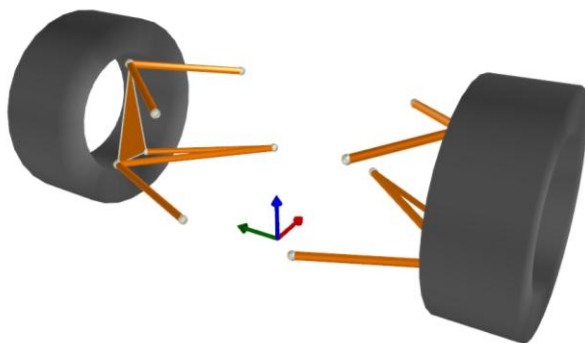


Figure 3.1 3-Dimensional A-Arm and tie rod geometry

suspension system is largely dependent on the tires. In order for a more controlled trade study between the two types of rear suspension systems, the same tires will be used for each. These tires are Goodyear 20 x 13 x 7in racing slicks. The club has a few sets of this tire available, giving plenty of opportunities for testing. The tires were originally chosen for the CP08 car due to their driver-friendly properties; unlike most race tires, these Goodyears do not have a steep peak followed by a drop-off in frictional properties, as seen in Figure 2.2. This typically means more predictable handling for an inexperienced driver. The rear track was initially chosen to be 44". This is one inch wider than with the solid rear axle, and was chosen primarily to better balance lateral weight transfer. A Matlab lap simulation was also run to check vehicle lap times through a set course with increasing rear track. Lap times were seen to decrease with increasing track. With minimal change as track increased from 44 to 54 inches, the initial selection was deemed suitable for this design.

With rear track, wheel size and rim diameter known, a suitable lower ball joint and toe link ball joint could be found. The toe link replaces the steering link in a front double wishbone suspension and

further constrains the motion of the wheel. The toe link was designed to be attached to the lower A-Arm instead of the upper A-Arm for two reasons. First, the upper ball joint was designed to be as far away from the lower ball joint as possible to distribute the loads more evenly. Second, after conducting an FBD of the suspension member forces, it was seen that more force would exist in the lower A-Arm members. The extra support of the toe link on the bottom was expected to lower the maximum force seen in each lower A-Arm member, allowing for smaller and lighter A-Arms.

The chassis pick up points were then iterated until suitable roll and heave characteristics were met. Initial design focused on keeping roll camber as low as possible. Roll camber is the change in tire camber as the chassis rolls. While cornering the chassis will roll to the outside of the turn, and due to lateral weight transfer the outside wheels will become more heavily loaded than the inside wheels.

$$\text{Roll Camber} = \frac{\Delta \text{Camber}}{\Delta \text{BodyRoll}} \quad [1]$$

Making sure the roll camber stays low is especially important for the outside wheels since they will provide the most lateral force, and a change in camber could greatly reduce the lateral forces the tires are capable of reaching. Our geometry has roll camber of $.49^\circ/\text{roll}$, and with a static tire camber of -1° , our outside tires will never be positively cambered even under 2.4° of chassis roll. Dynamic properties of the geometry can be seen in various plots and graphs in Appendix C.

Also important with the suspension geometry is to insure that the roll center stays relatively consistent both vertically and laterally under roll. A low roll center was desired in order to reduce jacking forces on the chassis and suspension. However, it was quickly found that a compromise would have to be made between roll camber gain and roll center height. A roll center of 2.4" was selected as the goal as it always maintained negative camber under 2.5° of roll, while remaining similar to the roll center height on the front suspension on the CP08 car.

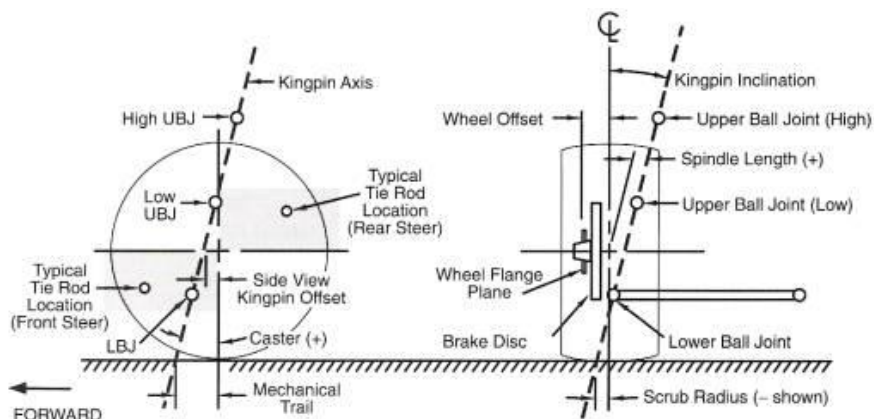


Figure 3.2: Suspension packaging and parameters

It was found that rear suspension geometry was much simpler to design than front suspension geometry due to the inability to steer the rear wheels. Front geometry is complicated by the fact that it must take into account steering parameters including the effect of bump steer on the car. Caster angle, kingpin inclination, wheel offset, mechanical trail and other parameters shown in Figure 3.2 were not as important in rear geometry. Nonetheless it was important to re-analyze the CP08 car's front geometry. This is shown later in the Detailed Design section.

Loading Conditions and Forces

The determination of loading forces started with tire data and loading conditions. The loads likely to occur under competitive situations were found using historical data, and a Matlab code was written to calculate normal, lateral and longitudinal (tractive) forces on each tire during a specific set of accelerations in a turn, based on tire properties and weight transfer. These conditions were assumed to occur during steady longitudinal acceleration. While this assumption is primitive and may need revision later, it functions well as an initial test, with a safety factor providing for any unknown loading and accelerating conditions.

With initial geometry and tire forces at the contact patch known, forces in the suspension members could then be solved for. In order to do this, each tension-compression member was assumed to be a two-force member, meaning it would only have axial forces acting on it. The forces are translated from the contact patch to the upright pickup points into the A-Arms axially, and lastly into the chassis through the chassis pickup points. Since a double A-Arm suspension has six members to it, only six equations are needed to solve for all the forces for each tire loading condition. These six members are the upper A-Arm (2 members), the lower A-Arm (2 members), the tie rod and the push rod, which will be attached to the lower A-Arm and act through the lower upright ball joint. Summing forces in three directions and moments about three axes yields the axial forces in each tension-compression member for each given set of tire contact patch forces.

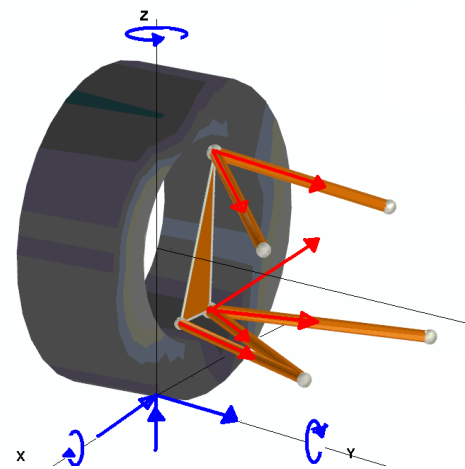


Figure 3.3: Loading Forces seen on tire and in suspension members



A program was created in Matlab (see Appendix E) which solves for these axial forces using matrix math. Inputs are the OptimumK coordinate points, which define the geometry of the suspension components. These forces are transmitted as reaction forces on the chassis through the A-Arm, which act as axial forces on each member. Next, tire contact patch forces and tire properties such as pneumatic trail are manually input.

The program then solves the system of quasi-static equilibrium equations and outputs axial forces in the suspension members. The development of the equations of quasi-static equilibrium and the FBD's can be seen in Appendix H. The first case was calculated using what was assumed to be worst case loading conditions of 1.5g's lateral acceleration, 1.0g longitude acceleration, and 3.0g's of bump. The resulting axial forces are then fed into a separate Matlab program that determines tubing sizes for each member. The program takes into account yield and buckling, and also includes deflection of the A-Arms.

Space Frame Adaption

The rear frame adaption is arguably the most difficult part to design given that it must interface and connect not only with all of our new suspension and drive train components, but also existing chassis and engine components, all while being easily removable. Due to the different design possibilities available, multiple concepts were created, and a concept evaluation matrix was used to select top rear frame adaption designs based on common criteria requirements. Concepts were designed with SolidWorks to better anticipate the manufacturing challenges and removability for each concept. At the time of the design no structural calculations were made for each frame, and designs were simply triangulated to provide stiffness. To make up for a lack of accurate concepts, criteria requirements were weighted qualitatively for each design as shown in Appendix D. The criteria for which we judged the concepts are listed below.

Weight: This is the largest area of concern and was weighted greatly in the decision process. Since frames were constructed in SolidWorks, the program allowed us to find the weight of each design using carbon steel tubing. Tubing geometry chosen was 1" O.D. by 0.0625" thickness for all members within the concept. These tube sizes could then be individually tuned using FEA analysis and results.

Stiffness: The concept's stiffness rating was considered by inspection because a more accurate FEA analysis was not done at this stage of the design process.

Manufacturability: Tube notching and welding can become extremely difficult the more complex a structure gets. The more branches a node contains the more difficult it will be to construct. Also, the structure's ability to adapt to existing pickup points on the chassis and frame will save the integrity of the current space frame design.

Engine Stress: This is currently an area of uncertainty. While a stressed or partially stressed design may result in fewer components to stabilize the structure, this could potentially compromise the strength and reliability of the engine. Engine testing should be done to determine the feasibility of stressing the engine.

Suspension Compromises: The design must follow the suspension geometry and little to no compromise should be accepted in this area. The concept must not pose complications to mounting locations for suspension components such as A-Arm and rocker pick-up points.

Other considerations such as appearance, cost, interference and system compliance were used in the decision making process but were not heavily weighted due to the fact that this is purely a test vehicle to compare performance results.

The top concepts from our design matrix are examined below, highlighting the pros and cons of each.

Concept 1:

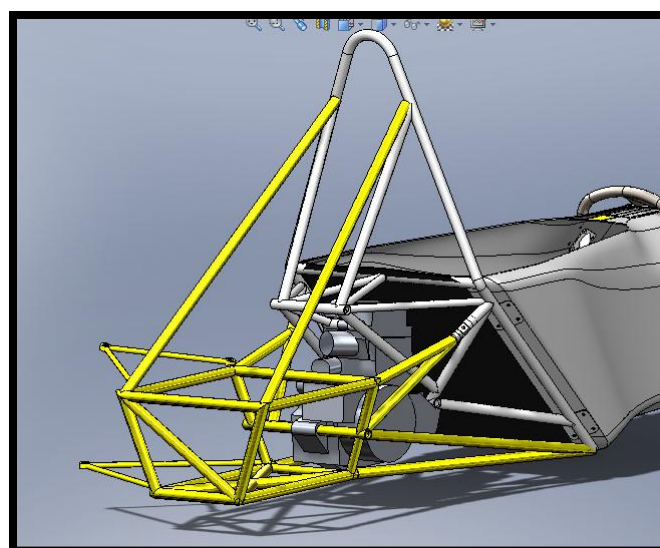


Figure 3.4: Top concept 1 from rear frame decision matrix

The first concept, shown above, starts with a trapezoidal box that is fastened to the engine's back mounts. This box will hold the differential components as well as provide the suspension mounting locations. The box is then further constrained to existing engine bung mounts in four locations. It also has members which run all the way up to the main roll hoop for added stiffness. The design initially weighed 22 lbs, and stiffness was expected to be high. It also was deemed to have the least possible interferences with existing components and was expected to not stress the engine. It was eventually chosen as the top choice to develop.

Concept 2:

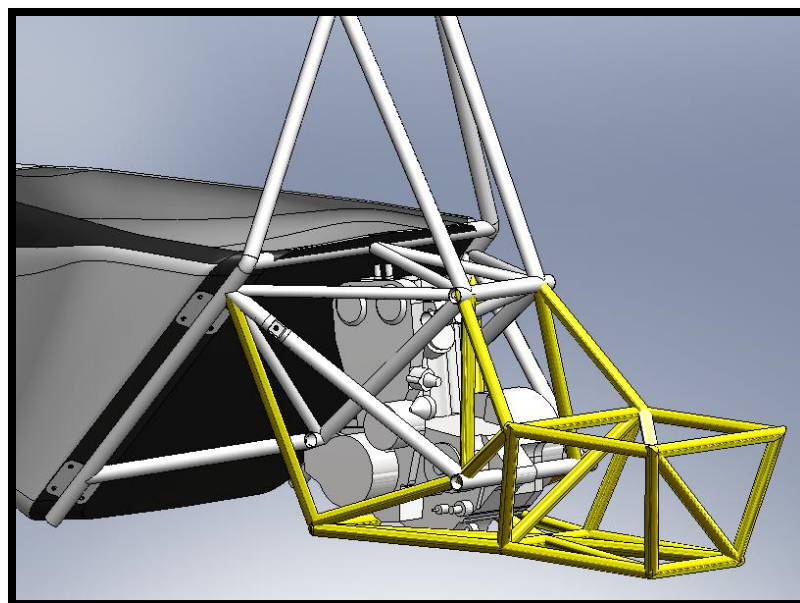


Figure 3.5: Concept 2 from rear frame decision matrix.

The second concept is a partially stressed engine design which mounts to removable engine arm tubes as well as the high corner of the roll hoop main down tube. This structure mounts to the bottom of the engine and the existing rear rocker. Relative to other structures, this design was one of the lightest, weighing in at 18 lbs. Few locations on the space frame and chassis are used to stabilize the structure, which is picked up by the engine mounting locations, which consequently causes a higher engine stress relative to other concepts. Mounting to the rocker was also deemed too difficult and it meant a new intake would absolutely need to be made.

Concept 3:

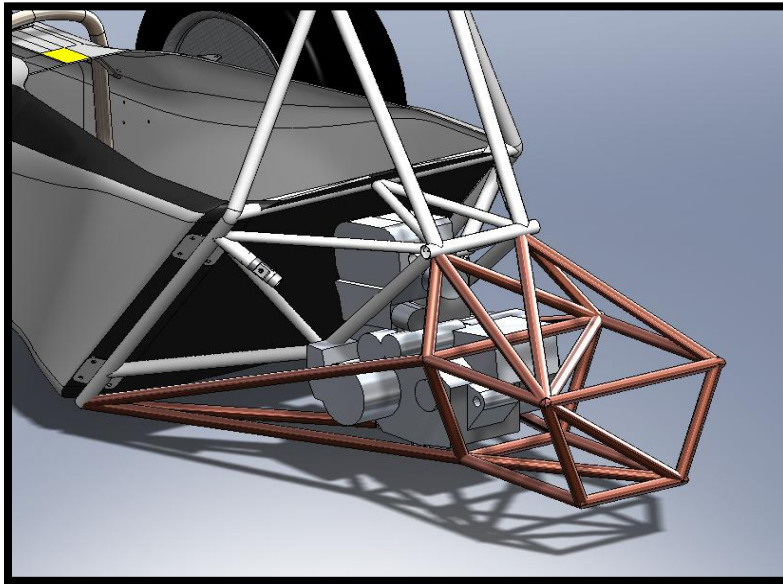


Figure 3.6: Concept 3 from rear frame decision matrix.

Concept 3 is a partially-stressed design mounting to the rocker and lower corner of the roll hoop. Although it was rated higher on stiffness due to triangular geometry, its weight was the same as Concept 1 at 22 lbs. Problems arose with its interference with differential components and the intake. The intake would need to be re-manufactured, as in Concept 2. Also, the rocker bar had over five members mounted to it. This would be hard to incorporate into a removable design.

The finalized design decision combined the best results of all design options and is shown in Appendix D. The final design will be constructed with 4130 normalized steel tubing. Cross-sectional area will be determined when further stress and stiffness calculations and FE models have been produced. The structure will be constructed by notching and welding and attached to the chassis and rear space frame using detachable bungs and existing pickup points.

Differential

The differential is an essential part of a car's drive train. When a car corners the outside wheels must travel a greater distance than the inside wheels, and therefore must spin at a faster speed. Without a differential (as in a solid axle) both wheels are forced to rotate at the same speed, scrubbing one tire under cornering. Performance can be improved through the use of a differential, which allows the wheels to rotate at different speeds. A couple of options were available for the selection of the differential. The differential selection was based on the following criteria.



Figure 3.7: Representation of a limited slip clutch differential

The most dominating factors were weight and accessibility. One option considered was modifying a differential from a quad. For our application the quad differential would be considerably overbuilt. To remove unnecessary weight from the housing, a new housing would need to be designed and manufactured.

Limited Slip: The differential needed to have limited slip characteristics, whether through a clutching device or an Invex gear mesh like those present in Torsen differentials. Although the desired life is

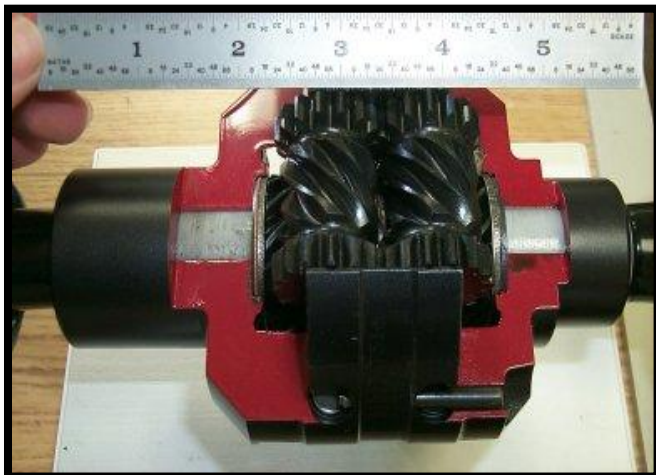


Figure 3.8: D12000 Torsen differential

assumed to not exceed 1000 hours, the life of the components must be considered. Clutches used for limited slip differentials will wear more significantly than gears like those present in the Torsen, but could possibly be lighter overall as has been proven by past Formula teams. An open differential would not supply the needed torque to both wheels under any substantial torque difference between drive axles. The torque bias ratio is also a main consideration. The bias ratio represents the "locking effect" and relates the torque supplied

to the wheel with the most traction to the torque supplied to the free spinning wheel.



Weight: Although there are many differential options available, most are not practical for FSAE applications. Most readily available options are over-built, and we would have to consider a high weight compromise for these options.

Cost: The differential is a substantial part of our budget. Keeping cost down is not absolutely necessary but aids in the positive outcome of our product.

Availability: Ease of purchase and procurement were considered purely for the ability to adapt half shafts and CV joints. Choices included ordering a new or rebuilt differential or rebuilding the old Torsen on the 2004 Formula car.

Torsen offers a limited slip differential specifically for FSAE teams. Their current university special Torsen D12000 weighs in at just 8 lbs. This model has a torque bias ratio of 3.2:1, which means that about 75% of the torque can be maintained at the wheel with the most traction. Also the Torsen is the only differential type that allows the use of a single inboard rear brake by design. Fortunately for Suspension Solutions, Formula Hybrid owns a spare version of Torsen's current university special, as shown in Figure 3.7. A housing will be manufactured out of aluminum to block dirt and debris from naturally settling inside the mesh of gears.

CV Joints and Half Shafts

Before making any design decisions, a strength calculation was performed to find the relative size of the drive train components. The CV joints and shafts must be compatible with the differential and the uprights. Many options were considered during this design process. The 2004 Formula car already has all the components needed for this design, and these could be used and customized to fit the 2008 Formula car or referenced as a template to make the design better. The half shaft and CV joint assemblies would be possible to manufacture in-house with few components needing to be outsourced. Also at our disposal are Formula Baja's out-of-service CV assemblies, which could be modified to fit our geometry. As a last resort, a more costly idea would be to purchase a rebuilt or new CV assembly from a manufacturer. Decisions were made based on the following criteria:

Weight: The selected design of the CV joint and half shafts needs to be compliant with our projected weight goals. Quad CV assemblies may be overbuilt for our application and thus would need to be modified or result in a weight penalty.

Buying vs. Manufacturing: Since this is a design project where learning is the most valuable experience gained, in-house manufacturing of the CV assemblies initially seemed like an intuitive decision. After further thought and consideration, possible cost savings due to in-house manufacturing over outsourcing would not be achieved at a significant level. Also, the ability to size and adapt components to each other may not be worth the time spent. If in-house manufacturing were



Figure 3.9. CV assembly including half shaft

to proceed, many more design criteria would need to be analyzed. The type of bearings used in CV assemblies range from the complicated tripod and cup to the traditional U-joint to splined collars which would be fitted to half shafts and mating components. Using different sources for all these components would make seamless integration difficult, as well as potentially requiring modification of purchased parts, possibly compromising the component's integrity. Despite these drawbacks, the team decided to use custom-manufactured tripod half shaft assemblies. The most important factor considered was that any pre-manufactured assembly would set our track width. Since this parameter was already set by the design team, a pre-manufactured assembly would have to be cut and welded to fit our design. This was not at all desirable, as the resulting stress concentrations and fatigue strength are very difficult to accurately determine. This consideration, as well as the relative greater difficulty and increased weight of modifying a pre-manufactured CV spindle to fit and rotate properly within the designed uprights, lead the team to choose custom-manufactured tripod assemblies. In-house manufacturing also gave the team more control over the weight of the assembly, as well as material choice and fit and finish.



Figure 3.10: Different bearing options for manufacturing of CV assembly.

Results: As mentioned above, custom manufactured half shaft assemblies have their drawbacks, mostly relating to increased design complexity. Despite these factors, the team decided to manufacture the assemblies in-house in order to give them more direct control over track width, weight, and fit and finish. This decision was also economical, because a set of tripod assemblies were available from a previous Cal Poly SAE vehicle.

Uprights

The rear uprights were sized based upon worst case loading of maximum grip, both laterally and longitudinally, while experiencing a large spike in normal force due to a bump. The design was driven by the following factors:

Design considerations: The upright design relies heavily on the choice of bearing and spindle assembly. There are many different ways to configure the half-shaft/spindle interface, mostly due to the live spindle, which is required of a rear upright. Some upright designs incorporate a larger bore in the center to encompass an entirely concentric CV joint/bearing combo. Such a design allows for longer half shafts, which has a few advantages, one of these being a less extreme angle for the CV joint to deal with. We decided against this design for a number of

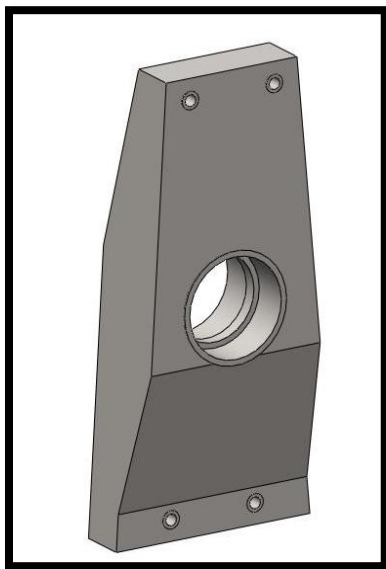


Figure 3.12: Steel upright concept

reasons. Firstly, it is a hard setup to manufacture due to critical press fits. Secondly, placing the CV joints inside the upright would likely weigh more. While the associated bore deducts from upright weight, it fills this void

with larger, heavier bearings. Many teams boast uprights of this design that weigh a little over a pound due to the large void in the center; however, they do not take into consideration the weight they will in turn be adding in bearings. For these reasons, we decided to use a tripod joint housing mounted to a flange on the spindle to the

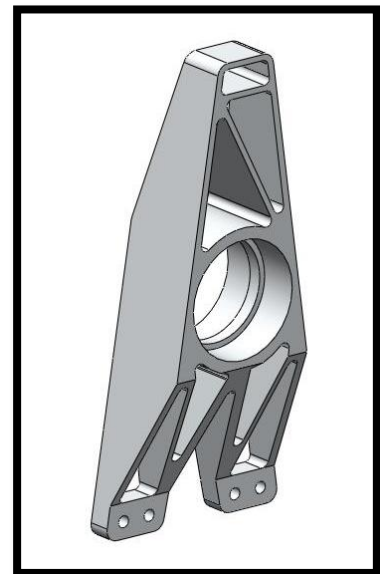


Figure 3.11: Aluminum upright concept



inside of the upright. This not only saves weight with smaller bearings, but also allows us to use tapered roller bearings to transfer thrust loads due to lateral grip forces. The roller resistance of this type of bearing was verified to be negligible through simple calculations, coming in at 1.5 in-lb.

Material: Material decisions were initially looked at for strength and weight. FSAE uprights are typically constructed either from sheet metal or aluminum, and these two options were examined to determine which was better suited for this project. 4130 normalized steel has high strength and stiffness properties relative to those of 6061 aluminum, but the 6061 can have weight advantages over steel, which is the primary area of concern. These properties will drive geometry alterations for the initial upright design. To pick the best design, the models will be imported into FEA software to more accurately predict stresses and stiffness. As for the relative cost of the materials it was determined that on the basis of just raw materials, the aluminum upright materials would cost about twice as much as those of the sheet metal uprights.

Manufacturing Cost: With the choice between two materials comes the choice between two different manufacturing processes, which will naturally contribute to the overall design decision. An aluminum upright would be outsourced to a CNC machinist, while a sheet metal upright would be welded in-house. Performing in-house construction, while somewhat less expensive, is quite time consuming, which creates a cost much higher than one might assume. We would have to associate our time with a value as high, if not higher, than that of a CNC machinist due to the simple fact that we will be constructing many of the other systems in-house and are therefore ultimately responsible for their being completed on time.

Deflection and strength Criteria: In order to accurately compare the two designs, both designs must have a deflection of no more than .005 inches, which would correspond to an arbitrary .05 degree change in camber. In terms of strength, both designs must have a factor of safety above 1.2, which is a safety factor based on conservative loading conditions.

Once preliminary designs of each type of upright were created through simple hand calculations and solid modeling, a decision matrix was created to drive the ultimate design to fruition. Each criterion was rated on a scale of one to five, with five being the most ideal and one being the least.



Table 3.1: Upright Material Trade Study

Criteria Concept	Criteria Weight	6061 Aluminum	Weighted Sum	4130 Steel	Weighted Sum
Weight	0.5	5	2.5	3	1.5
Material Cost	0.15	2	0.3	4	0.6
Manufacturing Cost	0.15	3	0.45	5	0.75
Strength	0.1	5	0.5	5	0.5
Stiffness	0.1	4	0.4	5	0.5
Total	1		4.15		3.85

Criteria Weight: The relative weights awarded to each criterion are percentage values that add up to 100 percent in total. Weight was decidedly the highest priority, and therefore it is worth 50% of the total points. Material and manufacturing costs were the next largest consideration, each coming in at 15%. Strength and stiffness were merely guesses at this point, and because of the fact that at the end of the design process either upright will meet the required allowances within the factor of safety, stiffness and strength each embody 10% of the overall score.

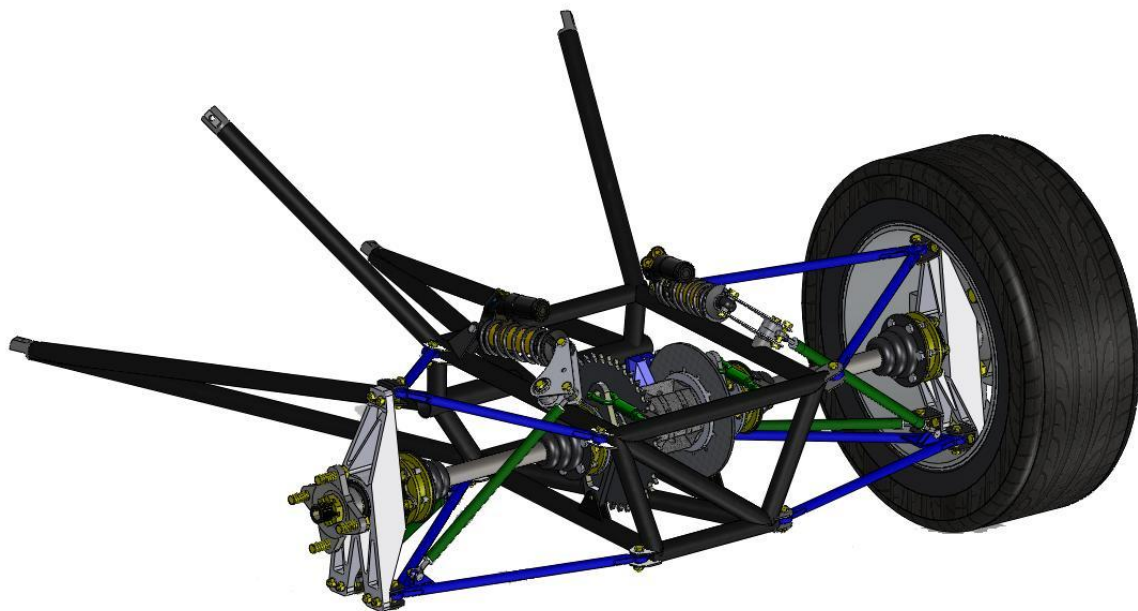
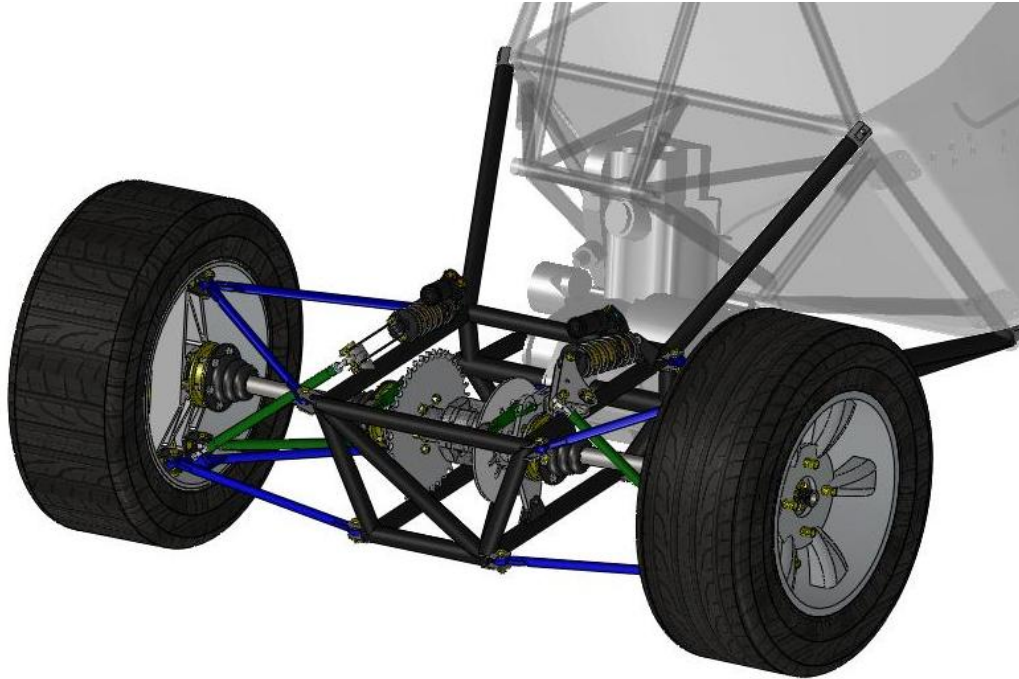
Results: Due mostly to the fact that the preliminary design weighed about a half pound less, the aluminum upright design came out ahead in the above matrix. From here, FE analysis results can determine whether the designs are ultimately adequate, and necessary design iterations will be performed as seen fit.

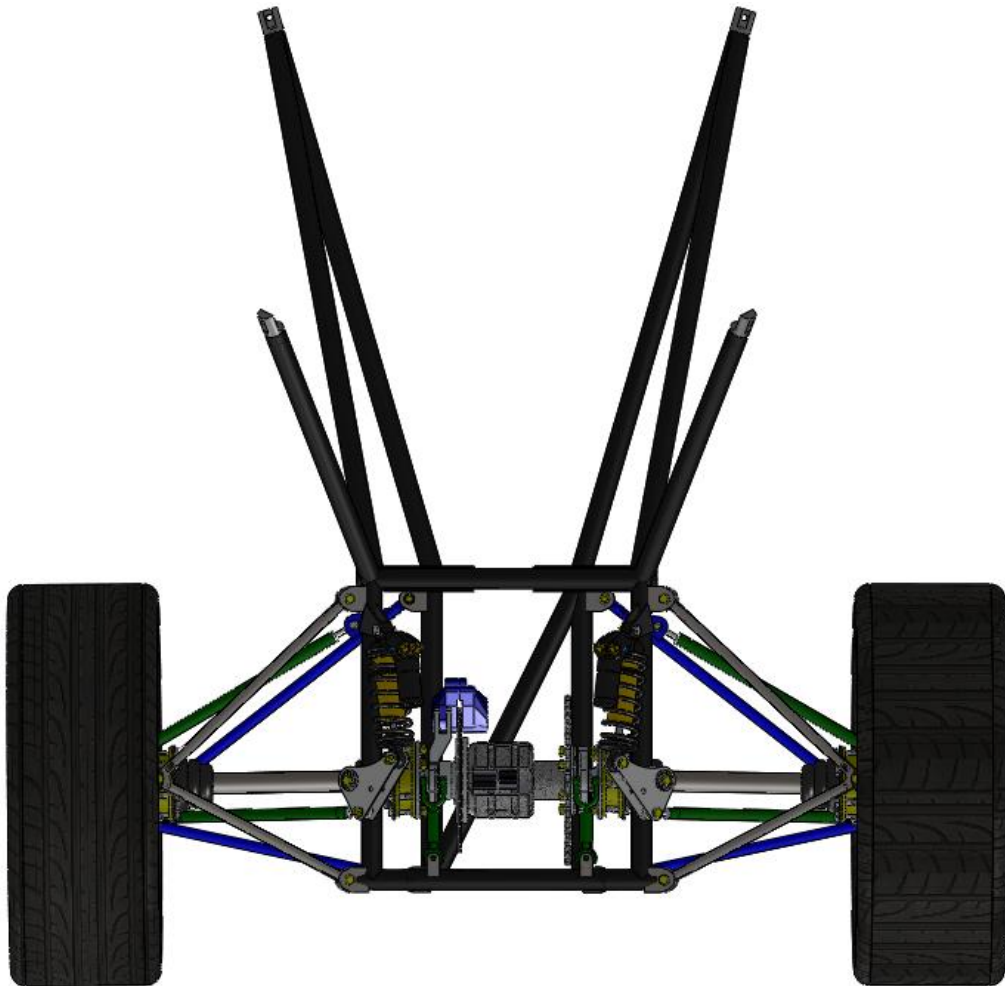
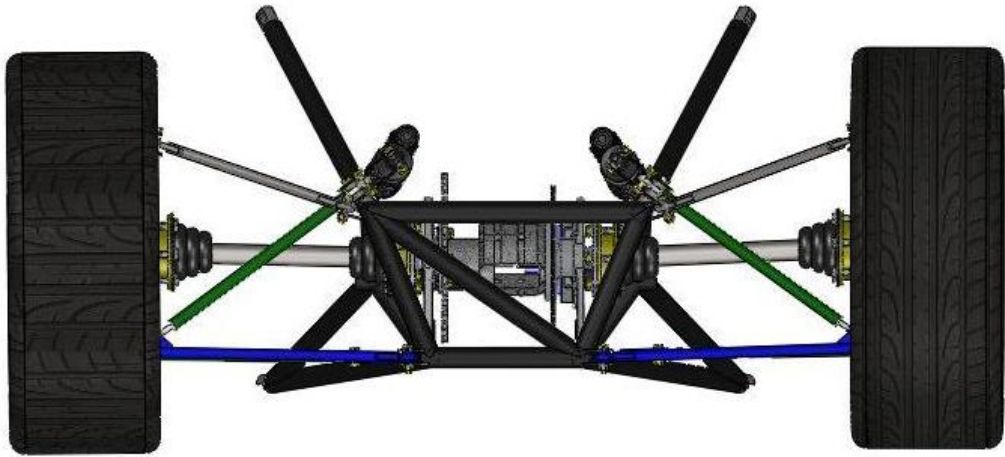


Chapter 4: Final Design

Summary and model

Presented below are some assembly models of all the current components within SolidWorks. This will allow us to accurately check all design interfaces before production. It also gives us a current prediction of interferences and weight comparisons between the IRS and solid rear axle systems.








Detailed Design Description and Analysis

Rear A-Arms

With a chosen rear frame adaptation concept, final chassis mounting points were determined, and final suspension coordinates could be found using Optimum K suspension software. Our final points can be seen in the following table. The coordinate system that defines these coordinates is on the ground plane and directly in the middle of rear track line which connects the contact patch points of the tires.

Table 4.1: Geometry of the rear suspension giving in Optimum K coordinates.

<i>OPTIMUM</i> 		Double A-Arm Rear							
OptimumK v 1.1		Left			in		Right		
Lower A-Arm	x	y	z	x	y	z			
Chassis Fore	9	4.875	4.78	9	-4.875	4.78			
Chassis Aft	-5	4.875	4.78	-5	-4.875	4.78			
Upright	-2	19	5	-2	-19	5			
Upper A-Arm									
Chassis Fore	9	8	12.5	9	-8	12.5			
Chassis Aft	-5	8	12.5	-5	-8	12.5			
Upright	0	17.5	15.5	0	-17.5	15.5			
Tie Rods									
Attachment	Lower A-Arm								
Attachment	9	4.875	4.78	9	-4.875	4.78			
Upright	2	19	5	2	-19	5			
Wheel geometry									
Half Track			22			22			
Longitudinal Offset			0			0			
Vertical Offset			0			0			
Static Camber			-1			-1			
Static Toe			0			0			
Rim Diameter			13			13			
Tire Diameter			20			20			
Tire Width			7			7			

Our final design incorporated shorter A-Arms than was originally designed. A-Arms are typically desired to be as long as possible to reduce significant camber changes during cornering. However, we

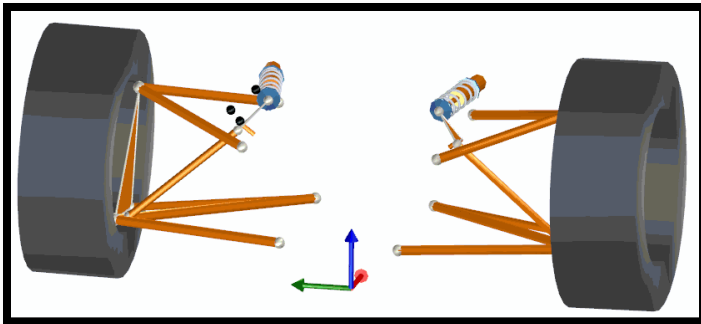


Figure 4.1: Back view of A-Arm geometry

were able to maintain a good camber curve with roll with relatively shorter A-Arms overall. The lower A-Arms were still longer than the upper A-Arms in order to produce the desired tire curvature towards negative camber during roll. Overall, shorter A-Arms were chosen to allow for easier insertion and mounting of the differential assembly. Shorter A-Arms leads to a larger rear frame bay, where the differential

will be housed. Since little-to-no changes were found within the dynamic suspension analysis, the larger rear frame bay was deemed more important to other areas of the project. The Differential Assembly will fit easily into the rear frame bay, allowing for easy accessibility.

Next, the axial forces in the A-Arms were solved for using our developed Matlab program. Three loading cases were examined: a steady state cornering case, a straight line acceleration case, and a full cornering and accelerating case with 3G's of bump. The latter was deemed to be most critical. This case, along with the steady state cornering at 1.5G case, can be seen below in Table 4.2. The tire coordinate system used is that of the SAE convention presented in the Milken's Racecar Vehicle Dynamics.

Table 4.2: Axial forces within the suspension members for two loading conditions

All Loads in (lbf)		Accelerating, cornering, and bump			Steady state cornering, no bump		
		F Tire X	F Tire Y	F Tire Z	F Tire X	F Tire Y	F Tire Z
Member	length (in)	350	342	801	0	342	267
Upper A-arm (fore):	11.53	206.64			-1.0		
Upper A-Arm (aft):	9.29	200.64			229.73		
Tie Rod (fore):	14.77	-515.23			-145.09		
Lower A-Arm (fore):	17.01	-382.4			203.65		
Lower A-Arm (aft):	13.94	-501.97			-768.49		
Push Rod:	11.25	925.72			276.82		

After examining all the loads it was found that the lower A-Arm aft member and the pushrod are the most heavily loaded members. The tie rod has the next highest loading, and lastly the upper A-Arms are relatively lightly loaded. The suspension member's tube size was then calculated based on yielding and bucking criteria. Deflection of the members was also calculated and led us to choose larger upper A-Arm members. All allowable and final tubing sizes can be seen below in Table 4.3. Each member was sized using a minimum 1.5 factor of safety. For the case of the upper A-Arms, it was found that .250" O.D. tubing would suffice for strength considerations; however, .4375" O.D. tubing was selected for manufacturing and stiffness reasons. Welding any smaller size of tubing would be very difficult, and wouldn't allow the bearing wafer design chosen below.

Table 4.3: Final A-arm Tubing Sizes.

Member	length (in)	Allowable O.D. (in)	Chosen O.D. (in)	thickness (in)	Deflection (in)
Upper A-arm (fore):	13.12	.250	0.4375	0.035	.003
Upper A-Arm (aft):	11.14	.250	0.4375	0.035	.003
Tie Rod (fore):	15.76	.313	0.4375	0.035	.001
Lower A-Arm (fore):	17.90	.375	0.4375	0.035	.005
Lower A-Arm (aft):	14.44	.500	0.500	0.035	.009
Push Rod:	13.0	.500	0.500	0.035	.008



Figure 4.2: Right Side of Suspension members

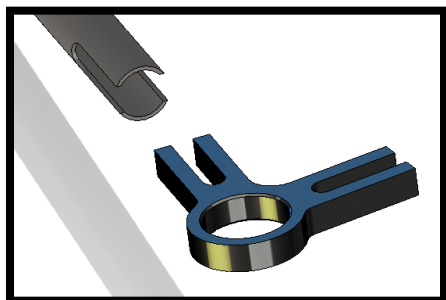


Figure 4.3: A-Arm end wafer/bearing carrier

With the tube sizes and lengths determined, design began on the bearing carrier that must be attached to the ends of each suspension member. The CP08 front suspension currently houses the spherical bearings as part of the upright and chassis tabs. However, designing the bearing into the arms seemed like a simpler manufacturing solution. We decided to use an A-Arm wafer design borrowed from the Formula Hybrid team. The design has already been proven as easy to manufacture and it allows for less deflection of the critical bearing surface during welding. The wafers will need to be CNC machined, but the code for the machining is already available.

Rear Rockers

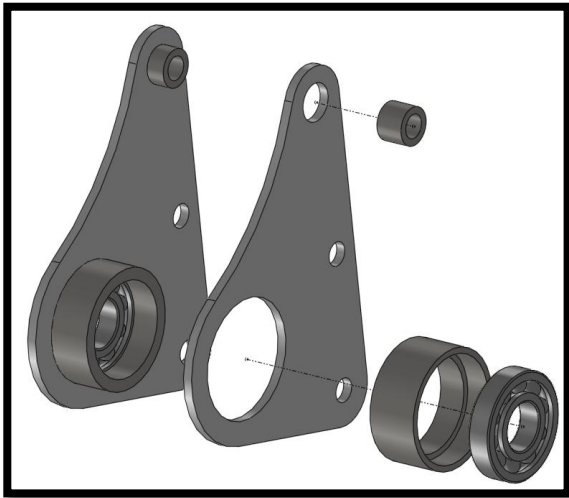


Figure 4.4: Final rear Rocker assembly

The rear rocker's design was started after suspension pickup points and space frame members were located. The master Solidworks assembly was then used to design the rocker and push rod length and place their locations. The first major concern was to place the rear rockers and the dampers that attached to them out of the way of other components. Another concern was easy accessibility to the damper to allow for tuning. Lastly, a motion ratio of 1:1 was desired, which must be built into the geometry of the rocker. The motion ratio relates the compression distance of the damper to the upward wheel travel. A motion ratio of 1:1 was chosen to

avoid a progressive spring rate, which would change the vehicle behavior during roll and lead to an inconstant roll gradient. This motion ratio also made use of most of the damper's stroke with the two inches of travel, increasing velocity in the damper and improving damping characteristics.

The upper horizontal member within the space frame box was found to be the most acceptable place to mount the rockers. This allows the damper to be mounted parallel along that member, giving plenty of room for other components. This position also allows for shorter push rods than originally expected, which led to thinner, lighter pushrods. The rocker itself will pivot about a machined steel post with a threaded insert to allow a top piece to hold the rockers in place. The bottom of the post will then be notched at the correct angle and be welded to the frame itself. Figure 4.5 shows this location on the rear space frame.

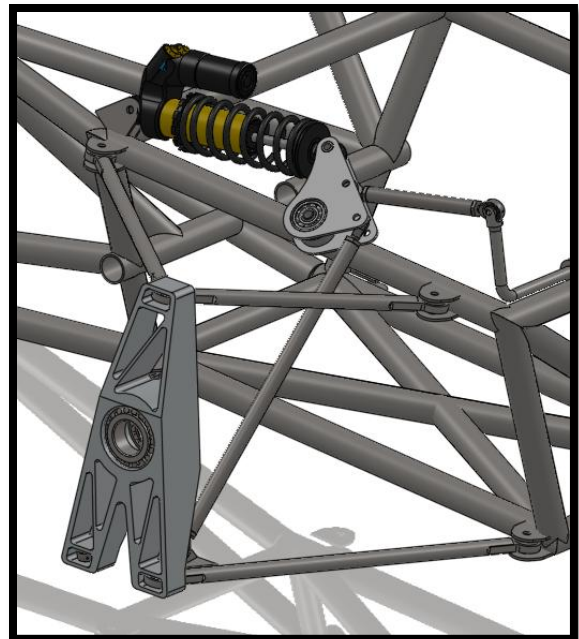


Figure 4.5: Final rear rocker location

With our geometry for a 1:1 motion ratio determined, a trade study was conducted to decide on the material to be used. There were two obvious competing choices, a machined aluminum rocker or a steel fabricated rocker. Since manufacturability and cost are high concerns, it was decided through a trade study that steel fabrication should be employed. Although aluminum pieces would be lighter, we believe the total weight penalty of less than 0.2lb is worth the cheaper alternative.

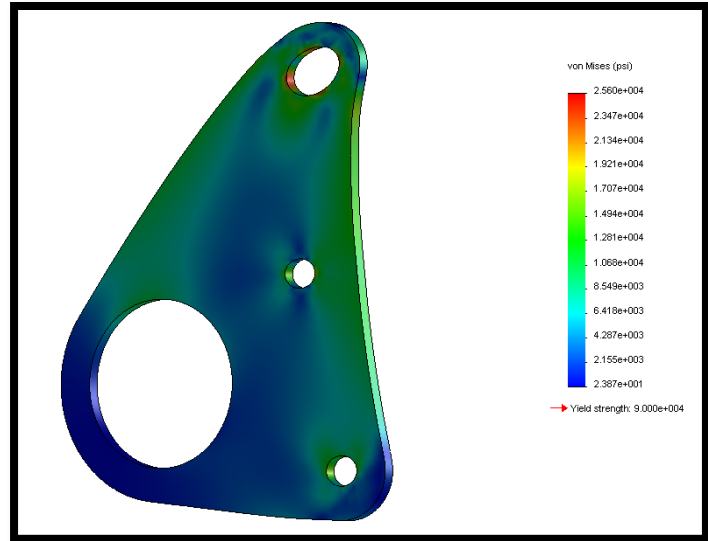


Figure 4.6: Stress analysis on the rear rockers

The steel rockers will consist of three pieces: a plate, an insert to hold the bearing, and an insert to support the shock spherical bearing.

The three pieces will then be TIG welded together to create the final part. The final rear rocker assembly can be seen in Figure 4.4. The rocker plate thickness was calculated using the CosmosWorks program and assuming the worst pushrod loads of upwards of 900lbf. A thickness of 0.060" was deemed adequate with a factor of safety of 1.4 for normalized 4130 steel. Results of this analysis can be seen in Figure 4.6.

Shocks and the Anti-Roll Bar (ARB)

The shocks to be used on this project are the shocks that are currently in use on the CP08 car. The current shocks are Cane Creek mountain bike shocks with adjustable dampers and springs. The ride frequencies to be used are 3.3Hz for the front and 3.6Hz in the rear. The front ride frequency was desired to be higher than the rear to allow for faster transient response at corner entry and reduce front ride height variation. However due to the lack of a front ARB, it was necessary to select springs for desired roll rates instead of ride rates, which lead to such high ride frequencies. With the previously stated ride frequencies and desired roll rates of 8400 ft-lbs/° in the front and 7900 ft-lbs/° in the rear, spring stiffness of 150 lbf/in and 175 lbf/in were chosen for the front and rear springs respectively. Roll Rates were decided based on matching the maximum lateral acceleration front to rear at 1.46 G and a

desired roll gradient of 1.5 °/G. Matching lateral acceleration front to rear is important for a neutral handling car. With a Front ARB available, a Rear ARB may have also been desired but with the lack of a front ARB, the addition of a rear ARB was deemed unnecessary. Instead high spring rates will be used to achieve desired roll stiffness, at the cost of high ride frequencies.

Front Suspension Analysis and Redesign

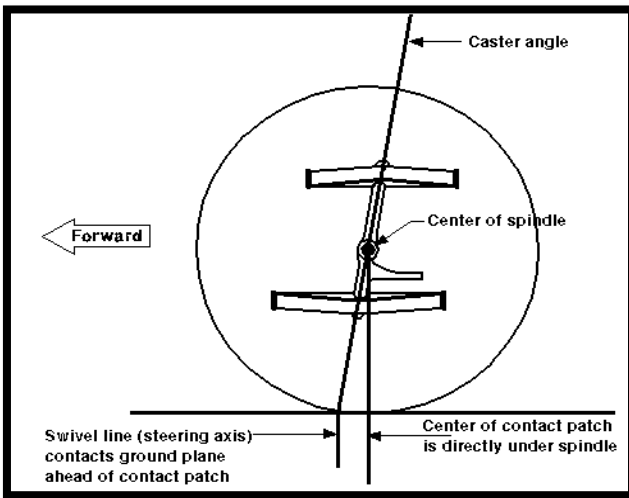


Figure 4.7: Caster angle

Although the bulk of this project focuses on the adaptation and design of an independent rear suspension, a considerable amount of time must be spent reevaluating the current front independent suspension of the 2008 FSAE car. The front and rear suspension systems must ultimately work in unison. The CP08 front suspension has a lot of unique attributes due to the constraints that drove the solid rear axle design.

With a solid rear axle it is necessary to unload the inside rear wheel while cornering, such as in a go-kart. In order to accomplish such a feat, karts have very high caster angles. Caster is the angle between the upper ball joint and the lower ball joint when looking at the side view of the wheel and upright. Caster angles for racing karts typically range around 20-25°, which is quite large in comparison to a typical FSAE car, which runs anywhere from 4-8° of caster.

Since more caster causes the wheel to rise and fall with steering, steering will give rise to roll, which will cause a diagonal weight shift from the inside front tire to the outside rear tire. This is how solid rear axle vehicles unload the inside tire while cornering. Diagonal weight transfer is also determined by other factors, such as spring rates and kingpin angle, but these contributions are considerably smaller than the contribution of caster angle.

The 2008 FSAE car was measured and currently has a caster angle of 9°. This is on the high side of FSAE cars, but not as bad as expected. The main advantage of an independent rear suspension, however, is to keep the weight as evenly distributed on the four tires as possible, leading to more

efficient tire performance and higher lateral force coefficients. If we leave the high caster angle on the CP08 car then it will induce excess jacking of the inside rear tire, which is not beneficial to our cause.

There are many options at our disposal in order to solve the front caster problem, all requiring different amounts of effort in both design and manufacturing. Since the front suspension is already built, it would be extremely convenient to recycle as many of the parts as possible, cutting down on the labor and time needed before the car is test ready. Solutions were thus aimed at changing as few parts as possible.

The front upright is a complex aluminum CNC machined part. However, the tabs on the upright that house the upper and lower ball joint, along with the spherical bearing, are removable and held to the upright by two bolts. Re-machining these aluminum tabs to change the caster and kingpin angle

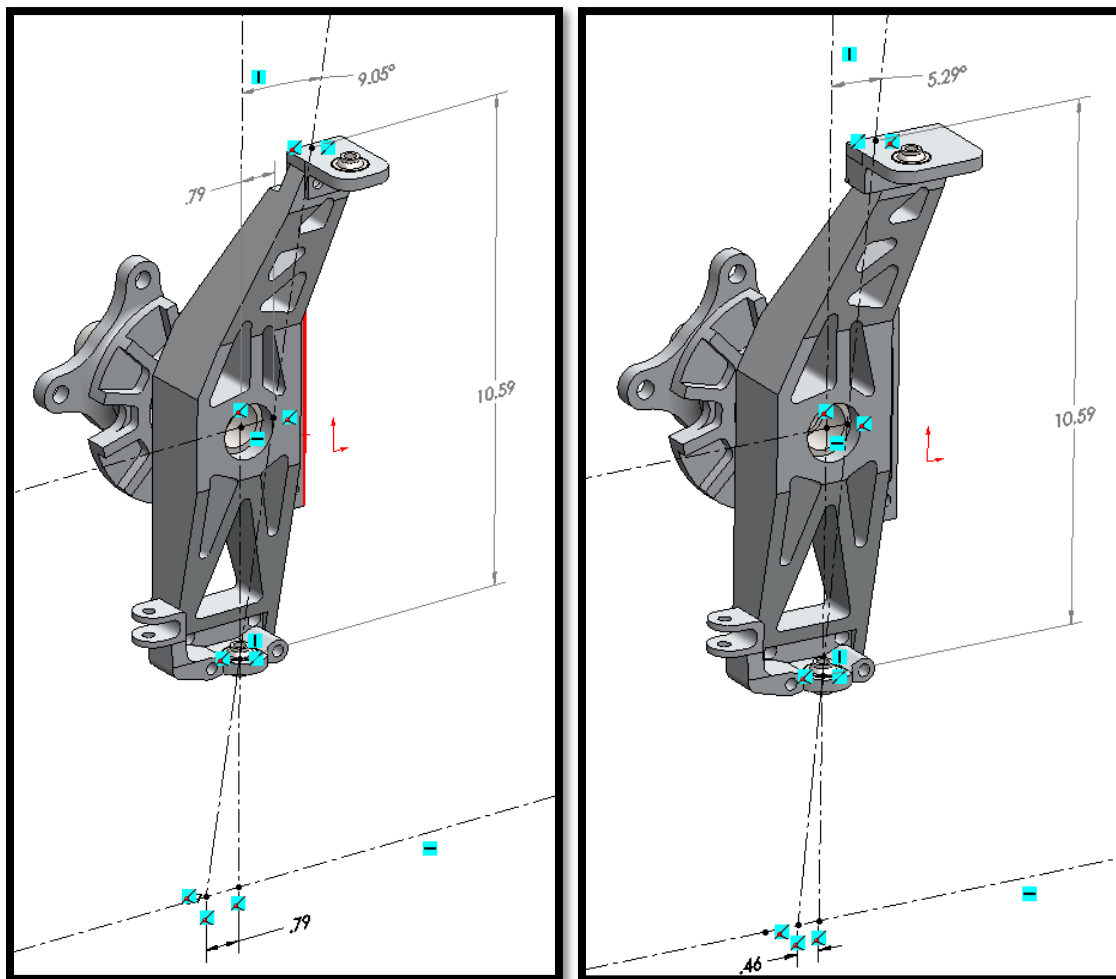


Figure 4.8. Solid models of current front caster and mechanical trail (left) and suggested changes (right).



would be much faster, easier, and cheaper than re-machining an entire upright. As for the other components, only new upper A-Arms will need to be made, which are relatively simple to fabricate.

The decision was made to re-manufacture the upper ball joint tab only, moving it forward with respect to the centerline 0.75in and changing the caster angle from 9° to 5.3° . The downside of changing just the upper ball joint tab, however, lies in the mechanical trail. This change would decrease the mechanical trail from 0.79in to 0.46in. Mechanical trail is what gives rise to the aligning moment around the tire. The aligning moment is the lateral force multiplied by the combination of mechanical and pneumatic trail where, typically, the pneumatic trail is much smaller than the mechanical. This is to ensure a consistent steering wheel feedback to the driver. The aligning moment is directly proportional to the amount of force the driver must provide at the steering wheel. High amounts of trail and consequently high forces through the wheel may give rise to a fatiguing driver, while too low an amount of trail may not give the driver enough feedback while cornering.

Although the mechanical trail will be decreased slightly by our manipulation, we anticipate that the car will still respond reasonably to the driver. During testing we expect to run both the old caster angle, along with the new one to determine if the diagonal weight jacking is even a problem. This information can be used in the future since caster angle affects many other aspects besides this diagonal weight transfer effect.

Rear Frame Adaptation

With the rear frame concept design chosen, optimization began on its individual members. Using the maximum suspension loads from our Matlab program and FEA software, each tube's relative size was considered and changed. Optimizing members lightened the structure where stiffness is not needed and stiffened the structure where it was found to be the weakest. The tubes that make the trapezoid with the engine mounts are all design to be .065" thick to reduce node deflection. Other members were found to be sufficient at a thickness of .035" thick. After an initial FEA it was found that the two members that mounted to the existing main roll hoop would not be needed, and were removed for a weight savings of 2.5 lbs. Additional members were then added from the original concept in order to support the differential and rocker loads. The final weight was calculated to be 15.06lbs, which is about 5.5lbs less than the original concept.

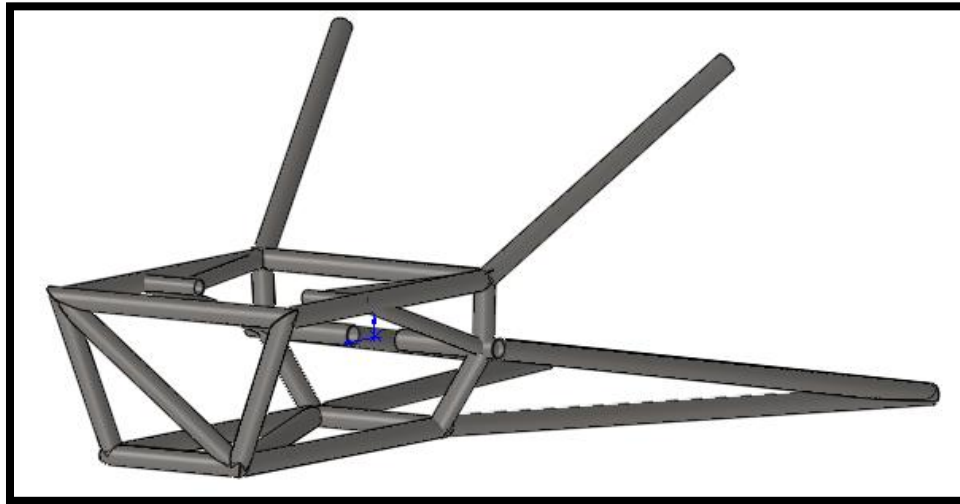


Figure 4.9: Final rear frame design

The strength and stiffness properties of the frame can be seen in the following figures and table. The worst case loads were found at each suspension point and used to perform the strength and stiffness calculations within FEA. Within the FE analysis the engine was assumed to be much stiffer than the frame itself, based on the thickness of the motor mounts. Deflection is biggest at the back bottom nodes at 0.015". This is not surprising considering that the lower A-Arms are the most heavily loaded. This analysis was conducted without a 3G bump load. If such a load is seen we are confident that the steel will not yield; however deflection will be much greater. Since such a load is so rare, we designed for stiffness assuming it will not happen during a racing situation.

Table 4.4: FEA Frame Performance Estimate.

FEA Frame Performance Estimate		
	Maximum Displacement	Maximum Stress
Frame	0.015 inch	12000 psi
Allowable	0.02 inch	52200 psi
S.F.	1.37	4.0

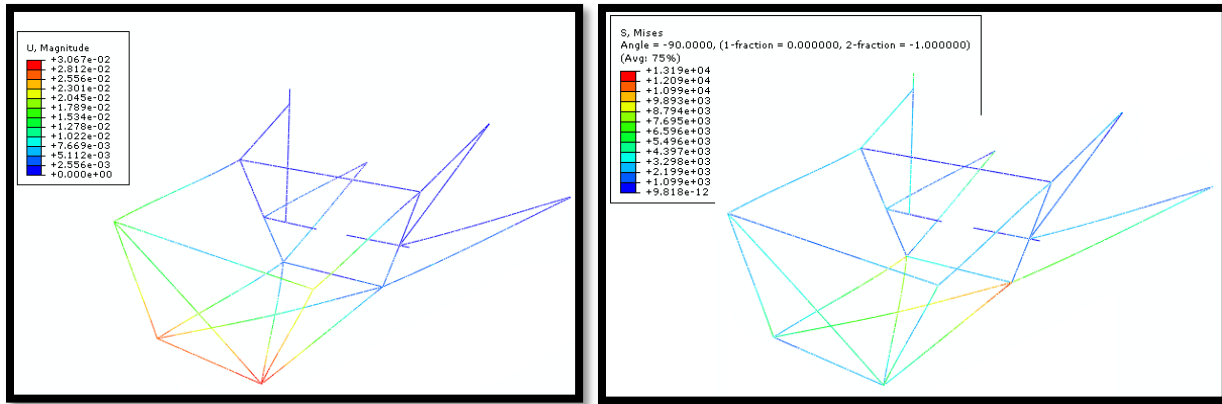


Figure 4.10: Stiffness and strength FEA results for max case loading, respectively

FEA was also used to calculate an estimate of the roll stiffness of the rear chassis. The A-Arm and upright members were modeled along with the frame and a known load was applied to one upright. The rear frame was constrained used pinned joints in all directions at each of the four nodes which would connect it existing rear space frame. Knowing this force, the deflection and the distance between the uprights, chassis roll stiffness could be found in units of lbf-ft/°. We found the rear chassis stiffness to be approximately 4200lbf-ft/°. The FEA deflection results used to calculate this are shown below.



Figure 4.11: Chassis stiffness simulation of rear frame

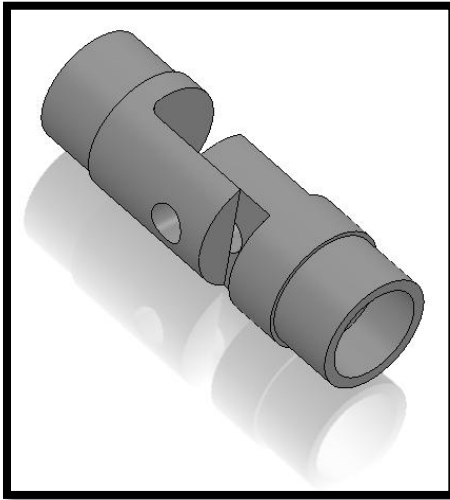


Figure 4.12: Frame Bung design

The rear frame will be attached to the existing sub frame using removable frame bungs. Similar bungs are already incorporated into the sub frame to aid in engine removability. Our new bung sets(4), however, will need to be in single shear, as shown in Figure 4.12. Though not ideal, placing the bolt in single shear is necessary for the frame to be removable due to the complex angles the tubes will be arranged in. Failure calculations were done on the joint, and it was found that bolt shear would be the cause of failure, at an axial tube member force of 3800lbs. Our FEA results show that this much force will not be seen in any of the frame members. We will be using a Grade 8 0.3125" bolt in each joint.

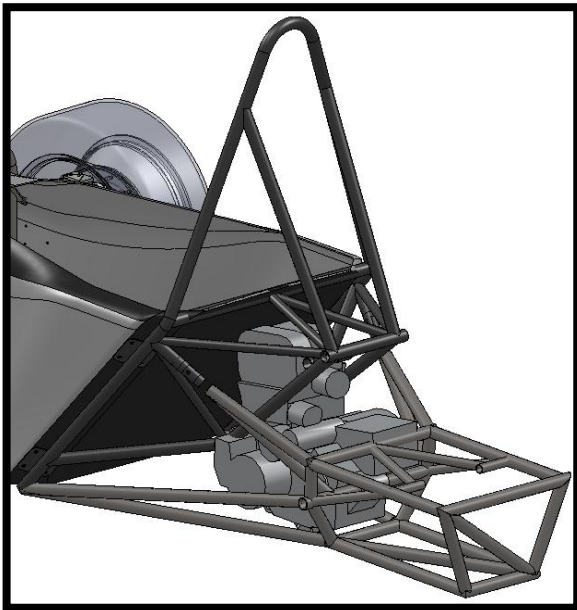


Figure 4.13 Rear Space Frame Assembly

The locations of the bungs were temporarily set at the uppermost node of the main roll hoops down tubes, and the very bottom of the down tubes. Initially we planned on reusing the frame bungs currently on the car as shown in Figure 4.13. However, we found that a lighter, stiffer frame will be possible by creating new hard points. Using the old bungs would force the tubes running to the rear box to “cheat” the node. Alternatively, the tube could be placed at the node and run off-axis to the bung, placing the tubes in bending. Both these designs could compromise the strength of the frame, and therefore new bung locations were placed to avoid these issues.

Differential Choice and Mounting

After considering the available options, Suspension Solutions selected a University Special Torsen differential. This choice provides an efficient torque transfer under a variety of conditions and supplies a torque-biasing ratio of 3.2:1. The University Special Differential is modeled off of an Audi Quattro AWD drive train and is more than strong enough to handle the torque requirements of our engine. Another factor contributing to us choosing the university special was ease of availability. Suspension Solutions was able to use an existing Torsen differential, freeing up funds for other aspects of the design.

Many Formula teams using the university special differential choose to abandon the stock housing in favor of a custom-manufactured enclosed assembly. This method is generally preferable, as the engineer is free to design the whole differential as one unit, as well as potentially removing some un-necessary weight and complexity from the assembly.

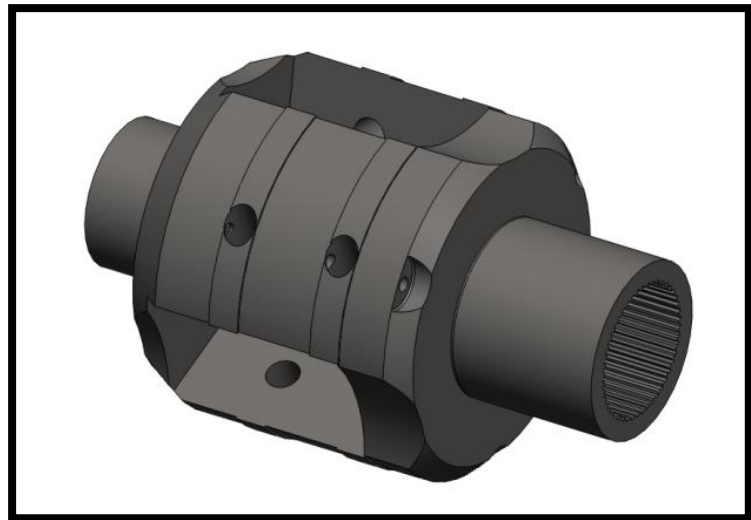


Figure 4.14: Torsen Differential

Despite these advantages, it was decided that the stock housing would

be used unaltered, as seen in Figure 4.14, due to the fact that we want to preserve the differential in its original state for use by future SAE teams. This is a design consideration because we are borrowing the differential from the Hybrid SAE team, and would like to return it to them as unaltered as possible. Effectively this means that the housing is not to be notched, ground, or bolted into unless absolutely necessary. Given this limitation, the design problem became how to effectively work around the existing differential housing without making sacrifices in weight or performance.

Differential Design Components

The first major consideration for the differential was how to effectively deliver torque from the engine. Although various methods exist for power transfer from engine to differential, the engine is currently configured to be chain-driven. In order to maintain equal final torque ratios are equal it was decided to use the same diameter 40 tooth sprocket found on the solid axle design. The final sprocket uses six ¼ inch grade 8 screws to fasten it to the sprocket differential insert. This insert will be machined

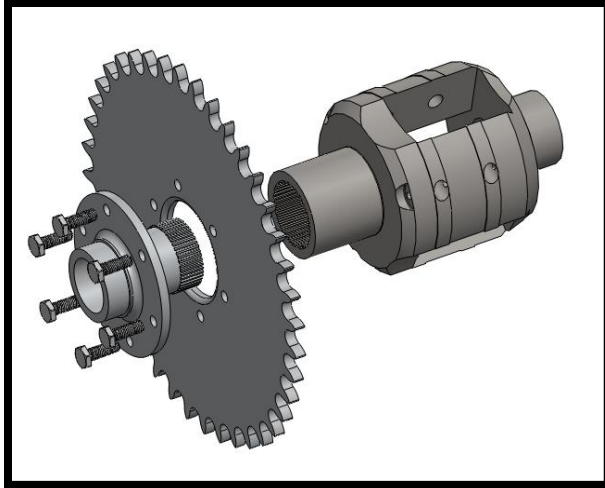


Figure 4.15: Sprocket insert with differential

out of T6 6061 aluminum because of the relative ease of manufacture. Performing stress calculations on the screws showed that this design is able to meet the stated design requirements, (See Figure 4.15). Since the purpose of the sprocket insert is to supply power to the drive train, a strong and reliable method of locking the sprocket insert to the differential body was needed. This was accomplished by using the differential housing's built-in large splined opening on one end. Using AGMA spline calculations it was determined that a splined insert with a 1/4" wall thickness would be sufficient to transmit torque from the sprocket to the differential. To ensure a secure and sealed environment this insert will have a slight press-fit tolerance of .001 inch. In addition to transferring torque to the differential, this splined insert will also provide a mounting point for two bearings, one inside the insert to isolate the drive shafts from the differential and one on the outside to mount the differential assembly to its supporting uprights. Because the inner bearing surface will only see rotation during cornering, and slow rotational speeds even then, an inexpensive and low-profile bronze bushing was used for the inner bearing. A spherical ball bearing was used for the outer surface, sized for at least 1×10^8 rotations.

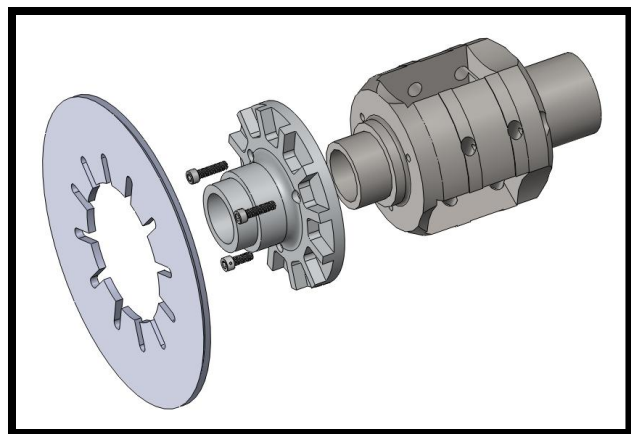


Figure 4.16: Brake Insert with Differential

Next to be designed was the opposing differential insert, whose function is to transmit the braking torque from the upright-mounted caliper to the rotor. Again we decided to use existing parts, and so the rotor being considered is the same carbon rotor used in the solid-axle setup. In order to transfer braking torque to the differential, this insert will use a combination of press-fit and (3)10-32 thread socket cap screws, shown in Figure 4.16. The corresponding screw holes in the differential are the only modifications to the Torsen housing, and were drilled because the original keyhole locking mechanism was determined to not be strong enough. The brake rotor is positively locked to the differential insert via built in splines, and inner and outer bearings support the axle stub and differential in the same way as described for the sprocket insert earlier. Spherical roller ball bearings were selected for differential support because of the lack of thrust loads.

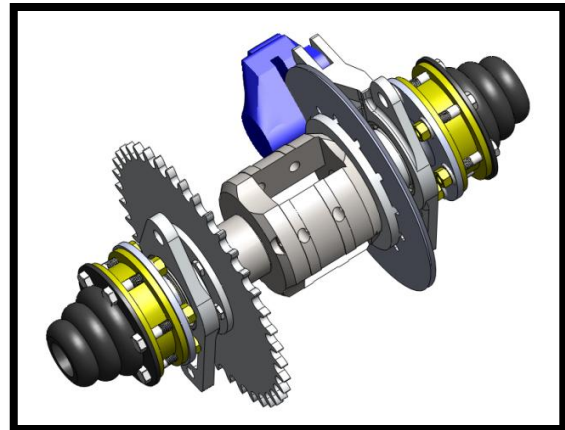


Figure 4.17: Differential Assembly

The inserts will be made of 6061-T6 aluminum stock. Early on in the life of this project it was determined that in order to maintain proper chain tension, the differential assembly would need to be adjustable, with between ½-1" longitudinal travel. In order to meet this requirement, as well as keep the whole differential assembly straight and true, the differential, inserts, sprocket, rotor, and caliper will all be mounted onto two 6061 aluminum uprights, shown in Figure 4.17. The whole differential assembly will pivot on the lower mounting hole, and will be accurately adjusted via turnbuckles mounted to the frame. This method allows for approximately ¾ inch maximum longitudinal travel. Lateral adjustment will be controlled by shims between the differential upright and the upright mounting brackets. This will allow for up to ¼ inch adjustment side-to-side, which given careful initial alignment and good build quality, should be sufficient. As mentioned above,

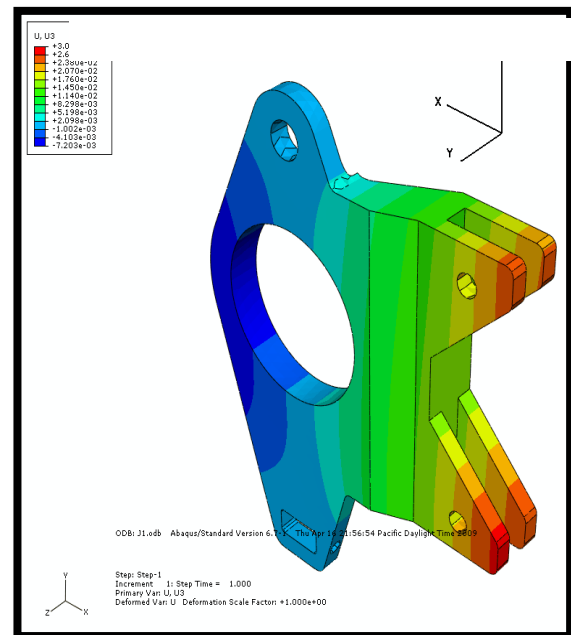


Figure 4.18: Deflection distribution of Upright

the brake caliper will be mounted directly on to the differential upright. The caliper is a Brembo-P32F opposing piston design and was selected because of it's availability and general suitability. The uprights are designed with an outside step to hold the differential bearings securely in line. One potential concern is the large moment applied by the caliper upright (Figures 4.18 and 4.19). An estimated 900 lbf-in braking moment was assumed for the rear inboard brake which is approximately 30% of the front braking torque (300lbf-in). To accurately identify the stress and deflection results of the complex shape, FE analysis was done which transferred the brake loading to the mounting points. Due to unknown factors in loading the analysis was done using a 1.5 safety factor on the reaction loads located where the caliper mounts to the upright. Maximum stress resulting in the upright, shown in Table 4.5 is within the yielding limits of the material used (Al 6061).

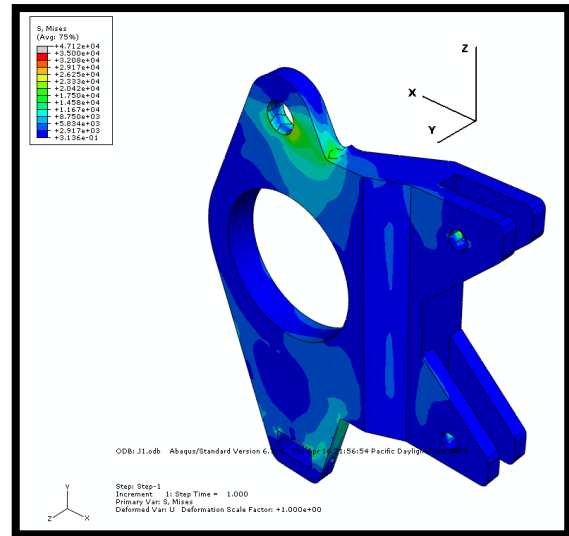


Figure 4.19: Von Mises stress in upright

When completely assembled, the differential assembly weighs approximately nine pounds. This weight is not entirely accurate as it does not include the weight of the differential gearing or the brake caliper mounting hardware. Taking these factors into account will put the total weight at around 12 pounds, which is in line with our expectations.

Table 4.5: Upright Results (S.F. 1.5)

Max Mises	24.4	ksi
Max Deflection	0.0282	in

The final component to the differential assembly is a housing cover. Because the stock housing is an open differential design, the bevel gearing is directly exposed to the outside elements, leaving it vulnerable to all kinds of environmental hazards, from rocks to mud to dust. The rotation of the differential would also tend to fling any lubricating grease out of the assembly, leading to premature wear and poor performance. For these reasons, Suspension Solutions has decided to manufacture a clamshell-style cover to snap onto the existing housing. This housing will be made out of either sheet metal or carbon fiber, depending on availability of materials at manufacture date. Because it is a totally non-structural part, almost any gauge of material will work, so we will attempt to make the clamshell

assembly as thin as possible. To prevent oil leakage and completely seal the differential housing from outside elements, a rubber gasket will be added around all edges.

Following the design plan outlined above, the differential assembly will be manufactured at a total material cost of under \$150, and with only minimal alterations to the differential housing. The differential's built-in outer splines will be used to transmit torque from the sprocket to the housing, and braking torque will be transmitted to the housing via a press-fit and bolts. Bearings will be cylindrical roller bearings, and differential inserts will be made from 1020 steel or 6061 aluminum. This design is sized for a minimum life of 2000 hours, with the aluminum brake rotor insert the driving part for design life.

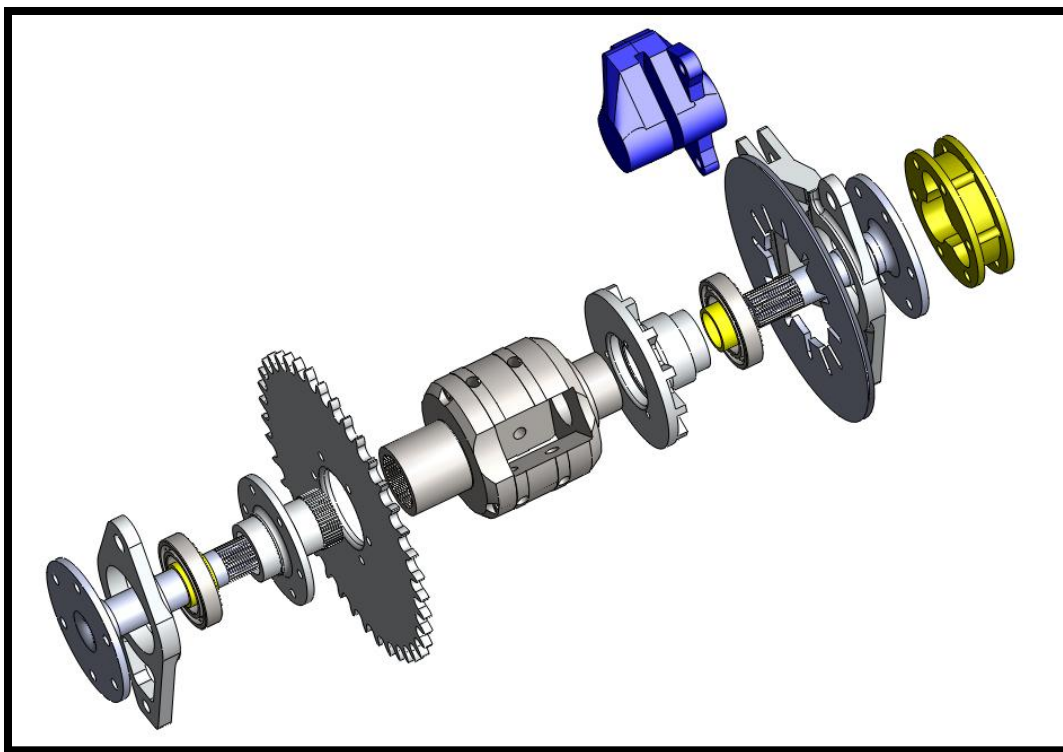


Figure 4.20: Exploded Differential Assembly



CV Joints, Half Shafts, Splines, and Axles

The objective of this project was to analyze and properly size various elements of an independent suspension Formula SAE car. A breakdown of typical formula power-transmission systems yielded five major components that would need to be designed in order to achieve a workable system. These components are as follows:

1. Inboard Axle Stub Splines
2. Halfshaft Splines
3. Halfshaft Fatigue Sizing
4. Spindle Fatigue Design and Sizing

Chromoly and 4130 steel members were sized for infinite life and aluminum parts for 1000 hours of service. All bearings in our design are rated for a minimum of 1000 hours as well. Following is a short description of each design process as well as the final design dimensions and safety factors.

Spline Analysis

The loading on a spline is typically pure torsion, either steady or fluctuating. Although it is possible for bending moments to be superposed, the spline analysis performed assumes that the bending loads are minimized due to proper bearing placement. Splines and half shafts were designed to transmit the maximum allowable torque needed to overcome the longitudinal friction force generated by the tires. This was computed knowing the frictional coefficient of the tire ($\mu=1.4$). A static calculation shows that the maximum torque transmitted to the wheels cannot exceed 233.3 ft lb_f for stable conditions to be obtained. Although the power supplied to the differential from the transmission can reach levels of 466.5 ft lb_f, this much torque cannot be contained due to the frictional properties of the tires and will cause unstable conditions. Due to internal splines already manufactured into the differential and tripod bearings, multiple analyses were done to verify components reliability. According to Norton there are two possible failure modes possible bearing and shear, with shear usually being the limiting mode. The shear stress calculated for the splines uses the SAE assumption that only 25% of the teeth are in contact due to inaccuracies in spacing and tooth form. For a more detailed analysis of spline calculations refer to Appendix C.

The result of our spline analysis is presented in the following tables:



Table 4.6 Spline analysis results of differential splines using equations provided by Norton

Spline Analysis – Differential (28 Splines)		
Material - 4130 Q&T @ 425°C		
Major Diameter	$d_o(in)$	0.919
Pitch Diameter	$d_p(in)$	0.875
Minor Diameter	$d_R(in)$	0.852
Inner Diameter (Hollow)	$d_i(in)$	0.0
Approximate Length	$l (in)$	0.808
Shaft Torque	$T (lb ft)$	467.6
Shear Stress	$\tau (psi)$	46210.9
Yeild Strength	$S_y(psi)$	173000
Safety Factor	SF	3.74

Table 4.7 Spline analysis results of half shaft splines using equations provided by Norton

Spline Analysis - Half Shaft (30Splines)		
Material - 4130 Q&T @ 425°C		
Major Diameter	$d_o(in)$	0.975
Pitch Diameter	$d_p(in)$	0.9465
Minor Diameter	$d_R(in)$	0.918
Inner Diameter (Hollow)	$d_i(in)$	0.5
Approximate Length	$l (in)$	0.864
Shaft Torque	$T (lb ft)$	467.6
Shear Stress	$\tau (psi)$	36943.3
Yeild Strength	$S_y(psi)$	173000
Safety Factor	SF	4.68



Half Shaft Fatigue

Half shaft sizing needs to be determined due to the abnormal amount of braking and accelerating during an endurance test. For our purposes a simplified model assumed a maximum accelerating torque of 2800 in-lb_f and a maximum braking torque of 2800 in-lb_f. This is the maximum torque required to overcome the frictional properties induced by the tires. The material used for this application is 4130 Q&T steel at 425°C with an ultimate strength of 236 Ksi. The cyclic loading induces fatigue loading, and modifying factors were used to find the modified endurance limit of the material.

Table 4.8 Endurance limit modifying factors

Modifying Factors	
ka Surface Factor	0.6522
kb Size Factor	0.9777
kc Loading Factor (Mises)	1
kd Temperature Factor	1
ke Reliability (99%)	0.814
Notch Sensitivity q	1.72

A surface factor was applied to the endurance limit assuming a machined cold drawn process. The size factor assumed an outer shaft diameter of 1 inch with a ¼ inch wall thickness. The loading factor was adjusted to a value of one due to the equivalent Mises stress applied to the alternating torsional stress. The temperature factor was adjusted to 1 due to the location of the half shafts and the surrounding conditions. The half shafts are located in ambient conditions and encounter high heat transfer rates due to the forced convective properties applied during a dynamic test of the vehicle. For this reason the assumption that the half shaft does not heat up is a valid one. A notch sensitivity factor was used as a result of the torsional effects on the spline.

The endurance limit was found using Equation [1].

$$S_e = k_a k_b k_c k_d k_e S_e' \quad \text{Equation [1]}$$

The safety factor of the shaft was found using Equation [2], the Goodman failure criteria.

$$S.F. = \frac{1}{\frac{\sigma_m}{S_e} + \frac{\sigma_a}{S_{ut}}} \quad \text{Equation [2]}$$



Table 4.9 Torsional Stress Values

Stress Values		
T_m	0	in lb_f
T_a	± 2800	in lb_f
τ_a	27.2	Ksi
σ_{ea} (Mises)	47.1	Ksi
S_e	51.9	Ksi
S_{ut}	236	Ksi
S.F.	1.1	

Due to the over-conservative estimate of the alternating torque being applied to the half shafts for infinite life, the safety factor and sizing the shaft resulting from fatigue analysis is an acceptable one. Using 4130 steel 1 inch OD $\frac{1}{4}$ inch wall thickness stock tubing to manufacture the half shafts will be able to withstand the maximum torsional loading of 2800 in lb_f during its intended use. A conservative model was chosen purposely due to the unknown loading conditions which act on half shafts.

Spindle Fatigue Sizing

Unlike half shafts, spindles are responsible for carrying the weight of the vehicle and thus are subjected to bending as well as torsional loading. To acquire the spindle moment, the tire patch forces were translated to the spindle, and two constant resulting moments were calculated, M_x and M_y . These were then added to the spindle cut FBD, and summing the moments in three planes about a generic cut gave the moment on the spindle. The following geometric dimensions were used:

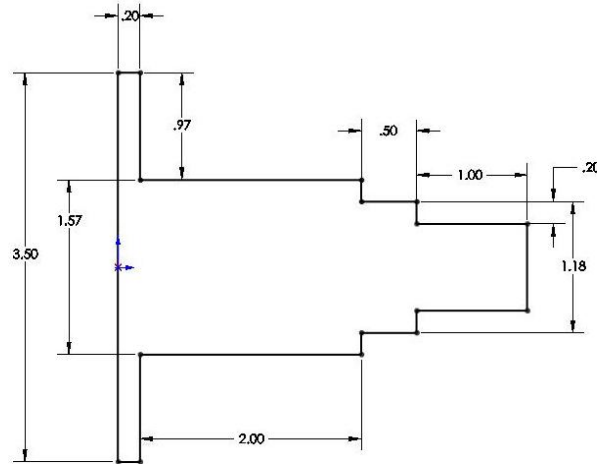


Figure 4.21: spindle geometric dimensions

The tire patch forces were calculated from a weight-transfer spreadsheet using six different loading conditions and then added up using the linear damage rule:

$$F_{eq} = \left[\frac{\sum_{i=1}^6 F_i^a l_i}{\sum_{i=1}^6 l_i} \right]^{1/a} \quad \text{Equation [3]}$$

Here an application factor of $a=2$ was used, signifying moderate impact operation. After evaluating the moment at the step and bearings, we decided that the shaft was critical at the step because of the added local stress concentrations. We originally planned to use 6061 aluminum sized for 1000 hours of life, but after consulting Mil-Handbook 5, we concluded that the shaft would need to be at least 45mm in diameter, which proved impractical. We therefore decided to use a 4130 chromoly hollow spindle, sized to infinite life. The results of these design parameters are as follows:

Table 4.10 Spindle sizing properties

Outer Diameter, D	1.57"
Outer Step Diameter, D_{step}	1.18"
Inner Diameter, d	0.79"
Modulus, E	30,000 ksi
Ultimate Strength	236 ksi
Yield Strength	212 ksi
Factor of Safety	2.15

Uprights

As mentioned before, the uprights were designed with worst-case scenario forces in mind. To achieve this we looked at forces on the outside rear corner of the car under 1G of longitudinal acceleration, 1.5 Gs of lateral acceleration, and 3Gs of vertical acceleration for the worst-case scenario of a sudden bump. The table below lists the resulting pick up point forces, calculated using a Matlab program and used in the FE analysis.

After some minor adjustment, the upright passed FE analysis, but the initial results were quite unexpected. The design failed at the lower tab of edge B, pictured in Figure 4.24. It was the result of a sharp corner causing a large stress concentration, resulting in local stresses upwards of 55,000 psi, well above the 35,000 psi yield strength of aluminum. This problem was solved by increasing the cross sectional area in that region slightly and creating a ½ inch fillet in place of the sharp edge.

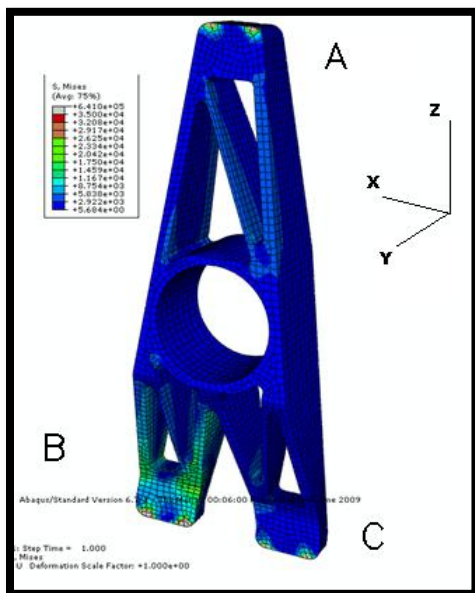


Figure 4.22: Final Upright FEA

The resulting local stress never exceeded 23,000 psi, and the design passed with a factor of safety of 1.5 at a weight of 1.74 lb per upright. This weight can be further reduced by making some adjustments to the dimensions above the bearing ring; for example, changing the upper legs from ¼ to 1/8 inch wide. Component weight could further be reduced by constructing the upright out of stronger, but much more expensive, 7075 aluminum.

Table 4.11: reaction forces on the upright

Point	Force X [lbf]	Force Y [lbf]	Force Z [lbf]
A	+220	+302	-41
B	+162	-290	+13.3
C	+361	-408	+700

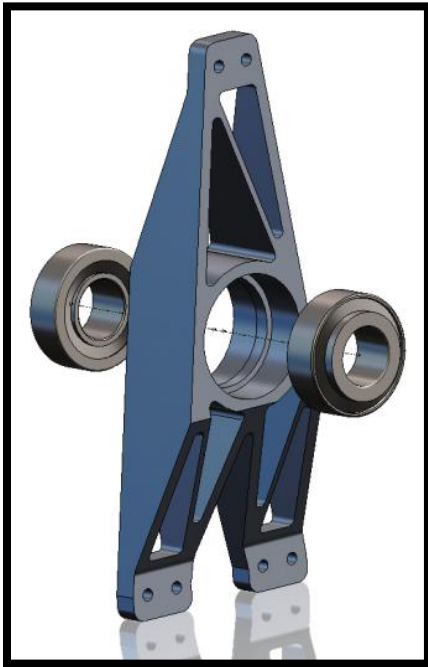


Figure 4.23: Exploded Upright View

Many of the critical dimensions of the upright stemmed from the given bearing dimensions. The bearings were sized using a Timken bearing life calculation, with a maximum life of 1000 hours and a spindle diameter of 30mm. The spherical bearings used to connect the A-Arms to the uprights will do so by means of pick up tabs, simple C channel devices that will be held to the upright with ¼ inch bolts. These are still in the design phase but will be constructed from 4130 steel. Such a setup allows for simple adjustment of camber angle by adding successive shims between the pickup tabs and upright, a desirable feature which will allow for greater suspension tune-ability. The Bearings to be used are tapered roller bearings, Timken #M86610 and #M86649. They were sized for infinite life and lightweight. Tapered Roller bearings were chosen do to their ability to take axial loads. And general removability.

Cost Analysis

Current cost analysis is based on recent component design. Pricing tables will fluctuate throughout the design process and will be documented and updated on the teams interactive spreadsheet. Total estimated pricing came to about **\$3670.15**, which is within our budget. This does not include an estimate for hardware or a large fluctuation in vendor pricing.

Table 4.12: Cost analysis of major components

Suspension				
Part No.	Components	Quantity	Description	Cost
08S0241-SS	Upper a-arm fore tube	2	4130 3/8x.035	\$6.00
08S0242-SS	Upper a-arm aft tube	2	4130 3/8 x.035	\$6.00
08S0243-SS	Tie rod tube	2	4130 7/16x.035(30inch)	\$11.00
08S0244-SS	Lower a-arm fore tube	2	4130 1/2x.035 (86)	\$11.00
08S0245-SS	Lower a-arm aft tube	2	4130 1/2x.035	\$11.00
08S0246-SS	Push Rod Tube	2	4130 1/2x.035	\$11.00
08S0604-SS	Shocks	4	Fox DHX 5.0	\$399.00
08S0647-SS	Space Frame Adaption	1	4130 .87" x .065"wall x 6'	\$30.80



DriveTrain				
Part No.	Components	Quantity	Description	Cost
08D0101-SS	Differential	1	Torsen University Special	\$415.00
08D0102-SS	Sprocket attachment	1	6061 2" OD 12" wide	\$17.84
08D0103-SS	Brake Hub attachment	1	4.5" OD 3" wide	\$30.40
08D0104-SS	Differential Support Right	1	4140 multipurpose	\$40.33
08D0105-SS	Differential Support Left	1	4140 multipurpose	\$40.33
08D0106-SS	Sprocket	1	chain # ANSI 35	\$13.15
08D0108-SS	Mounting Bracket Right	1	6061 Al 12"x3"x.5"	\$13.18
08D0109-SS	Mounting Bracket Left	1	6061 Al 12"x3"x.5"	\$13.18
08D0201-SS	TriPod Bearing	4	Tripod Joint 22-Spline RT40/41	\$62.99
08D0202-SS	TriPod Bearing Housing	4	Tripod Joint Housing 94mm dia, 26mm thick	\$182.99
08D0203-SS	Half Shaft Right	1	4130 Unpolished; 1"OD 1/4"wall x 6'	\$86.33
08D0204-SS	Half Shaft Left	1	Included in Half Shaft Right Cost	
08D0205-SS	Rotor Side Inner Shaft Bearing	1	2"OD 1"IDx9/16" Doubley sealed ball bearing	\$18.38
08D0206-SS	Rotor Side External Bearing	1	2.5"OD 1.25"ID x 5/16" Doubley sealed ball bearing	\$25.87
08D0207-SS	Sprocket Side External Bearing	1	2.5"OD 1.25"ID x 5/16" Doubley sealed ball bearing	\$25.87
08D0208-SS	Sprocket Side Inner Shaft Bearing	1	2" OD 1" ID x 1/2" ABEC 1 Doubley sealed ball bearing	\$10.92

Upright				
Part No.	Components	Quantity	Description	Cost
08U0101-SS	Rear Upright Right	1	6061 12"x6"x2"	\$78.03
08U0102-SS	Rear Upright Left	1	6061 12"x6"x2"	\$78.03
08U0201-SS	Rear Spindle	1	12" x 4" x 1.25" 4140	\$76.92
08U1AS2-SS	Upright Bearings	4	30mm Id x 6r mm OD Tapered Roller Bearing	\$14.95

Total Cost

\$3700.10



Manufacturing Plan

Most components will be manufactured in house by students to cut down on labor costs. Many drivetrain components include splines and will therefore need to be outsourced due to their complexity. Several local sources have been contacted for these jobs, such as Helical in Santa Maria. For ease of manufacturability, most large components will be made out of 6061aluminum, which can be easily machined. Components such as the rear spindles needed a material with higher strength properties to accommodate the relatively large load levels, and small shaft diameter dictated by the upright bearings. The stock 4130 tubing priced out for the half shafts are slightly larger than what the required design calls for. The decision to price out the larger diameter gave us flexibility to turn down the sides to a smaller corresponding wall thickness. Flanges will need to be welded onto the differential axle stub to support mounting locations for the tripod bearing housing.

A-Arms, tie rods, and push rods will use stock tubing which will be notched to fit bearing wafers (Part # 08S247-SS). The 4130 steel bearing wafers will be manufactured in house using a CNC mill and an existing wafer jig. Spherical bearings will be ordered from Coast Fabrication (Part # HAB-4TG), and will be pressed into the wafers and secured using a staking tool. Simple tabs will be ordered to save time, while complex tabs such as the push rod mounting tab (Part # 08S0250-SS) will be cut and welded in the hangar. The rear rocker assembly will include sheet metal, which will be cut and grinded to shape. The space frame adaption will be one of the more complicated manufacturing jobs of the project. A network of multiple tubes will have to be notched and welded to one another. This will require the care of a carefully designed jig and a professional welder.

The rear frame is going to have to be very carefully jigged and notched. With multiple nodes having more than three members joined at them, notching will become very difficult unless properly mapped out to the manufacturer and welder. The extra time taken to properly measure and notch tubes will produce a stronger frame that is easier to weld. TIG welding will be used to weld the frame; tubes will be 4130 normalized steel and ordered from Aircraft Spruce.

The complexity of the upright will require the accurate manufacturing ability of a CNC. Upper and lower A-Arms, tie rods, and push rod tabs will be bolted onto the upright. The tapered roller bearing will be press fit inside the upright.



Chapter 5: Manufacturing Process

Suspension:

A-Arms

One of the unique aspects of this project's A-Arms were the bearing wafer designs. During the design phase it was determined that using wafers instead of bearing cups would produce a better quality part, though it did produce some manufacturing challenges. The wafers required a special tooling jig to hold the part during machining; fortunately, this jig was already constructed and used for production by the Formula Hybrid team. The jig (shown in the background of Figure 5.1) held the wafer blanks (seen



Figure 5.1: A-Arm wafer jig, blanks, and finished single wafers

in the back right of the figure) during the CNC machining operation to produce the completed wafers. The blanks themselves were prepared manually from $\frac{1}{4}$ " thick 4130 steel, with the center hole drilled and reamed to the proper size for the spherical bearings. With the only critical dimension being the distance of the hole from the edge (ensuring a tight fit in the jig), these blanks were quick to manufacture on a properly set up mill.

The CNC machining was done after coding in CamWorks was completed. Since these parts had been produced before by Formula Hybrid, only minor changes had to be made to the code to adapt to this project's suspension geometry. Machining of the wafers was done with $\frac{1}{4}$ " carbide endmills, and took approximately six minutes per single wafer and 15 for each outboard double wafer.



Figure 5.2: Notched A-Arm tubing

The A-Arm tubing was cut to length on the chop saw, and then sent to the mill to be notched. Notching involved one pass per side with a $\frac{1}{4}$ " endmill to produce the slots shown in Figure 5.2 at left. When the tube was flipped for notching on the second side, a $\frac{1}{4}$ " plate was inserted into the first notch. A digital angle finder was secured to the plate and was used to ensure that the slots were in plane with each other.

With the wafers and tubes complete the A-Arms could be mounted on the jig plate. The jig was created from 3/16" steel with all A-Arm points located, drilled and tapped for 1/4" bolts. Spacers were cut on a lathe to fit inside the bearing holes on the wafers while mounting to the jig plate. Prior to placing on the jig, all tubes and wafers were cleaned on the wire wheel around the welding area to remove any contaminants. Once assembled on the jig the A-Arms were tack welded in two places at both ends of each tube, final TIG welded on one side, flipped on the jig, and welded on the other side.

The lower A-Arms also required the addition of a gusset for mounting the pushrod tabs. This piece was made from 0.060" steel and was cut so it would rest tangent to the top tubes. After being welded in place, the A-Arm was mocked up to get the proper location for the push rod tabs. These tabs were then bolted onto a rod end and welded on to the A-Arms. Similarly, tie rod tabs were created and aligned so that the tie rod acted in line with the nodes at the upright and chassis.

Rockers

The rocker assembly consisted of three main parts that needed to be manufactured. The first parts manufactured were the main rocker plates. These plates (4) were plasma cut out of 0.060" thick 4130 steel plate stock. The drawing shown in Appendix F was traced by the plasma cutter in order to cut the rocker plate to its proper shape. With excess slag removed, the rocker plates were then stacked together and tack welded to for an easier drilling process. The bolt holes for pushrods and shocks were done on a simple drill press, while the hole for the bearing insert cup was done on a mill. This bigger hole required a 1" drill which proved to be too much load for the smaller clamps of the drill press. Using the mill was much more stable and produced a clean finish. With all the drilling done on the plates the tack welds holding them together was ground off, and the parts were prepared for welding.

The next parts manufactured were the rocker bearing insert cups (4). These parts were created from 1" x .125" 4130 steel tube stock. The bearing cups were cut to length and then welded to the previously drilled out hole in the bearing rocker plates. Since boring for the rocker bearing was done after the welding process,



Figure 5.3: Rockers after welding of bearing cups

no special jig was used. Figure 5.3 shows the rockers after the TIG welding of the two parts. Once the

parts had cooled down from welding they were chucked up on the CNC lathe to bore out the proper diameter for the rocker bearing. The bore was cut to allow for a bearing press fit of 0.001". Once this process was complete, the bearings were easily pressed into the rockers using the hydraulic press.

The third main component was the rocker posts(2) which the bearings pivot on and connect the rockers to the frame. These were turned down from 1" 4130 steel bar stock using the CNC lathe. A perfect slip fit was needed to allow easily removability of the parts, while also making sure the inner race would not spin on the post. Figure 5.4 shows a rocker post bearing surface being turned down. With the bearing surface slip fit done, the rocker was drilled and tapped for a ¼"-28 bolt. This bolt would apply axial force to the bearing races, keeping the rockers in place. Next the rocker post were flipped on the lathe and the back end was bored out and then notched on the tube notcher to allow for clean, easy welding to the rear frame.

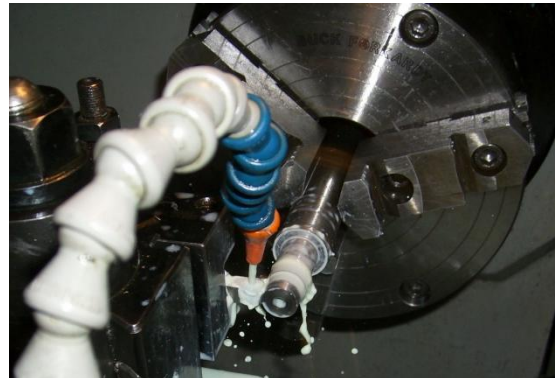


Figure 5.4: Rocker bearing post being machined



Figure 5.5: Final Rocker Location.

The suspension was then mocked up to find the final placement of the rocker post. It was then tacked in place and then fully TIG welded. Figure 5.5 shows the final rocker location.

Push-rod's/Tie-rods:

Carbon pushrods were originally designed for the car, but due to the uncertainty of carbon properties, they needed to be tested for buckling before being used on the car. 0.5" diameter carbon tubes were laid up manually around an aluminum mandrel, with a $[0^{\circ}_2/90^{\circ}]_{sym}$ laminate of unidirectional AS04carbon. Tapped inserts were machined out of 4130 steel and bonded to both ends of the finished rods. The carbon pushrods meet or exceeded expected failure loads for buckling but the manufacturing difficulty led us to build steel parts for the final assembly. A more complete description of the carbon rod manufacturing and testing is in another report which has been handed down to the current FSAE

team members. The '08 solid rear axle push rods became our new tie-rods to speed up manufacturing of other parts.

Chassis

Manufacturing of the chassis began with the construction of some basic jigs to properly locate the tubes. The rear frame was constructed in several stages; first, the upper and lower rectangles were made, then connected to each other, and finally connected to the existing frame. For the upper and lower rectangles, angle iron was welded to the frame table to restrain the tubes to the dimensions specified during design. Tubes were mitered at 45° and carefully cut down until they could fit inside the jig with minimal gaps. In the design for the lower rectangle, a cross piece was used to triangulate the base. This tube required a more complex notching and made use of the PipeMaster, a tool used to



Figure 5.6: Rear box aligned with the existing frame and engine

fishmouth the tubes for welding. The almost completed rear section was next aligned with the connection points on the engine, as shown in Figure 5.6. This stage in the fabrication was very critical,



Figure 5.7: Single shear chassis bungs for upper frame mounts

indicate the shape required for fitting tubes. After careful notching, the tubes were tacked in several places at each corner and then TIG welded while still in the jig.

With the upper and lower rectangles complete, a temporary notched tube welded to the table was used as a jig to space the upper and lower rectangles vertically. At this point the back trapezoid was created to connect the two parts, again using the PipeMaster and tubing notcher to properly

fishmouth the tubes for welding. The almost completed rear section was next aligned with the connection points on the engine, as shown in Figure 5.6. This stage in the fabrication was very critical, and extra steps were taken to ensure that the frame was level, centered and at the proper height for our suspension design. The down tubes on the engine side were then cut, notched, and tacked in place while still attached to the car. At this point, the rear box was sturdy enough to remove from the car, and all joints were cleaned and finish welded.

With the rear box complete the connections could be made to the existing steel chassis. For the sake of removability these connections were all made using machined bungs as shown in Figure 5.7 at left. The bungs were machined from 4130 steel on a manual lathe and mill, and were designed to slip inside the frame tubing for welding. Two styles of connectors were made; those designed for the upper frame pickup were single side, single-shear bungs, while the lower bungs were for a double-shear mount. With the lower mount was already in place on the old chassis it was simply a matter of connecting the lower node of the rear box to the new bung bolted onto the chassis. The upper connecting tubes required new mounts on the old chassis in order to maintain pure tension-compression members; again, this was just a matter of bolting the bungs together and running tubing in a straight line between the frame and upper node on the rear box. A key factor in the design was the orientation of the bungs. The connections had to be aligned in such a way that the rear frame could be easily removed; improperly done, the new frame could be trapped in place, forcing tubes to be bent for removal. The bungs were welded onto the tubes running to the rear box, and the mating tubes and bungs were welded onto the existing frame to complete the chassis fabrication.

With the frame completely welded, the 16 “unique” suspension pick up tabs were assembled into the completed A-Arms, and lined up with their appropriate nodes on the chassis. Then they were tack welded in place, one A-arm set as a time. With all the tabs tack welded, the a-arms were removed and the tabs were fully TIG welded. A similar process was carried out for the chain guard tabs, and diff turnbuckle tabs. Figure 5.8 shows the rear frame complete assembled with all the suspension components.



Figure 5.8: Rear frame completely welded and assembled with the suspension components

Drivetrain:

The drivetrain subsystem proved to have the most complex and high precision parts needed for the project. Many parts included multiple set ups on both manual and CNC mills and lathes; some parts also requiring fourth axis splining operations. For easier manufacturability, most the drivetrain parts were machined from 6061-T6 aluminum round stock. Any highly loaded parts were sized to a fatigue life of at least 500 hours, to ensure safe testing. However, the spindles and half-shafts were manufactured from 4340 and 4130 steel respectively, due to higher expected loads.

Differential Inserts

The sprocket insert and brake Insert were machined down from the appropriate 6061 Al round stock following the drawings in Appendix F. First, the stock was turned down on the CNC lathe located at the Bonderson machine shop to match the profile for each insert. Both inserts required turning, drilling, boring, and facing operations, from both sides of the parts. Once the lathe work was completed, the parts had their bolt holes drilled using the manual mills and a rotary table at the hangar machine shop. Finally, the parts were sent to the CNC mills at Bonderson for splining. The brake spline on the brake insert was coded using CamWorks and cut with a standard ½” three flute end mill. The involute spline on the sprocket insert was splined using a fourth axis operation.

Luckily only one major problem was encountered during the entire machining process of these parts. On the sprocket Insert, the bearing surface was accidentally turned down too much resulting in a 0.080” slip fit. This of course was unacceptable, and a separate sleeve piece was needed to increase the bearing surface diameter. The sleeve was machined separately from the same material and pressed on the bad surface with a 0.002” press fit using the hydraulic press. With the parts now one, the correct bearing surface diameter was machined. the sleeve was later welded on, when it was found the press fit was not enough.



Figure 5.9: Top- drilling of Sprocket bolt holes. Middle-Bearing surface after sleeve was pressed on. Bottom- final part after splining

Differential Axle Stubs

The differential axle stubs were also started from 6061 Al round bar stock, and consisted of three processes for each axle stub. First the bulk of the material was turned down until the proper bushing surface diameter was reached on a CNC lathe. The full profile, including radius dimensions and spline major diameter, were then machined following the drawings in Appendix F. Next, the axle stubs had the bolt holes for the tri-pod bearing housings drilled using a manual mill and rotary table. Lastly, the parts were put on the fourth axis mill for splining.

The axle stubs were originally designed to be constructed of steel, however due to time and cost constraints they were redesigned for aluminum.



Figure 5.10: Differential axial stubs and sprocket insert completed and assembled in differential

As will be discussed later, a new set of Axles were machined out of 4340 steel following yielding of the aluminum axles after the first drive. the steel material for these parts was ordered already splinned. the steel parts were then heat treated, along with the half shafts for better hardness properties.

Differential Uprights

The two differential uprights were fully machined on a CNC mill. The process was coded and cut by shop technician Matt Ales. CamWorks was used to code the tool paths for both parts. The process included two sides of machining for each part as well as creating soft jaws for the second side processes. They were machined from 6061 Al 0.5" plate stock. Figure 5.11 shows both differential uprights, one



Figure 5.11: Left- Brake side differential upright after first side of machining. Right- Sprocket side differential upright fully machined.

after the first side of machining complete and one fully complete. The only problem encountered during the manufacturing process was when one

differential upright

got shot out of the soft jaw due to a random incorrect tool path. This unfortunate event, however, did not damage the part beyond use. Lastly, a manual milling operation was needed to face away the gap for the brake caliper on the corresponding upright. With the uprights complete the bearings could then be pressed into their respective spots.

Differential Half Shafts

The half shafts were manufactured from a long 1" O.D. by .25" thick stock pipe. Two pieces were first cut to length using a horizontal band saw. Next the ends of the 13" long parts were turned down on a manual lathe to the correct spline O.D. of 0.975". Lastly the parts were put on the fourth axis mill for their 30 tooth splining operation using a slot mill.



Figure 5.12: Spined half-shaft with tri-pod bearing

Similarly to the aluminum axle stubs, the cutter was not appropriately sized, and the teeth needed to be cut deeper than anticipated. Also after the splining operation, they required post lathe work. They needed to be turned down past the spline O.D. by up to 0.005" in order for the tripod bearings to slide on. Although the bearings fit on nice and snug, a new cutter would be ordered if these parts were to be manufactured again.

Differential Drilling

The differential was drilled with a bolt pattern to match that of the brake Insert. The operation was done on a manual mill with the rotary table and no difficulties were experienced.

Drive train Assembly

With all the parts manufactured, assembly of the drivetrain subsystem could occur. The only initial problems while assembling the subsystem were with the sprocket bolts. The bolt heads needed to be slightly faced down to avoid making contact with the differential upright. Also, shim stock was needed to ensure a good fit between the bushings and the sprocket insert.

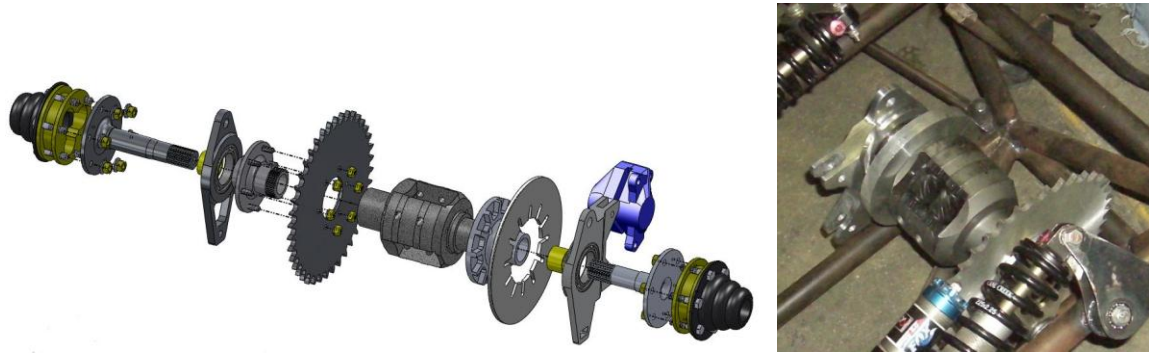


Figure 5.13: Drive train assembly

After assembly, the subsystem was placed within the rear frame. The differential tabs, which connect the uprights to the bottom frame members, were welded in place. Also, the diff turnbuckles were mocked up and welded in place.

Uprights:

Wheel Uprights

The uprights were machined from solid 6061 Aluminum blocks using a HAAS CNC mill. Eric Pulse at Bonderson helped with converting the SolidWorks model into CamWorks code for fabrication. Due to the thickness of the design, each upright had to be flipped half way through the cutting process to mill the back geometry. This was done in order to keep end mill stress at safe levels during the machining process.



Figure 5.14: Finished upright, in wheel

Once the uprights were fully machined, it was discovered that the back bearing opening on both uprights were out of tolerance by -



Figure 5.15: Upright right after machining process

.004" and had to be bored out in order to achieve the desired press fit between the bearing outer race and the upright. The uprights were chucked up on a lathe with reverse chuck jaws to remove .004" material from the rear openings. Once the press fit was down to 0.0015", the outer races were pressed using a hydraulic press. About 300psi was needed.

Upright Suspension Tabs

The upright tabs were constructed from .080" steel plate. They were cut using a plasma cutter. The top tabs were designed to accept the A-arm bearings at a slight angle, so a block of aluminum was milled to the correct tab geometry to fixture the tabs for the welding process.

For future upright CNC fabrication, it would be beneficial to put more consideration into how complex of a fixture will be required so that it is easier to remain within specified tolerance. Also, it was found through trial and error that quenching the tabs in water after the plasma process resulted in hardening the slag, making it much more difficult to grind off. From that point on, all plasma cut items were air cooled prior to grinding.

Spindles

The spindles(2) for the wheel uprights required many manufacturing processes. They started as 4" round stock of 4340 steel. This steel was chosen over the designed steel of 4140, due to its availability in our stock size. The parts required two alternating CNC lathe and CNC mill processes. First the parts were turned down to the end of the sinusoidal spline. The rest of the part was left uncut to give room to grab the part in the mill's vice. Next, the sinusoidal spline was cut using the CNC mill and an extra long ½" four flute end mill. After the sinusoidal spline was cut, the rest of the bushing surface was turned down back on the lathe and a perfect slip fit was achieved. Then, the part was put back on the mill to machine the bearing housing bolt hole pattern. Lastly, a die was used to thread the 1"-20 thread for the center lug nut.

Cutting the thread proved to be more difficult than expected due to the ease of cross-threading. However, much care was taken and after a great deal of time chasing, tightening the die, and re-chasing, a perfect fit was achieved. Figure 5.16 shows the two spindles and castle center locking nut, one with the tread completed and one without.



Figure 5.16: Final Steel Spindles and castle nut showing thread and sinusoidal spline.

Hubs

The wheel hubs were manufactured in two phases. First, the stock 6061 Al round stock was cut to length and turned down to the right profile using a CNC Lathe. The complex profile required chamfers to be machined from both sides of the part. All dimensions were machined following the drawings in Appendix F. With the side profile complete, the part was sent to the CNC mill and the matching female sinusoidal spline and wheel bolt pattern was machined. Soft jaws were needed in order to properly secure the part in the vice. The spline was purposely cut too small on the first pass and carefully taken down to the correct size, cutting 0.002" per cycle of the program. After each cycle we would check the hub with the matching spindle spline until a perfect slip fit was achieved.

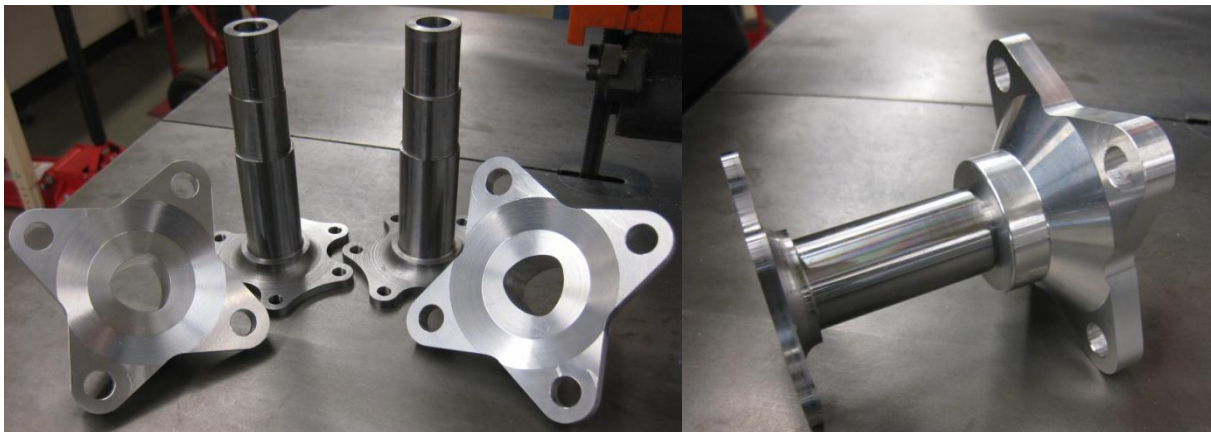


Figure 5.17. Right-Completed hubs and Spindles. Left-Spindle and hub slip fit.



Chapter 6: Design Verification



Weight Results

An important design goal decided early in our project was to limit the amount of weight added to the 2008 car. We had calculated that we could gain 35lbs and still have a cornering advantage over a solid rear axle even at a tire's highest slip angles. Thus, we set a goal of 25lbs of additional weight for our system. After all components were manufactured and assembled, we weighed our complete IRS Interchangeable assembly and compared it to the amount of weight we had removed with the solid rear axle assembly. The total weight removed was 42.6 lbs while total weight added was 64.4lbs. This led to total weight addition of 21.8lbs, surpassing our goal of 25 lbs. Table 6.1 below shows the weight of various assemblies and components.

Table 6.1: Weight of Assemblies.

		Weight (lbs)
Solid Rear Axle Components	Axle Assembly - Axle, spacers, axle nuts, wheel hubs, sprocket/brake inserts, sprocket, brake disk	(18.81)
	A-Arm Assemblies - Lower A-Arms, lower links, bearing blocks, jacking bar, push rods, rocker, brake caliper, shock	(18.55)
	Engine Arm's - Left engine arm, chain guard, right engine arm	(5.3)
IRS Assembly	IRS Assembly - Rear frame, A-Arms, rockers, shocks, differential assembly, upright assembly, half shafts, tri-pod bearings (Aluminum Differential axle stubs)	64.47
Total Weight Added:		21.81

Although we met our weight goal, looking back at certain parts, we are confident that an extra 10 lbs could have easily been saved. For example, in order to make our system interchangeable, we needed to adapt our new frame to the old frame. If designing an IRS from scratch we believe we could have combined the two separate frames and saved anywhere from 5-10 lbs in chassis alone. Also, many of our drive train components are oversized and heavy. For example, aluminum tri-pod bearing housings could have been used over steel ones. We chose steel based on cost and availability, however using aluminum could have saved us an estimated 3 lbs. Our half shafts themselves are also over designed and probably could shed a third of their weight, saving another 1 lb. If the extra weight of an IRS over a solid rear axle was down to 10 pounds or less, it would be much harder to justify the use of a solid rear axle design.

Dynamic Test Plan and Equipment

The 2008 Formula car was to be run through a rigorous set of tests to experimentally quantify the advantages of either setup. These tests were to include skid pad trials to determine maximum lateral G forces, a 75 meter straight line run to gain data on the traction and acceleration differences between the two systems due to weight transfer and weight difference, some wet pavement testing in order to observe handling responses in poor weather conditions, and a repeatable slalom/Autocross course in order to grasp transient cornering stability. Due to time limitations, we were only able to accomplish skid pad testing. We choose skid pad, since we believe we could gain the most information from this test and it is relatively easy and repeatable with the 08 car with both IRS and Solid rear Axle configurations.

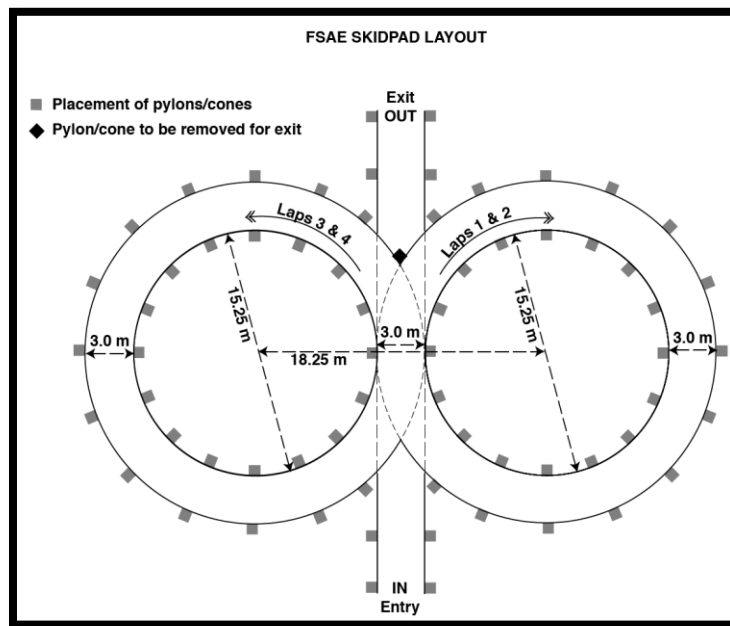


Figure 6.1: FSAE Specified Skid-Pad Course

In the design phase of the IRS setup in question, it was calculated that during steady state cornering at 1.5 G of lateral acceleration, the pushrod would be under a compressive load of 276 lbf. A second case, the worst case scenario, attained simultaneous suspension loads during 1.5 G lateral acceleration, 1 G longitudinal acceleration and a 3 G bump. This can be seen below in Table 1 whose values were calculated using the Matlab vehicle dynamic simulation.



Table 6.2: Simulated Loads in each suspension member based on 1.5 G lateral acceleration

All Loads in (lbf)		Accelerating, cornering, and bump			Steady state cornering, no bump		
		F Tire X	F Tire Y	F Tire Z	F Tire X	F Tire Y	F Tire Z
Member	length (in)	350	342	801	0	342	267
Upper A-arm (fore):	11.53	206.64			-1.0		
Upper A-Arm (aft):	9.29	200.64			229.73		
Tie Rod (fore):	14.77	-515.23			-145.09		
Lower A-Arm (fore):	17.01	-382.4			203.65		
Lower A-Arm (aft):	13.94	-501.97			-768.49		
Pushrod:	11.25	925.72			276.82		

In order to see if these numbers make any real world sense, a series of tests were conducted on the real life prototype during “steady state cornering”. The vehicle was outfitted with the following equipment:

- Motec Data acquisition system
- Strain gage bridge attached to one of the pushrods to act as a load transducer
- A 3 axis accelerometer mounted on the chassis of the vehicle to measure accelerations

With the above equipment mounted, the vehicle was taken through skid pad testing in order to obtain the system’s maximum lateral acceleration. The skid pad test was set up in accordance to formula SAE event regulations: a circle with a 50 ft diameter that the vehicle is driven around at maximum velocity without tire slippage. Accelerometer data was obtained and checked against a hand calculation based on the vehicles lap time around the ring. Load transducer data was recorded from the pushrod which correlated to the accelerations acting upon the vehicle. Due to the fact that all the data was time stamped, it was a simple task to compare the pushrod loads to the lateral accelerations attained.

Strain Gages

Finding the amount of strain in the pushrod of the car experimentally required a variety of different equipment. Strain gages were utilized to measure the amount of strain in the pushrod and were wired to compensate for bending and temperature effects. The gages were wired into a full Wheatstone bridge as shown below in Figure 4.

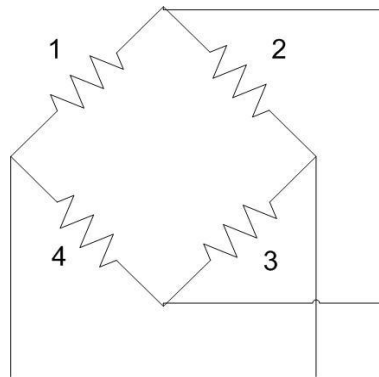


Figure 6.2: Wiring diagram for a full Wheatstone bridge.

Wiring the strain gages to compensate for the above characteristics required that the strain gages be applied in a certain manner on the pushrod. The layout of the strain gage application is shown below in Figure 6.3. The pushrod contained four strain gages attached at the center section of the shaft; two were aligned axially along the shaft (1 and 3) while the other two were aligned in the transverse direction (2 and 4). The numbers labeled on the gages in Figure 5 denote their wiring position in the Wheatstone bridge in Figure 4. Figure 6 shows the pushrod load transducer installed as part of the IRS for the mini Formula car.

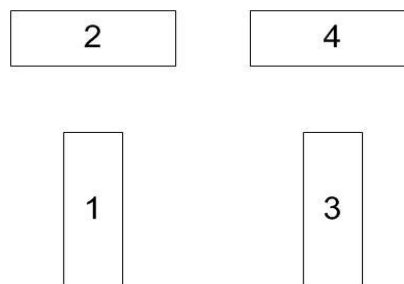


Figure 6.3: Strain Gage Application schematic. Gages 1 and 2 are 180 degrees out of plane with gages 3 and 4.

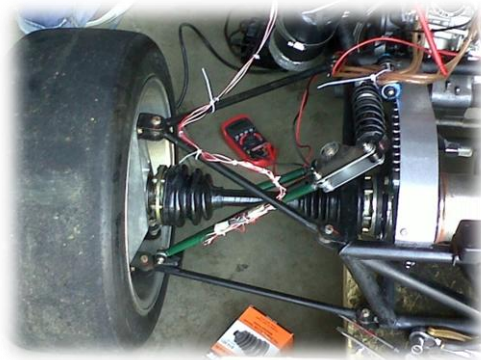


Figure 6.4: Pushrod Load Transducer installed on car.

Transducer Calibration

Strain gages output a differential voltage that is converted into micro-strain. This can then be converted to force using a calibration constant. The calibration constant was computed experimentally using an Instron tensile test machine and a Vishay P3 box.

Specially manufactured clevises were bolted to the rod ends of the pushrod so the Instron could grip the part without damaging it. Once the pushrod was firmly fixed in place, the Instron applied a tensile load to the pushrod which gave a corresponding strain reading. Figure 7 shows the pushrod loaded in the Instron.

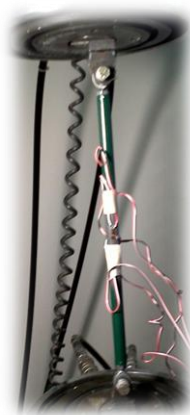


Figure 6.5: Pushrod Load Transducer fixed in Instron machine.

A P3 data acquisition box was used to read the strain gage bridge output during calibration. The P3 is capable of converting the bridge millivolts to micro-strain using the gage factor provided with the strain

gages. With the load applied by the Instron and the micro-strain readings from the P3, a calibration curve was produced. A trend line was fit to the calibration curve with the slope being the calibration constant. The wiring for the calibration test that was conducted can be seen in Figure 8.



Figure 6.6: Full Wheatstone bridge wired into P3 data acquisition box.

Accelerometer

Measuring the strain in a pushrod is important information; however it does not mean much or correlate to anything relevant without knowing its relation to the dynamics of the vehicle. Accelerometers were used in this case to provide relative comparative data to the strain readings. The accelerometer used in this experiment was a Dimension Engineering Buffered ± 3 G Triple Axis Accelerometer part number ADXL330. This accelerometer is a 3-axis accelerometer that has an operating range of ± 3 G and operates off of 3-15 V. The accelerometer outputs a voltage much like the strain gages, and in order to get relevant data, a calibration constant is required. For the ADXL330, this constant is equivalent to 333 mV/G. The mounted accelerometer can be seen below in Figure 9



Figure 6.7: Accelerometer mounted on rear frame. This location proved to be vibration prone, so it was later relocated to a more dampened location on the monocoque.

DAQ

The data acquisition system (DAQ) that was used in this experimental process was manufactured by Motec which specializes in vehicle data acquisition and engine control systems. The FSAE car was outfitted with a Motec Advanced Central Logger (ACL) and Variable Input Module (VIM) shown in Figure 10. The ACL interfaces with a computer to retrieve data across an Ethernet cable.

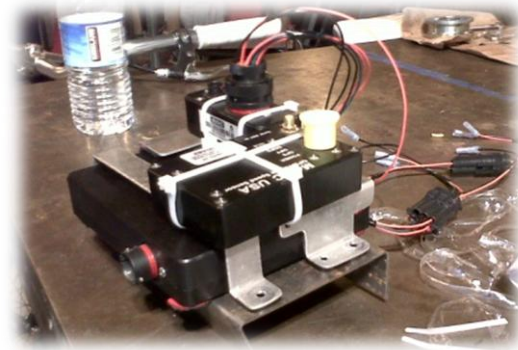


Figure 6.8: ACL and VIM wired together and mounted on a makeshift bracket.

The sensors used were connected to the DAQ system through the VIM. The VIM is a module that has a 55 pin connector that connects all of the sensors being used. For this experiment, nine pins were used to connect both the accelerometer and the Wheatstone bridge. The Wheatstone bridge requires four of the nine pins; a +5 volt supply, ground, Sensor +, and Sensor -. The accelerometer requires five pins due to the fact that it is a 3-axis accelerometer; one pin is used for each the X, Y, and Z accelerations, as well as a +5 volt supply and ground. The VIM interfaces with the ACL across a CAN-BUS. This CAN-BUS serializes and prioritizes the data to be relayed. It is comprised of a twisted trunk pair of wires and two 100Ω resistors at either end of the cable. A five pin connector was used to connect the CAN-BUS to the VIM and a 22 pin connector was used to connect to the ACL. The mounted and Connected ACL and VIM can be seen in Figure 11.

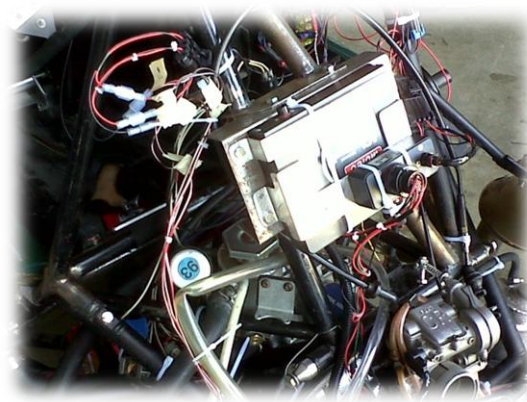


Figure 6.9: Motec DAQ mounted on the racecar

The ACL is the brain for the VIM in that it stores all of the data read and relayed by the VIM. The ACL required power from the battery with an auxiliary power switch. This auxiliary power switch controlled whether the ACL was on or off, and it was wired this way because the memory in the ACL is volatile and can be corrupted if the logger is not powered down correctly. The ACL is a robust device that is set up to handle power overloads; with an optimum voltage for the system of 12 Volts.

The ACL is configured by software provided by Motec called ACL Manager which allows the user to specify which channels to monitor and what rates to sample at. These rates can be changed for all channels being monitored, and the sampling rates do not have to be the same. The software also provided built in anti-aliasing filtering and start/stop conditions for the data logging. The start/stop conditions can be set with a multitude of options, for this experiment the start/stop condition used was that data was to begin logging when the Wheatstone bridge received power and stop when the power was pulled.

Once the data is logged on the ACL it can be read on a computer via an Ethernet cable, however the data cannot be read live. The data can be later viewed and manipulated using either i2 Standard or i2 Pro, both of which are also supplied by Motec. These programs allow for the data to be displayed graphically as well as for more advanced filtering to be applied to the data.

Initial Installation Testing

Axle Stubs

The first test trial with the Independent Rear Suspension yielded some predictable failure results. Due to time constraints and ease of manufacturability the team agreed that temporary aluminum axle stubs could work for testing, but steel axle stubs should be manufactured during this time which would eventually replace the aluminum parts. Unfortunately, machining splines into our 4130 stock tubing was turning out to be too time consuming and expensive with the consistent replacement of cutting tools. Fortunately the team was able to find splined material which would mate to the internal Torsen splines.

After the first test trial with the IRS, the aluminum axle stubs were removed for inspection.



Figure 6.10: Results of torsional twist on sprocket side (right) axle stub



Figure 6.11: Result of torsional twist on brake side (left) axle stub

A 4 degree twist was measure on the worst case axles stub ($\pm \frac{1}{2}$ degree). A calculation was done to find maximum torque acting on the axle stubs. The calculation was done assuming the following conditions:

- 1.) Modulus of Elasticity for Aluminum is 3.4 Msi
- 2.) Diameter of the splined tube: $D=.85$ inches
- 3.) Length of twist is 3.775

The length of twist starts at the beginning of the splines and ends where the diameter changes considerable at the flange.



Figure 6.12: Length of twist is 3.775 inches

Table 6.3: Axle stubs stress and deflection calculations

Aluminum Axle Stubs	
Angle of Twist	4 degrees
Length of Splines	3.775 inches
Diameter	.85 inches
Max Applied Torque	422 lb-ft
Max Shear Stress	42 ksi
Max Stress	72 ksi

The maximum applied torque is higher than our worst case torque at the differential in first gear which is 351 ft-lbs. This could possibly be due to impulse or shock from a dropped clutch or a stall. Needless to say we did not continue testing until steel axle stubs were available.

The steel axle stubs and half shafts were heat treated to ensure proper material properties. The four parts were heated to 1600 °F for an hour then oil quenched until ambient conditions then tempered to 750°F for an hour then air cooled.

Upright Thrust Bearing

High Friction and long term repetitive movement can be destructive if a bearing is not properly lubricated. This lesson was demonstrated with Suspension Solutions upright thrust bearing. High temperature lithium grease was applied to the new and existing bearing.



Figure 6.13: Bearing FAIL



Dynamic Testing Results

The two suspension systems were run in a skid-pad test similar to that of the FSAE competition seen in Figure 6.1. For our test however, double ski pad circles were not used. Instead just a single circle was used for simplicity and to cut down on experimental variables. Cones were set at the appropriate diameters, and each suspension system was timed around the circle track. The car was driven by two different drivers for both configurations. Each driver then drove to maximize lateral acceleration while maintaining traction and minimizing wheel spin. Both a stopwatch and Data acquisition were used to determine the maximum lateral acceleration attained.

Stopwatch

The drivers were Danny Nunes, FSAE's former drive train lead, and Matt Ales, FSAE's former team lead and engine lead. All IRS testing was done first then the axle was assembled back on the car (a 24hr turn around) and tested the next weekend. Before driving, the setups were weighed and balanced with a 150lb driver (a compromise between both drivers). They were also set with 0° toe angle at each tire and set up with static caster of between 0° and -1° for each tire.

Testing was performed on campus at CalPoly's H1 Lot off Bishops road. The skid pad was moderately swept and weather conditions are shown in Table 6.2. This table also shows the Skid pad times and calculated lateral accelerations from these times. To calculate Lateral Acceleration, Equation 6.1 was used.

$$\frac{((D_{skidpad} * \pi) / t)^2}{g * D_{skidpad} / 2} = A_{lateral} \text{ (g's)} \quad (6.1)$$

Table 6.2 shows mixed results, which suggest more testing is needed, however we can first easily conclude that the IRS car can at minimum match the solid rear axle car in terms of ski pad timed results. Before one can conclude whether it is indeed faster, further study of the data is required along with some more background information. Nunes' results can be thought to represent the beginner driver, as this was his 2nd time driving an IRS FSAE car, and 1st time driving a Solid Axle FSAE car. He was able to put both faster and more consistent skid pad results in the IRS car. After driving both set ups, Nunes' went on to say:



“Driving the Axle is definitely fun, but you can’t really tell when the rear will slide out, the IRS starts to under steer at the limit, which lets you control it easier, this could be play in the throttle though, with isn’t very responsive.”

Consistency seemed to be harder to achieve in the Solid Axle car for Nunes, whose fewer timed laps are a result of the car and driver over steering and spinning out more often. Interestingly, tire lift with the Solid Axle was also a bit inconsistent for Nunes when compared to Ales. We believe this a combination of poor throttle response, but also perhaps of lighter weight. With the car weighing 30lbs less, due to driver, the normal load could vary more with vibration, and weight jacking. This would be counter intuitive to our original analysis which showed lighter weight is better. It is still true that less total vehicle weight means greater lateral force coefficients. However if it leads to driving frequencies which inconsistency lift the inside tire, then they do not matter as much. This is a design parameter that is affected by many things however, so a conclusion cannot be reached by our limited testing.



Table 6.4: Lateral Acceleration Testing results by stopwatch.

Skidpad Diameter:	50		ft					
Driver:	Danny Nunes				Matt Ales			
Direction:	CW		CCW		CW		CCW	
	time(s)	G's	time(s)	G's	time(s)	G's	time(s)	G's
IRS Weather: Cloudy, 59° F, dry	6.9	0.64	6.5	0.73	6.8	0.66	6.5	0.73
	6.7	0.68	6.4	0.75	6.7	0.68	6.4	0.75
	6.0	0.85	6.0	0.85	6.5	0.73	5.5	1.01
	6.1	0.82	5.6	0.98	6.0	0.85	5.5	1.01
	5.9	0.88	5.6	0.98	6.0	0.85	5.5	1.01
	5.7	0.94	5.6	0.98	6.0	0.85	5.3	1.09
	5.7	0.94	5.6	0.98	5.6	0.98		
	5.7	0.94	5.6	0.98	5.5	1.01		
	5.6	0.98	5.5	1.01	5.5	1.01		
					5.5	1.01		
Average of Best 4	<i>5.7</i>	<i>0.95</i>	<i>5.6</i>	<i>0.99</i>	<i>5.5</i>	<i>1.004</i>	<i>5.5</i>	<i>1.03</i>
Direction:	CW		CCW		CW		CCW	
	time(s)	G's	time(s)	G's	time(s)	G's	time(s)	G's
Solid Rear Axle Weather: Clear, 68° F, Dry	6.3	0.77	6.8	0.66	6.3	0.77	6.5	0.73
	6.0	0.85	6.4	0.75	6.3	0.77	5.8	0.91
	5.8	0.91	6.2	0.80	6.0	0.85	5.6	0.98
	5.7	0.94	6.1	0.82	6.0	0.85	5.6	0.98
	5.6	0.98	6.0	0.85	5.9	0.88	5.5	1.01
					5.8	0.91	5.4	1.05
					5.7	0.94		
					5.5	1.01		
					5.5	1.01		
					5.4	1.05		
Average of Best 4	<i>5.8</i>	<i>0.92</i>	<i>6.2</i>	<i>0.81</i>	<i>5.5</i>	<i>1.005</i>	<i>5.5</i>	<i>1.00</i>

Ales' results can be thought to represent a more experienced driver within FSAE. He has driven both CalPoly's IRS and Solid Axle cars multiple times, both in and out of competition. Ales did put down a slightly faster time of 5.3s in the IRS compared to 5.4s in the Solid Axle. However looking at an average result between the fastest four runs shows Ales is similar in both cars, with only a slighter higher average in one direction in the IRS car. Experience showed with Ales, who did not spin out as frequently in either set up. He did agree with Nunes that the IRS is more stable saying:



“ The (IRS) is more predicable than the solid rear axle. It doesn't slide out...If it starts to slide you can either counter it by changing your steering input, or by giving it a little bit of brake it will come back around... it feels pretty consistent”

Data Acquisition System

Lateral Acceleration of IRS Setup and Pushrod Strain During Skidpad

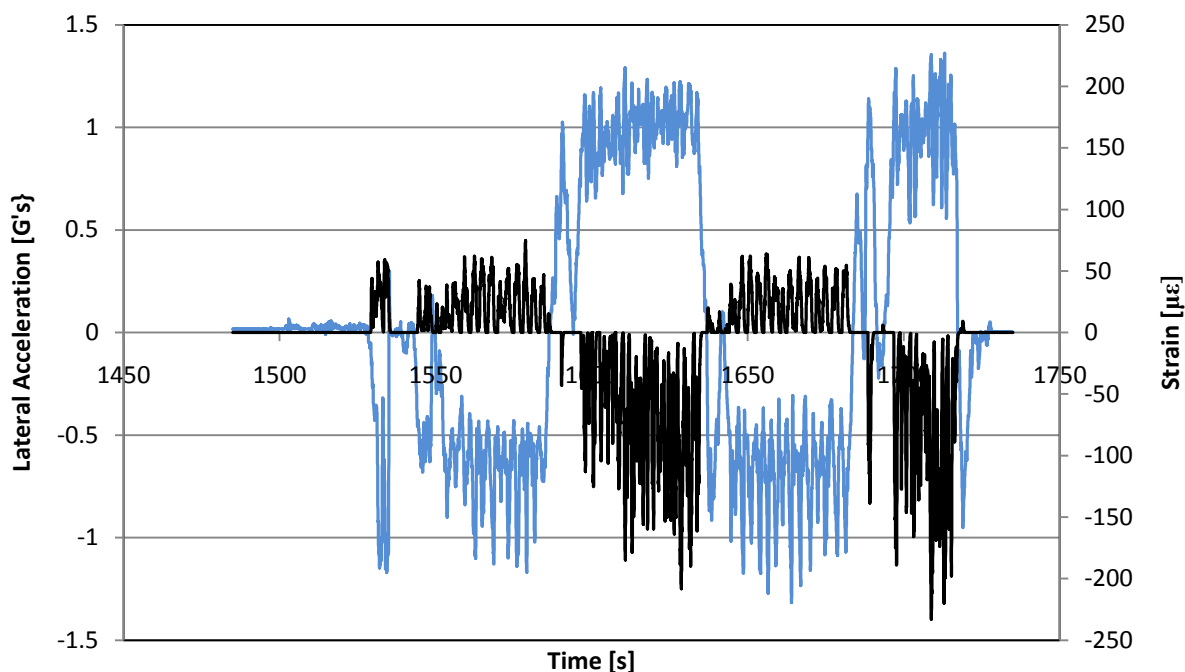


Figure 6.14: Lateral acceleration during skid pad test, plotted with pushrod strains. Note the positive and negative fluctuations about the axis of zero acceleration. These correspond to right turn (+) and left turn (-) laps. Strain experienced in the pushrod during testing fluctuated between tension and compression. During a right hand turn, the left pushrod (the one the transducer was on) was on the outside rear corner of the car, which saw high compressive forces. During a left hand turn, the left pushrod was on the inside rear corner of the car, which was unloaded and put into tension. This checked out with the direction the car rolled in cornering, and more importantly it makes physical sense.



Table 6.5: Accelerations at peak strain during skid pad test. X is longitudinal, which is due mostly to changes in throttle position. Y is lateral (radial acceleration, a measure of a cars grip) and Z is vertical, which is influenced by bump.

Accelerations at Peak Strain	
Axis	G
X	0.09
Y	1.27
Z	0.21

Table 6.6: Peak strains seen by the pushrod due to cornering. Compressive strains indicate a right hand turn; tensile loads indicate a left hand turn. The tensile load was considerably less. This can be related directly to the inside rear tire's tendency to want to lift during cornering.

Peak Strain Data	
Peak Compressive Strain [$\mu\epsilon$]	232.22
Peak Tensile Strain [$\mu\epsilon$]	74.58

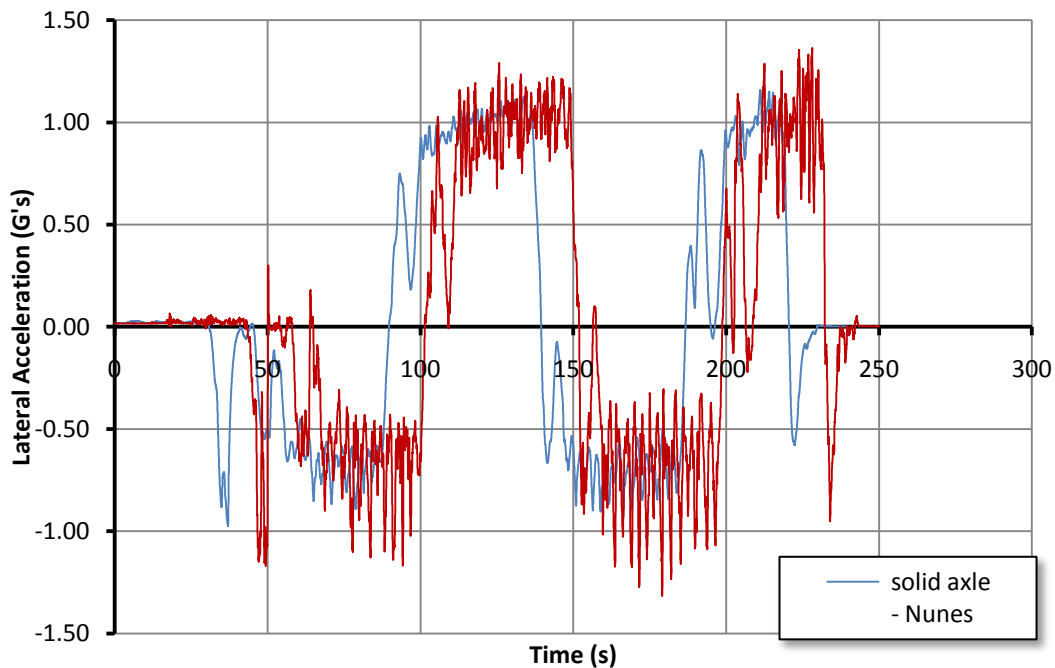


Figure 6.15: Solid axle and IRS lateral acceleration results plotted on same axis. Peak IRS lateral acceleration: 1.27 g. Peak solid axle lateral acceleration: 1.16 g.

Discussion

The data obtained seems reasonable based on the hand calculations in Appendix A and simulated dynamic modeling performed by the Suspension Solutions Senior Project team. According to the accelerometer data, lateral acceleration reached a peak value of 1.27 G during skidpad testing for the IRS car. Stopwatch acceleration calculations, which represent more of an average acceleration based on the time it takes to complete a lap, show lateral acceleration reaching 1.05 G. These numbers are both reasonable due to the fact that it is assumed at the onset of the hand calculated lateral acceleration that the car's velocity around the track is constant. We know for sure this is not the case, primarily because the motor of this car surges and spikes due to a poor carburetion. It is also assumed during the hand calculation that the radius of the turn remains constant. This also is not entirely true; video footage confirms that the car's distance from the marker line varied between 6 inches and 2 feet. For these reasons, it is entirely logical that at some point around the skidpad, the car did in fact feel a lateral acceleration of 1.27 G. This maximum was also verified by occurring at the point of maximum pushrod strain.



Maximum strain throughout the skid pad test was found to be 232.22 $\mu\epsilon$ which converts to 645.06 pounds of force applied to the pushrod. These numbers seem reasonable when you consider that the car weighs approximately 535 pounds with the driver and is undergoing 1.27 G lateral, .09 G longitudinal and .21 G vertical acceleration. When checked against the dynamic simulation results in Table 1, the force that was present experimentally in the pushrod lies between the two design conditions listed. The worst case design condition was a simulation of the car accelerating around the skid pad with a 3 G bump present, while the other was steady state cornering with no bump. The design condition with the 3 G bump predicted a force of 925.72 pounds in the pushrod. On the other hand, the steady state design condition with no bump predicted 276.82 pounds of force in the pushrod. It makes physical sense that the load measured by the transducer in our experiment ended up somewhere in between these design cases.

Future Testing

The following are a series of dynamic test which we believe the FSAE team should follow up our skid pad testing with. They will better show the differences between the handling and dynamic properties of the independent and solid rear axle car.

Acceleration Test

The FSAE competition features an acceleration event over a 75m track. For this test, a straight, flat 75m track will be measured. The two suspension systems will be timed from a standing start on multiple runs to ensure consistent data. Data acquisition will also be used to measure maximum longitudinal acceleration.

Autocross Test

A test track consisting of straights, slaloms, constant radius, changing radius and hairpin turns will be constructed. The vehicle will be timed with each suspension system through the track at increasing speeds. The fastest lap time of each car will be compared, and data acquisition will be used to plot accelerations through the track. This data will be compared to determine which vehicle has superior performance in the autocross event.



Chapter 8: Conclusion



Conclusion and Recommendations

Following the design presented in this report, the Suspension Solutions team successfully converted the CP08 Formula car to an independent rear suspension with a differential. The design of an independent rear suspension system had not been attempted by the FSAE club in over five years. Although many of our designs had to be compromised to allow for interchangeable rear ends, we believe the car still performs competitively, not only against the solid rear axle FSAE car, but also against other school teams' FSAE cars which were designed to have independent rear suspensions. The results of this project will allow the FSAE team to gain more knowledge, which will hopefully lead to better design decisions regarding rear suspensions systems and differentials.

Although we were able to complete skid pad dynamic testing, we believe more testing needs to be done to better justify either design decision. We also believe there are still many improvements that can be made, the biggest with respect to weight. We calculated early in the design process that total vehicle weight was most likely the driving factor that would lead to a performance advantage of either an independent rear suspension or solid rear axle car. A Formula SAE design team starting from scratch for a new year could easily surpass our prototype in lightness. However, allowing for the testing of both rear suspension systems by designing an interchangeable system was worth the extra weight and complexity. The following recommendations to improve upon a generic independent rear suspension are listed below with respect to particular components and systems.

Rear Suspension Members and Geometry

With regards to suspension geometry, more dynamic possibilities could be analyzed to better understand the handling characteristics of the car. Within our design it was quickly found that suspension geometry, whether front or rear, is always a compromise between two or more competing characteristics. More optimization could have occurred, but the man-hours were needed on other components. Also, the rear A-Arms were designed for the limitations on the rear frame adaptation of the car. More freedom to determine geometry could likely improve the dynamic ride characteristics of the car, resulting in a better performance.



Differential choice

The differential being borrowed from Formula Hybrid for this project is the Torsen university special used by many FSAE teams. Although a Torsen has its advantages, such as allowing the use of a differential mounted brake rotor, there are other options available. The Torsen was chosen for its limited slip capabilities, but more importantly because it was readily available and commonly used within FSAE. However the differential is arguably overweight and lighter options exist within the world of ATV differentials. The design team would recommend extensive research into ATV differential's if the FSAE teams were to return to an independent rear suspension car. ATV clutch-type limited slip differential will likely be lighter and more effective than the Torsen university special, a theory which has been proven by a handful of FSAE teams. Half shafts and tripods/CV joints also need to be properly researched to ensure that compatibility of parts are available or machine-able when choosing a differential.

Uprights

The upright is a very complicated part that went through many design iterations during this project. Its complexity lies in the complete understanding of all the components it must connect and all the forces that act on it. Live spindles must be used with rear differentials, which are more complicated than typical front dead spindles.

Rear Frame

Had an independent rear suspension been the car's design from the start, it is believed that some weight could be taken off the rear sub-frame. The extra sub frame we had to create is our heaviest addition to the car, and had to be designed against the already fixed engine position of the previous rear sub frame. Once again, a knowledgeable understanding of all the loading conditions and where they act is most important for conducting FE analysis on a chassis. The rear frame was also limited by our hesitation to design a stressed engine frame. We did not have the availability and time to complete an engine stress test. It is suggested that FSAE use a strong table and lever mechanism to experimentally determine the strength and stiffness of the WR-450 engine. If results show a strong and stiff enough block, the stressed engine design, which is a lighter design, could be justified.



Final Thoughts

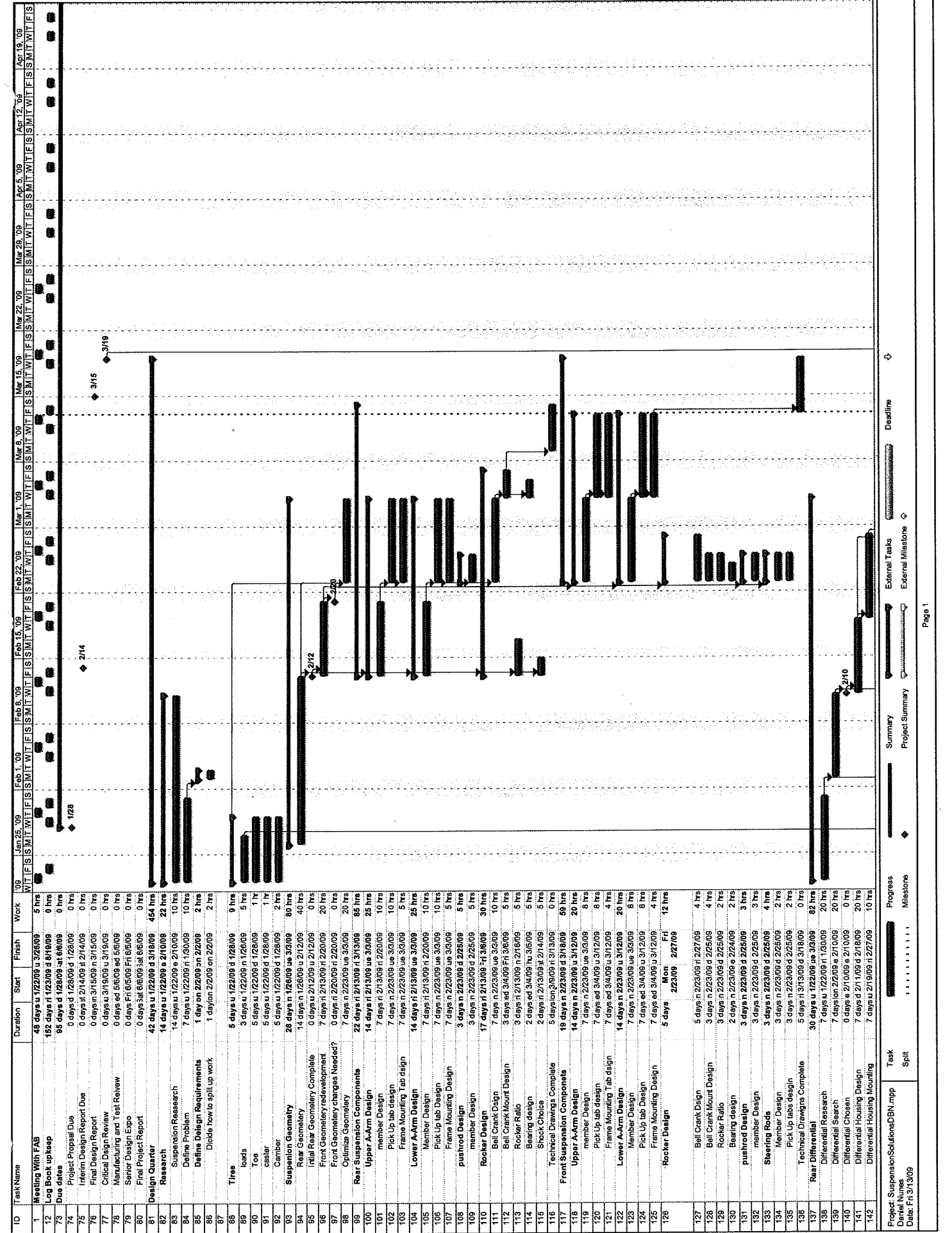
In conclusion, Suspension Solutions was able to design, manufacture, and test an independent rear suspension system for the 2008 Formula car. The finished product met all our major design goals: it was fully interchangeable, taking less than 30 minutes for two people to remove or attach with just five bolts needing to be fastened. The components were all easily accessible; bleeding or removing the brakes, removing the differential assembly, and changing the shocks are all straightforward jobs. Finally, the system met our weight goal, tipping the scales at just 22 lbs added when we designed for 25 lbs.

Limited dynamic testing shows mixed results. However, it was agreed by both drivers that the IRS is a more stable and predictable car. With further testing, we suspect it to *clearly* be seen as the faster design as well. This project did teach us a number of valuable lessons. First, it is important to have a complete, adequate design before manufacturing begins. The longer you wait, the harder it gets to make changes in a project. This is due to the constraints created by already built parts and the time available. Second, it is important to design within your manufacturing abilities or have a complete plan for how parts will be manufactured. This includes knowing the processes needed to manufacture the part, or knowing companies who are able to create the part for you.

Most importantly, we learned that the weight savings associated with the solid rear axle might not be worth it when it comes to performance, reliability, and accessibility. This is a lesson that can be passed down to future FSAE teams to allow them to more easily quantify the advantages and disadvantages of solid rear axle and independent suspension designs.

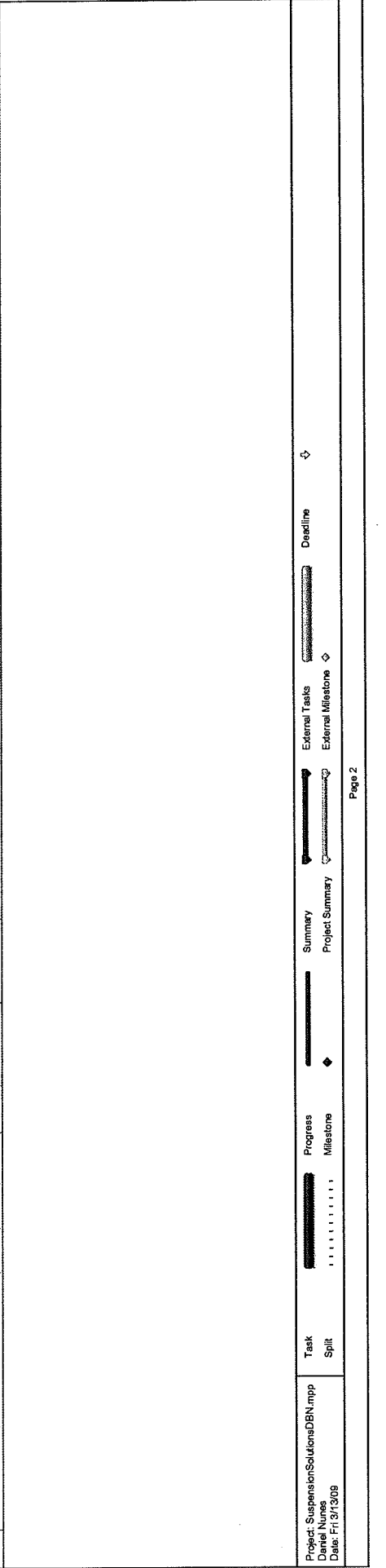


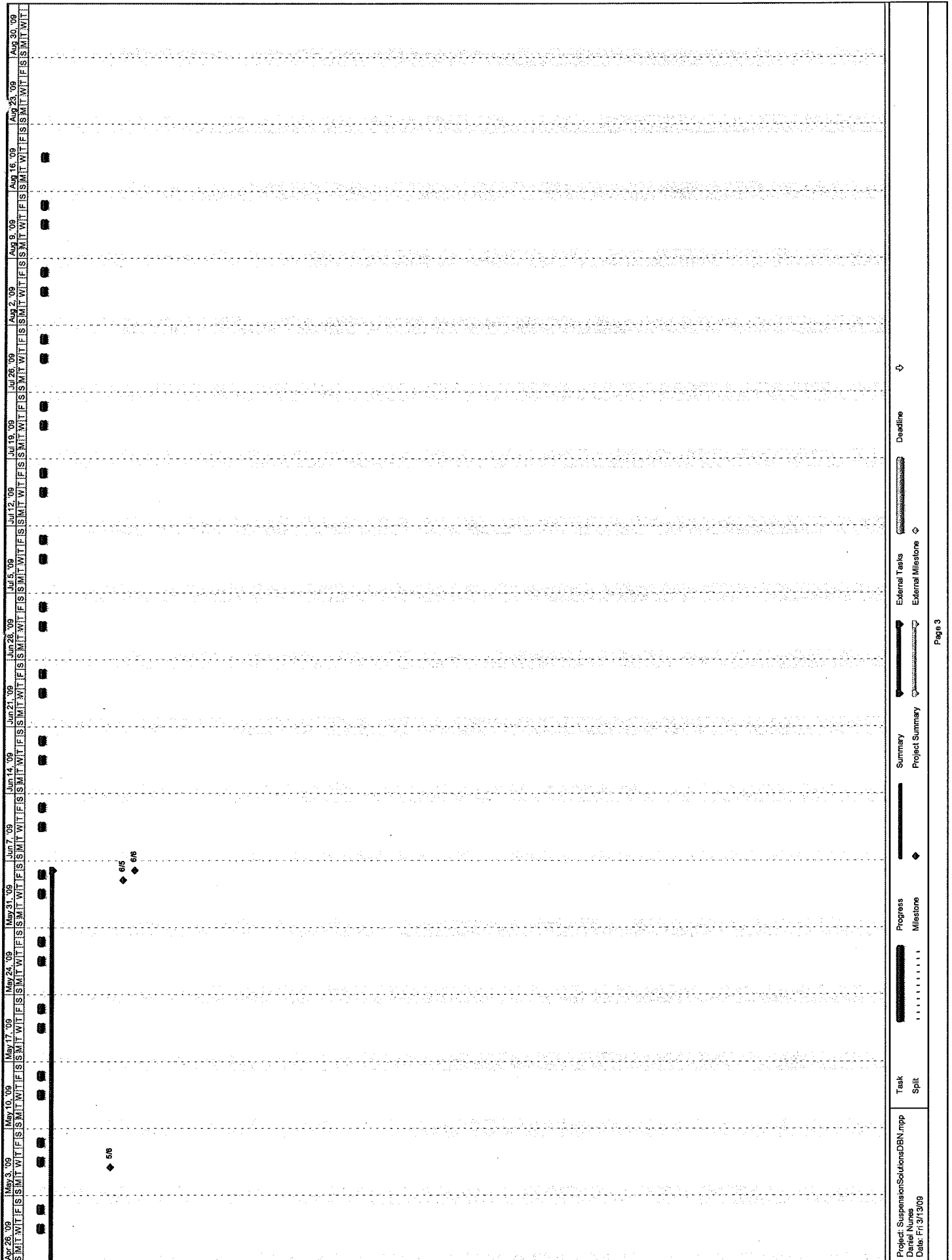
Appendix A: Gantt Chart

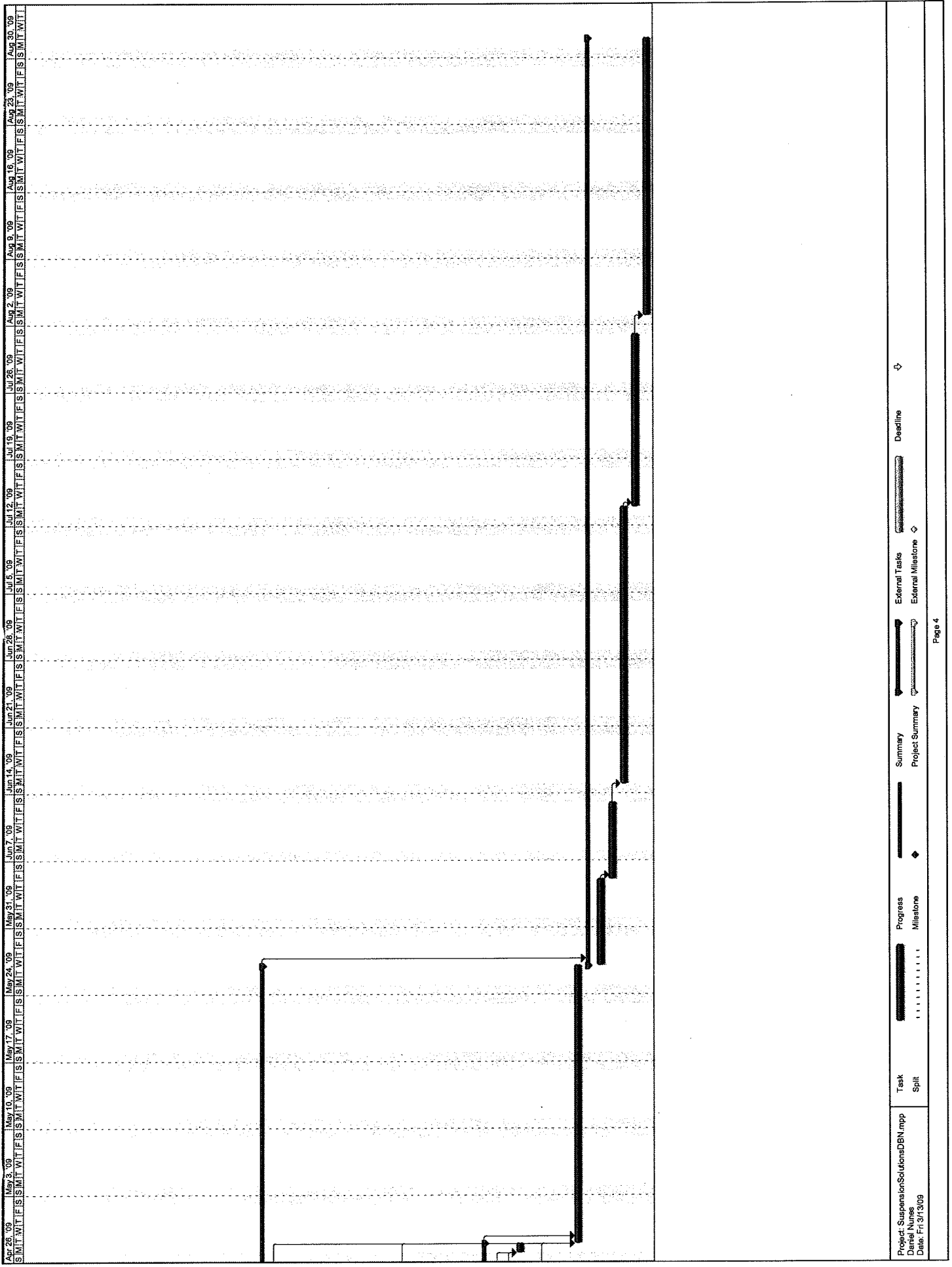


ID	Task Name	Duration	Start	Finish	Work
1	Meeting With FAB	45 days u 1/22/09 d 3/26/09		5 hrs	
2	Log Book upkeep	85 days u 1/23/09 d 8/19/09		0 hrs	
3	Due dates	0 days d 1/28/09 at 8/6/09		0 hrs	
74	Project Proposal Due	0 days d 1/28/09 d 1/28/09		0 hrs	
75	Inferior Design Report Due	0 days d 2/14/09 d 2/14/09		0 hrs	
76	Final Design Report	0 days u 3/15/09 u 3/15/09		0 hrs	
77	Critical Design Review	0 days d 3/15/09 d 3/15/09		0 hrs	
78	Manufacturing and Test Review	0 days d 5/6/09 d 5/6/09		0 hrs	
79	Senior Design Expo	0 days Fri 6/5/09 Fri 6/5/09		0 hrs	
80	Final Project Report	0 days Sat 6/6/09 Sat 6/6/09		0 hrs	
81	Design Quarter	45 days u 1/22/09 d 3/18/09		454 hrs	
82	Research	14 days u 1/22/09 d 2/10/09		22 hrs	
83	Suspension Research	14 days u 1/22/09 d 2/10/09		10 hrs	
84	Define Problem	7 days u 1/22/09 d 1/30/09		10 hrs	
85	Define Design Requirements	1 day on 2/2/09 on 2/2/09		2 hrs	
86	Divide how to split up work	1 day on 2/2/09 on 2/2/09		2 hrs	
87					
88	Tires	5 days u 1/22/09 d 1/28/09		9 hrs	
89	loads	3 days u 1/22/09 d 1/26/09		5 hrs	
90	Toe	5 days u 1/22/09 d 1/28/09		1 hr	
91	caster	5 days u 1/22/09 d 1/28/09		1 hr	
92	Camber	5 days u 1/22/09 d 1/28/09		2 hrs	
93	Suspension Geometry	26 days n 1/26/09 ue 3/3/09		80 hrs	
94	Rear Geometry	14 days n 1/26/09 u 2/12/09		40 hrs	
95	Infil Rear Geometry Complete	0 days u 2/12/09 u 2/12/09		0 hrs	
96	Front Geometry redevelopment	7 days n 2/13/09 d 2/20/09		20 hrs	
97	Front Geometry changes needed?	0 days n 2/20/09 d 2/20/09		0 hrs	
98	Optimize Geometry	7 days n 2/23/09 ue 3/3/09		20 hrs	
99	Rear Suspension Components	22 days n 2/13/09 d 3/13/09		85 hrs	
100	Upper A-Arm Design	14 days n 2/13/09 ue 3/5/09		25 hrs	
101	member Design	7 days n 2/13/09 d 2/20/09		10 hrs	
102	Pick Up lab design	7 days n 2/23/09 ue 3/3/09		10 hrs	
103	Frame Mounting Tab design	7 days n 2/23/09 ue 3/3/09		5 hrs	
104	Lower A-Arm Design	14 days n 2/13/09 ue 3/3/09		25 hrs	
105	Member Design	7 days n 2/13/09 d 2/20/09		10 hrs	
106	Pick Up lab Design	7 days n 2/23/09 ue 3/3/09		10 hrs	
107	Frame Mounting Design	3 days n 2/23/09 d 2/26/09		5 hrs	
108	pushrod Design	3 days n 2/23/09 d 2/26/09		5 hrs	
109	member Design	3 days n 2/23/09 d 2/26/09		5 hrs	
110	Rocker Design	17 days n 2/13/09 d 3/6/09		30 hrs	
111	Ball Crank Design	7 days n 2/23/09 ue 3/3/09		10 hrs	
112	Ball Crank Mount Design	3 days d 3/4/09 Fri 3/6/09		5 hrs	
113	Rocker Ratio	3 days n 2/13/09 n 2/16/09		5 hrs	
114	Bearing design	2 days d 3/4/09 Tu 3/5/09		5 hrs	
115	Shock Choice	2 days n 2/13/09 d 2/14/09		5 hrs	
116	Technical Drawings Complete	5 days on 2/9/09 d 3/13/09		0 hrs	
117	Front Suspension Components	18 days n 2/23/09 d 3/18/09		69 hrs	
118	Upper A-Arm Design	14 days n 2/23/09 ue 3/12/09		20 hrs	
119	member Design	7 days n 2/23/09 ue 3/3/09		8 hrs	
120	Pick Up lab design	7 days d 3/4/09 u 3/12/09		8 hrs	
121	Frame Mounting Tab design	7 days d 3/4/09 u 3/12/09		4 hrs	
122	Lower A-Arm Design	14 days n 2/23/09 u 3/12/09		20 hrs	
123	Member Design	7 days n 2/23/09 ue 3/3/09		8 hrs	
124	Pick Up lab Design	7 days d 3/4/09 u 3/12/09		8 hrs	
125	Frame Mounting Design	7 days d 3/4/09 u 3/12/09		4 hrs	
126	Rocker Design	5 days Mon 2/23/09 Fri 2/27/09		12 hrs	
127	Ball Crank Design	5 days n 2/23/09 d 2/27/09		4 hrs	
128	Ball Crank Mount Design	3 days n 2/23/09 d 2/25/09		4 hrs	
129	Rocker Ratio	3 days n 2/23/09 d 2/25/09		2 hrs	
130	Bearing design	2 days n 2/23/09 u 2/24/09		2 hrs	
131	pushrod Design	3 days n 2/23/09 d 2/25/09		3 hrs	
132	member Design	3 days n 2/23/09 d 2/25/09		3 hrs	
133	Steering Rods	3 days n 2/23/09 d 2/25/09		2 hrs	
134	Member Design	3 days n 2/23/09 d 2/25/09		2 hrs	
135	Pick Up tabs design	3 days n 2/23/09 d 2/25/09		2 hrs	
136	Technical Drawings Complete	5 days u 1/22/09 ue 3/3/09		0 hrs	
137	Differential Research	7 days u 1/22/09 n 1/30/09		20 hrs	
138	Differential Search	7 days on 2/2/09 u 2/10/09		20 hrs	
139	Differential Chosen	0 days d 2/10/09 u 2/10/09		0 hrs	
140	Differential Housing Design	7 days d 2/10/09 d 2/18/09		20 hrs	
141	Differential Housing Mounting	7 days u 2/19/09 n 2/27/09		10 hrs	

ID	Task Name	Duration	Start	Finish	Work	109	Jan 28, '09	Feb 1, '09	Feb 8, '09	Feb 15, '09	Feb 22, '09	Mar 1, '09	Mar 8, '09	Mar 15, '09	Mar 22, '09	Mar 29, '09	Apr 5, '09	Apr 12, '09	Apr 19, '09	
143	Rear Shafts Design	3 days on 2/20/09 to 2/24/09			10 hrs															
144	Bearing Design	3 days on 2/20/09 to 2/24/09			2 hrs															
145	Differential Design Complete	0 days on 2/27/09 to 2/27/09			0 hrs															
146	Technical Drawings Complete	2 days on 3/2/09 to 3/3/09			0 hrs															
147	Rear Upright Design	28 days on 1/27/09 to 3/5/09			63 hrs															
148	research Uprights	7 days on 1/27/09 to 2/4/09			20 hrs															
149	CAD Up, Current Witness	4 days on 1/27/09 to 1/30/09			2 hrs															
150	Upright	12 days on 2/5/09 to 2/19/09			12 hrs															
151	Spindle	12 days on 2/5/09 to 2/19/09			12 hrs															
152	bearings	2 days on 2/20/09 to 2/23/09			5 hrs															
153	brakes on Uprights?	7 days on 2/20/09 to 3/2/09			12 hrs															
154	Rear uprights Complete	0 days on 3/2/09 to 3/2/09			0 hrs															
155	Technical Drawings Complete	3 days on 3/3/09 to 3/5/09			0 hrs															
156	Rear Frame Adaptation	31 days on 1/22/09 to 3/4/09			54 hrs															
157	ReBuild Rear Frame in CAD	7 days on 1/22/09 to 1/30/09			12 hrs															
158	Structure Geometry	14 days on 2/2/09 to 2/18/09			20 hrs															
159	Member Design	7 days on 2/19/09 to 2/27/09			10 hrs															
160	frame bungs design	7 days on 2/11/09 to 2/18/09			8 hrs															
161	Differential Housing mount	3 days on 3/2/09 to 3/4/09			0 hrs															
162	Technical Drawings Complete	48 days on 3/19/09 to 5/28/09			331 hrs															
163	Build Quarter	20 days on 3/19/09 to 4/15/09			160 hrs															
164	Rear Suspension Components	20 days on 3/19/09 to 4/15/09			80 hrs															
165	Upper A-Arms	14 days on 3/19/09 to 4/7/09			40 hrs															
166	Jig	2 days on 4/8/09 to 4/9/09			10 hrs															
167	Tubes Touched	2 days on 4/8/09 to 4/9/09			10 hrs															
168	Tabs Made	2 days on 4/14/09 to 4/15/09			10 hrs															
169	Welded	7 days on 3/19/09 to 3/27/09			80 hrs															
170	Lower A-Arms	4 days on 3/19/09 to 3/24/09			40 hrs															
171	Jig	1 day on 3/25/09 to 3/25/09			10 hrs															
172	Tubes Notched	2 days on 3/25/09 to 3/26/09			20 hrs															
173	Tabs Made	1 day on 3/27/09 to 3/27/09			10 hrs															
174	Welded	7 days on 3/19/09 to 3/27/09			51 hrs															
175	Rear Upright Components	7 days on 3/19/09 to 3/27/09			40 hrs															
176	Uprights	7 days on 3/19/09 to 3/27/09			40 hrs															
177	Jig	7 days on 3/19/09 to 3/27/09			40 hrs															
178	SpindalHub	7 days on 3/19/09 to 3/27/09			10 hrs															
179	Jig	1 day on 3/19/09 to 3/19/09			1 hr															
180	Bearings	1 day on 3/19/09 to 3/19/09			1 hr															
181	ordered	8 days on 4/16/09 to 4/27/09			80 hrs															
182	Frame Adaptation	7 days on 4/16/09 to 4/24/09			40 hrs															
183	Tubes Notched	7 days on 4/16/09 to 4/24/09			20 hrs															
184	Frame Bungs Machined	1 day on 4/27/09 to 4/27/09			10 hrs															
185	Welded	4 days on 3/19/09 to 3/24/09			0 hrs															
186	Differential mounted	21 days on 4/28/09 to 5/26/09			30 hrs															
187	Differential	4 days on 3/19/09 to 3/24/09			0 hrs															
188	Ordered	4 days on 3/19/09 to 3/24/09			0 hrs															
189	Brakets	70 days on 5/27/09 to 8/31/09			120 hrs															
190	Assembly	7 days on 5/27/09 to 6/4/09			20 hrs															
191	Testing Quarter	7 days on 5/27/09 to 6/4/09			20 hrs															
192	Safety inspection	21 days on 6/15/09 to 7/13/09			20 hrs															
193	Brake Testing	14 days on 6/15/09 to 7/13/09			20 hrs															
194	Shockpad Testing	21 days on 6/15/09 to 7/13/09			20 hrs															
195	Acceleration Testing	14 days on 7/14/09 to 7/31/09			20 hrs															
196	AutoCross Testing	21 days on 8/3/09 to 8/31/09			40 hrs															







ID	Task Name	Duration	Start	Finish	Work	edecessc	16	19	22	25	28	May 2009	1	4	7	10	13	16	19	22	25	28	Ju
1	Meeting With FAB	58 days	Thu 1/22/09	Thu 3/26/09	5 hrs																		
12	Log Book upkeep	188 days	Fri 1/23/09	Wed 8/19/09	0 hrs																		
73	Due dates	125 days	Wed 1/28/09	Sat 6/6/09	0 hrs																		
81	Design Quarter	42 days	Thu 1/22/09	Tue 3/10/09	464 hrs																		
87																							
163	Build Quarter	42 days	Sun 4/19/09	Sat 5/30/09	153.75 hrs	77																	
164	Rear Chassis	24 days	Sun 4/19/09	Tue 5/12/09	39 hrs																		
165	Rear Frame Box	12 days	Sun 4/19/09	Thu 4/30/09	31 hrs																		
166	Rear Box Jig Set Up	2 days	Sun 4/19/09	Mon 4/20/09	4 hrs																		
167	Tubes Cut/Notched	7 days	Sun 4/19/09	Sat 4/25/09	20 hrs																		
168	Rear Box Welded	1 day	Sun 4/26/09	Sun 4/26/09	4 hrs	167																	
169	Suspension Pickup Tabs Cut	1 day	Sun 4/19/09	Sun 4/19/09	2 hrs																		
170	Tabs Welded	1 day	Thu 4/30/09	Thu 4/30/09	1 hr	169,168																	
171	Frame Adaptation	15 days	Tue 4/28/09	Tue 5/12/09	8 hrs																		
172	Chassis & Rear Box Set Up	1 day	Tue 4/28/09	Tue 4/28/09	0 hrs	168																	
173	Tubes Cut/Notched	3 days	Thu 5/7/09	Sat 5/9/09	0 hrs	172																	
174	Frame Bungs Machined	3 days	Sat 5/2/09	Mon 5/4/09	4 hrs																		
175	Connecting Tubes Welded	3 days	Sun 5/10/09	Tue 5/12/09	4 hrs	173,174																	
176	Rear Suspension Components	28 days	Sat 4/25/09	Fri 5/22/09	45.75 hrs																		
177	Upper A-Arms	21 days	Sat 5/2/09	Fri 5/22/09	17 hrs																		
178	Jig	1 day	Sat 5/2/09	Sat 5/2/09	0.5 hrs																		
179	Wafer Blanks Cut	2 days	Fri 5/8/09	Sat 5/9/09	1.5 hrs																		
180	Wafer Blanks Drilled	1 day	Sat 5/9/09	Sat 5/9/09	1 hr																		
181	Wafer CNC Machining	1 day	Sat 5/16/09	Sat 5/16/09	3 hrs																		
182	Tubes Cut/Notched	1 day	Thu 5/21/09	Thu 5/21/09	1 hr																		
183	Welded	1 day	Fri 5/22/09	Fri 5/22/09	10 hrs	182																	
184	Lower A-Arms	21 days	Sat 5/2/09	Fri 5/22/09	11.75 hrs																		
185	Jig	1 day	Sat 5/2/09	Sat 5/2/09	0.25 hrs																		
186	Wafer Blanks Cut	2 days	Fri 5/8/09	Sat 5/9/09	1.5 hrs																		
187	Wafer Blanks Drilled	1 day	Sat 5/9/09	Sat 5/9/09	1 hr																		
188	Wafer CNC Machining	1 day	Sat 5/16/09	Sat 5/16/09	4 hrs	187																	
189	Tubes Cut/Notched	1 day	Thu 5/21/09	Thu 5/21/09	1 hr																		
190	Tabs Made	1 day	Thu 5/21/09	Thu 5/21/09	2 hrs																		
191	Welded	1 day	Fri 5/22/09	Fri 5/22/09	2 hrs	189,190																	
192	Push Rods	2 days	Sat 4/25/09	Sun 4/26/09	2.5 hrs																		
193	Cut Tube	1 day	Sat 4/25/09	Sat 4/25/09	0.5 hrs																		
194	Machine Threaded Inserts	1 day	Sat 4/25/09	Sat 4/25/09	1 hr																		
195	Weld	1 day	Sun 4/26/09	Sun 4/26/09	1 hr	194,193																	
196	Tie Rods	2 days	Sat 4/25/09	Sun 4/26/09	2.5 hrs																		

Project: SuspensionSolutionsDBN
Daniel Nunes
Date: Thu 4/16/09

Task Split Progress

Milestone Summary Project Summary

External Tasks External Milestone Deadline

Page 1

ID	Task Name	Duration	Start	Finish	Work	edecessc	16	19	22	25	28	May 2009	1	4	7	10	13	16	19	22	25	28	Ju	31
197	Cut Tube	1 day	Sat 4/25/09	Sat 4/25/09	0.5 hrs																			
198	Machine Threaded Inserts	1 day	Sat 4/25/09	Sat 4/25/09	1 hr																			
199	Weld	1 day	Sun 4/26/09	Sun 4/26/09	1 hr	198, 197																		
200	Rockers	10 days	Sat 5/9/09	Mon 5/18/09	12 hrs																			
201	Build Rocker Jig	1 day	Sat 5/9/09	Sat 5/9/09	2 hrs																			
202	Cut Rocker Sheet	2 days	Sat 5/9/09	Sun 5/10/09	2 hrs																			
203	Machine Bearing Cups	1 day	Sat 5/16/09	Sat 5/16/09	2 hrs																			
204	Machine Rocker Mount	2 days	Sat 5/16/09	Sun 5/17/09	4 hrs																			
205	Weld Rockers	2 days	Sun 5/17/09	Mon 5/18/09	2 hrs	202, 203																		
206	Rear Upright Components	25 days	Thu 4/23/09	Sun 5/17/09	34 hrs																			
207	Uprights	16 days	Sat 5/2/09	Sun 5/17/09	12 hrs																			
208	Billet Cut to Size	2 days	Sat 5/2/09	Sun 5/3/09	3 hrs																			
209	CNC Machining	14 days	Sun 5/3/09	Sat 5/16/09	8 hrs																			
210	Bearings Pressed In	1 day	Sun 5/17/09	Sun 5/17/09	1 hr	209																		
211	Spindle	18 days	Sat 4/25/09	Tue 5/12/09	12 hrs																			
212	Spindle Machined	3 days	Sat 4/25/09	Mon 4/27/09	8 hrs																			
213	Spines Cut	14 days	Tue 4/28/09	Mon 5/11/09	2 hrs	212																		
214	Spindle Threaded	1 day	Tue 5/12/09	Tue 5/12/09	2 hrs	213																		
215	Hubs	19 days	Thu 4/23/09	Mon 5/11/09	10 hrs																			
216	Hubs Machined	3 days	Thu 4/23/09	Sat 4/25/09	8 hrs																			
217	Spines Cut	14 days	Tue 4/28/09	Mon 5/11/09	2 hrs	216																		
218	Front Suspension Components	8 days	Sat 5/23/09	Sat 5/30/09	11 hrs																			
219	Front Tabs Machined	5 days	Sun 5/24/09	Thu 5/28/09	8 hrs																			
220	Upper A-Arm Jig	1 day	Sat 5/23/09	Sat 5/23/09	1 hr																			
221	Upper A-Arm Tubes Cut/Notched	1 day	Sun 5/24/09	Sun 5/24/09	1 hr	220																		
222	Upper A-Arms Welded	1 day	Sat 5/30/09	Sat 5/30/09	1 hr																			
223	Differential	28 days	Sat 4/25/09	Fri 5/22/09	24 hrs																			
224	Outer Housing	5 days	Sat 4/25/09	Wed 4/29/09	8 hrs																			
225	Brake Rotor Mount Machined	14 days	Sat 5/2/09	Fri 5/15/09	4 hrs																			
226	Sprocket Mount Machined	14 days	Sat 5/9/09	Fri 5/22/09	4 hrs																			
227	Differential Uprights Billet Cut to Size	1 day	Sat 4/25/09	Sat 4/25/09	2 hrs																			
228	CNC Machining of Uprights	14 days	Sun 4/26/09	Sat 5/9/09	6 hrs	227																		
229	Testing Quarter	70 days	Sun 5/31/09	Tue 8/25/09	120 hrs	163																		

Project: SuspensionSolutionsDBN
 Daniel Nunes
 Date: Thu 4/16/09

Task

Split

Progress

Milestone

Summary

Project Summary

External Tasks

External Milestone

Deadline



Appendix B: QFD

Suspension Solutions QFD		Engineering Requirements																		Benchmarks					
		Owner	Mechanic	Driver	add no more 20 lb of weight	Reduce Normal Load Variation on tires	Minimum Suspension travel of 2in	Chassis must be 1 in above ground	Lock all four tires in a straight line	Meet Budget Requirements	Maximum deflection of .01 in	Design Components Safety Factor=1.5	Components Life Span of 1000 miles	Create multiple mounting configurations	Limited Adjustability with Camber and Track	No Steering Reversal at the Steering Wheel	Consistent Steering Force	Design closely to neutral steer	Most components manufactured in the shop	Assembled with Standard Shop Tools	Ready Access to Maintenance elements	2008 FSAE SRA	2004 FSAE IRS	F1	
Customer Requirements	PERFORMANCE																							9	
	Light Weight*	7	3	6	●		Δ						●	Δ					Δ			8	6	9	
	Lateral Grip	8	1	9	○	●				○				●	○	○	●					7	8	9	
	Longitudinal Grip	8	1	9	○	●		●		○				●	○	○	●					5	9	9	
	Consistent Dependable Braking	6	1	7	●	●		●				○		○		●						5	6	9	
	Stiffness	5	2	7			●	○			●	●		○			●	●				8	7	9	
	Strength	4	2	6			Δ				●			●				●				7	7	5	
	Tunability	5	8	6			●							●								6	6	8	
	Driver Feedback (response)	4	6	10	○	○				○					●	●	●	●				6	7	9	
	MARKETABILITY																								
	Cost	10	1	7	Δ					●		○	Δ	○					●	Δ	Δ	7	6	1	
	Life Span	7	5	7							Δ	●	●									n/a	8	2	
	Aesthetics	10	2	2										Δ								8	8	7	
	SAFETY																								
	Non-Critical Components Fail First	10	1	10							●	●										n/a	n/a	4	
	Interchangeability *	1	9	1	○									○	○				○	●	Δ	n/a	n/a	6	
	Safe Assembly Procedures	2	9	1															○	●		8	8	3	
	MANUFACTUABILITY																								
	Ease of Manufacturability*	1	10	1	○									○	○				●		○	5	8	1	
	Compatibility with subsystems	1	10	1	○									○	○				○	○		n/a	n/a	3	
	Ease of Assembly	1	10	1	○									○	○				●	●	○	7	8	2	
	Skill of Manufacturability*	1	10	1	○									○	○				●			4	7	2	
	MAINTENANCE																								
	Accessibility*	3	10	1										Δ	○				Δ		●	6	6	6	
	Frequency	9	10	1					Δ					Δ								n/a	6	2	





Appendix C: Selection of Detailed Analysis

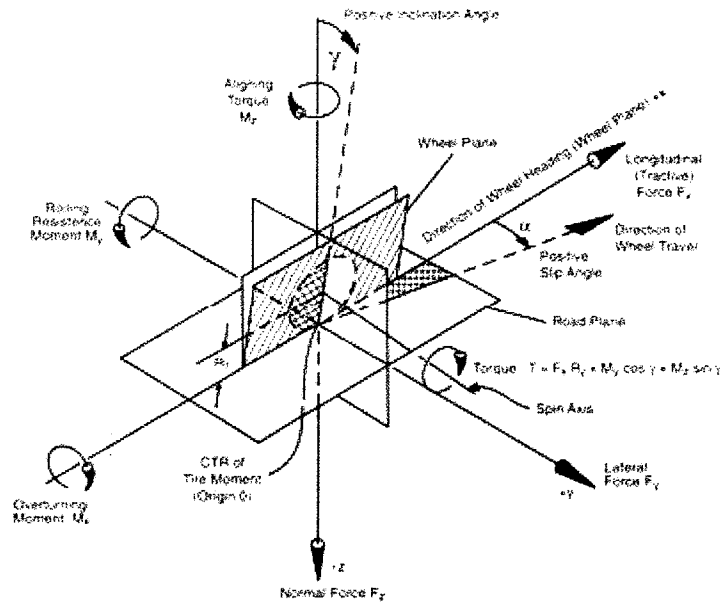


Figure C2 Six degrees of generated tire forces

The longitudinal (tractive), lateral, and normal force do not necessarily act in the center plane of the tire, especially when camber, toe and caster are adjusted. Generally, all forces generated are acting just offset to the center plane of the tire especially when cornering. The offsets create moments about all axis which are represented by the aligning moment (M_z) and the overturning moment (M_x).

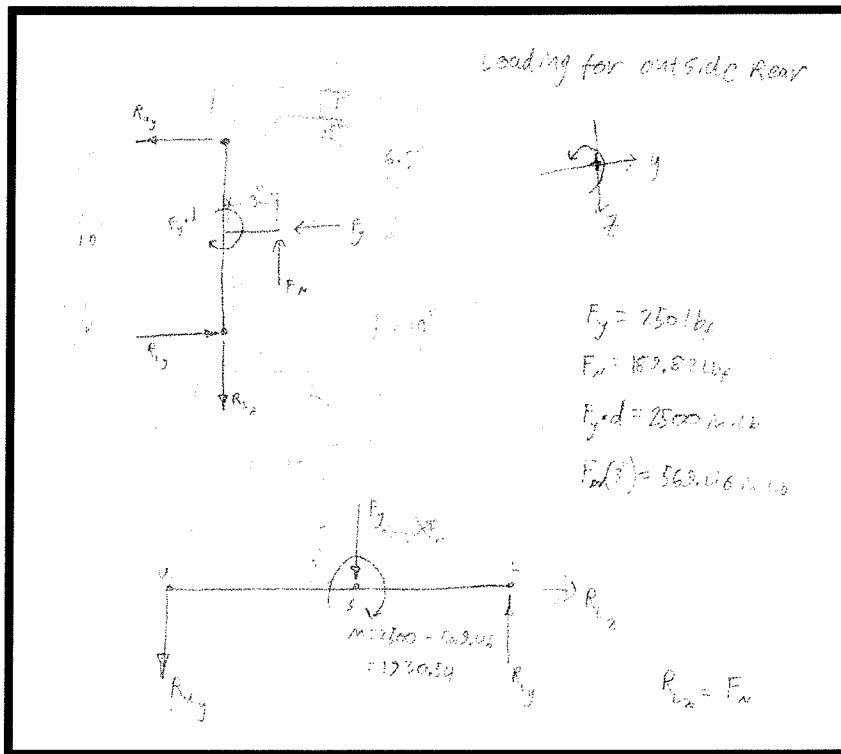


Figure C3 Initial Loading Estimates for Upper and Lower A-Arm pick-up points

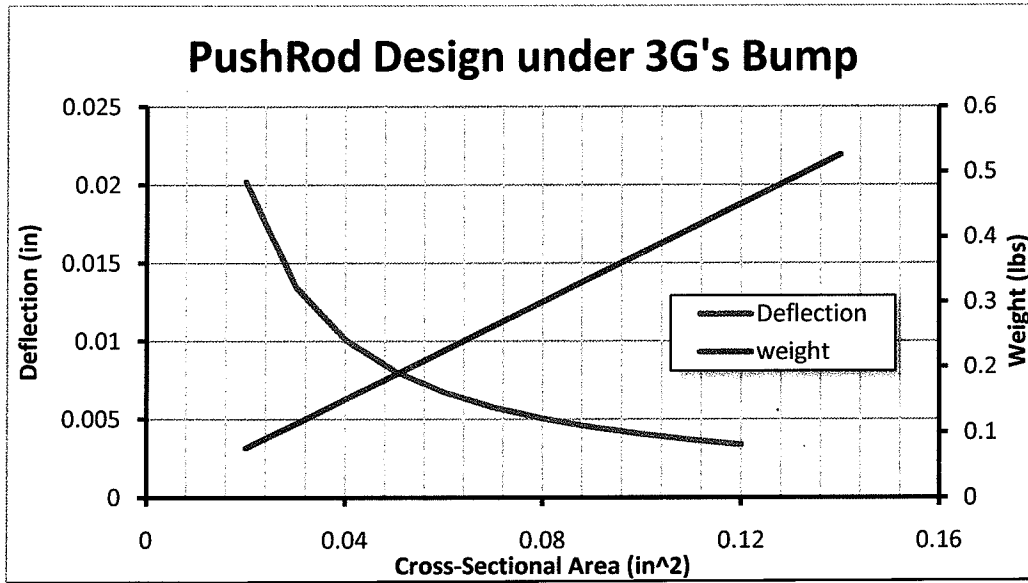


Figure C5 Push Rod Deflection with respect cross sectional area

A) System Inputs, and Initial Calculated Values

Input Tire Forces, off weight dist.	
Normal	
1	F-Outside Acc. (lbf) 265.17
2	F-Outside Dec. 174.34
3	F-Inside Acc. 125.41
4	F-Inside Dec. 34.58
5	F-Straight Acc. 195.29
6	F-Straight Dec. 104.46
Lateral	
1	F-Outside Acc. 340.6
2	F-Outside Dec. 223.66
3	F-Inside Acc. 160.65
4	F-Inside Dec. 43.66
5	F-Straight Acc. 0
6	F-Straight Dec. 0
μ longitudinal 1.4	

Life Inputs	
# hours	1000
avg speed (mph)	40
wheel diameter (in)	20
edge fillet radius (in)	0.2

Spindle Geometry	
Tapered Brg Width (in)	0.75
Hub-Spindle Contact Width	0.5
Upright Width	2
Assumed Shaft Diameter	
d_b1 (mm)	45
d_step (mm)	40
d_b1 (in)	1.771654
d_step (in)	1.574803
Distance between brg reactions	
x1 (in)	1.25
x2	0.625
Moment of Inertias	
I_b1 (in ⁴)	0.483599
J_b1	0.967197
I_step (in ⁴)	0.301908
J_step	0.603817

B) Statics and Stress Calculations

Force Inputs-Tire Loads Applied to Spindle					
	Fx	Fy	Fz	Mconstant	T
1	371.238	340.6	265.17	6812	3712.38
2	244.076	223.66	174.34	4473.2	2440.76
3	175.574	160.65	125.41	3213	1755.74
4	48.412	43.66	34.58	873.2	484.12
5	273.406	0	195.29	0	2734.06
6	146.244	0	104.46	0	1462.44
eq (lin-dam)	233.3448257	179.6973	166.6749	3593.94652	2333.448257

Moment eq'ns-- brg reactions at center	
M(bearing1) (psi)	1699.072
M(step)	1756.274
Torque	2333.448
Look at failure at step	
σ_m (psi)	5270.479
σ_a (psi)	4580.506
Strength Considerations	
r/d	0.127
D/d	1.125
q	0.81
Kt	1.5
Kt_torsion	1.5
Kf	1.405
Kf_torsion	1.405
New σ_m and σ_a	
σ_m (psi)	7405.023
σ_a	6435.611

C) Strength and Safety Factor

Strength	
Use 6061 T6 Aluminum	
Su (psi)	42000
Sy	35000
Sf @ 4e7 cycles	16000
# cycles	40336229
Application Factor, a	2
Safety Factors	
Ka	1.003
Kb	0.83743
Kc	1
Kd	1
Ke	0.814
Fatigue Strength	
Sf	10939.41
ASME Elliptic Factor Safety	
n	



Appendix D: Decision Matrices

APPENDIX D

Customer Reqs	WGT	Concept 1	Concept 2	Concept 3	Concept 4	Concept 5	Concept 7	Concept 8	Concept 9
Weight	20		+	S	+	+	+	+	S
Rigidity	20		-	S	-	-	-	S	+
Compliance	13		S	+	S	S	S	S	+
Engine Stress	10		-	S	S	-	-	+	+
Accessibility	10		+	S	-	+	+	S	-
Manufacturing	15	DATUM	+	S	S	+	-	-	S
Time to remove	5		+	+	+	+	+	S	S
Cost	5		+	+	+	+	-	S	+
Appearance	2		+	-	+	+	+	+	+

100	Weighted +	57	23	32	57	37	32	50
	Weighted -	30	2	30	30	50	15	10
	TOTAL SCORE	27	21	2	27	-13	17	40



Appendix E: Suspension Forces Matlab Code

```
%Rear_Susp_Forces_OPK.m
```

```
%
%Program is to assist Suspension Solutions Design Team in determining
%rear suspension forces that act through the control arms. The program
%inputs suspension from an OptimumK output file to determine a-arm
%geometry and computes tension/compression forces in each member for a
%variety of loading conditions. Maximum loads in each member are output
%to Rear_Susp_Stresses.m in order to determine tubing sizes.
```

```
%Designers Notes:
```

```
%2/15/09 started by: Daniel Nunes
% matrix created that attempts to solve for suspension forces at the
% uprights, however i soon discover that this leads to 9 unknowns;
% reaction in 3 directions (x,y,z) for the upper AA pick up point
% lower AA pick up point and the tie rod pick up point, with only
% 6 equations.
% for now will have to assume three more equations to constrain
% matrix, will ask Fab about this later.
```

```
%2/17/09 Recalculated equations of quasi-static equilibrium solving for
% unknown compressive(or tensive)forces in each member.
% member(1) is the Upper A-Arm fore T-C rod
% member(2) is the Upper A-Arm aft T-C rod
% member(3) is the Tie rod
% member(4) is the Lower A-Arm fore T-C rod
% member(5) is the Lower A-Arm aft T-Crod
% member(6) is the push rod, assumed attached to the lower A-Arm and
% acts on the Lower A-Arm upright ball joint
```

```
% These force directions are obtained by constraining the rods to be
% two-force members allowing us to solve for the forces acting on
% them. Thus a fully defined (3-D) A-Arm geometry is needed, and must be input
```

```
% initial A-arm and chassis pick up point forces solved for
```

```
#####
#####
```

```
clc
clear
```

```
#####
% OptimumK Data %
#####
```

```
file_name = input('Enter spreadsheet filename, including .xls extension: ','s');
```

```
opk = xlsread(file_name);
```

```

LAA_b = lf(1); % (in) Horizontal distance from fore chassis
pickup to upright pickup

%Lower inclination
LAA_phi=atand(la(3)/la(2)); % (deg) Angle of lower a-arm relative to
horizontal

%Tie Rod
tr=abs(Tie_Up-Tie_Arm);
TIE_L2 = (tr(1)^2+tr(2)^2+tr(3)^2)^0.5; % (in) Total length of tie rod
TIE_b = abs(Tie_Up(1)-Lower_Fore(1)); % (in) Horizontal distance to tie rod
TIE_phi = atand(tr(3)/tr(2)); % (deg) Tie rod inclination

%-----%

%Upright and wheel geometry, relative to ground plane at the tire contact patch.

%Upper A-Arm Upright pick up point
Dist_X_UAA=Upper_Up(1); % (in) Negative means aft of wheel
Dist_Y_UAA=half_track-Upper_Up(2); % (in)
Dist_Z_UAA=Upper_Up(3); % (in) Positive means upward from ground

%Lower A-Arm Upright pick up point
Dist_X_LAA=Lower_Up(1); % (in)
Dist_Y_LAA=half_track-Lower_Up(2); % (in)
Dist_Z_LAA=Lower_Up(3); % (in)

%Tie Arm Upright pick up point
Dist_X_TIE=Tie_Up(1); % (in)
Dist_Y_TIE=half_track - Tie_Up(2); % (in)
Dist_Z_TIE=Tie_Up(3); % (in)

%-----%

%Upper A-Arm geometry

%Calculated
UAA_L3=UAA_a+UAA_b;
UAA_alpha=acosd((UAA_L2^2-UAA_L1^2-UAA_L3^2)/(-2*UAA_L1*UAA_L3));
UAA_theta=90-UAA_alpha;
UAA_h=sind(UAA_alpha)*UAA_L1;
UAA_beta=acosd((UAA_L1^2-UAA_L2^2-UAA_L3^2)/(-2*UAA_L2*UAA_L3));
UAA_gamma=acosd((UAA_L3^2-UAA_L1^2-UAA_L2^2)/(-2*UAA_L1*UAA_L2));

%-----%

%Lower A-Arm geometry
%inputs

LAA_eps1=50; % (deg) Push rod angle from horizontal

%Calculated
LAA_L3=LAA_a+LAA_b;

```

```

%Rolling resistance moment
MTy=20;           %(lbf-in) Rolling resistance moment

%Torque about the spin axis
MTt=0;           %(lbf-in) Torque about wheel axis

%solving matrix for upright pickup point forces (crazy ass matrix!!)

A=      [cosd(UAA_phi)*cosd(UAA_beta), cosd(UAA_phi)*cosd(UAA_alpha), cosd(TIE_phi)
*cosd(TIE_beta), cosd(LAA_phi)*cosd(LAA_beta), cosd(LAA_phi)*cosd(LAA_alpha), 0;
      cosd(UAA_phi)*sind(UAA_beta), cosd(UAA_phi)*sind(UAA_alpha), cosd(TIE_phi)*sind
(TIE_beta), cosd(LAA_phi)*sind(LAA_beta), cosd(LAA_phi)*sind(LAA_alpha), cosd(LAA_epsl);
      sind(UAA_phi), sind(UAA_phi), sind(TIE_phi), sind(LAA_phi), sind(LAA_phi), sind
(LAA_epsl);
      (-cosd(UAA_phi)*cosd(UAA_beta)*Dist_Z_UAA)-(sind(UAA_phi)*Dist_X_UAA)), ((cosd
(UAA_phi)*cosd(UAA_alpha)*Dist_Z_UAA)-(sind(UAA_phi)*Dist_X_UAA)), (-cosd(TIE_phi)*cosd
(TIE_beta)*Dist_Z_TIE)-(sind(TIE_phi)*Dist_X_TIE)), (-cosd(LAA_phi)*cosd(LAA_beta)
*Dist_Z_LAA)-(sind(LAA_phi)*Dist_X_LAA)), ((cosd(LAA_phi)*cosd(LAA_alpha)*Dist_Z_LAA)-
(sind(LAA_phi)*Dist_X_LAA)), (sind(LAA_epsl)*Dist_X_LAA);
      ((cosd(UAA_phi)*sind(UAA_beta)*Dist_Z_UAA)+(sind(UAA_phi)*Dist_Y_UAA)), ((cosd
(UAA_phi)*sind(UAA_alpha)*Dist_Z_UAA)+(sind(UAA_phi)*Dist_Y_UAA)), ((cosd(TIE_phi)*sind
(TIE_beta)*Dist_Z_TIE)+(sind(TIE_phi)*Dist_Y_TIE)), ((cosd(LAA_phi)*sind(LAA_beta)
*Dist_Z_LAA)+(sind(LAA_phi)*Dist_Y_LAA)), ((cosd(LAA_phi)*sind(LAA_alpha)*Dist_Z_LAA)+
(sind(LAA_phi)*Dist_Y_LAA)), ((cosd(LAA_epsl)*Dist_Z_LAA)-(sind(LAA_epsl)*Dist_Y_LAA));
      (-cosd(UAA_phi)*cosd(UAA_beta)*Dist_Y_UAA)+(cosd(UAA_phi)*sind(UAA_beta)
*Dist_X_UAA)), ((cosd(UAA_phi)*cosd(UAA_alpha)*Dist_Y_UAA)+(cosd(UAA_phi)*sind
(UAA_alpha)*Dist_X_UAA)), (-cosd(TIE_phi)*cosd(TIE_beta)*Dist_Y_TIE)+(cosd(TIE_phi)
*sind(TIE_beta)*Dist_X_TIE)), (-cosd(LAA_phi)*cosd(LAA_beta)*Dist_Y_LAA)+(cosd(LAA_phi)
*sind(LAA_beta)*Dist_X_LAA)), ((cosd(LAA_phi)*cosd(LAA_alpha)*Dist_Y_LAA)+(cosd(LAA_phi)
*sind(LAA_alpha)*Dist_X_LAA)), (cosd(LAA_epsl)*Dist_X_LAA)];
A;

b=[-FTire_X;
   -FTire_Y;
    FTire_Z;
   -MTx;
   -MTy+MTt;
   -MTz];

b;
det(A);

X=inv(A)*b;

%Upright forces at the pick up points
disp('(-)=Tension in members, (+)=Compression in members')
%Upper A-Arm
  UAA_fore=X(1)   %(lbf)
  UAA_aft=X(2)   %(lbf)

%Lower A-Arm

```

```
Rear_Susp_Forces_OPK();
```

```
#####%
%   Input Variables from Rear_Susp_Forces_OPK   %
#####%
%
%   NAME           DESCRIPTION           UNITS
%   UAA_fore       Upper fore link force   lbf
%   UAA_aft        Upper aft link force   lbf
%   TIE_fore       Tie rod force          lbf
%   LAA_fore       Lower fore link force   lbf
%   LAA_aft        Lower aft link force   lbf
%   LAA_push       Push rod force         lbf
%   UAA_L1         Upper aft link length   in
%   UAA_L2         Upper fore link length  in
%   LAA_L1         Lower aft link length   in
%   LAA_L2         Lower fore link length  in
%   TIE_L2         Tie rod length          in
```

```
#####%
%               Define New Variables           %
#####%
```

```
% Material Properties for 4130 Alloy Steel
```

```
E = 30000000;           %Modulus of Elasticity (psi)
ys = 52;                %Yield strength (kpsi)
```

```
C = 1;                 %Column Effective Length Factor
```

```
n=11;
a_stress = 1;
```

```
#####%
%   Calculate Critical Area for Each Member   %
#####%
```

```
a_UAA_fore = abs(UAA_fore/(ys*1000));   % Area needed for Upper Fore (in^2)
a_UAA_aft = abs(UAA_aft/(ys*1000));     % Area needed for Upper Aft (in^2)
a_TIE_fore = abs(TIE_fore/(ys*1000));   % Area needed for Tie Rod (in^2)
a_LAA_fore = abs(LAA_fore/(ys*1000));   % Area needed for Lower Fore (in^2)
a_LAA_aft = abs(LAA_aft/(ys*1000));     % Area needed for Lower Aft (in^2)
a_LAA_push = abs(LAA_push/(ys*1000));   % Area needed for Push Rod (in^2)
```

```
% Matrix of standard tubing sizes (OD,WALL);)
tubes = [0.25,0.035;
         0.25,0.058;
         0.3125,0.065;
```

```

while (a_UAA_aft<a_tube(n)) && (n>1)
    n = n-1;
    a_tube(n) = (pi/4)*(tubes(n,1)^2-(tubes(n,1)-2*tubes(n,2))^2);
end
n=n+1;
a_stress = a_tube(n);

%Check critical load for buckling

I = (pi/64)*(tubes(n,1)^4-(tubes(n,1)-2*tubes(n,2))^4);

P_cr = C*(pi^2)*E*I/(UAA_L2^2);

%Check against tubing load
if P_cr>abs(UAA_aft)
    Tube2 = sprintf('Select tube with %.3f OD and %.3f wall',tubes(n,1),tubes(n,2))
else
    % Increase the area until tube passes
    while P_cr<abs(UAA_aft)
        n = n+1
        I = (pi/64)*(tubes(n,1)^4-(tubes(n,1)-2*tubes(n,2))^4);
        P_cr = C*(pi^2)*E*I/(UAA_L2^2);
    end
    Tube2 = sprintf('Select tube with %.3f OD and %.3f wall (buckling dependent)',tubes
(n,1),tubes(n,2))
end

n = 11;

a_tube(n) = (pi/4)*(tubes(n,1)^2-(tubes(n,1)-2*tubes(n,2))^2);

#####%
%           Tube 3 (Tie Rod)           %
#####%

while (a_TIE_fore<a_tube(n)) && (n>1)
    n = n-1;
    a_tube(n) = (pi/4)*(tubes(n,1)^2-(tubes(n,1)-2*tubes(n,2))^2);
end
n=n+1;
a_stress = a_tube(n);

%Check critical load for buckling

I = (pi/64)*(tubes(n,1)^4-(tubes(n,1)-2*tubes(n,2))^4);

P_cr = C*(pi^2)*E*I/(TIE_L2^2);

%Check against tubing load
if P_cr>abs(TIE_fore)

```



```

%           Tube 5 (Lower A-Arm Aft)           %
%#####%

while (a_LAA_aft<a_tube(n)) && (n>1)
    n = n-1;
    a_tube(n) = (pi/4)*(tubes(n,1)^2-(tubes(n,1)-2*tubes(n,2))^2);
end
n=n+1;
a_stress = a_tube(n);

%Check critical load for buckling

I = (pi/64)*(tubes(n,1)^4-(tubes(n,1)-2*tubes(n,2))^4);

P_cr = C*(pi^2)*E*I/(LAA_L2^2);

%Check against tubing load
if P_cr>abs(LAA_aft)
    Tube5 = sprintf('Select tube with %.3f OD and %.3f wall',tubes(n,1),tubes(n,2))
else
    % Increase the area until tube passes
    while P_cr<abs(LAA_aft)
        n = n+1;
        I = (pi/64)*(tubes(n,1)^4-(tubes(n,1)-2*tubes(n,2))^4);
        P_cr = C*(pi^2)*E*I/(LAA_L2^2);
    end
    Tube5 = sprintf('Select tube with %.3f OD and %.3f wall (buckling dependent)',tubes
(n,1),tubes(n,2))
end

n = 11;

a_tube(n) = (pi/4)*(tubes(n,1)^2-(tubes(n,1)-2*tubes(n,2))^2);

%#####%
%           Tube 6 (Push Rod)           %
%#####%

while (a_LAA_push<a_tube(n)) && (n>1)
    n = n-1;
    a_tube(n) = (pi/4)*(tubes(n,1)^2-(tubes(n,1)-2*tubes(n,2))^2);
end
n=n+1;
a_stress = a_tube(n);

%Check critical load for buckling

I = (pi/64)*(tubes(n,1)^4-(tubes(n,1)-2*tubes(n,2))^4);

P_cr = C*(pi^2)*E*I/(LAA_L2^2);

%Check against tubing load

```

Enter spreadsheet filename, including .xls extension: SS_4.3.09.xls

UAA_L1 =

11.1467

UAA_L2 =

13.4257

LAA_L1 =

14.4417

LAA_L2 =

17.9043

TIE_L2 =

15.7659

Results of Simulation for each loading conditons
(-)=Tension in members, (+)=Compression in members

UAA_fore =

109.8435

UAA_aft =

287.3598

TIE_fore =

-391.7811

LAA_fore =

-207.6702

UAA_aft =

-241.9155

TIE_fore =

-275.8172

LAA_fore =

-765.6549

LAA_aft =

892.2730

LAA_push =

131.6088

(-)=Tension in members, (+)=Compression in members

UAA_fore =

-59.1232

UAA_aft =

108.0985

TIE_fore =

15.7379

LAA_fore =

126.9398

LAA_aft =

Tube3 =

Select tube with 0.313 OD and 0.065 wall (buckling dependent)

Tube4 =

Select tube with 0.375 OD and 0.035 wall (buckling dependent)

Tube5 =

Select tube with 0.500 OD and 0.035 wall (buckling dependent)

Tube6 =

Select tube with 0.500 OD and 0.035 wall (buckling dependent)

>>

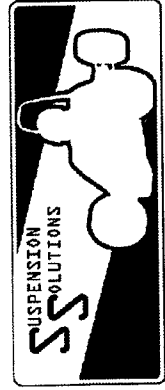
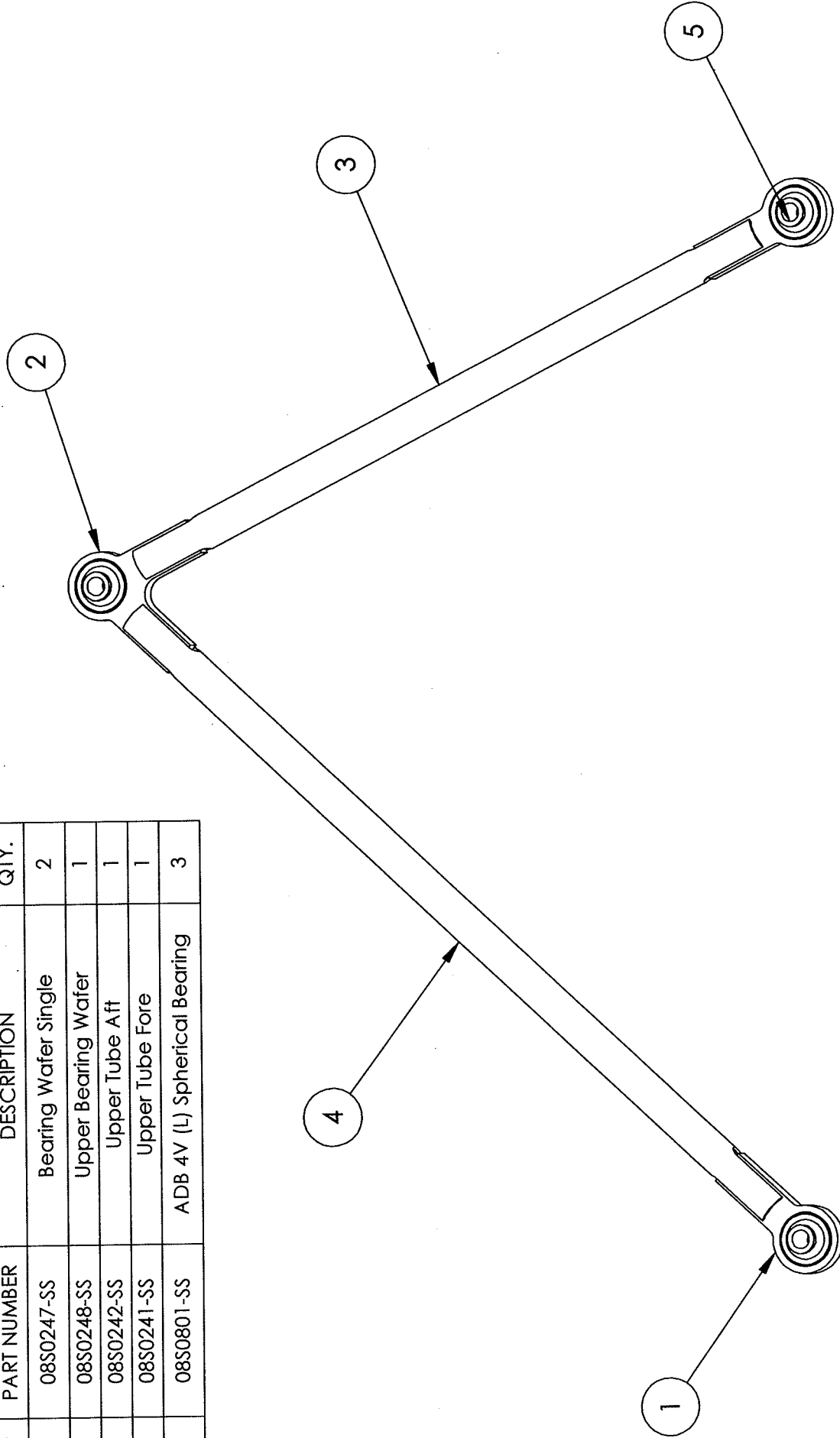


Appendix F: Detailed Engineering Part Drawings.

C. Poly Formula SAE Suspension Solutions

Part #: 08S04AS4-SS

ITEM NO.	PART NUMBER	DESCRIPTION	QTY.
1	08S0247-SS	Bearing Wafer Single	2
2	08S0248-SS	Upper Bearing Wafer	1
3	08S0242-SS	Upper Tube Aft	1
4	08S0241-SS	Upper Tube Fore	1
5	08S0801-SS	ADB 4V (L) Spherical Bearing	3



Part Name: Upper A-Arm Assembly

Sub Team: Suspension

Next Assembly: MasterAssm

Material:

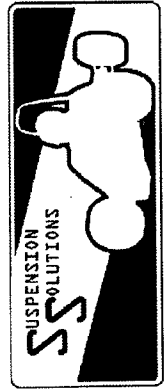
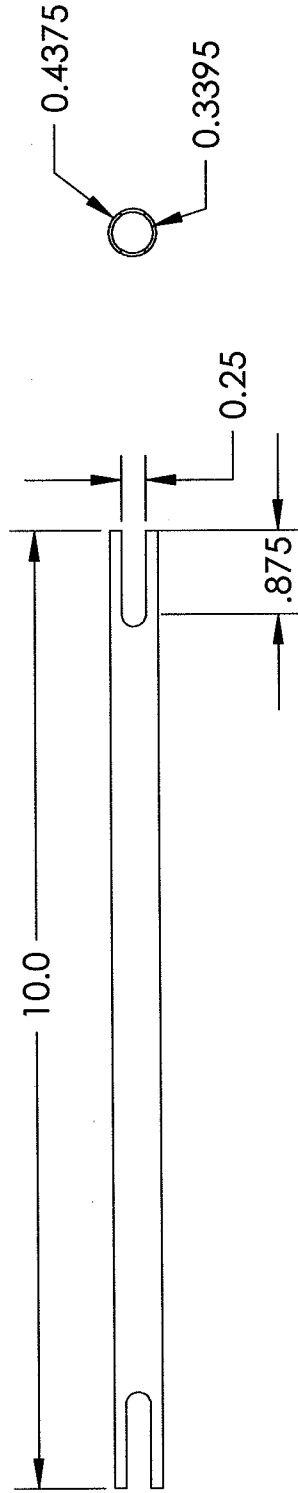
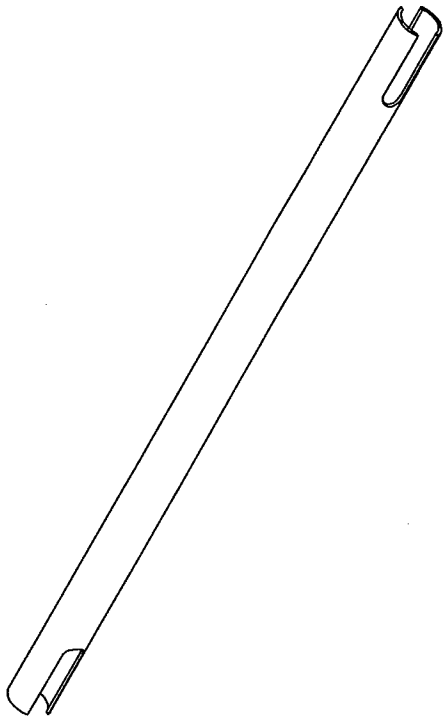
Units: INCHES

Scale: 1:2

Tolerance: ±.01

Date: 4/16/09

Drawn By: MAP



Part Name: Upper Aft A-Arm Tube

Sub Team: Suspension

Next Assembly: 08S04AS4-SS

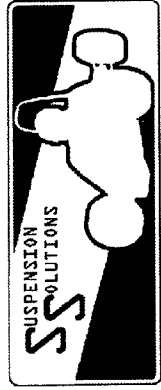
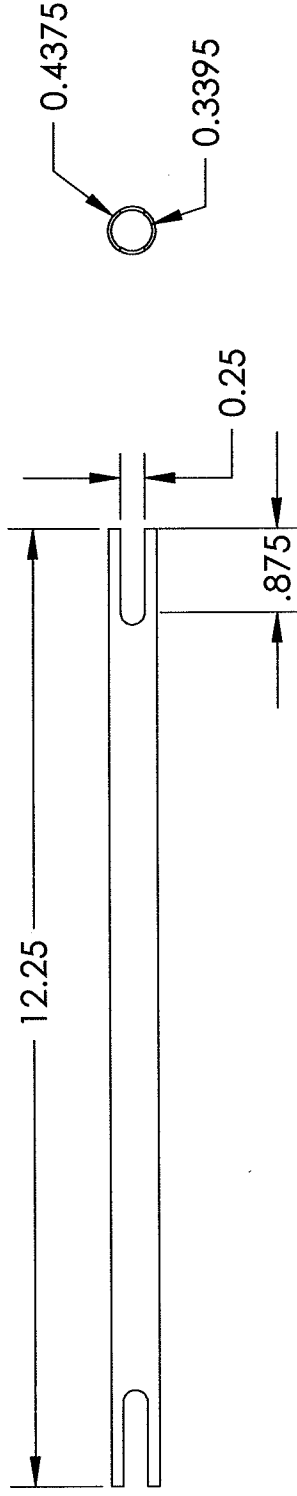
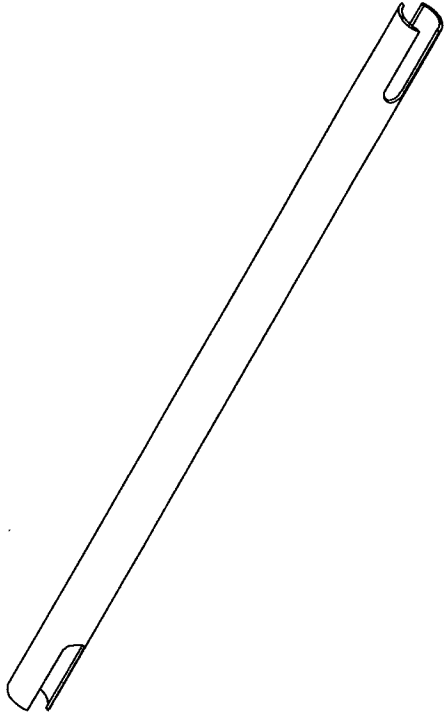
Material: 4130 Steel

Scale: 1:2

Tolerance: ±.01

Date: 4/16/09

Drawn By: MAP



Part Name: Upper Fore A-Arm Tube

Sub Team: Suspension

Next Assembly: 08S04A4-SS

Tolerance: ±.01

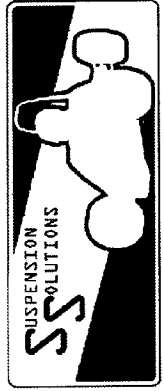
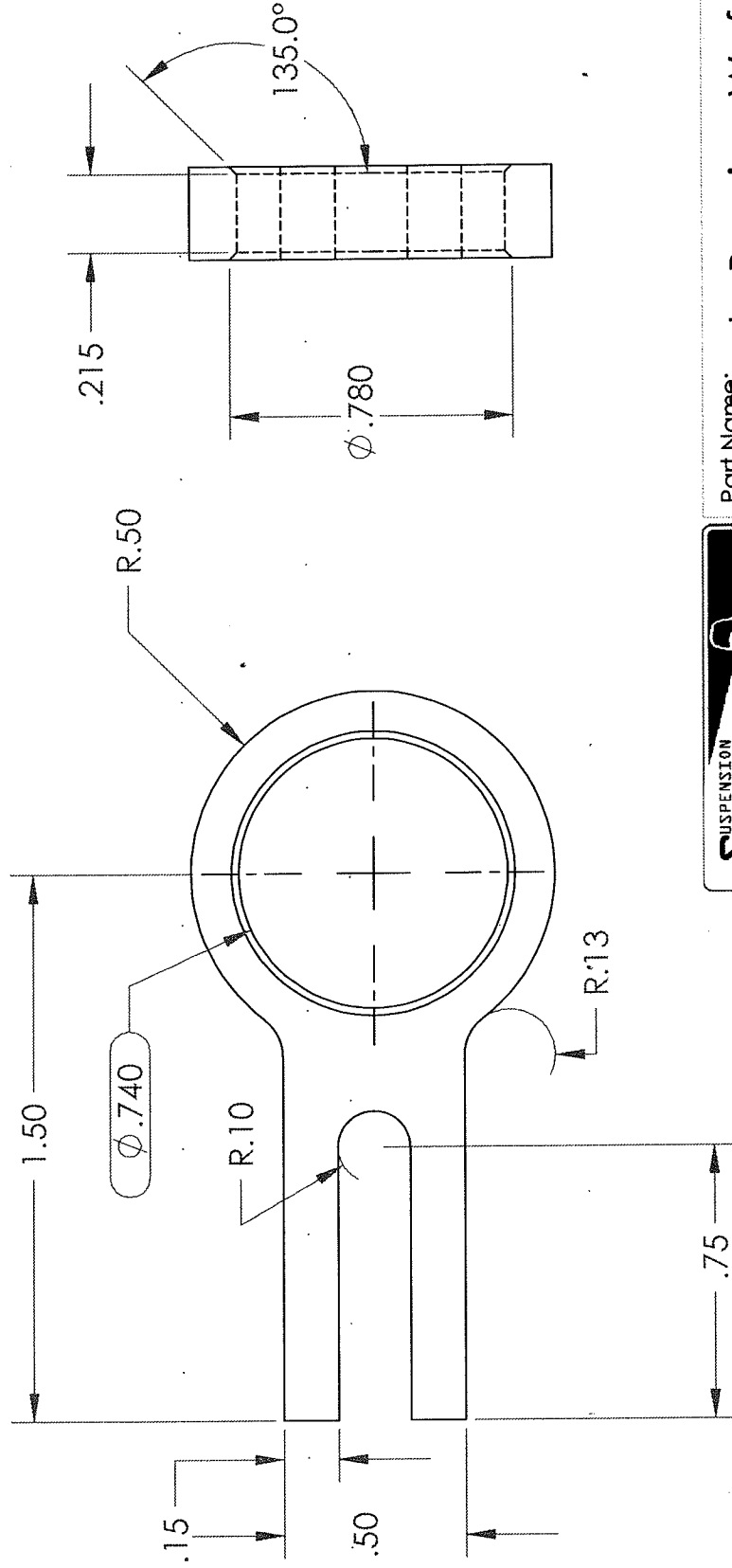
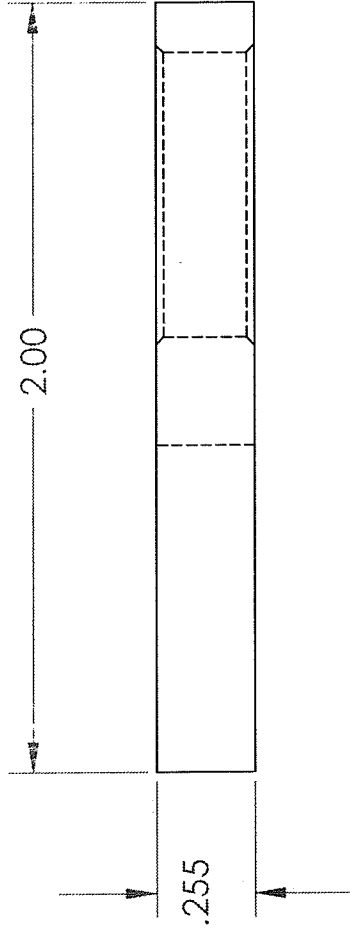
Material: 4130 Steel

Units: INCHES

Scale: 1:2

Date: 4/16/09

Drawn By: MAP



Part Name: Single Bearing Wafer

Sub Team: Suspension

Next Assembly: 08S02AS4-SS

Material: 4130 steel

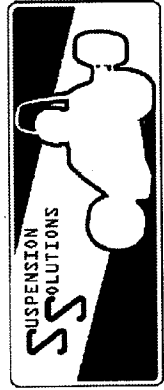
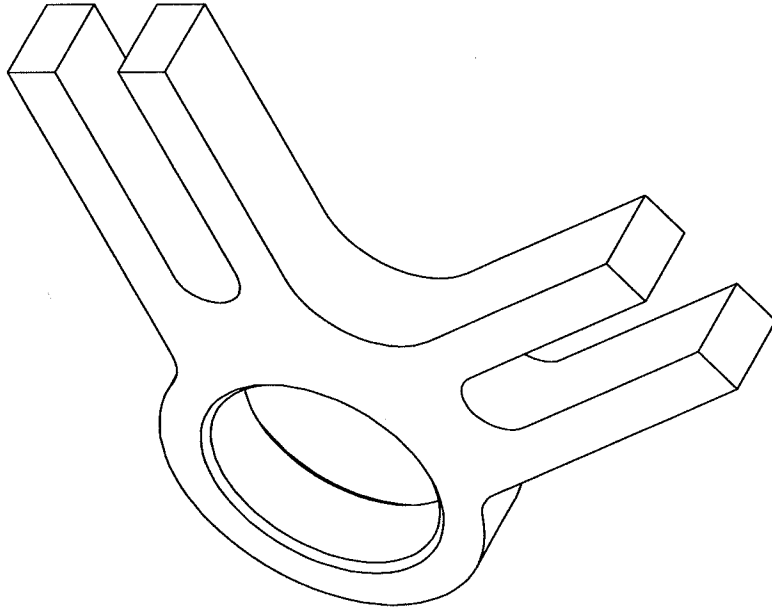
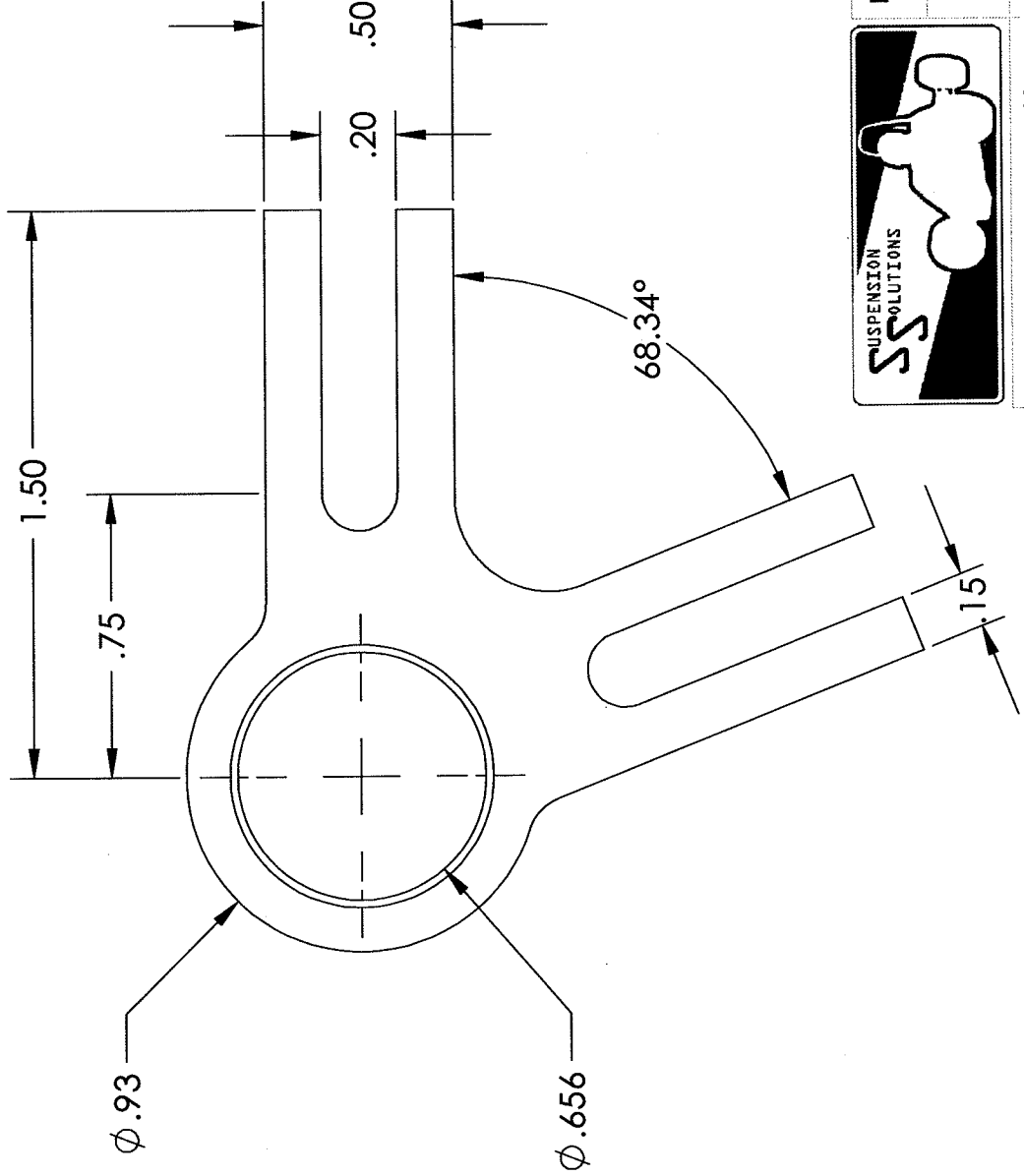
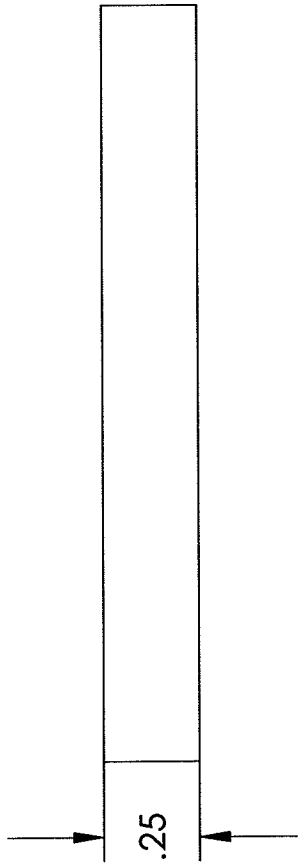
Units: INCHES

Scale: 2:1

Tolerance: $\pm .005$

Date: 3/11/09

Drawn By: DBN



Part Name: Upper Bearing Wafer

Sub Team: Suspension

Next Assembly: 08S02AS4-SS

Material: 4130 Steel

Units: INCHES

Scale: 1:2

Tolerance: ±.01

Date: 4/16/09

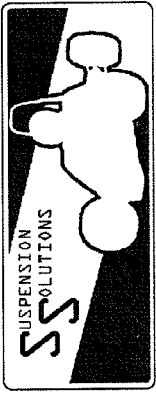
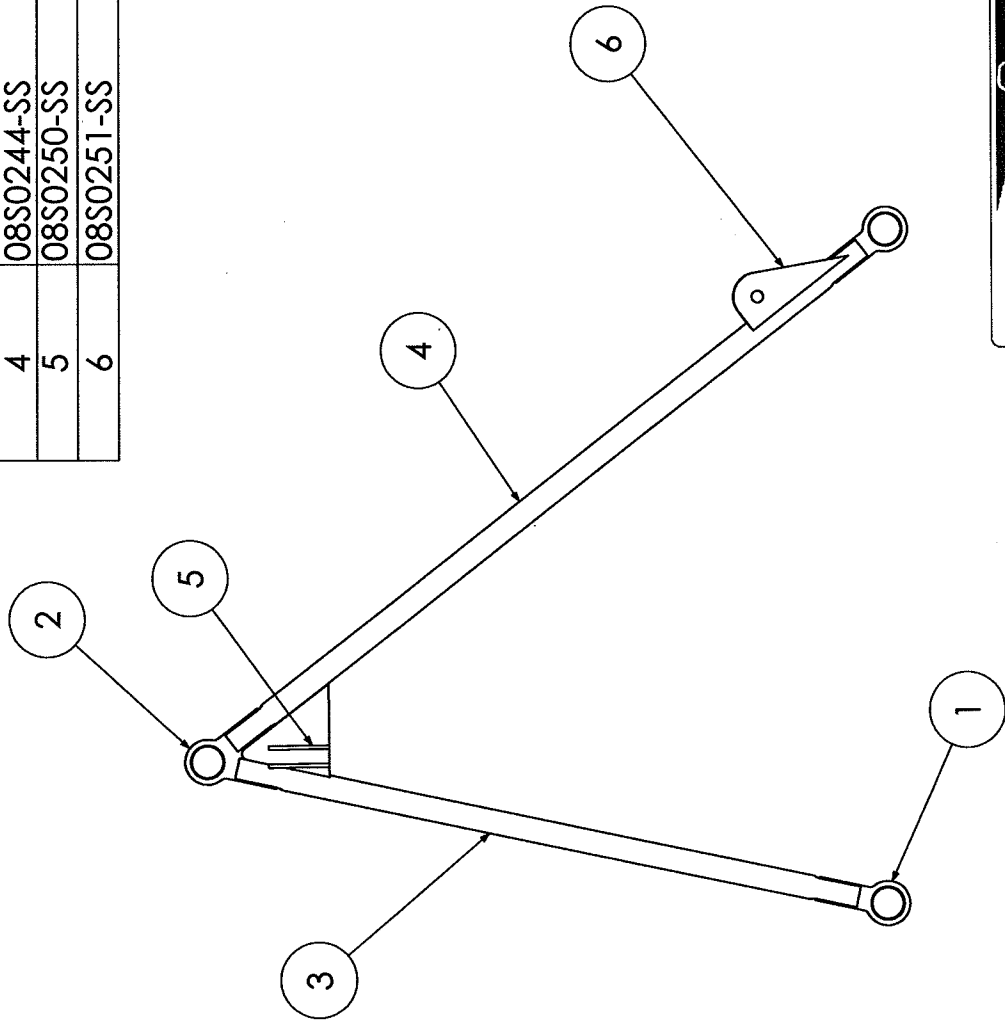
Drawn By: MAP

Caj Poly Formula SAE

Suspension Solutions

Part #: 08S04AS5-33

ITEM NO.	PART NUMBER	DESCRIPTION	QTY.
1	08S0247-SS	Single Bearing Wafer	2
2	08S0249-SS	Lower A-Arm joint bearing wafer	1
3	08S0245-SS	Lower A-Arm aff tube	1
4	08S0244-SS	Lower A-Arm fore Tube	1
5	08S0250-SS	PushRod Mounting Tab left	1
6	08S0251-SS	Tie-Rod Tabs	1



Part Name: Lower A-Arm

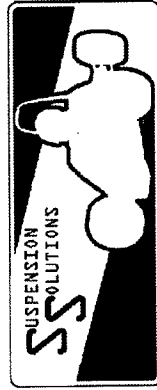
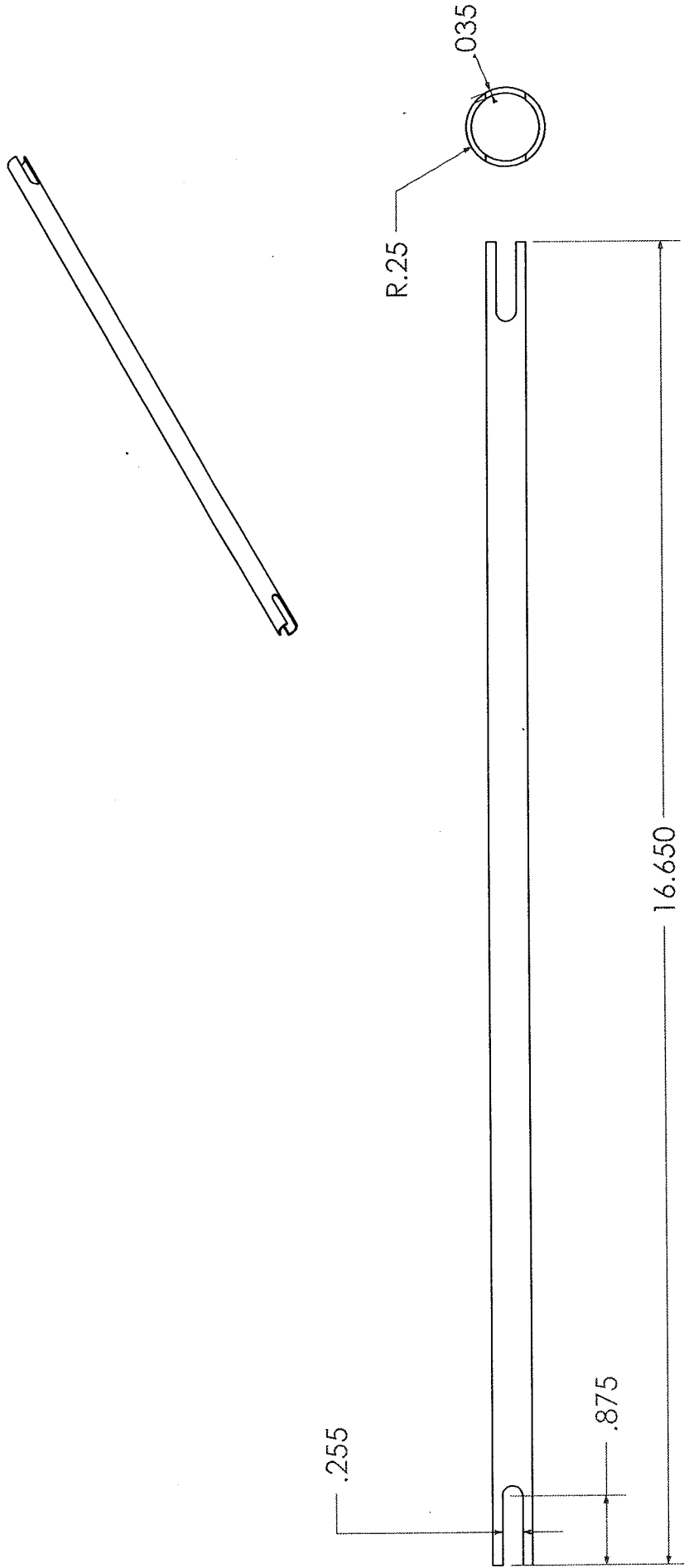
Sub Team: Suspension

Next Assembly: Master Assm

Material: 4130 steel Units: INCHES Scale: 1:2

Tolerance: ±.01

Date: 4/15/09 Drawn By: DBN



Part Name: Lower A-Arm fore tube

Sub Team: Suspension

Next Assembly: 08S04AS5-SS

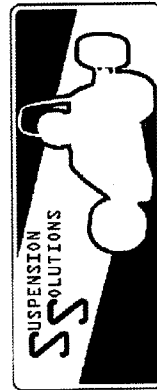
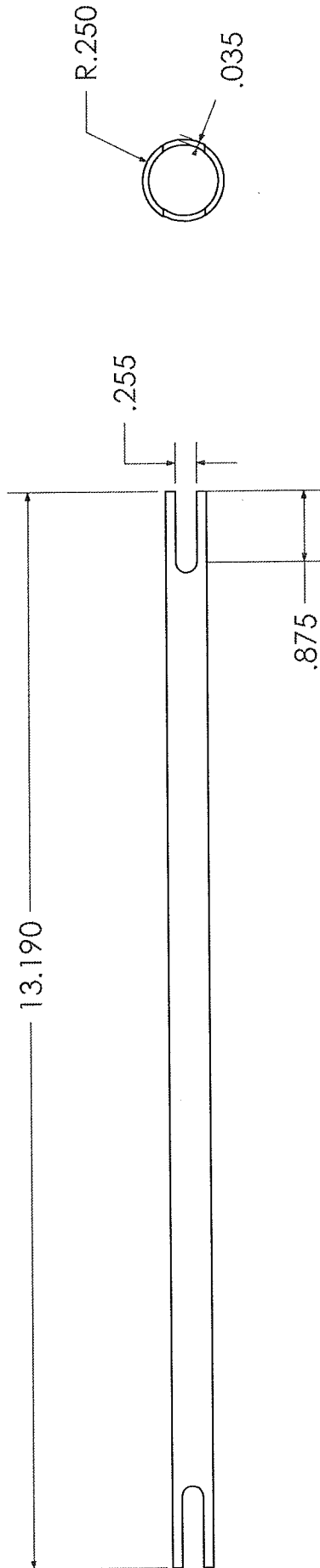
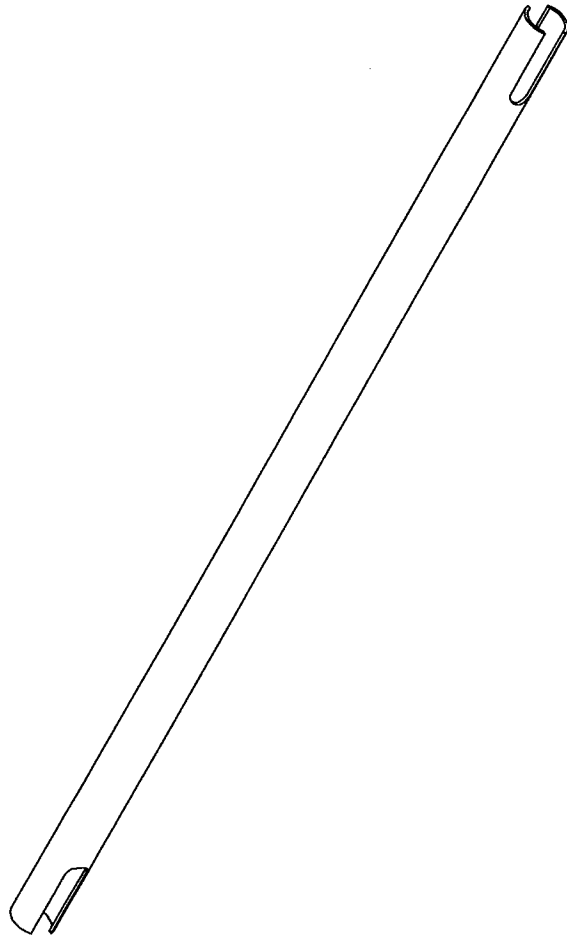
Material: 4130 steel

Scale: 1:2

Tolerance: ±.01

Date: 4/15/09

Drawn By: DBN



Part Name:

Lower A-Arm aft tube

Sub Team:

Suspension

Next Assembly: 08S04AS5-SS

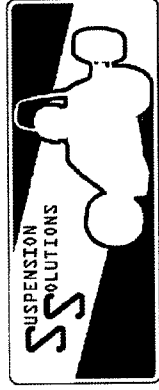
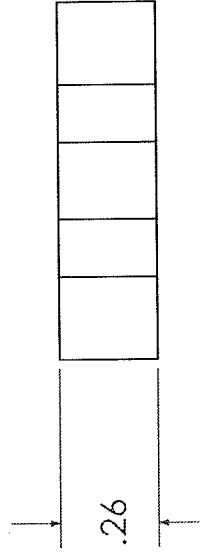
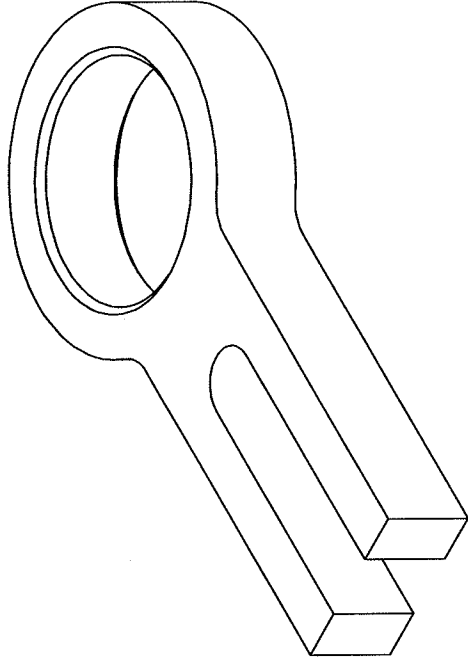
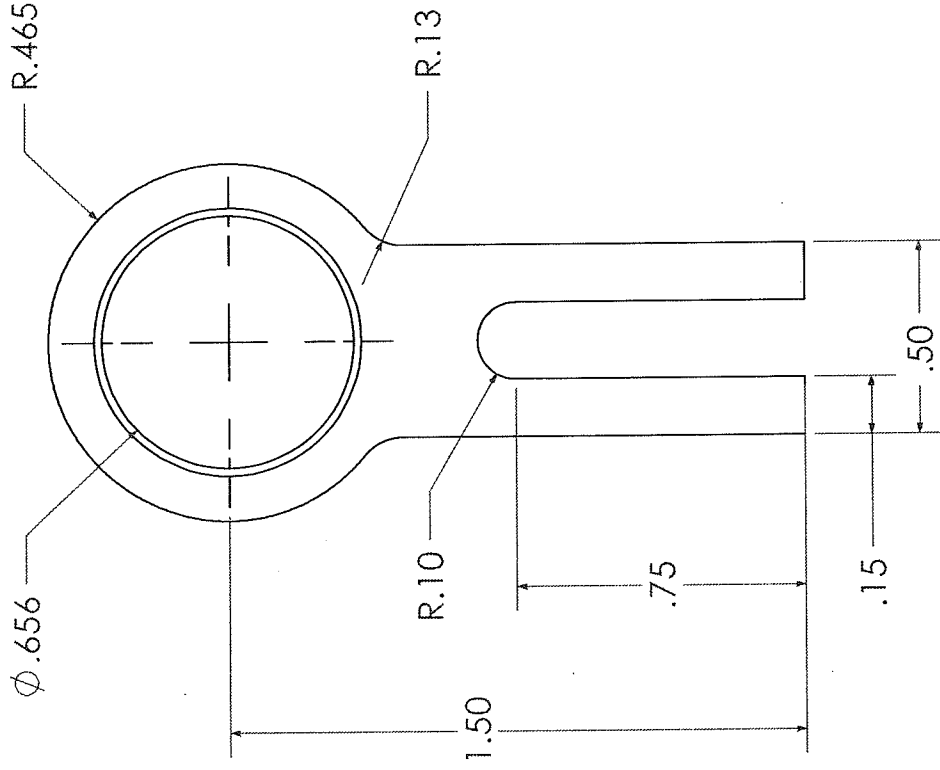
Material: 4130 steel

Scale: 1:2

Tolerance: ±.01

Date: 4/15/09

Drawn By: DBN



Part Name: Single Bearing Waffer

Sub Team: Suspension

Next Assembly: 08S04AS5-SS

Material: 4130 steel

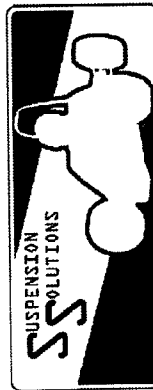
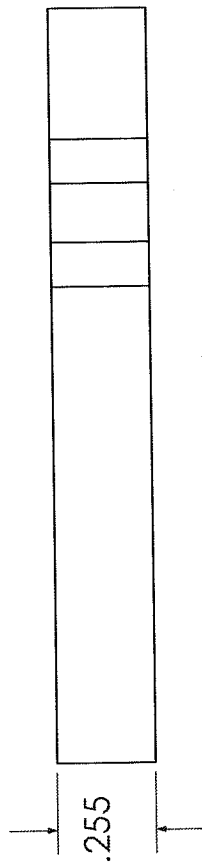
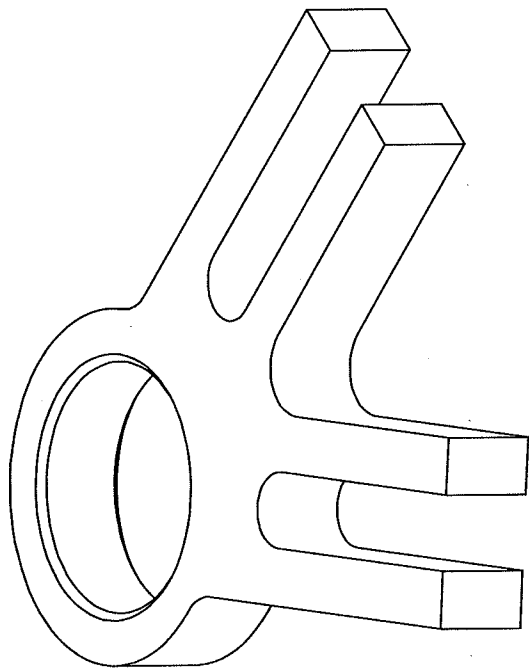
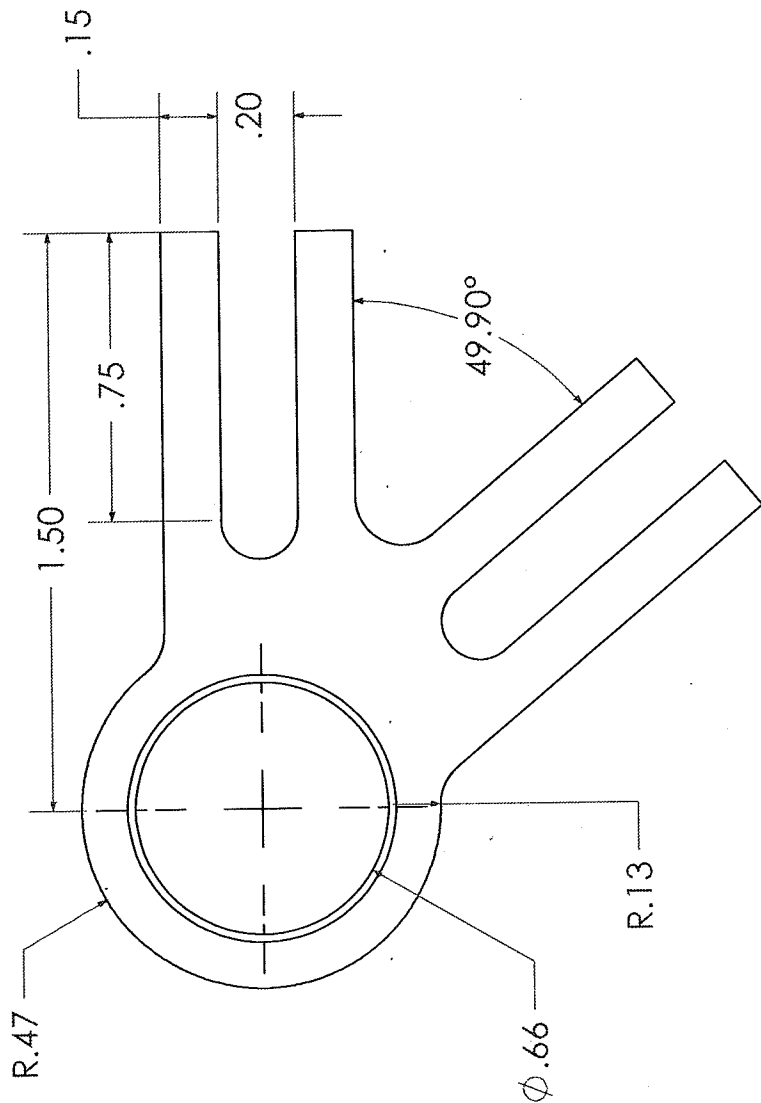
Units: INCHES

Scale: 2:1

Tolerance: $\pm .01$

Date: 4/15/09

Drawn By: DBN



Part Name: LAA Joint Bearing Waffle

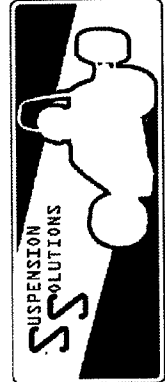
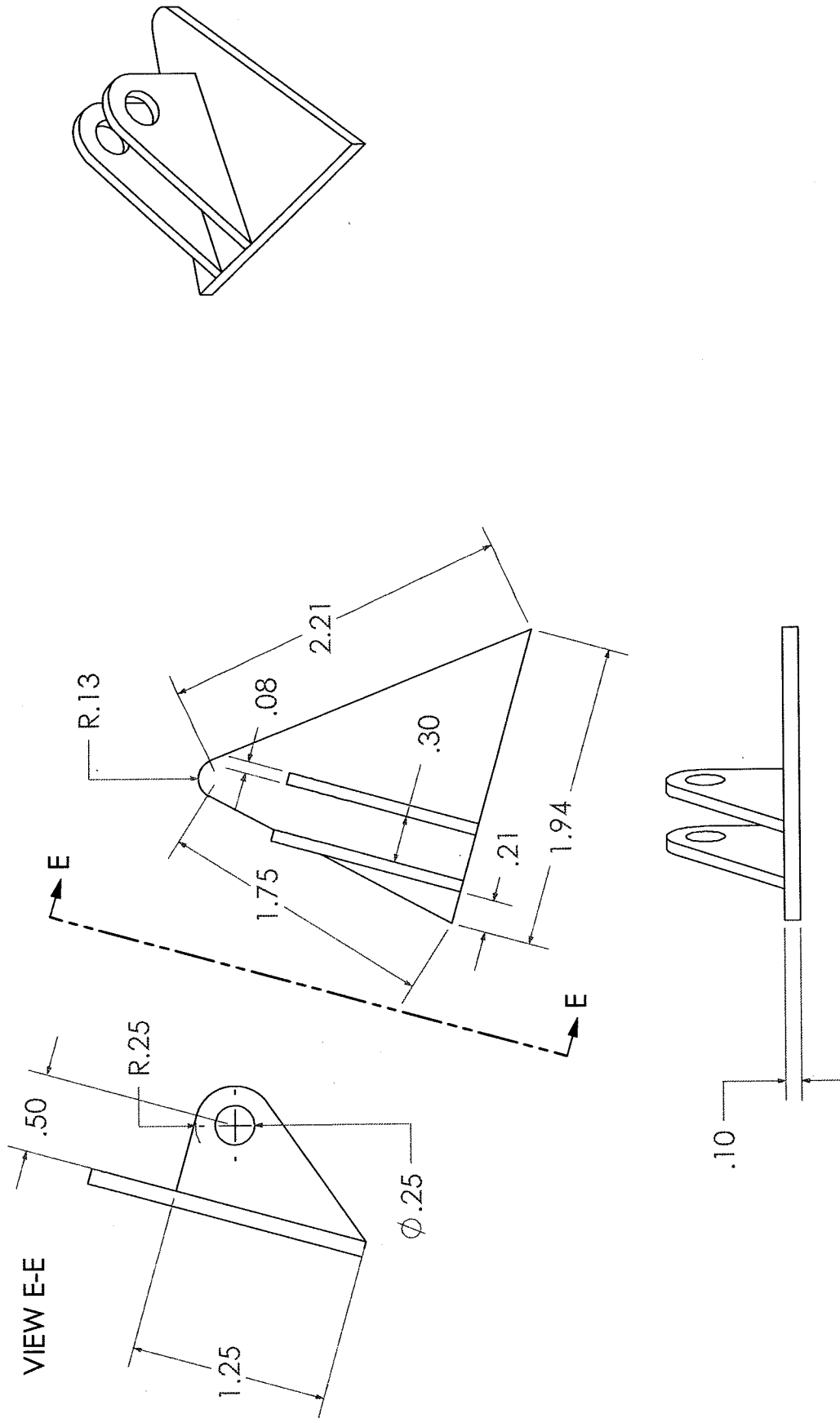
Sub Team: Suspension

Material: 4130 steel Units: INCHES Scale: 2:1

Date: 4/15/09 Drawn By: DBN

Next Assembly: 08S04AS5-SS

Tolerance: ±.01



Part Name: Push Rod Mounting Tabs

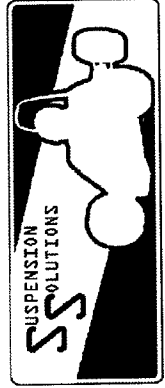
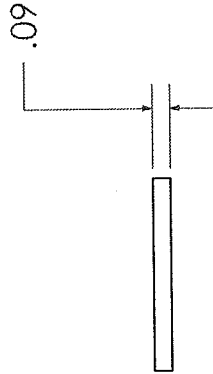
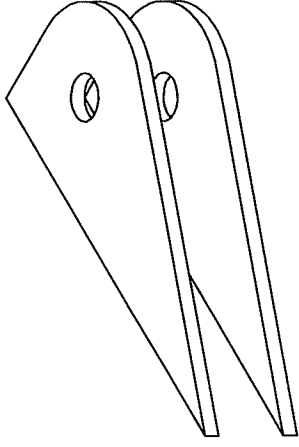
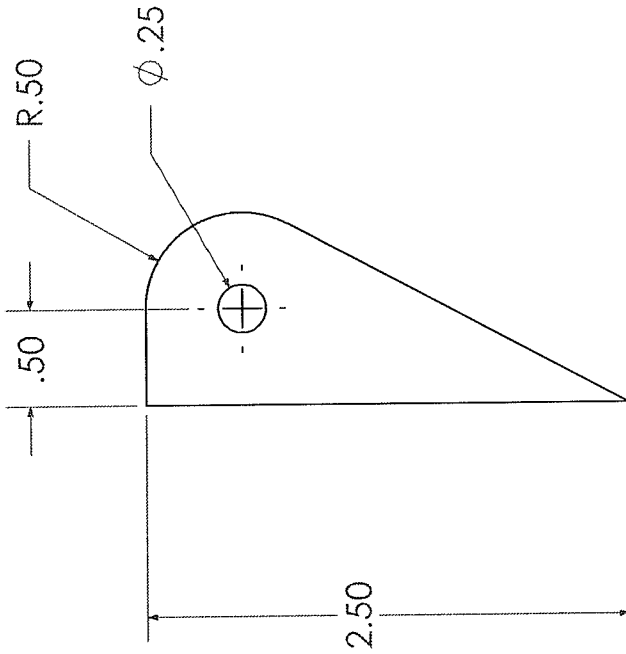
Sub Team: Suspension

Next Assembly: 08S04AS5-SS

Material: 4130 steel Units: INCHES Scale: 1:1

Tolerance: ±.01

Date: 4/15/09 Drawn By: DBN



Next Assembly: 08S04AS5-SS

Tolerance: $\pm .01$

Part Name: Tie Rod Mounting Tabs

Sub Team: Suspension

Material: 4130 steel

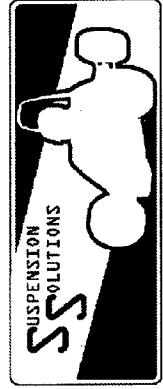
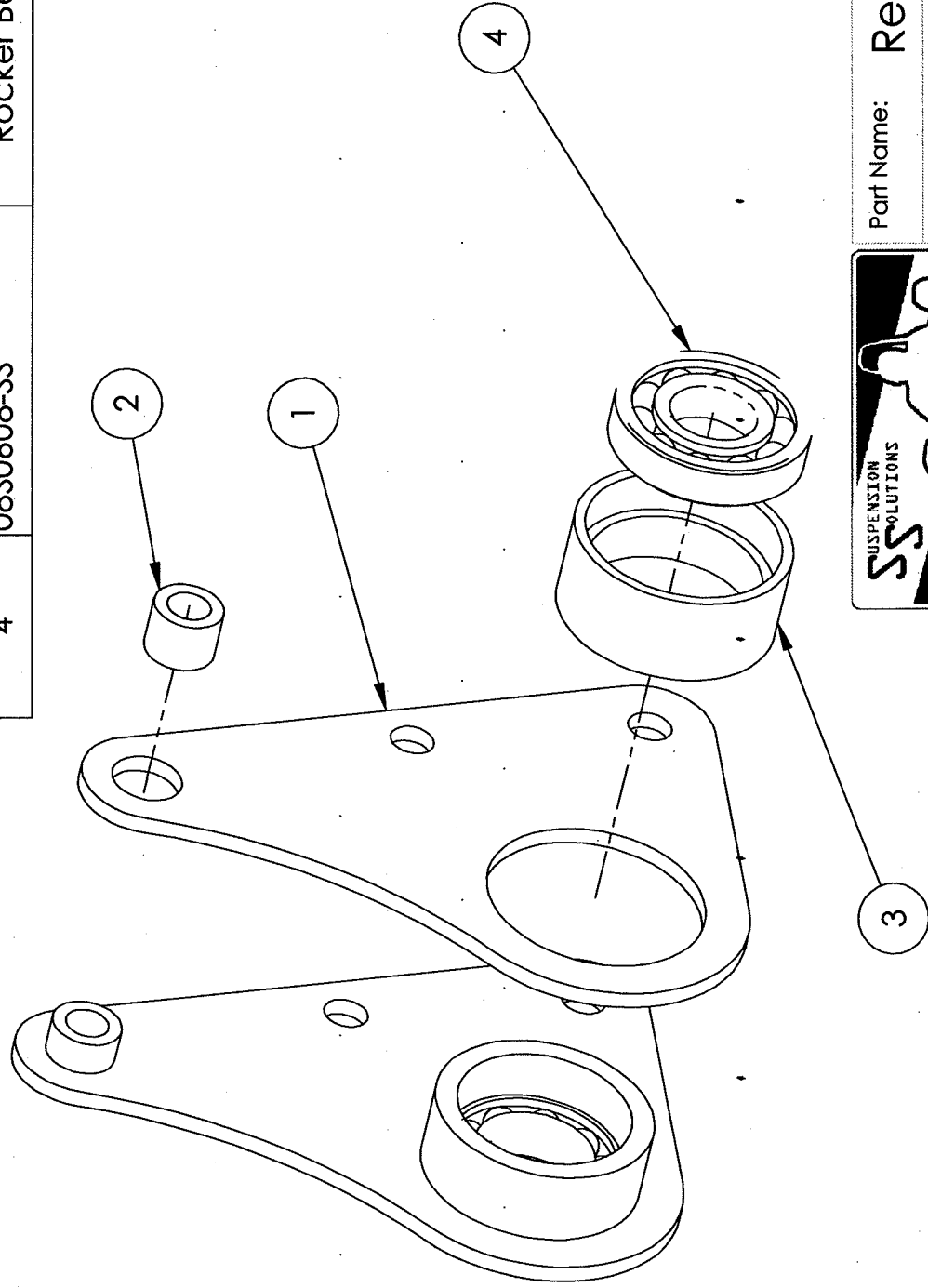
Scale: 1:1

Units: INCHES

Date: 4/15/09

Drawn By: DBN

ITEM NO.	PART NUMBER	DESCRIPTION	QTY.
1	08S0601-SS	Rocker Plate	2
2	08S0606-SS	steel rocker shock bolt insert	2
3	08S0607-SS	Rocker Bearing Insert	2
4	08S0608-SS	Rocker Bearing .5 x .1.125	2



Part Name: Rear Rocker Assembly

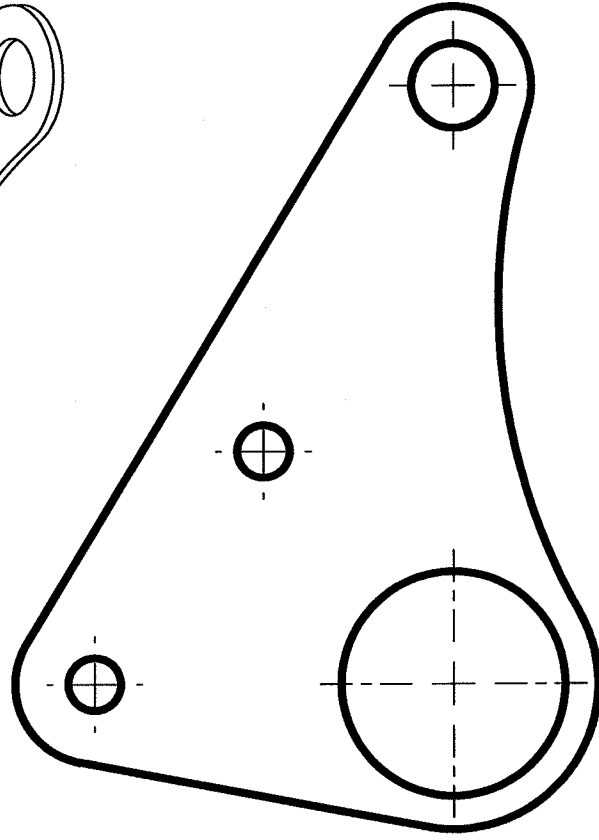
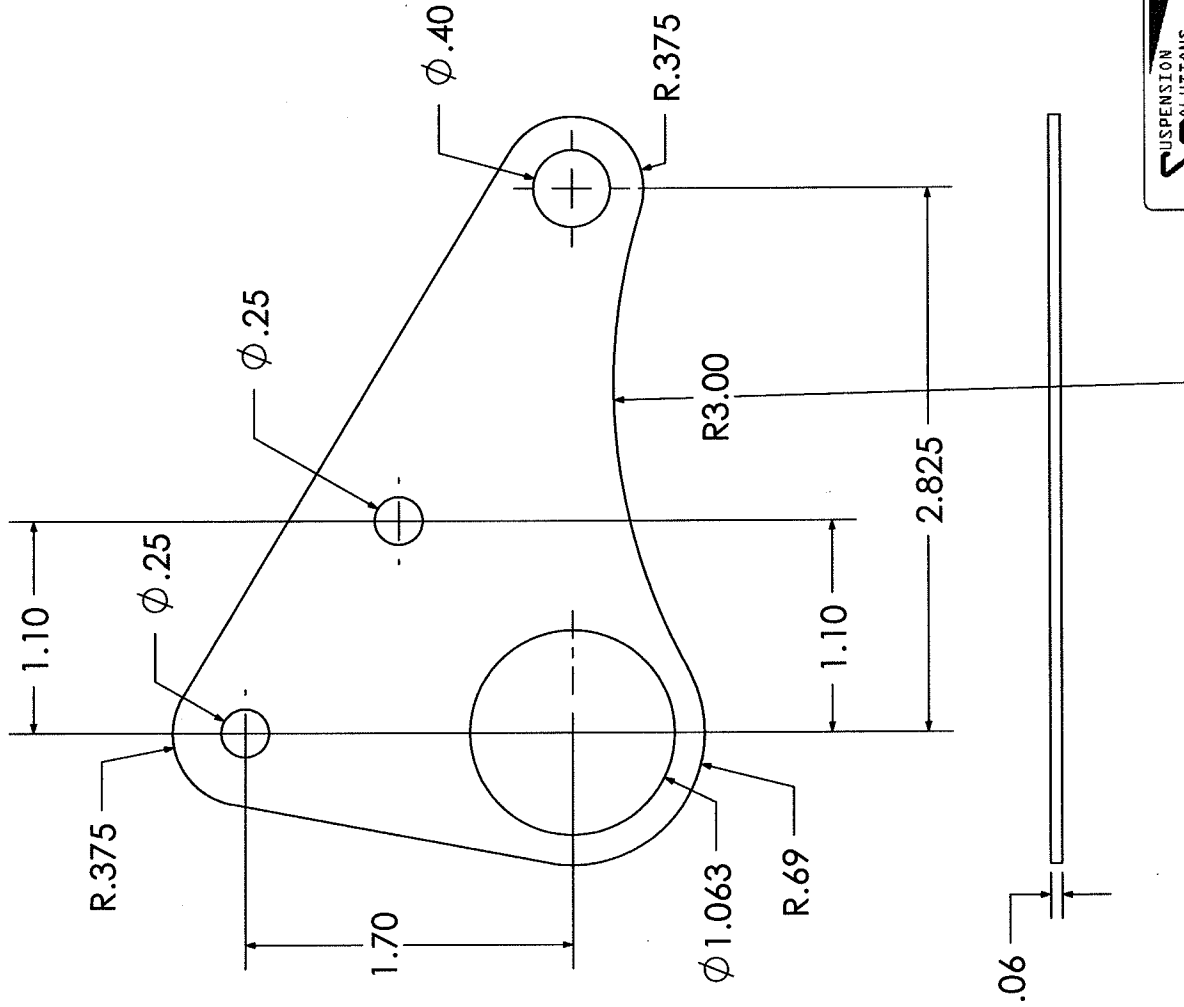
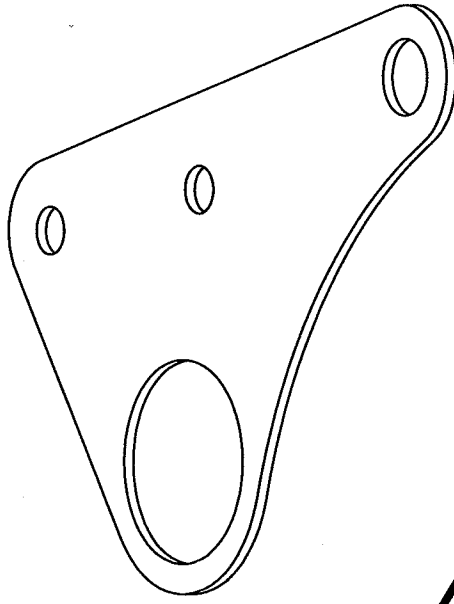
Sub Team: Suspension

Material: MATRL' Units: INCHES Scale: 1:1

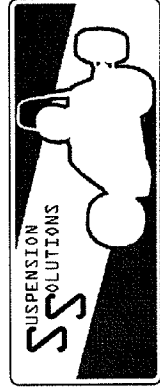
Date: 3/11/09 Drawn By: DBN

Next Assembly: #####

Tolerance: ±.01



1:1:1 scale for plazma cutter



Part Name: **Rocker Plate**

Sub Team: **Suspension**

Next Assembly: 08S06AS1-SS

Material: 4130 steel

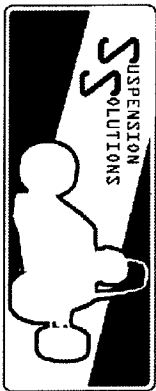
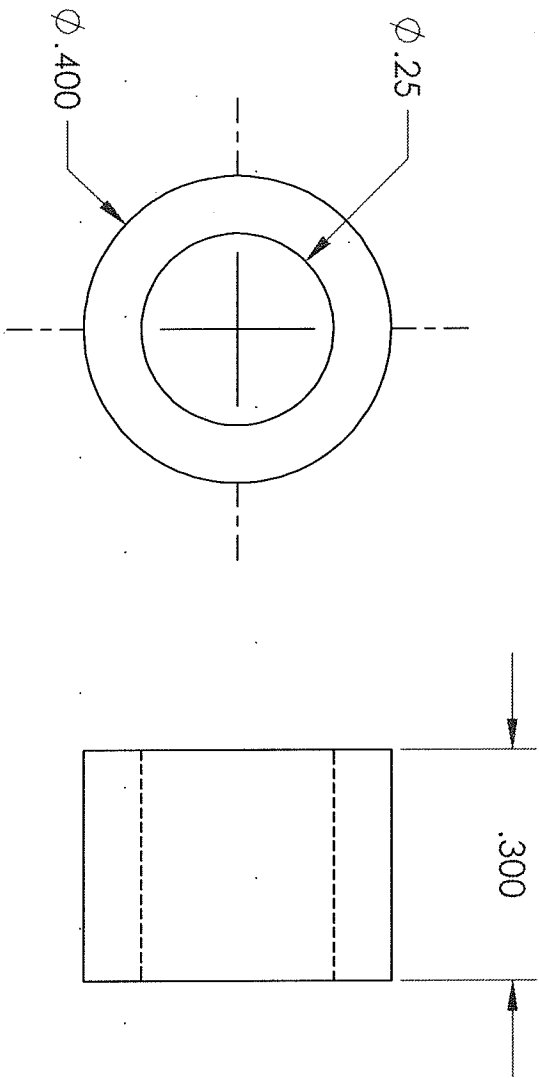
Units: INCHES

Scale: 1:1

Tolerance: $\pm .005$

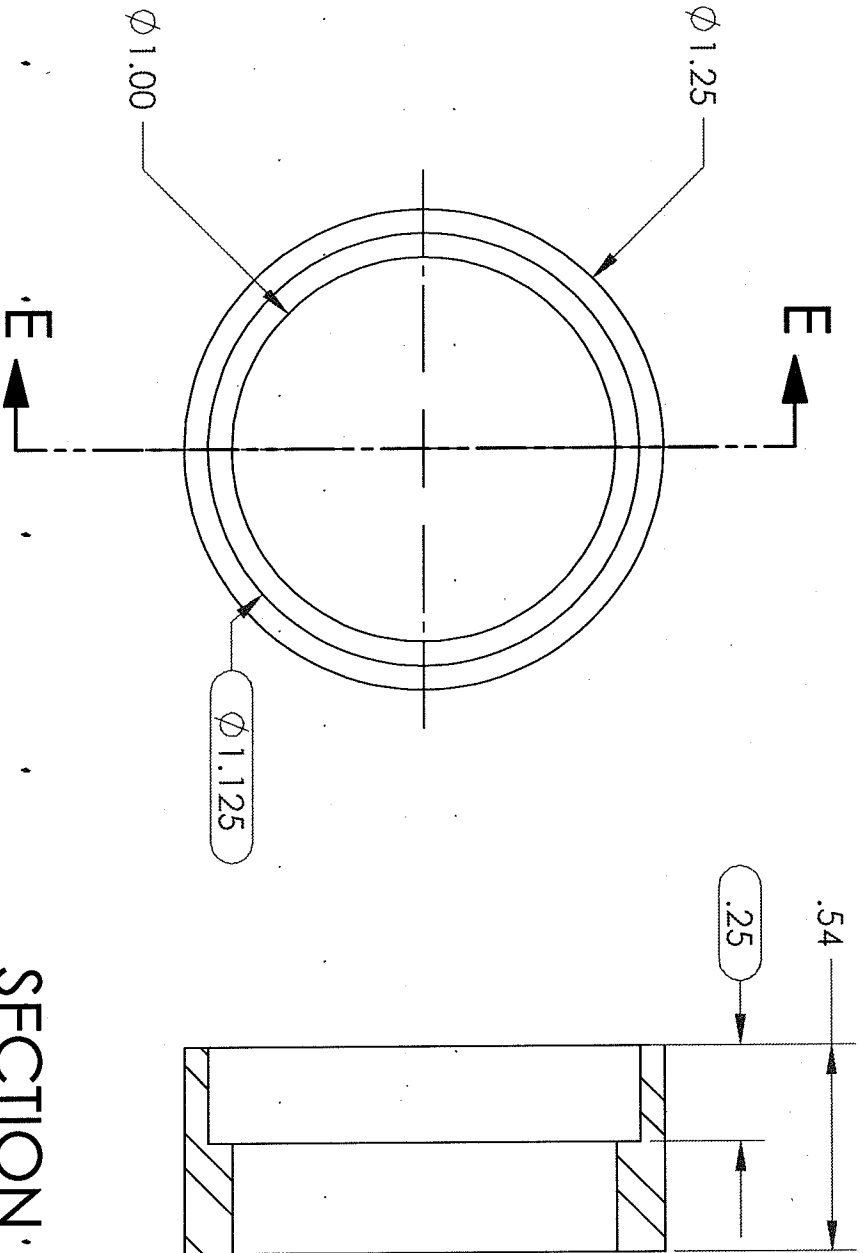
Date: 4/15/09

Drawn By: DBN



Part Name: **Rear Rocker shock bolt insert**
Sub Team: **Suspension**

Next Assembly: 08S06AS4-SS	Material: 4130 steel	Units: INCHES	Scale: 4:1
Tolerance: ±.01	Date: 3/11/09	Drawn By: DBN	

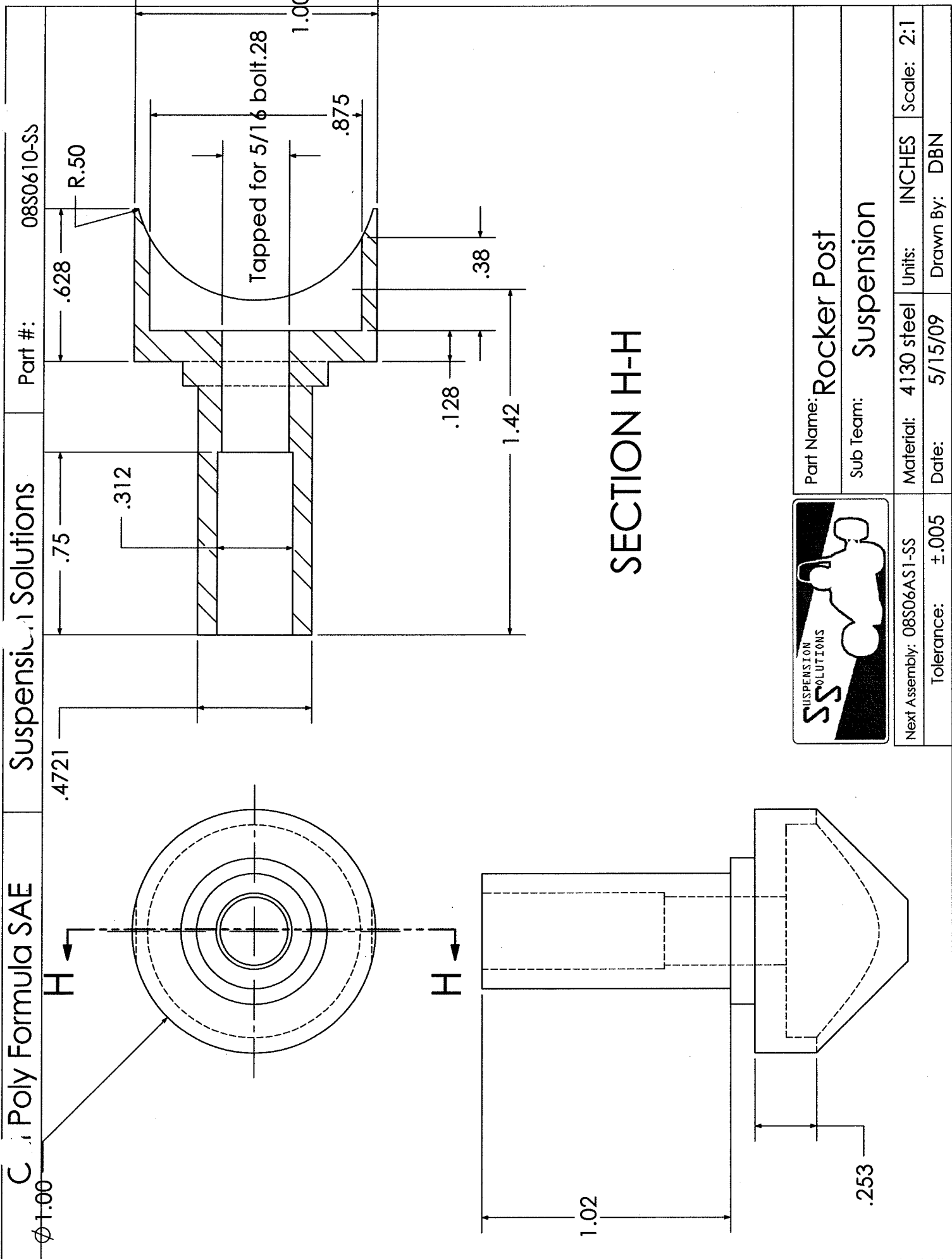


SECTION E-E

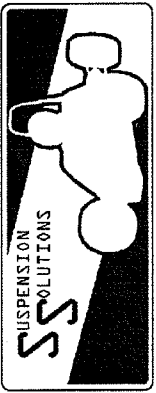


Part Name: Rear Rocker Bearing Insert
Sub Team: Suspension

Next Assembly: 08S06AS4-SS	Material: 4130 steel	Units: INCHES	Scale: 2:1
Tolerance: $\pm .01$	Date: 3/11/09	Drawn By: DBN	



SECTION H-H

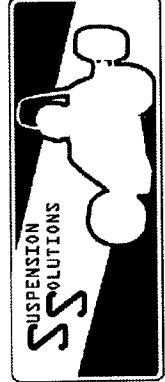
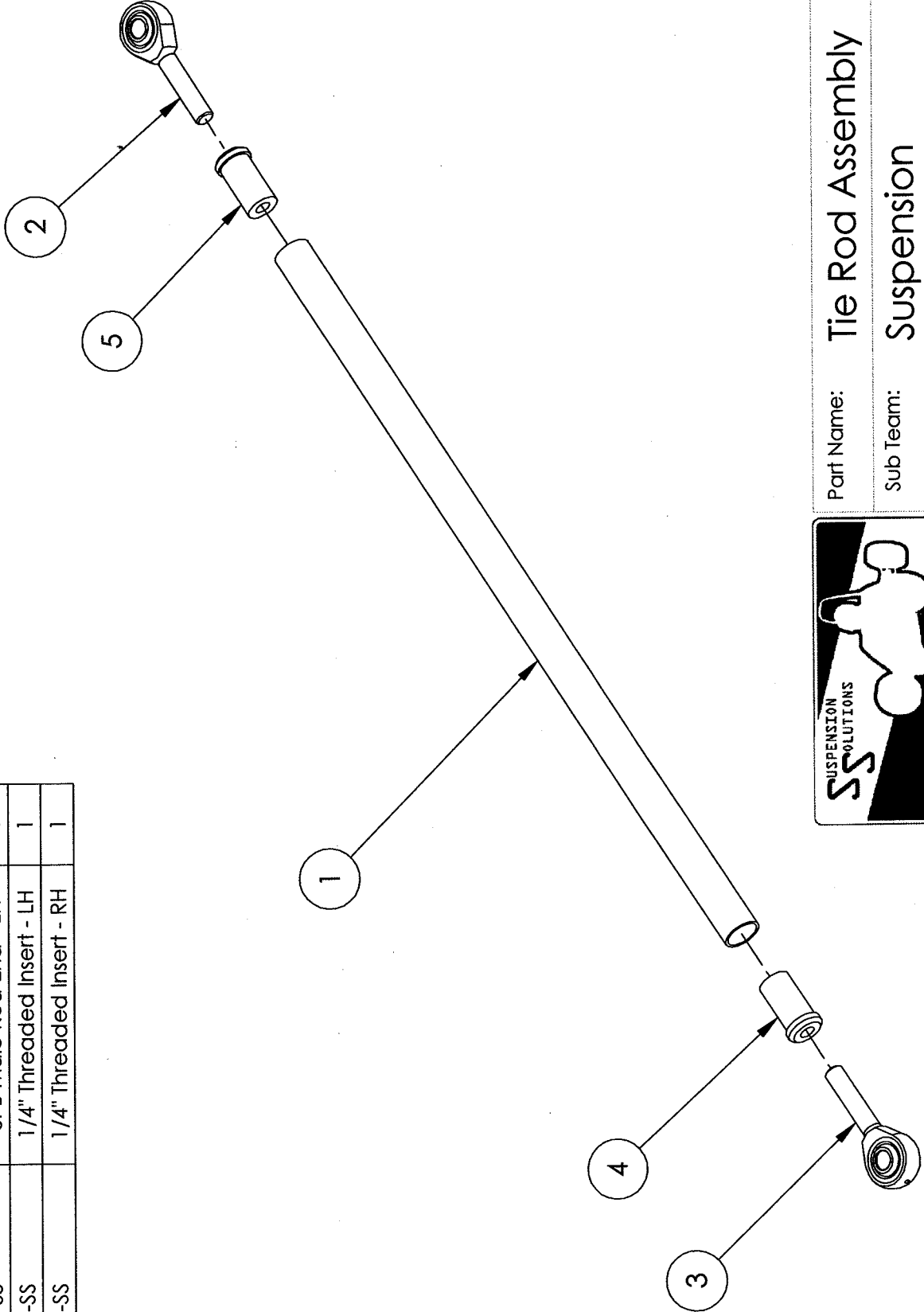


Part Name: Rocker Post	
Sub Team: Suspension	
Next Assembly: 08S06AS1-SS	Material: 4130 steel
Tolerance: $\pm .005$	Units: INCHES
Date: 5/15/09	Scale: 2:1
	Drawn By: DBN

al Poly Formula SAE Suspension Solutions

Part #: 08S04AS6-SS

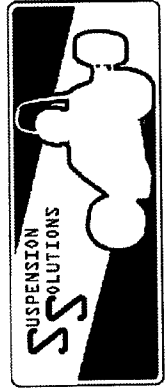
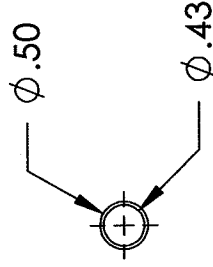
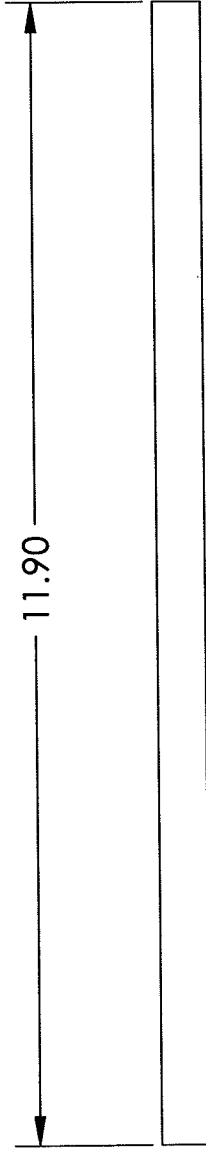
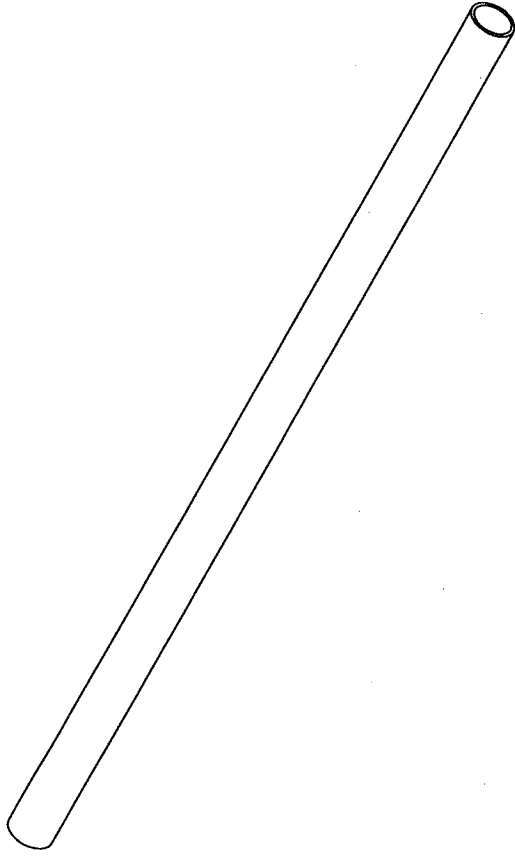
ITEM NO.	PART NUMBER	DESCRIPTION	QTY.
1	08S0243-SS	Tie Rod Tube	1
2	08S0802-SS	SPM Male Rod End - RH	1
3	08S0805-SS	SPB Male Rod End - LH	1
4	08S0252-SS	1/4" Threaded Insert - LH	1
5	08S0251-SS	1/4" Threaded Insert - RH	1



Part Name: Tie Rod Assembly
 Sub Team: Suspension

Next Assembly: Master ASM
 Tolerance: ±.01

Material: UNK
 Date: 4/16/09
 Units: INCHES
 Drawn By: MAP
 Scale: 1:2



Next Assembly: 08S04AS6-SS

Tolerance: $\pm .01$

Part Name: Tie Rod Tube

Sub Team: Suspension

Material: 4130 Steel

Scale: 1:2

Date: 4/16/09

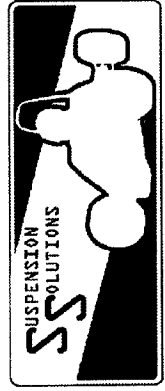
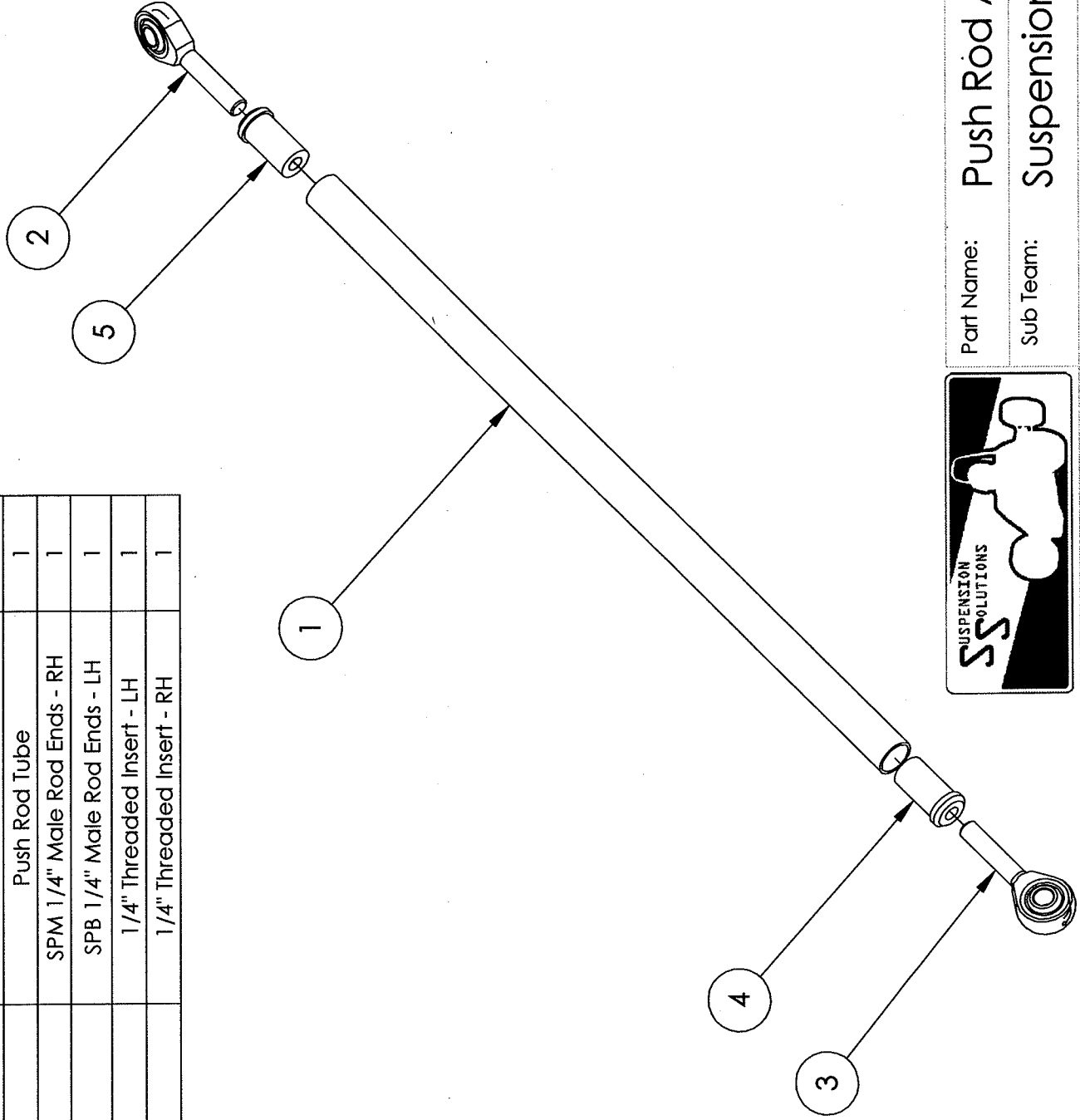
Units: INCHES

Drawn By: MAP

al Poly Formula SAE Suspension Solutions

Part #: 08S04AS7-SS

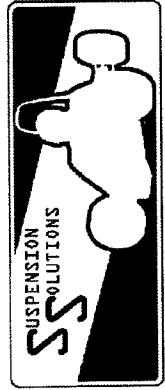
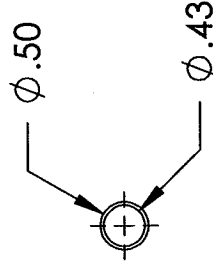
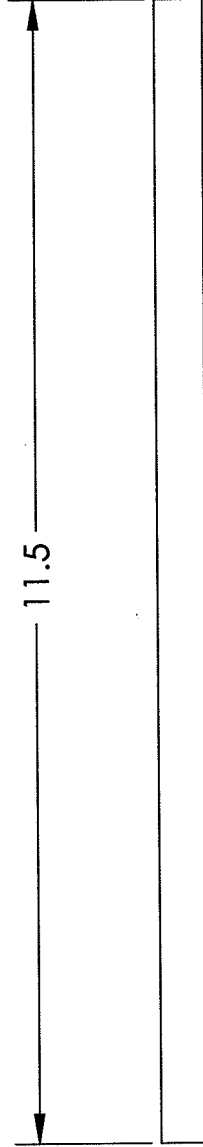
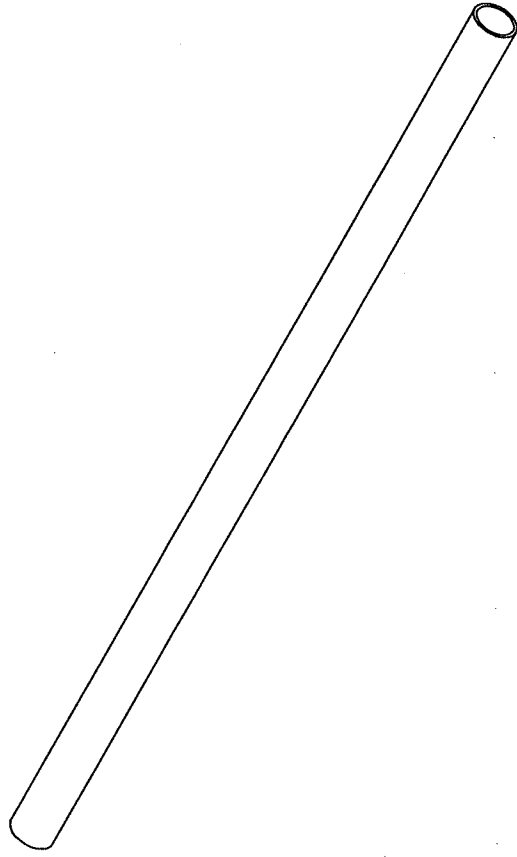
ITEM NO.	PART NUMBER	DESCRIPTION	QTY.
1	08S0246-SS	Push Rod Tube	1
2	08S0802-SS	SPM 1/4" Male Rod Ends - RH	1
3	08S0805-SS	SPB 1/4" Male Rod Ends - LH	1
4	08S0252-SS	1/4" Threaded Insert - LH	1
5	08S0251-SS	1/4" Threaded Insert - RH	1



Part Name: Push Rod Assembly

Sub Team: Suspension

Next Assembly: Master ASM
 Tolerance: ±.01
 Material: INCHES
 Date: 4/16/09
 Units: INCHES
 Scale: 1:2
 Drawn By: MAP



Part Name: Push Rod Tube

Sub Team: Suspension

Next Assembly: 08S04AS7-SS

Material: 4130 Steel

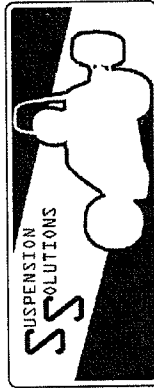
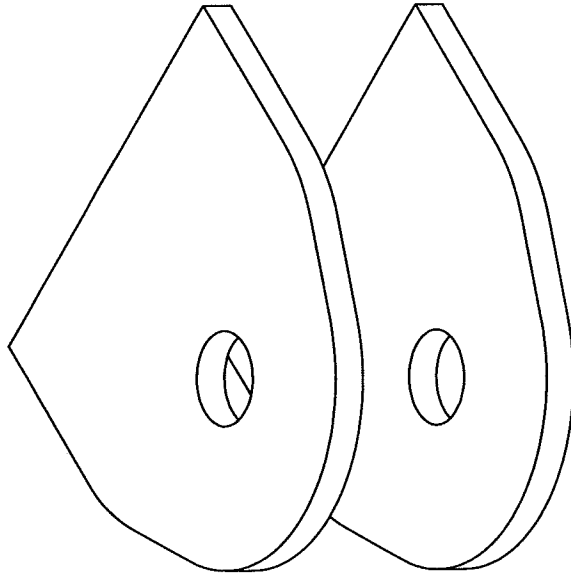
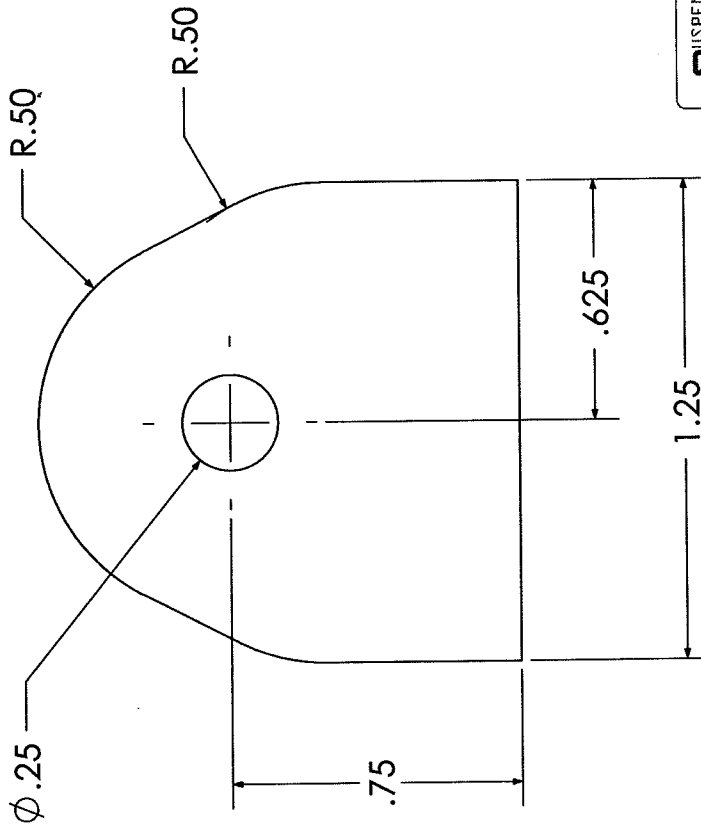
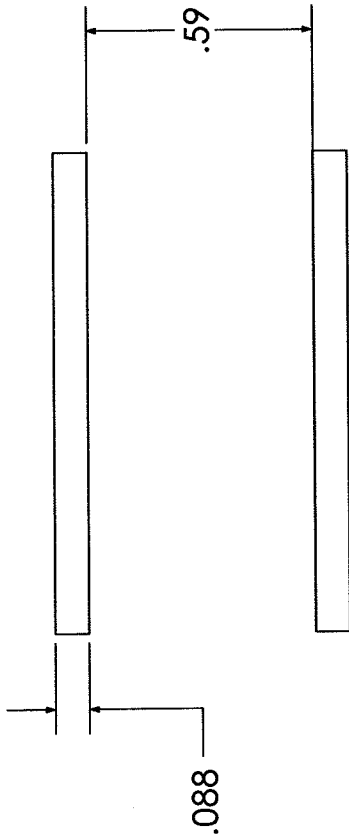
Scale: 1:2

Tolerance: $\pm .01$

Date: 4/16/09

Drawn By: MAP

Units: INCHES



Part Name: Suspension pick up tab

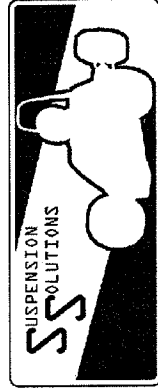
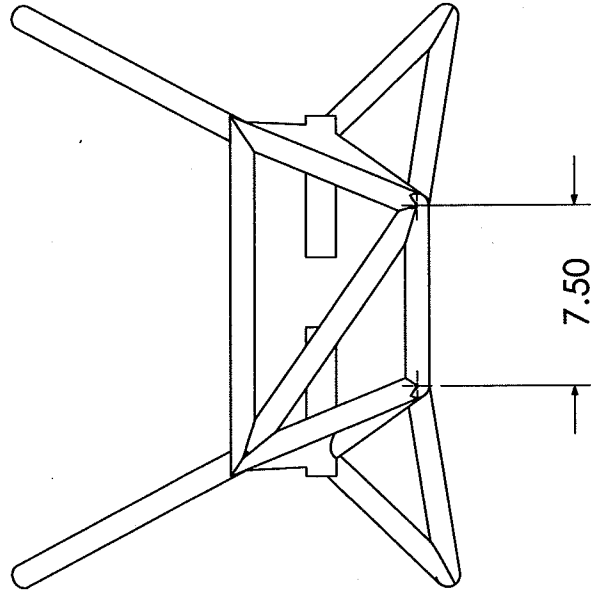
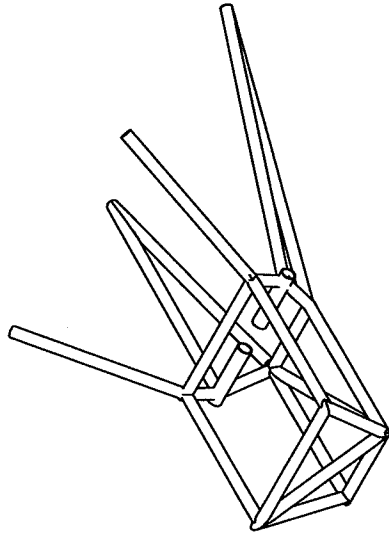
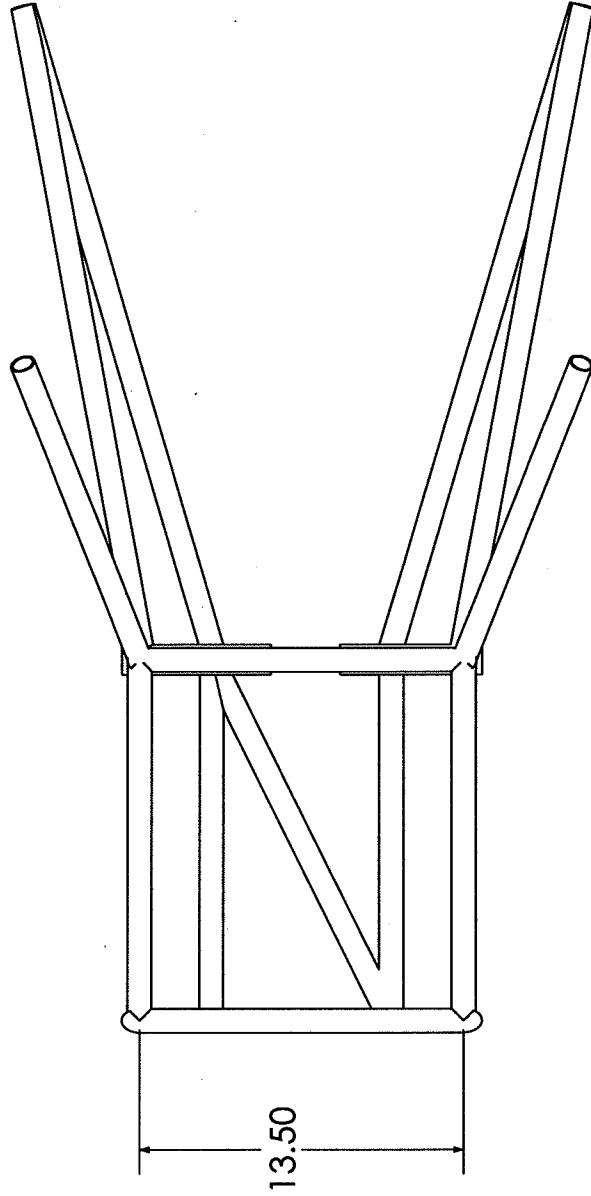
Sub Team: Chassis

Next Assembly: MasterAssm

Material: 4130 steel Units: INCHES Scale: 2:1

Tolerance: $\pm .01$

Date: 4/15/09 Drawn By: DBN



Part Name: Rear Frame Addition

Sub Team: Chassis

Next Assembly: MasterAsm

Material: 4130 steel

Tolerance: $\pm .150$

Date: 4/15/09

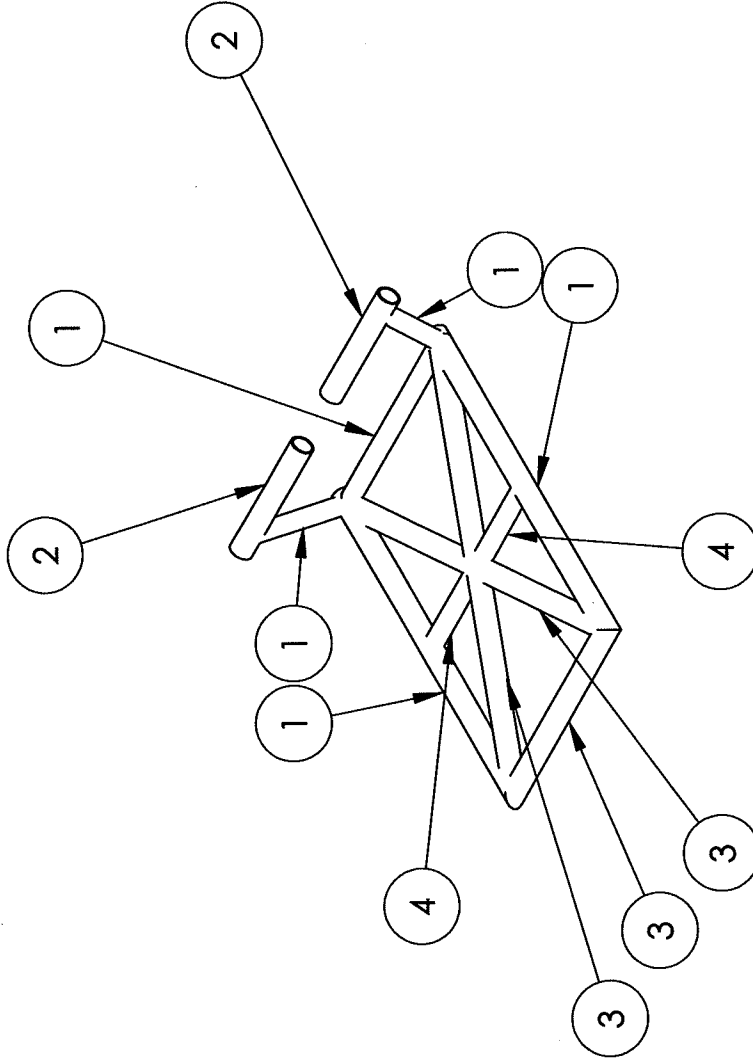
Units: INCHES

Scale: 1:8

Drawn By: DBN

Manufacturing Note: Sheet 2 of 5

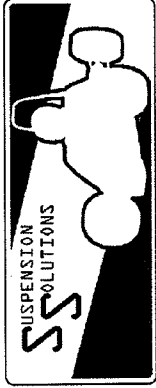
Phase 1: Cut and Notch rear tray tubes as pictured below
 Notch and place outer rectangle first then add inner members
 Mock up Old rear frame and engine to position Engine pick up tubes



NOTE: FRAME OVERAL GEOMETRY CHANGED BUT
 TUBE SIZES FOLLOW THESE DWGS

Tubing Sizes:

- 1: 1.0in O.D. by .87in I.D.
- 2: 1.0in O.D. by .75in I.D.
- 3: 1.0in O.D. by .93in I.D.
- 4: .75in O.D. by .6125in I.D.



Part Name: Rear Frame Adaptation

Sub Team: Chassis

Next Assembly: MasterASM

Material: 4130 Tubing

Scale: 1:8

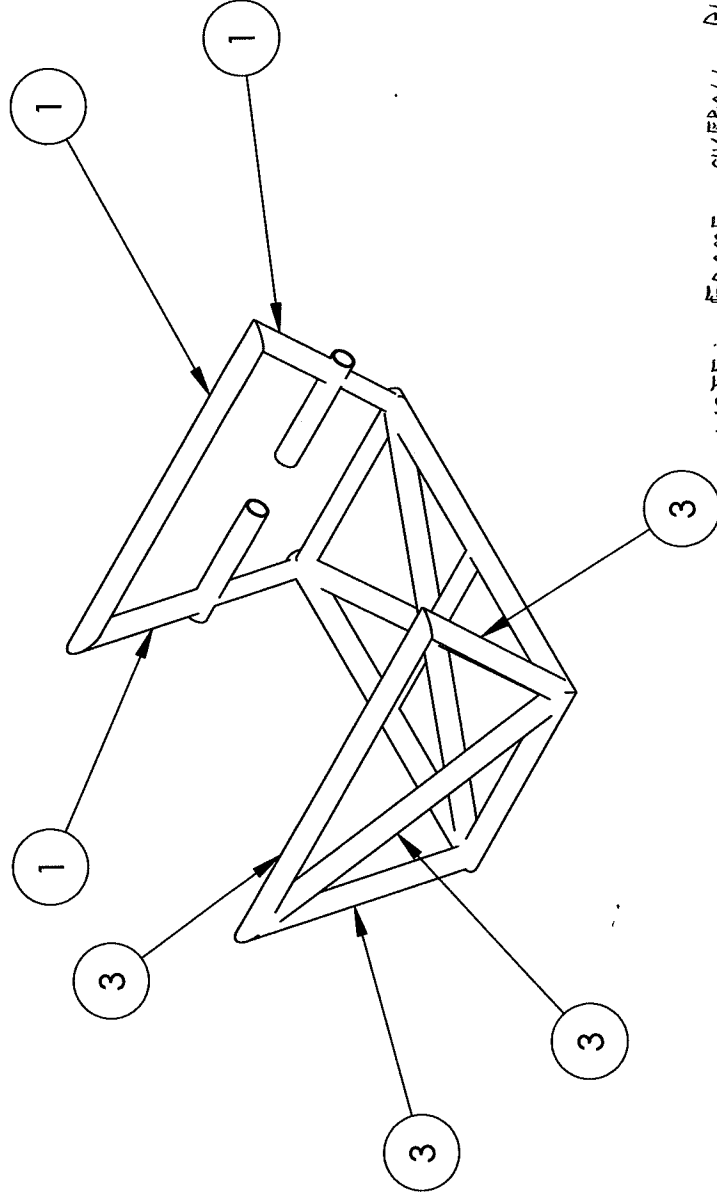
Tolerance: ±.01

Date: 3/11/09

Drawn By: DBN

Manufacturing Note: Sheet 3 of 5

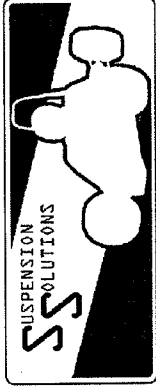
Phase 2: Added Trapezoid front and back planes as pictured below
Notch and place outer trapezoid first then add inner members



NOTE: FRAME OVERALL DIMENSIONS CHANGED BUT
TUBE SIZES FOLLOW THESE QW&G

Tubing Sizes:

- 1: 1.0in O.D. by .87in I.D.
- 2: 1.0in O.D. by .75in I.D.
- 3: 1.0in O.D. by .93in I.D.
- 4: .75in O.D. by .6125in I.D.



Part Name: Rear Frame Adaptation

Sub Team: Chassis

Next Assembly: MasterASM

Material: 4130 Tubing

Scale: 1:8

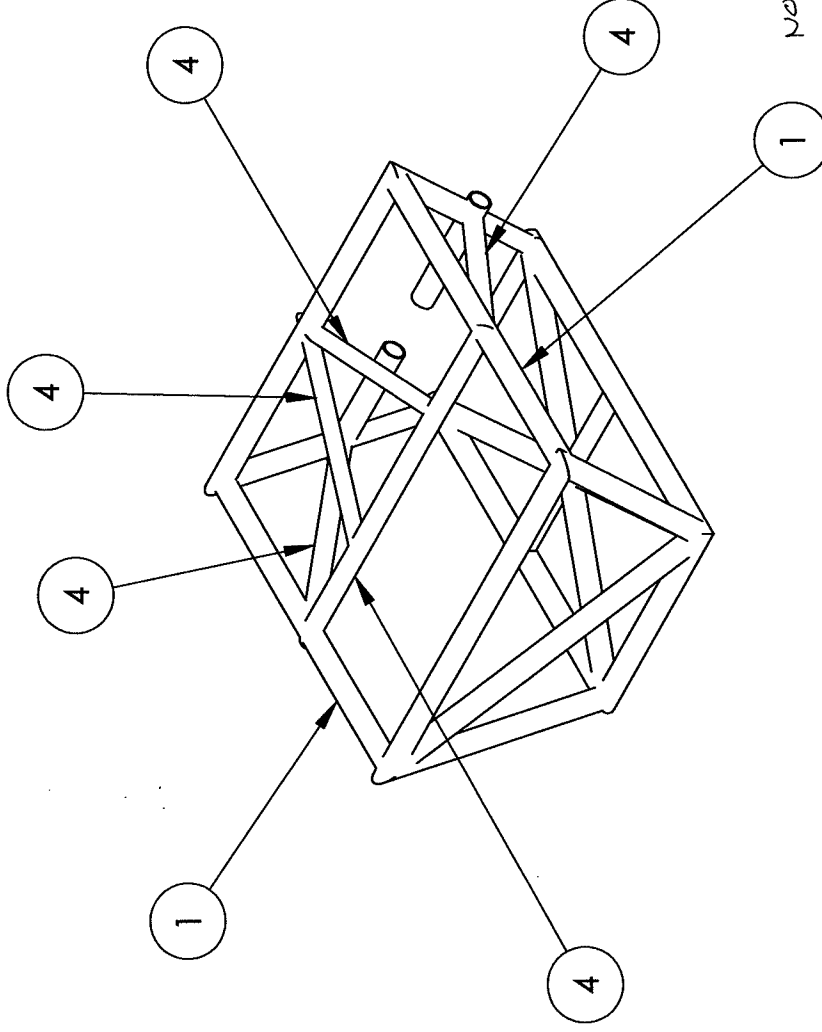
Tolerance: ±.01

Date: 3/11/09

Drawn By: DBN

Manufacturing Note: Sheet 4 of 5

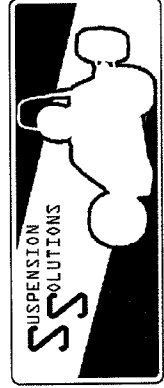
Phase 3 : Add Top Rails which connect to trapizoidal planes
Notch center member



NOTE: FRAME CUFFRAIL DIMENSIONS CHANGED
BUY TUBE SIZES FOLLOW THESE DIMS

Tubing Sizes:

- 1: 1.0in O.D. by .87in I.D.
- 2: 1.0in O.D. by .75in I.D.
- 3: 1.0in O.D. by .93in I.D.
- 4: .75in O.D. by .6125in I.D.



Part Name: Rear Frame Adaptation

Sub Team: Chassis

Next Assembly: MasterASM

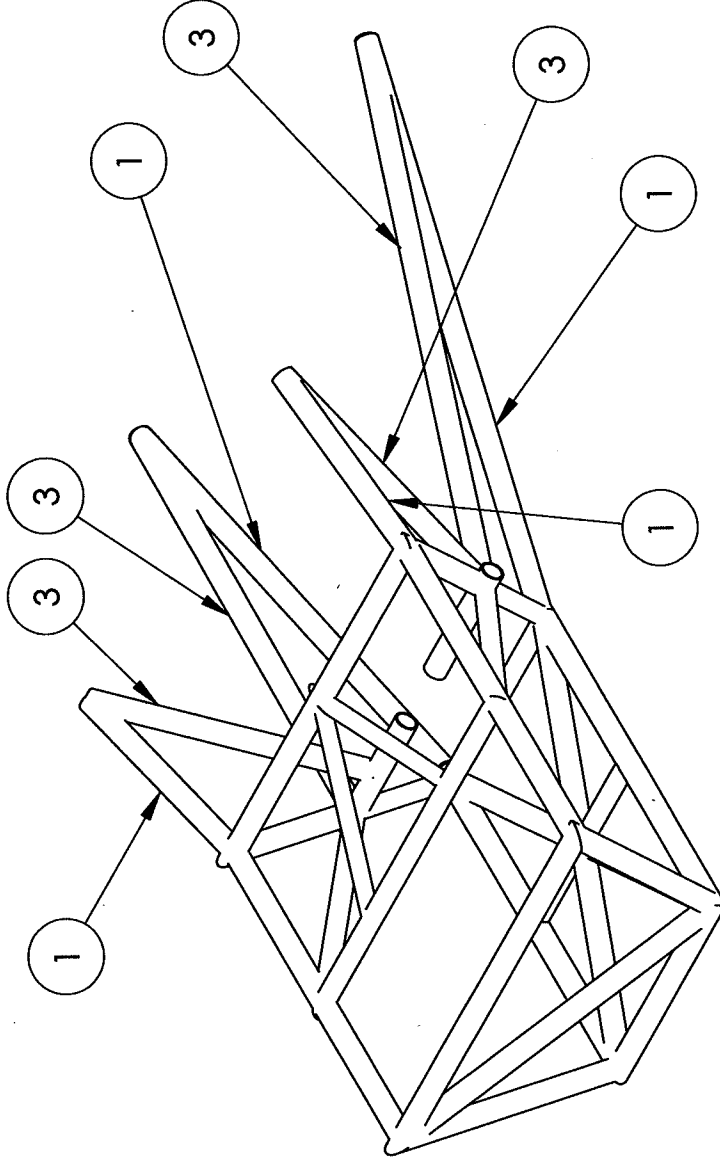
Material: 4130 Tubing Units: INCHES Scale: 1:8

Tolerance: ±.01

Date: 3/11/09 Drawn By: DBN

Manufacturing Note: Sheet 5 of 5

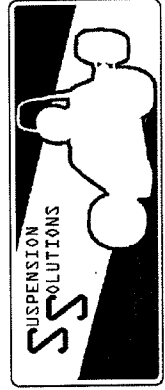
Phase 3 : Notch all teh members which will connect the final frame box to previous frame bungs



NOTE: FRAME OVERALL DIMENSIONS CHANGED
BUT TUBE SIZES FOLLOW THESE NUMS

Tubing Sizes:

- 1: 1.0in O.D. by .87in I.D.
- 2: 1.0in O.D. by .75in I.D.
- 3: 1.0in O.D. by .93in I.D.
- 4: .75in O.D. by .6125in I.D.



Part Name: Rear Frame Adaptation

Sub Team: Chassis

Next Assembly: MasterASM

Material: 4130 Tubing

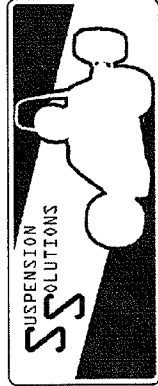
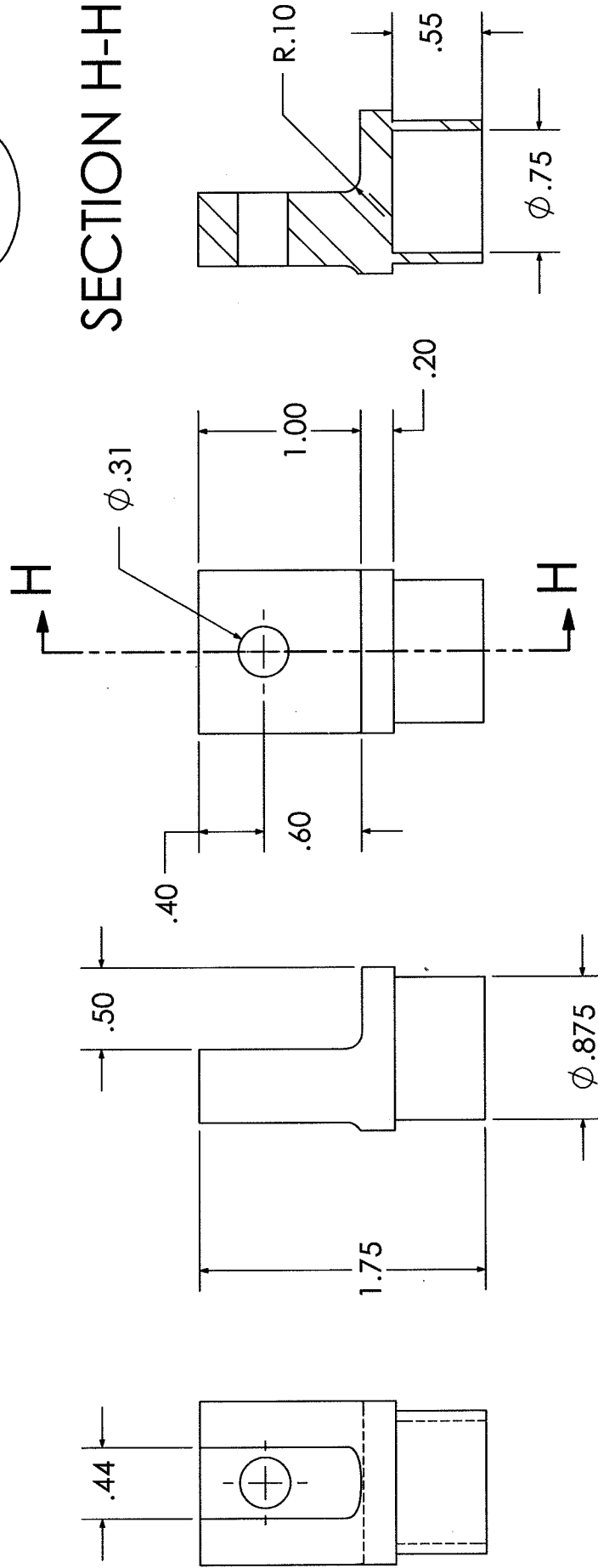
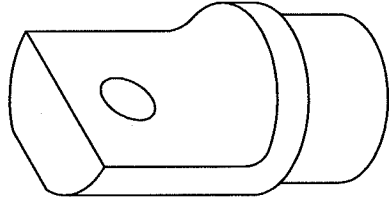
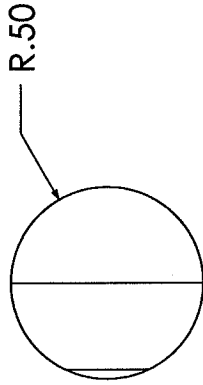
Scale: 1:8

Tolerance: ±.01

Date: 3/11/09

Units: INCHES

Drawn By: DBN



Next Assembly: MasterAsm
Tolerance: $\pm .005$

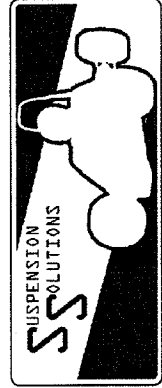
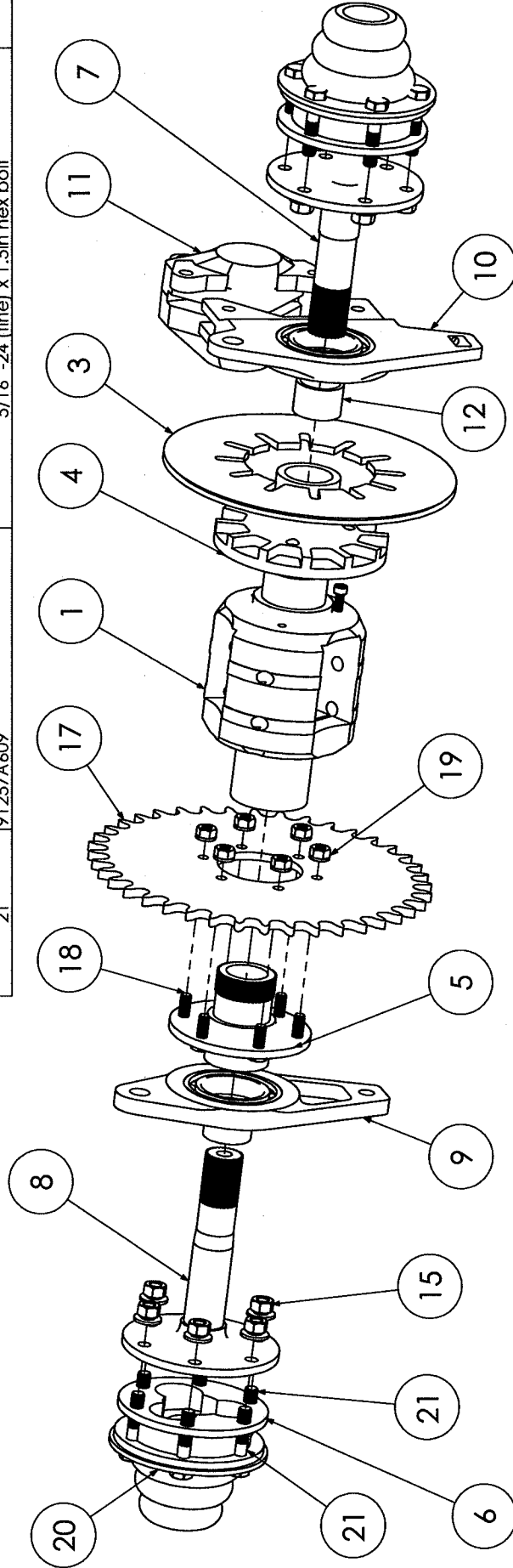
Part Name: Single Shear Frame Bung

Sub Team: Chassis

Material: 4130 steel Units: INCHES Scale: 1:1

Date: 4/15/09 Drawn By: DBN

ITEM NO.	PART NUMBER	DESCRIPTION	QTY.
1	08D0101-SS	Torsen Diff	1
2	SKF - 61908 - 20.DE.NC.20_68	External Diff Bearing	2
3	Brake Disk	Carbon Brake Rotor	1
4	08D0109-SS	Brake Insert	1
5	08D0108-SS	Sprocket Insert	1
6	TripodOuterOld	old outer tripod pegagus (the black cars)	2
7	08D0208-2-SS	Axle stub Right for bushing	1
8	08D0208-3-SS	Axle stub left for bushing (sprocket side)	1
9	08D0105-SS	Large Hole Diff Insert	1
10	08D0105-SS	Large Hole Diff Insert	1
11	08D0115-SS	Brake Caliper	1
12	Inner Bushing	Inner Bushing for axle stub	2
13	90117A193		2
14	91251A345	10-32 socket head screw X .75" long	2
15	HNUT 0.3125-24-D-N	5/16"-24 Hex Nut	12
16	Preferred Narrow FW 0.3125		12
17	08D0106-3-SS	40 tooth 520 chain Sprocket	1
18	92620A563	1/4-28 x 1.0 bolt "special sprocket bolts"	6
19	.25-28-Nut-Washer		6
20	Boot	TriPod Bearing Boot	2
21	91257A609	5/16"-24 (fine) x 1.5in hex bolt	12



Part Name: Differential Assembly

Sub Team: Drivetrain

Next Assembly: MasterAsm

Tolerance: ±.005

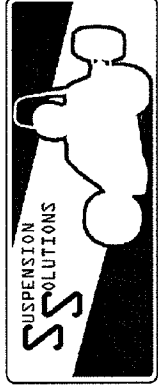
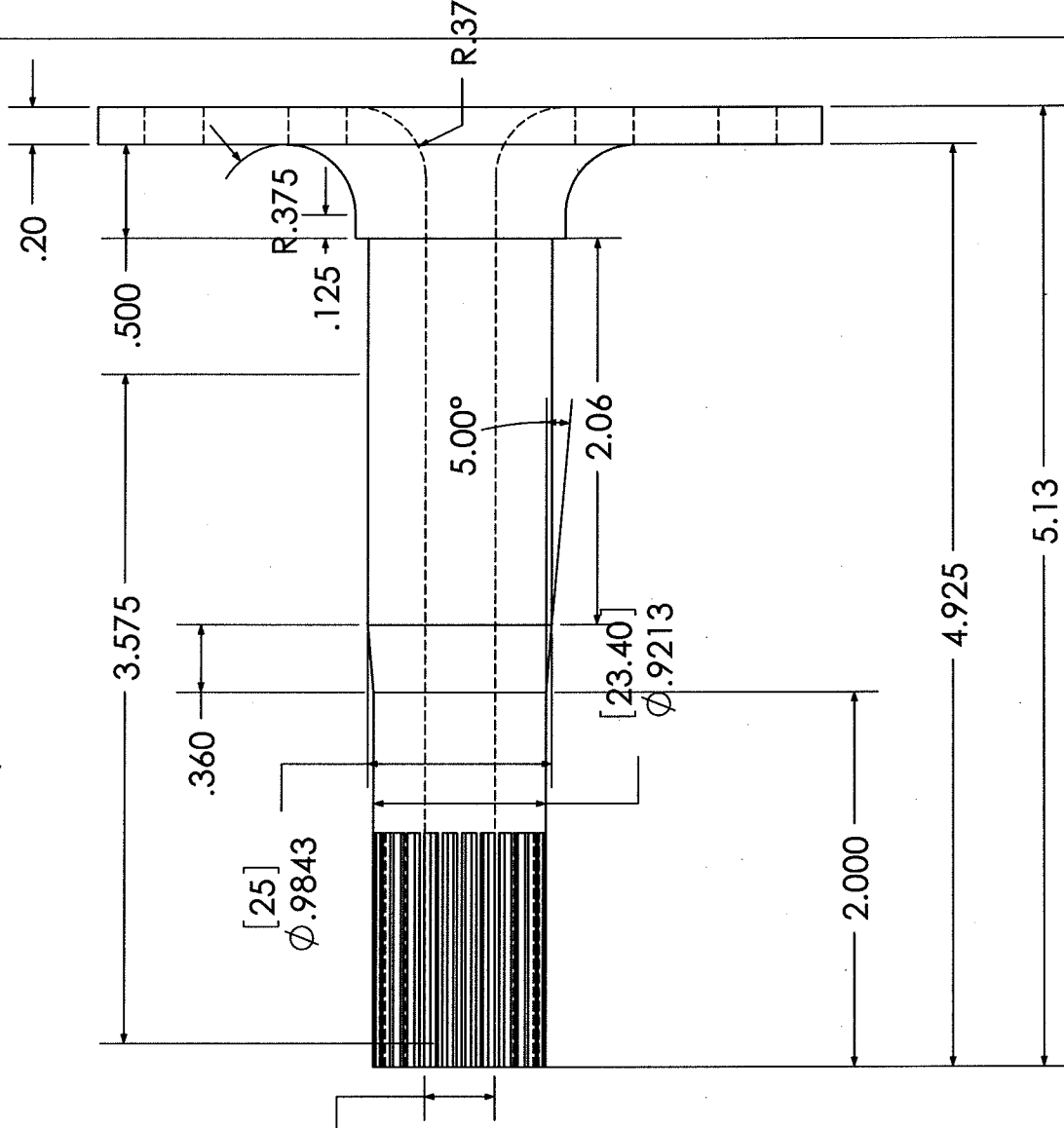
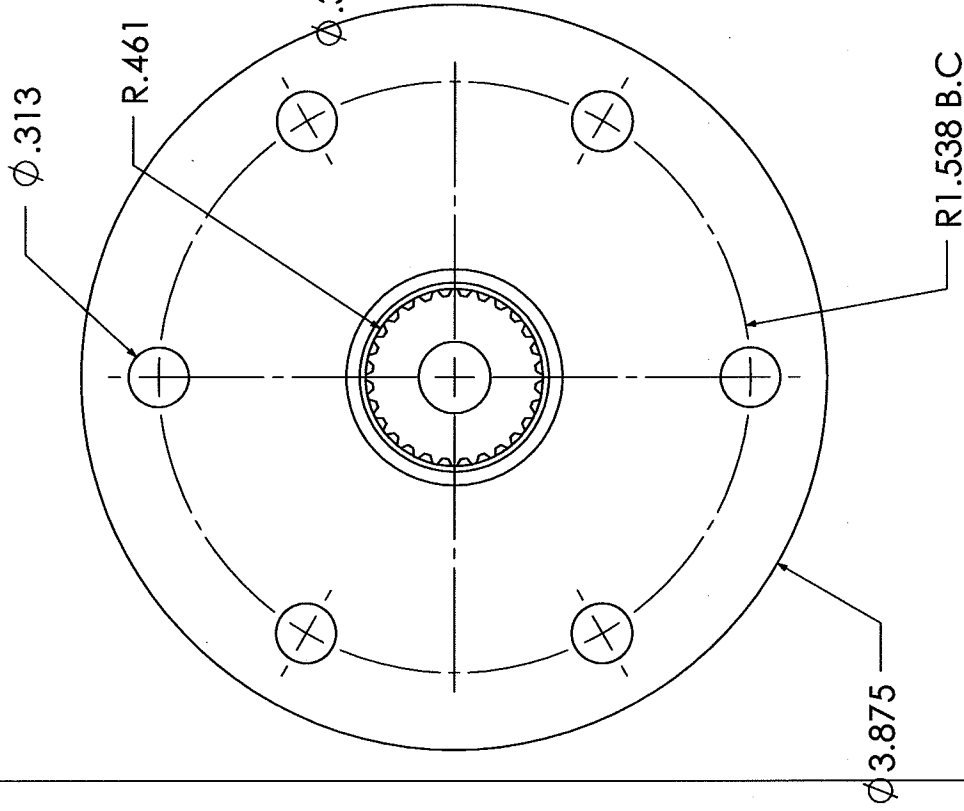
Material: -

Units: INCHES

Scale: 1:4

Date: 12/2/09

Drawn By: DBN



Part Name: Sprocket Side axle stub

Sub Team: Drivetrain

Next Assembly: MasterAssm

Material: 6061 Alum

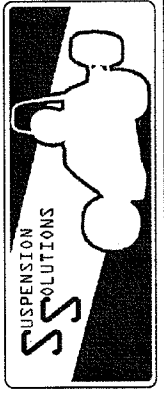
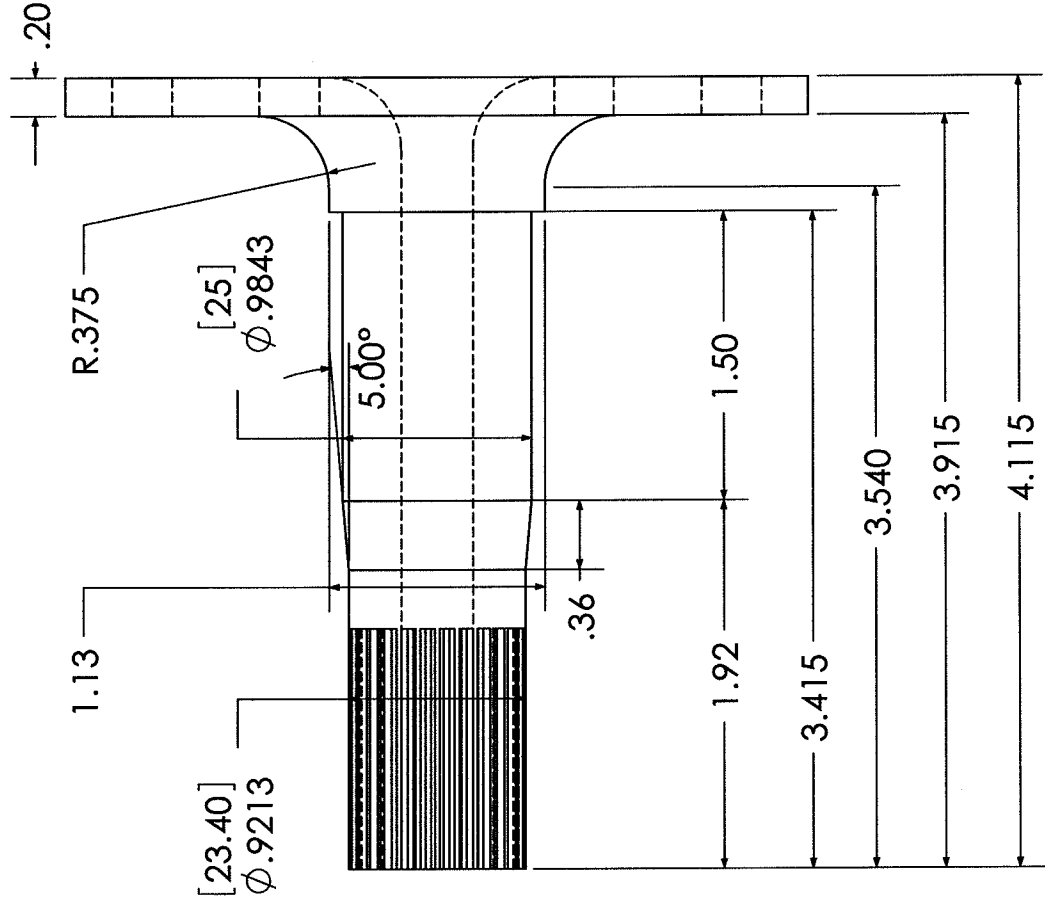
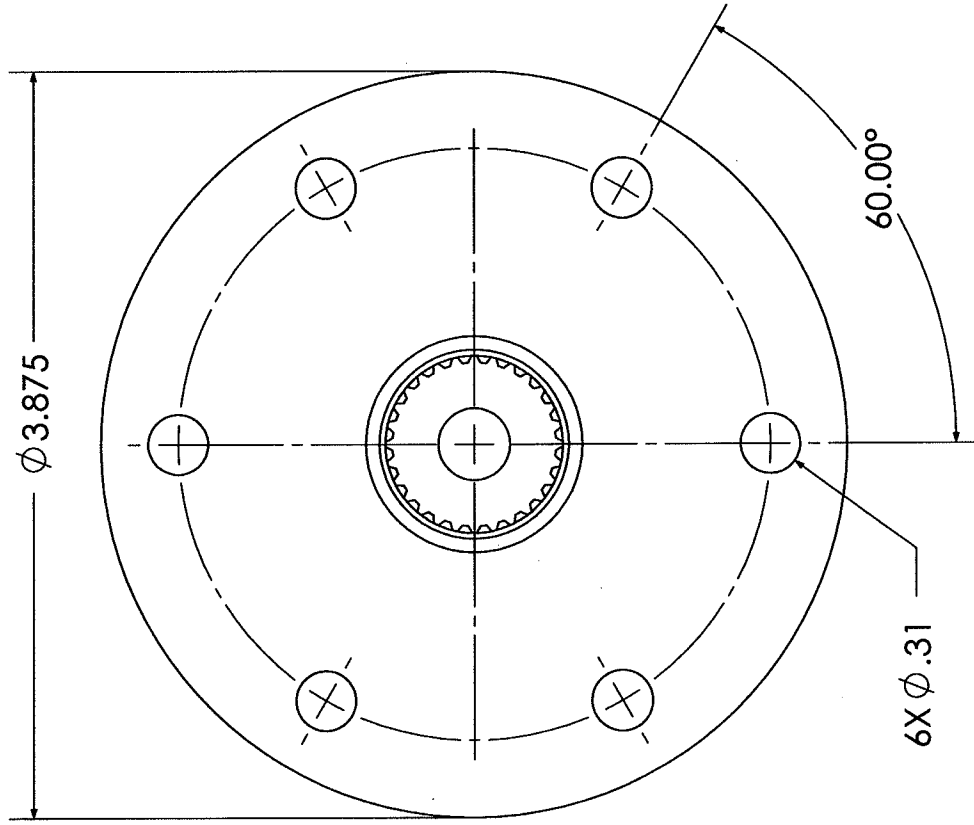
Scale: 1:1

Tolerance: $\pm .01$

Date: 10/1/09

Units: INCHES

Drawn By: DBN



Part Name: Sprocket Side axle stub

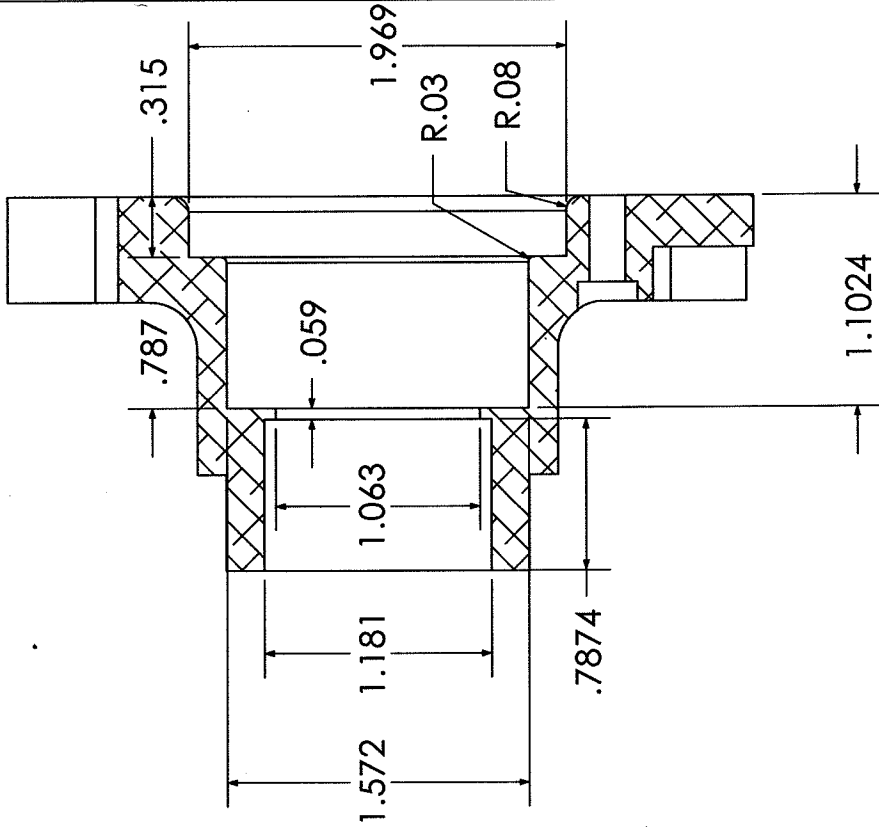
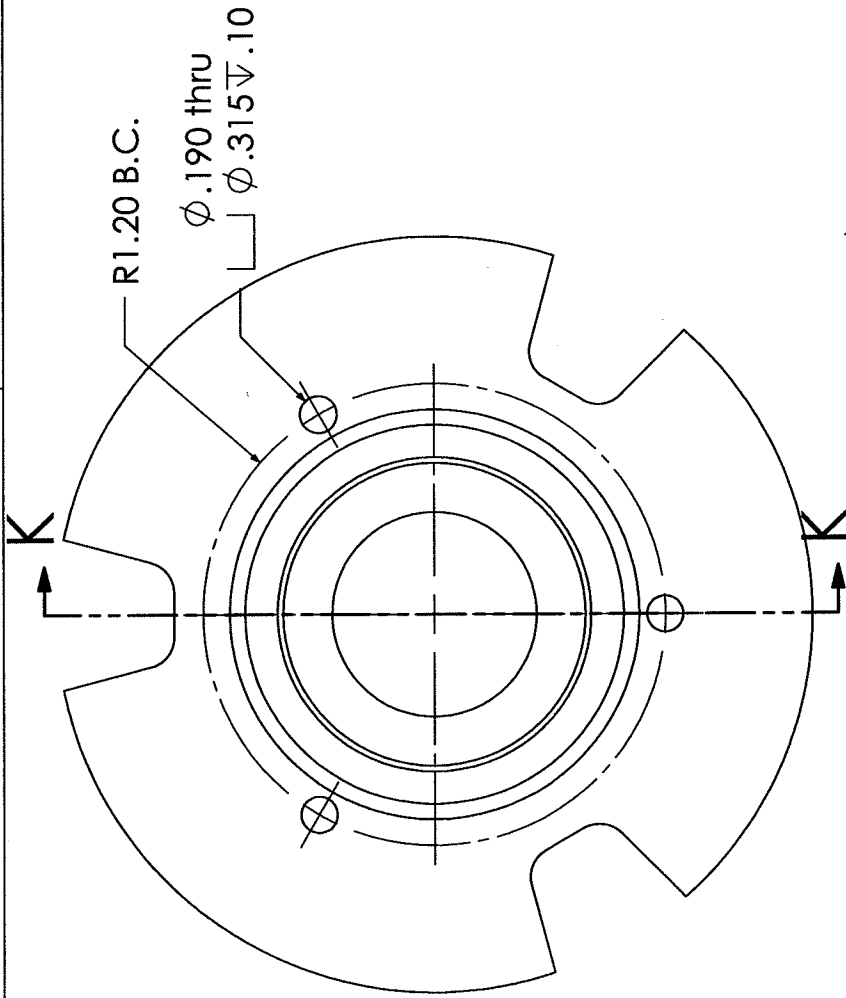
Sub Team: Drivetrain

Next Assembly: MasterAssm

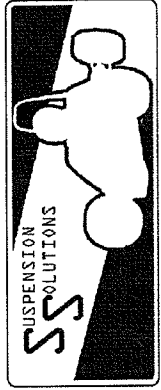
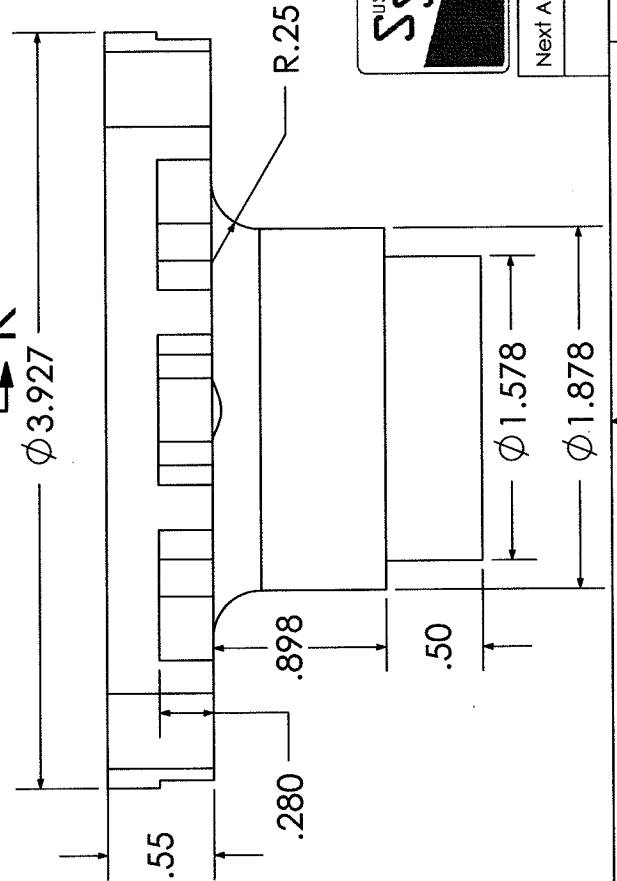
Material: 6061 Alum Units: INCHES Scale: 1:1

Tolerance: $\pm .01$

Date: 10/1/09 Drawn By: DBN



SECTION K-K
SCALE 1:1



Part Name: Brake Hub Insert

Sub Team: Drivetrain SS

Next Assembly: 08S06AS1-SS

Material: 6061 Al

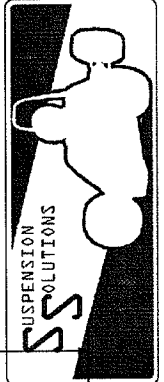
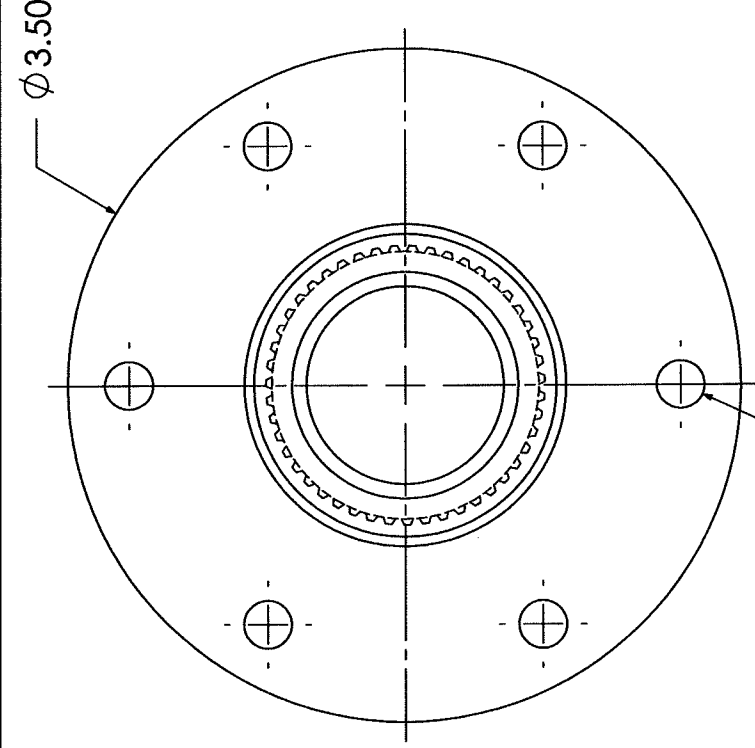
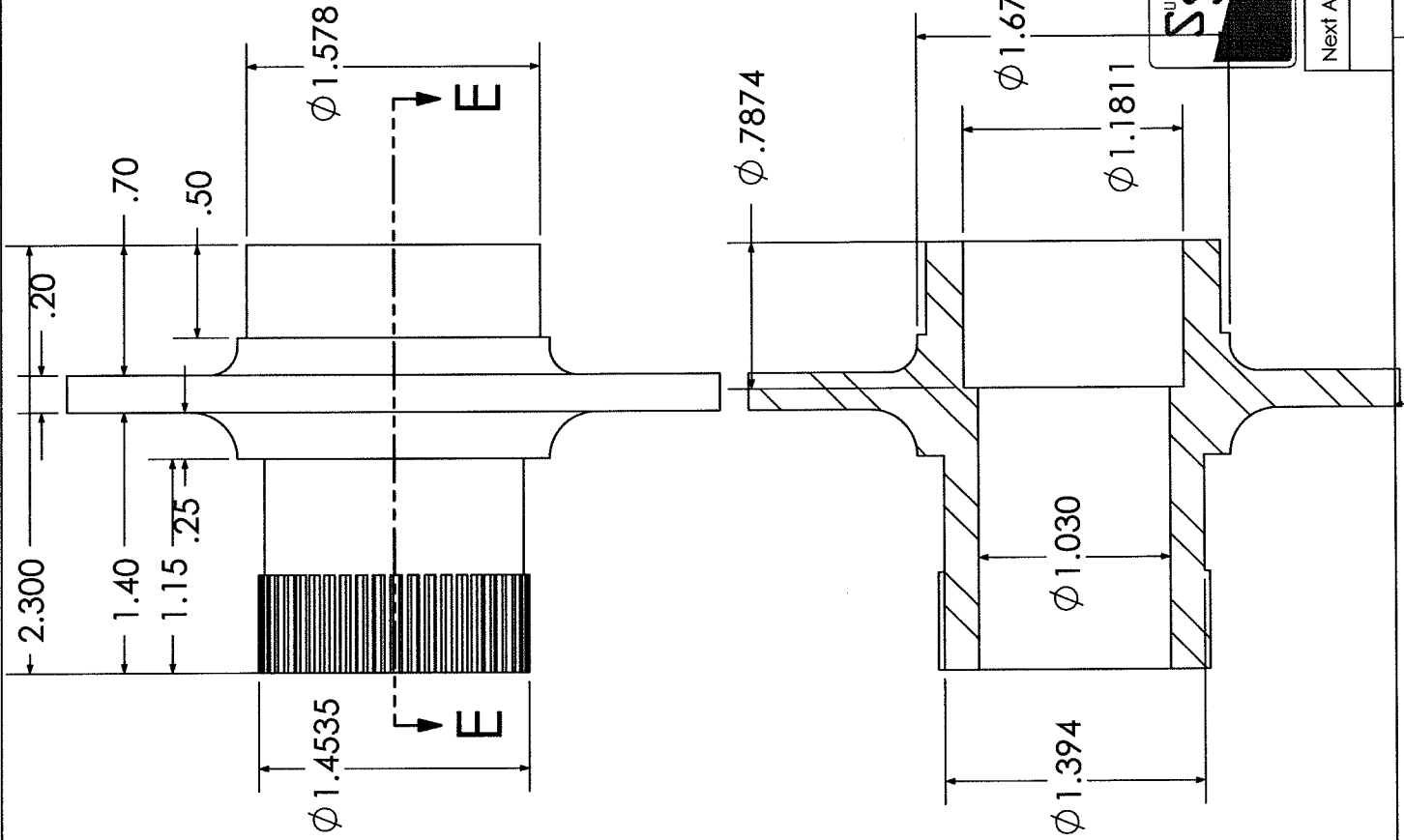
Units: INCHES

Scale: 1:1

Tolerance: $\pm .002$

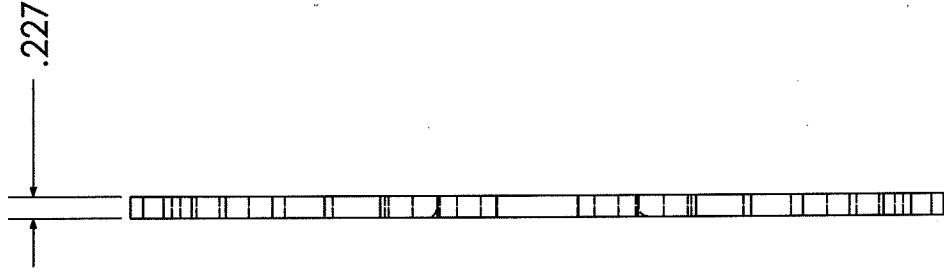
Date: 9/9/09

Drawn By: DBN

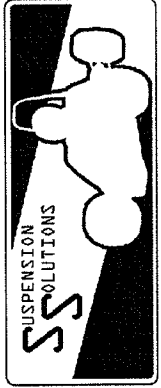
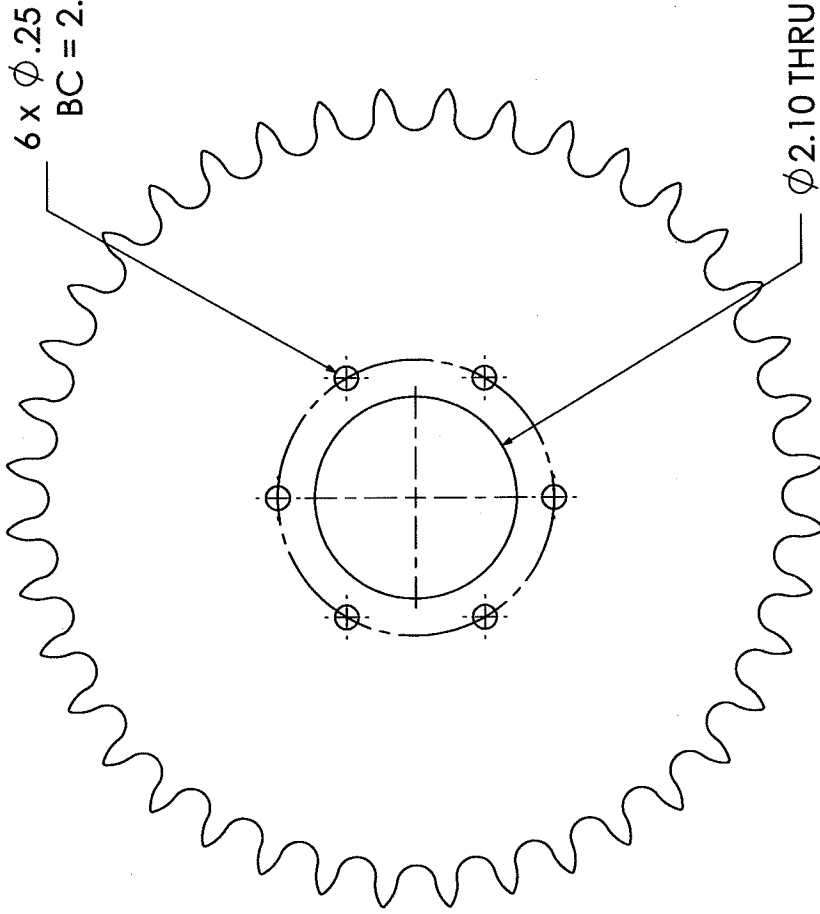


Next Assembly: MasterAssm
 Tolerance: ±.01

Part Name:	Sprocket Side axle stub		
Sub Team:	Drivetrain		
Material:	6061 Alum	Units:	INCHES
Date:	10/1/09	Drawn By:	DBN
			Scale: 1:1



6 x $\phi .25$ THRU
BC = 2.875



Part Name: (520) 40 tooth Sprocket

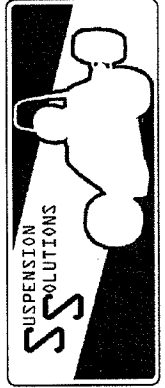
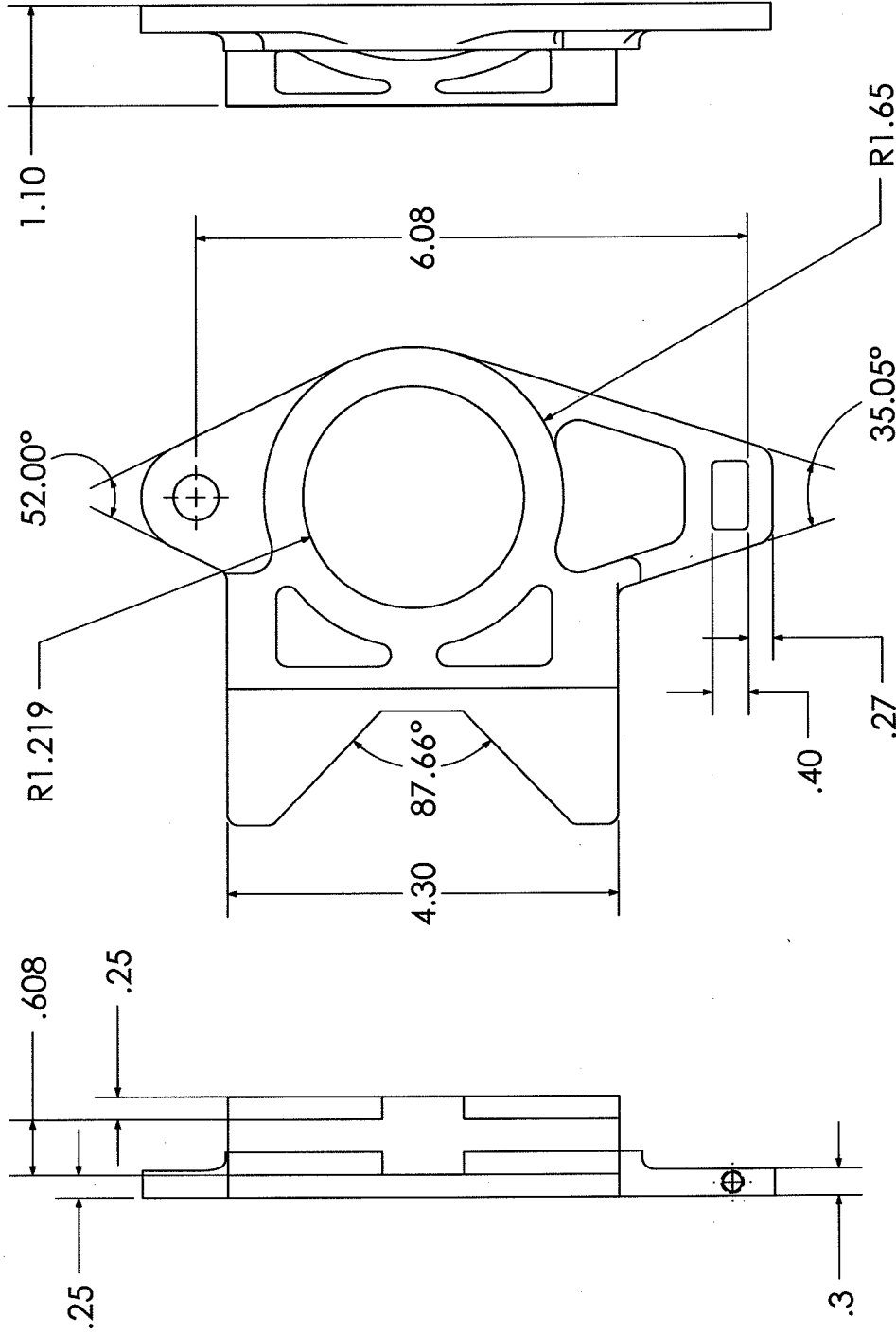
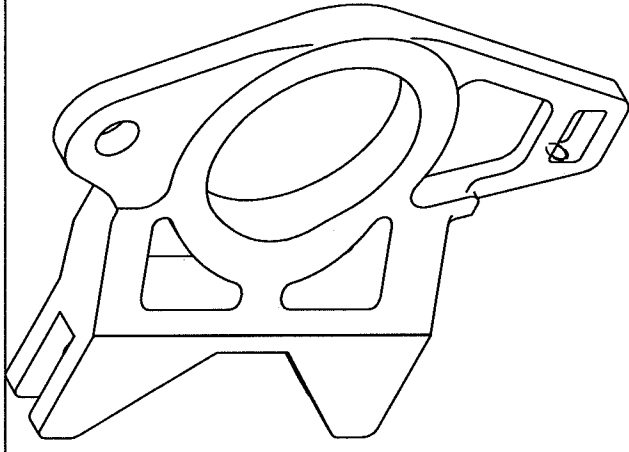
Sub Team: Drivetrain

Material: 6061 Alum Units: INCHES Scale: 1:2

Date: 12/2/09 Drawn By: DBN

Next Assembly: 08D01AS1-SS

Tolerance: $\pm .005$



Part Name:

Brake Side Diff Upright

Sub Team:

Drivetrain

Next Assembly: MasterAssm

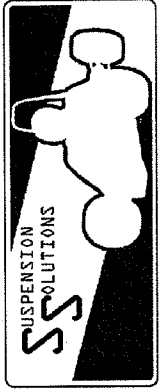
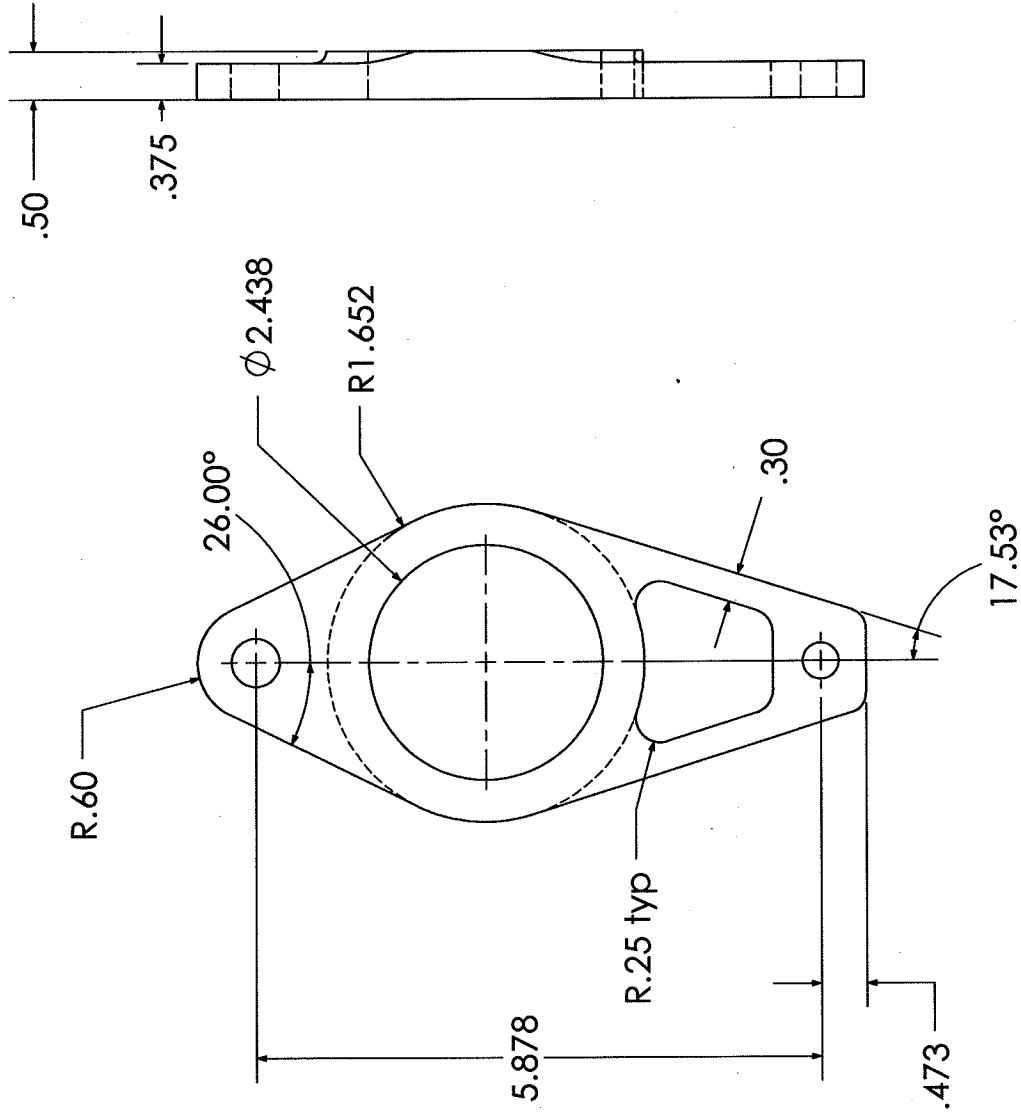
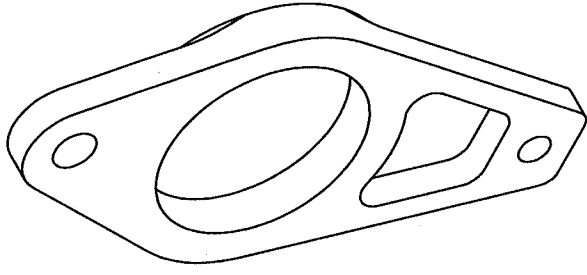
Material: 6061 Alum

Scale: 1:2

Tolerance: ±.005

Date: 10/1/09

Drawn By: DBN



Part Name: Sprocket Side Diff Upright

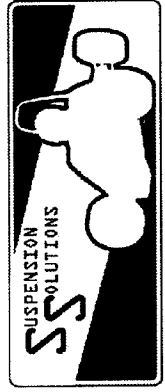
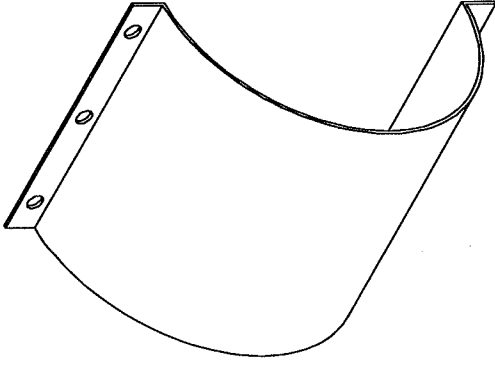
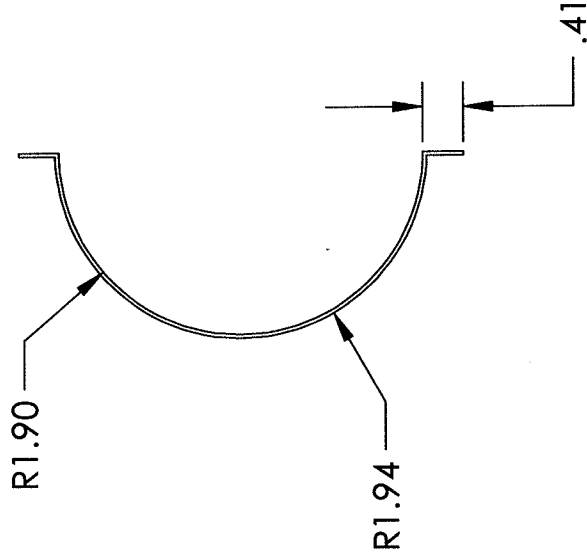
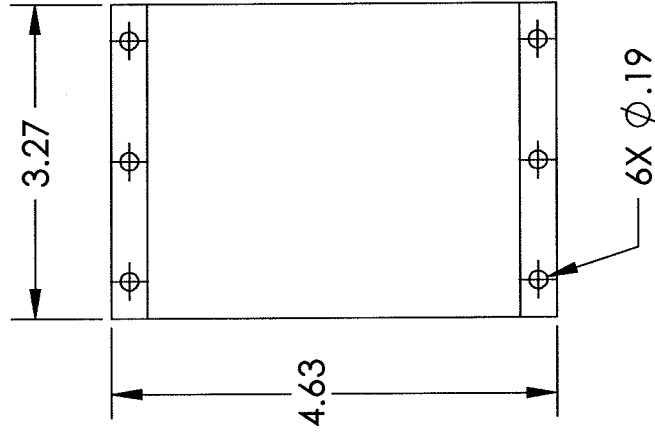
Sub Team: Drivetrain

Material: 6061 Alum Units: INCHES Scale: 1:2

Date: 10/1/09 Drawn By: DBN

Next Assembly: MasterAssm

Tolerance: ±.005



Part Name: Differential Clamshell

Sub Team: Diff

Next Assembly: 08D01AS1-SS

Material: 1020 Steel

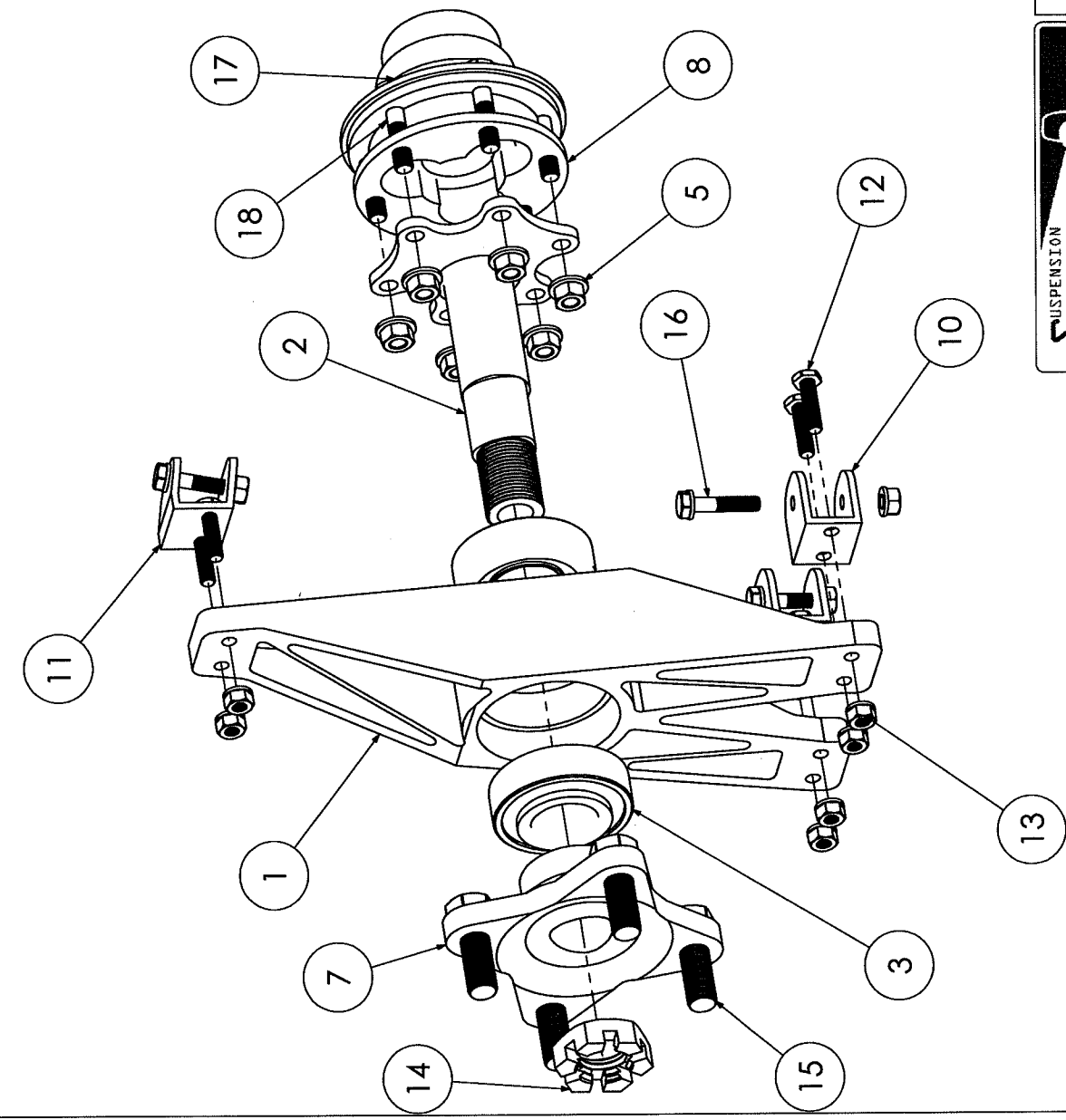
Units: INCHES

Scale: 1:2

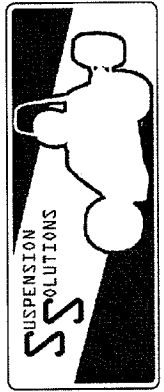
Tolerance: \pm .01

Date: 3/5/09

Drawn By: MBM

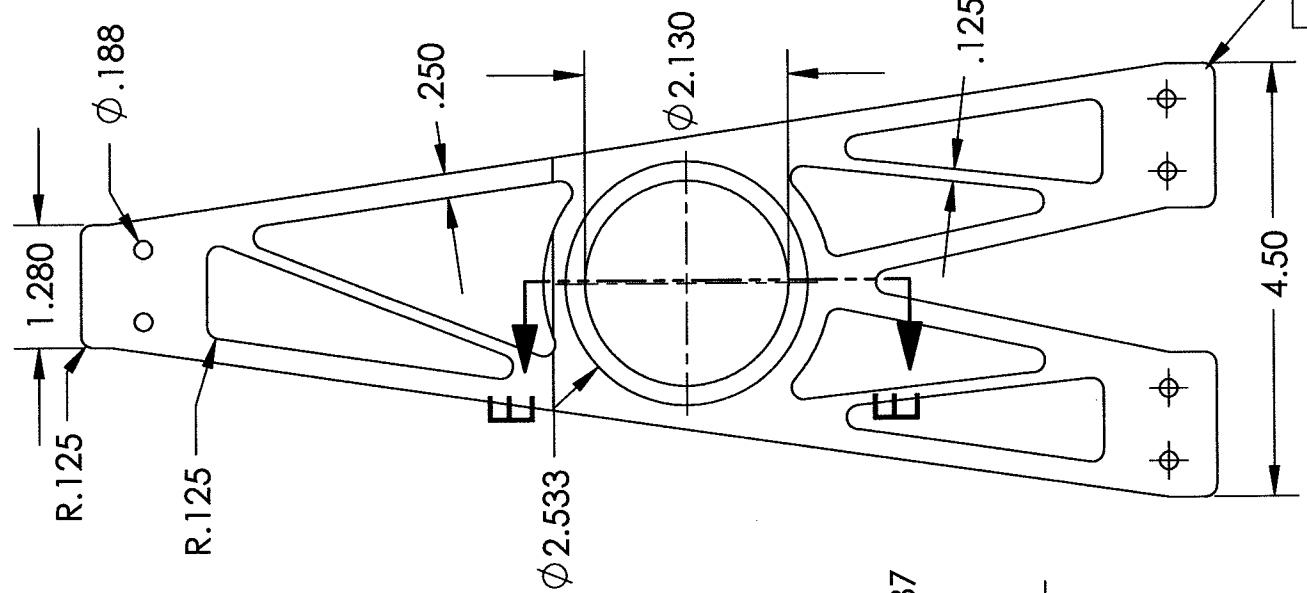
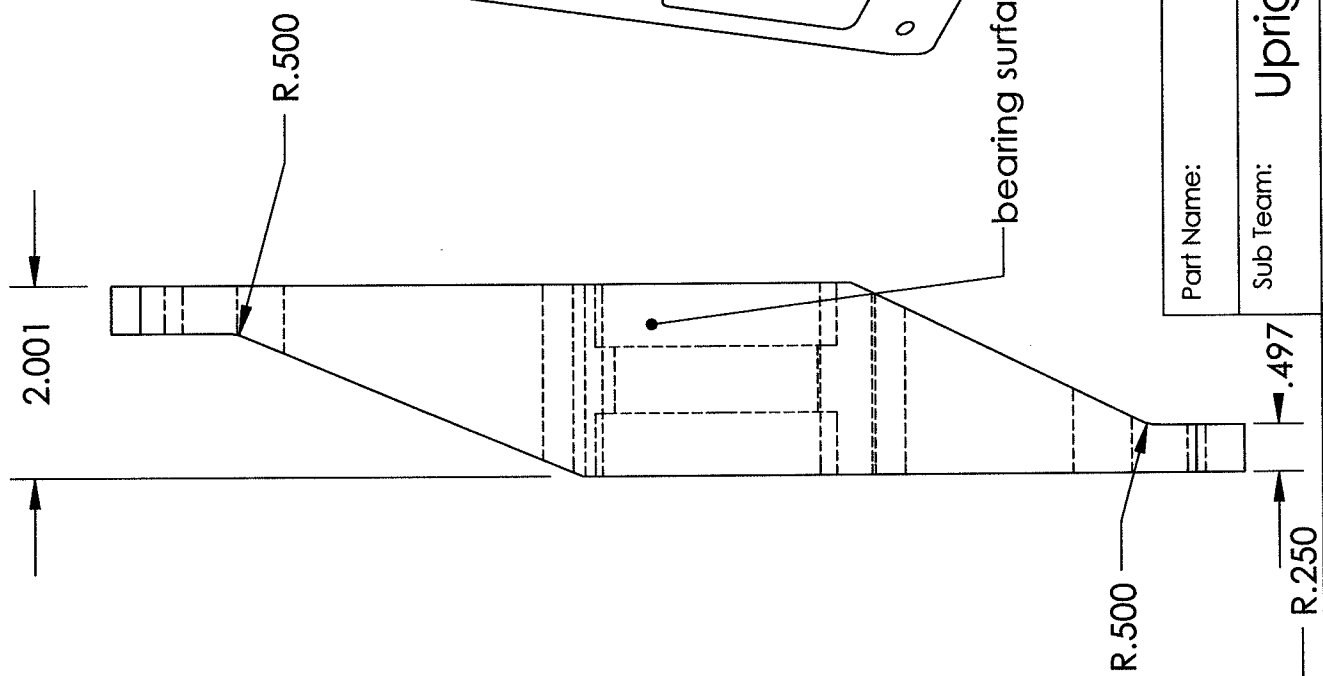
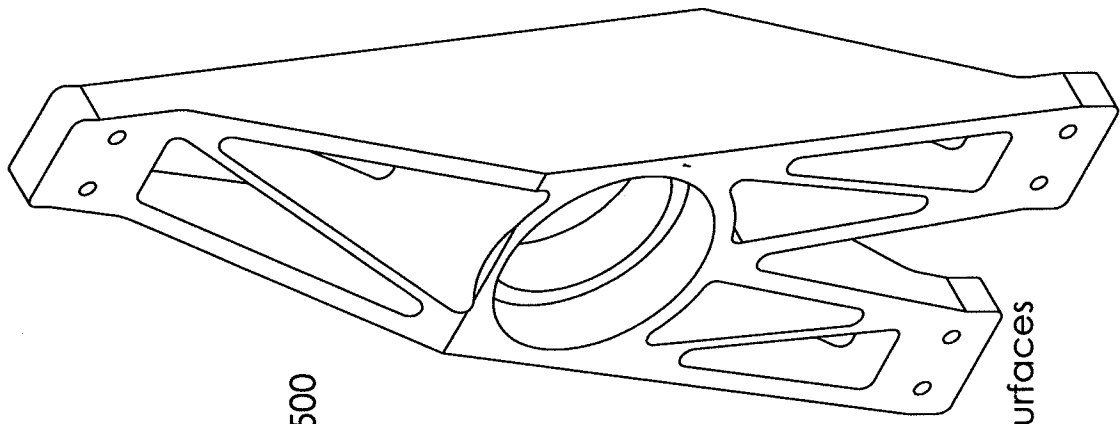


ITEM NO.	PART NUMBER	DESCRIPTION	QTY.
1	08U0101-SS	CNC machined, 6061 aluminum	1
2	08U0201-SS-2	Rear Steel Spindle 2	1
3	SKF - 32206 - 16.SI,INC,16	Roller Bearings	2
4	HNIUT 0.3125-24-D-N	5/16"-24 Hex Nut	6
5	Preferred Narrow FW 0.3125		6
6	UltraLight wheel	UltraLight rear wheel (looks like my chevy SS's)	1
7	08U0202-SS	AIHUB	1
8	TripodOuterOld	old outer tripod pegasus (the black cars)	1
9	FSAEC-09-023-WT-00100	Tire, Goodyear, 20x7-13	1
10	LowerPickuptabs		2
11	UpperPickup tab		1
12	92620A.563	1/4-28 x 1.0 bolt "upright tab bolts"	6
13	.25-28-Nut-Washer		9
14	91853A038	1"-14 Castle nut ("model actually has 1"-14 thread)	1
15	92620A746	1/2"-20 wheel bolts grade 8	4
16	.25-28-1.5-washer	1/4"-28 x 1.5" blot with washer	3
17	Boot	Tripod Bearing Boot	1
18	91257A609	5/16"-24 (fine) x 1.5in hex bolt	6

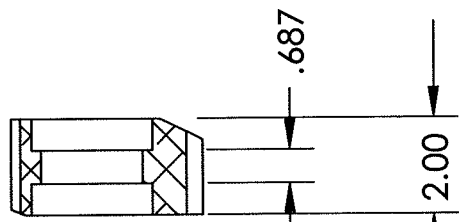


Part Name: Upright Assembly
 Sub Team: Suspension
 Material: -
 Date: 12/2/09
 Units: INCHES
 Scale: 1:3
 Tolerance: ±.005
 Drawn By: DBN

Next Assembly: MasterAsm
 Tolerance: ±.005



SECTION E-E



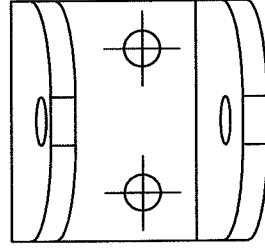
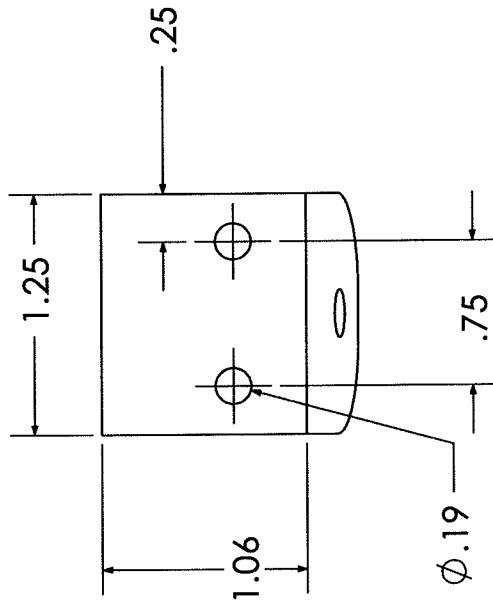
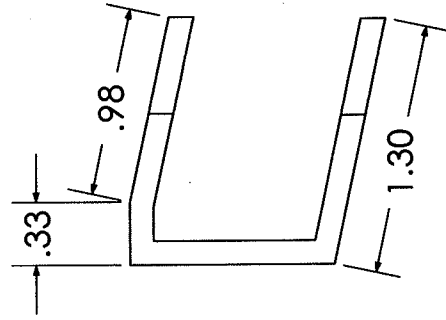
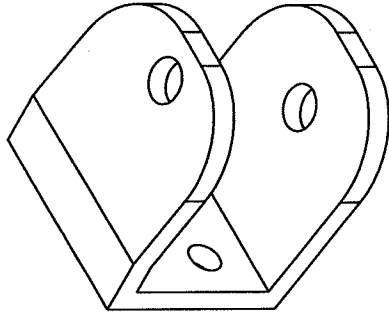
Part Name: Rear Upright

Sub Team: Upright

Next Assembly: #####
Material: 6061 Al
Units: INCHES
Scale: 1:2

Tolerance: ±.01

Date: 3/5/09
Drawn By: EAS



Part Name: Upper Upright Tab

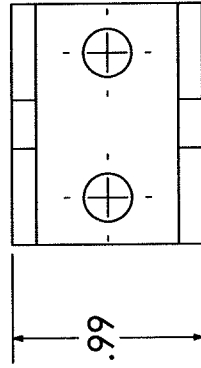
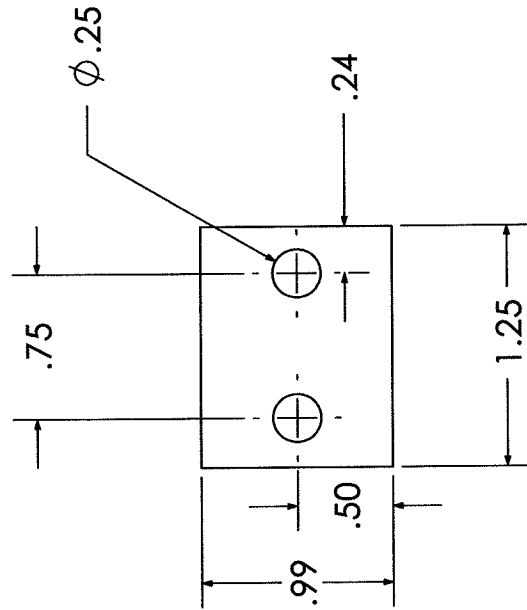
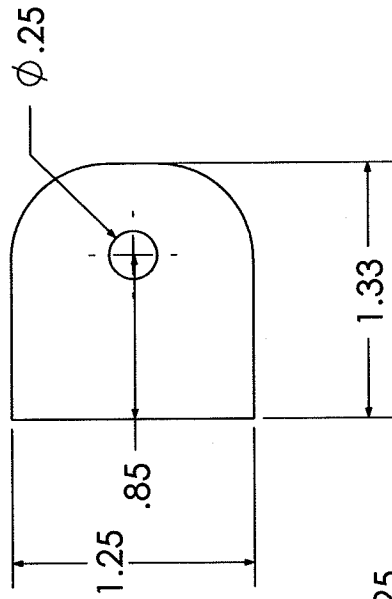
Sub Team: Drivetrain/Upright

Next Assembly: 08U01AS1-SS

Tolerance: $\pm .002$

Material: 6061 AL Units: INCHES Scale: 1:1

Date: 8/12/08 Drawn By: EAS



Part Name: lower upright tab

Sub Team: Drivetrain/Upright

Next Assembly: 08U01AS1-SS

Tolerance: $\pm .002$

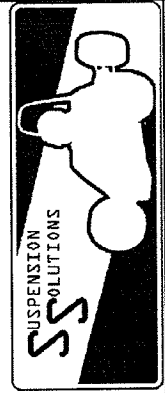
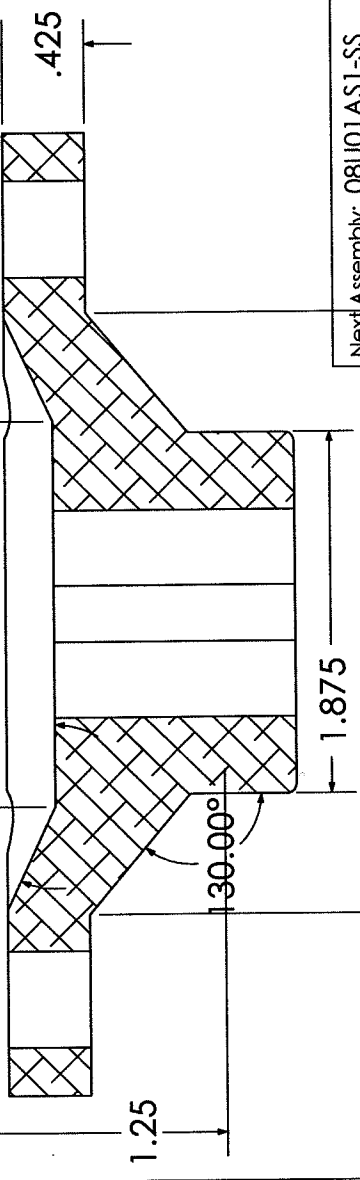
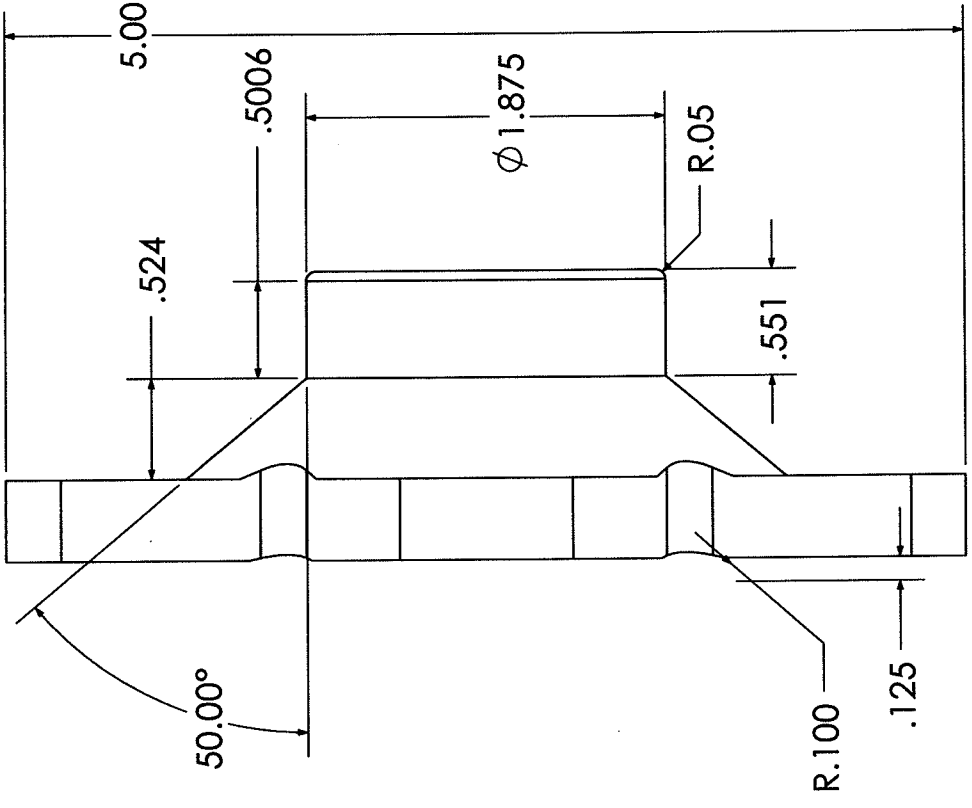
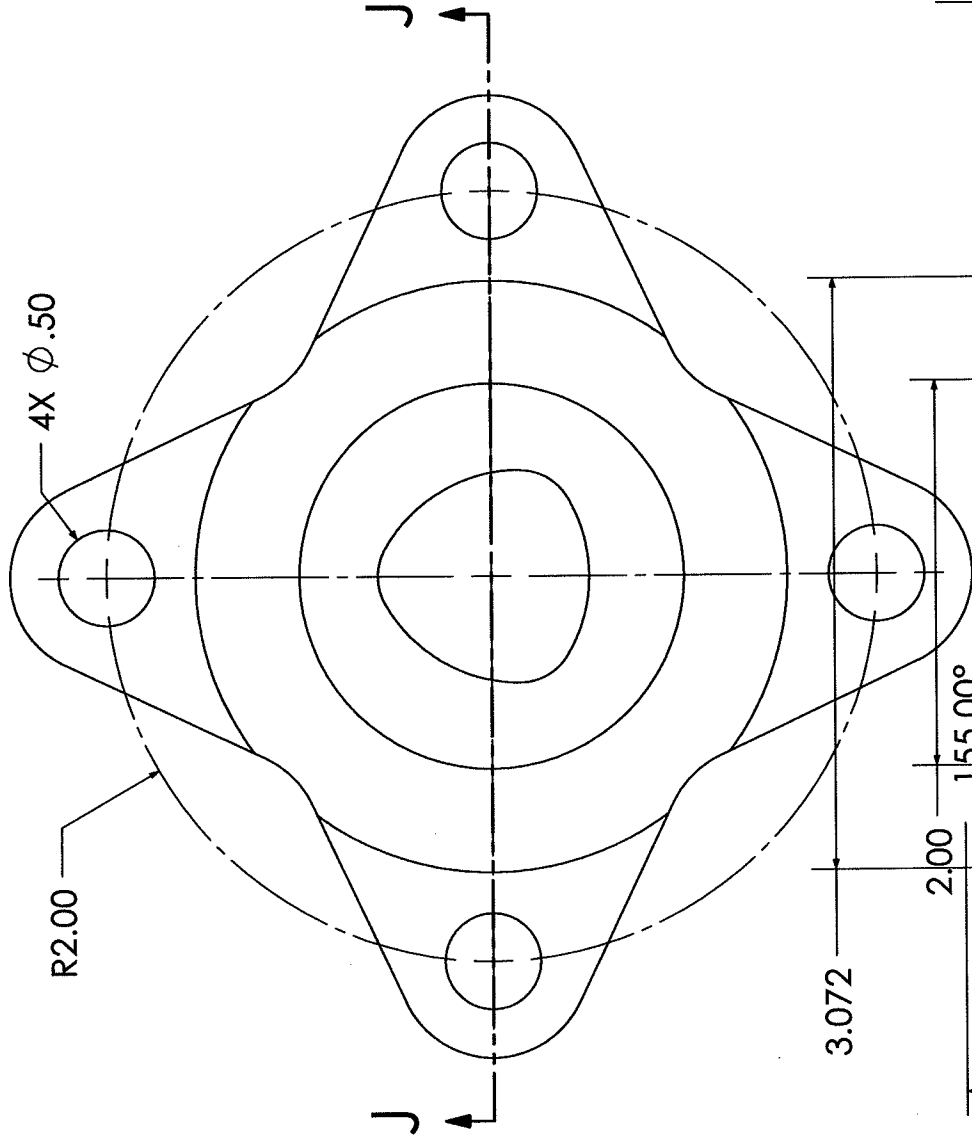
Material: 6061 AL

Date: 8/12/08

Units: INCHES

Scale: 1:1

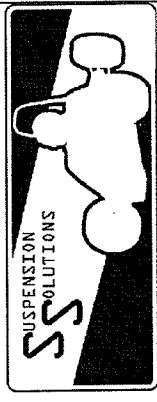
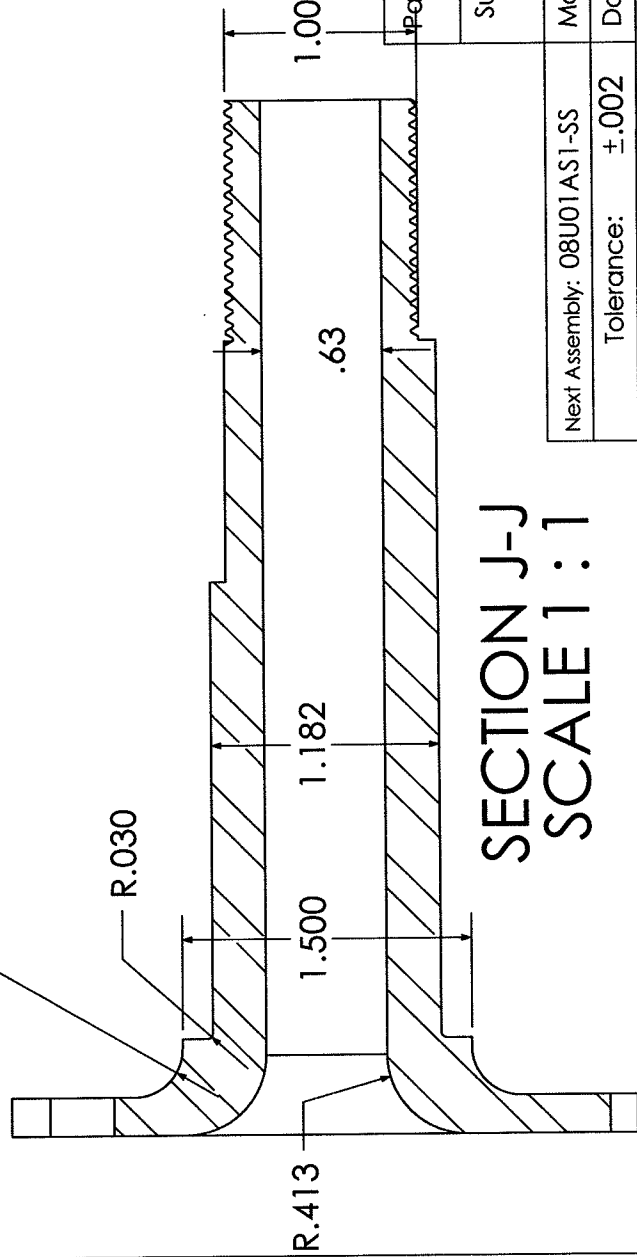
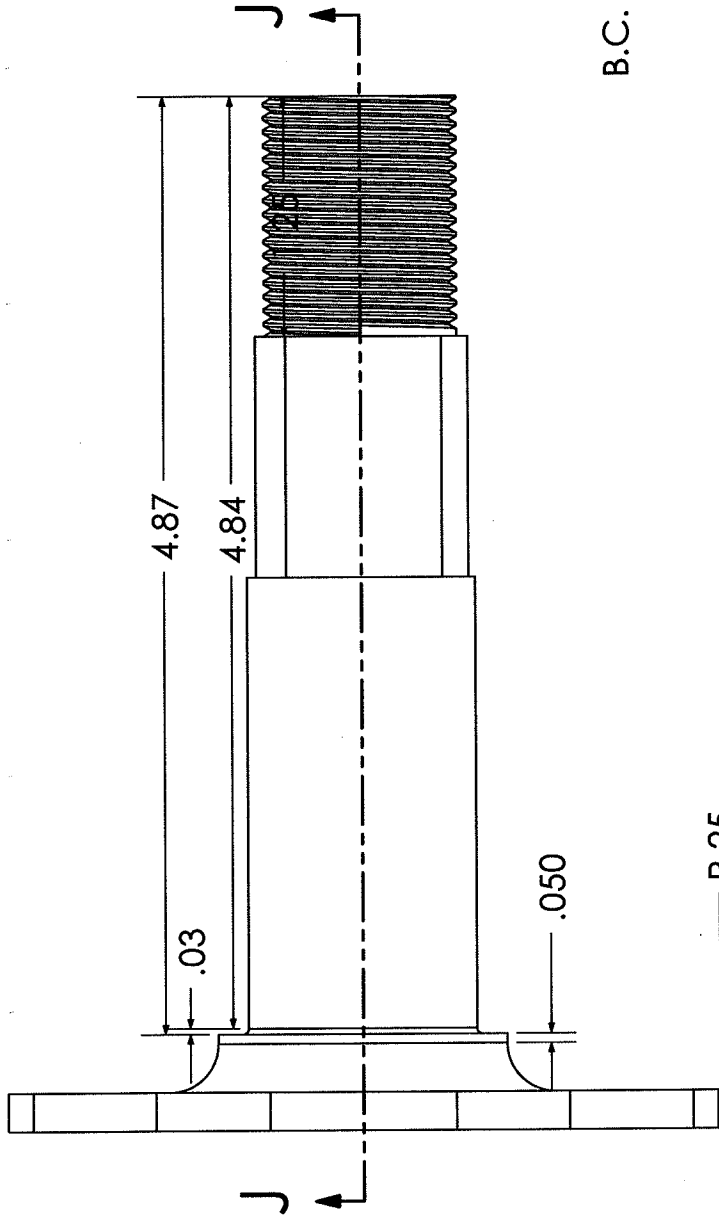
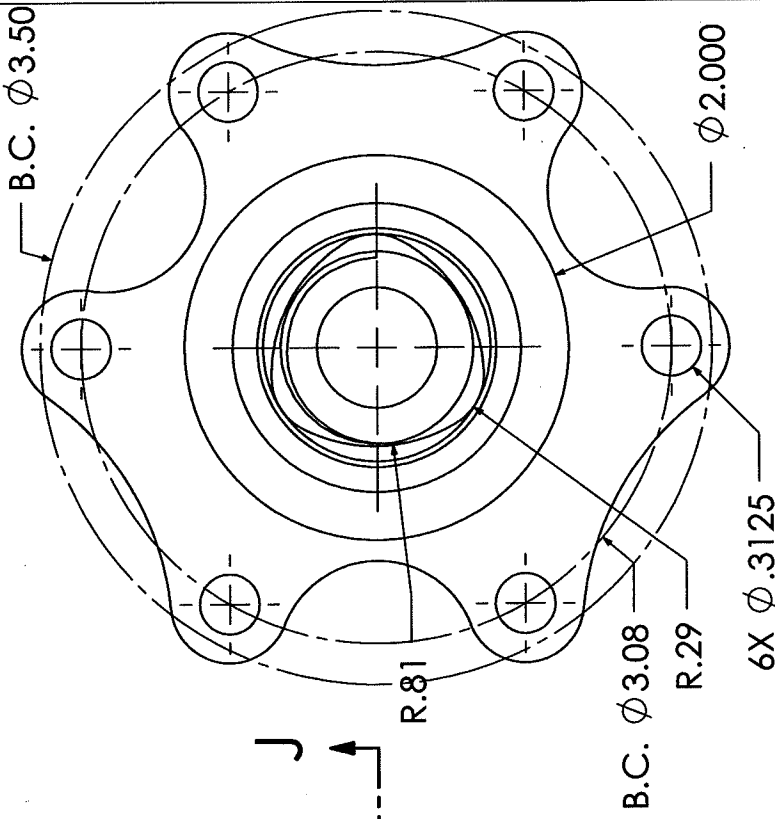
Drawn By: EAS



Part Name: **Rear Hub**
 Sub Team: **Drivetrain/Upright**

Next Assembly: 08U01AS1-SS	Material: 6061 AL	Units: INCHES	Scale: 1:1
Tolerance: $\pm .002$	Date: 8/12/08	Drawn By: DBN	

SECTION J-J
SCALE 1:1



Part Name: Rear Steel Spindle

Sub Team: Drivetrain

Next Assembly: 08U01AS1-SS	Material: 4130 steel	Units: INCHES	Scale: 4:1
Tolerance: \pm .002	Date: 7/17/09	Drawn By: DBN	

SECTION J-J
SCALE 1 : 1



Appendix G: Bill of Materials

Appendix G - Bill of Materials

Part Number	Description	Quantity	Material	Supplier	Vendor Part #
08D0101-SS	Torsen Differential	1	-	Torsen Traction	12000
08D0104-SS	Differential Support Right	1	1" 6061 Aluminum plate	McMaster-Carr	
08D0105-SS	Differential Support Left	1	1" 6061 Aluminum plate	McMaster-Carr	
08D0106-SS	Sprocket	1	Aluminum	Go Kart Galaxy	
08D0107-SS	Brake Rotor	1	Carbon	Tilton	
08D0108-SS	Sprocket Insert	1	4" 6061 round	McMaster-Carr	
08D0109-SS	Brake Insert	1	5" 6061 round	McMaster-Carr	
08D0110-SS	Mounting Bracket Right Top	2	0.10" 4130 steel	McMaster-Carr	
08D0111-SS	Mounting Bracket Left Top	2	0.10" 4130 steel	McMaster-Carr	
08D0112-SS	Mounting Bracket Right Bottom	2	0.10" 4130 steel	McMaster-Carr	
08D0113-SS	Mounting Bracket Left Bottom	2	0.10" 4130 steel	McMaster-Carr	
08D0114-SS	Differential Clamshell	2	-	McMaster-Carr	
08D0115-SS	Brake Caliper	1	-	Brembo	P32-F
08D0201-SS	Tripod Bearing	4	-	Pegasus Auto Racing	1476-002
08D0202-SS	Tripod Bearing Housing	4	Steel	Pegasus Auto Racing	1476-010
08D0203-SS	Half Shaft Right	1	1" x 0.25" 4130 tube	McMaster-Carr	
08D0204-SS	Half Shaft Left	1	1" x 0.25" 4130 tube	McMaster-Carr	
08D0205-SS	Rotor side inner shaft bushing	1	Oil impregnated bronze	McMaster-Carr	
08D0206-SS	Rotor side external bearing	1	-	Timken	9310K
08D0207-SS	Sprocket side inner shaft bushing	1	Oil impregnated bronze	McMaster-Carr	
08D0207-SS	Sprocket Side external bearing	1	-	Timken	
08D0208-SS	Axle Stub Left	1	4" 6061 round	McMaster-Carr	
08D0209-SS	Axle Stub Right	1	4" 6061 round	McMaster-Carr	
08D01A51-SS	Rear Differential Assembly	1	-	-	
08D02A51-SS	Half shaft Assembly right	1	-	-	
08D02A52-SS	Half shaft Assembly left	1	-	-	
08S0109-SS	Upper A-Arm aft tube	2	0.5" x 0.035" 4130 tube	Aircraft Spruce	
08S0110-SS	Upper A-Arm fore tube	2	0.5" x 0.035" 4130 tube	Aircraft Spruce	
08S0102-SS	Upper A-Arm end	4	0.060" 4130 sheet	Aircraft Spruce	
08S0111-SS	Upper A-Arm B1 tab	2	0.10" 4130 steel plate	Aircraft Spruce	
08S0142-SS	Left Upper Ball Joint Tab	1	0.080" 4130 sheet	Aircraft Spruce	
08S0139-SS	Right Upper Ball Joint Tab	1	0.080" 4130 sheet	Aircraft Spruce	
08S0241-SS	Upper a-arm fore tube	2	0.5" x 0.035" 4130 tube	Aircraft Spruce	
08S0242-SS	Upper a-arm aft tube	2	0.5" x 0.035" 4130 tube	Aircraft Spruce	
08S0243-SS	Tie rod tube	2	0.5" x 0.035" 4130 tube	Aircraft Spruce	
08S0244-SS	Lower a-arm fore tube	2	0.5" x 0.035" 4130 tube	Aircraft Spruce	
08S0245-SS	Lower a-arm aft tube	2	0.5" x 0.035" 4130 tube	Aircraft Spruce	
08S0246-SS	push rod tube	2	0.5" x 0.035" 4130 tube	Aircraft Spruce	
08S0247-SS	Single Bearing Wafer	8	1/4" 4130 plate	Aircraft Spruce	
08S0248-SS	Upper a-arm bearing wafer	2	1/4" 4130 plate	Aircraft Spruce	
08S0249-SS	Lower A-arm bearing wafer	2	1/4" 4130 plate	Aircraft Spruce	
08S0250-SS	Push rod mount and tabs	2	0.060" 4130 sheet	McMaster-Carr	
08S0251-SS	Tie Rod Tabs	4	0.060" 4130 sheet	McMaster-Carr	
08S0252-SS	Threaded Insert - RH	4	0.5" 4130 rod	McMaster-Carr	

Differential & Mounting

Bearings & Halfshafts

Assemblies

Front Suspension Members

Rear Suspension Members

Drivetrain

Suspension

Suspension	Rear Rocker	08S0253-SS	Threaded Insert - LH	4	0.5" 4130 rod	McMaster-Carr	ADB-4V (L)
		08S0254-SS	Spherical Ball Bearing	12	-	Coast Fabrication	
Upright	Rear Uprights	08S0601-SS	Rear rocker upper half	4	0.060" 4130 sheet	McMaster-Carr	
		08S0603-SS	Rocker mounting pipe	2	1" 4130 steel rod	McMaster-Carr	
		08S0604-SS	Rear Shock	2	-	Fox Shocks	DHX 5.0
		08S0605-SS	Rear Shock Bracket mount	2	0.080" 4130 sheet	McMaster-Carr	
		08S0606-SS	rocker shock mount insert	4	0.5" 4130 rod	McMaster-Carr	
		08S0607-SS	Rocker bearing insert	4	1" x 0.125" 4130 tube	McMaster-Carr	
		08S0608-SS	Rocker Pipe Bearing	4	-	China	
		08S0801-SS	Spherical Ball Bearing	10	-	Coast Fabrication	ADB-4V (L)
		08S0802-SS	1/4" rod end RH	6	-	Aurora Bearings	
		08S0805-SS	1/4" Rod End LH	6	-	Aurora Bearings	
	Assemblies	08S04AS4-SS	Upper A-arm	2	-	-	
		08S04AS5-SS	Lower A-arm right	1	-	-	
		08S05AS6	Lower A-arm left	1	-	-	
		08S06AS1	Rear Rocker Upper	1	-	-	
		08S06AS2	Rear Rocker Lower	1	-	-	
		08S06AS3	Rear Rocker Double	1	-	-	
		08U0101-SS	Rear Upright Right	1	4"x5"x12" 6061 Billet	McMaster-Carr	
		08U0102-SS	Rear Upright Left	1	4"x5"x12" 6061 Billet	McMaster-Carr	
		08U0103-SS	Ball joint Tab	3	0.080" 4130 sheet	McMaster-Carr	
		08U0201-SS	Rear Spindle	2	4" 4340 round	McMaster-Carr	
Rear Frame	Rear Spindles & Hub	08U0202-SS	Rear Hub	2	5" 6061 round	McMaster-Carr	
		08U01AS1-SS	Rear Upright and spindle left	1	-	-	
	Assemblies	08U01AS2-SS	Rear Upright and spindle Right	1	-	-	
		08U1AS2-SS	Upright Bearings	4	-	-	
		08C0501-SS	Rear Space Frame	1	1" 4130 steel tube	Aircraft Spruce	
		08C0502-SS	Engine Bungs, single shear	4	1" 4130 steel rod	McMaster-Carr	
		08C0503-SS	Frame Bungs, male	2	1" 4130 steel rod	McMaster-Carr	
		08C0504-SS	A-arm Pick up tab	8	0.080" 4130 sheet	McMaster-Carr	
		08C05AS1-SS	08C05AS1-SS	1	-	-	
		08C05AS2-SS	Suspension Pick Up tab assm	1	-	-	



Appendix H: Testing Summary

TEST PLAN

Item No	Specification or Clause Reference	Test Description	Acceptance Criteria	Test Stage
1	Rear Frame Stiffness	Fix chassis side of frame, load and measure displacement	Minimal deflection	DV
2	Upright Deflection	Mount upright on test bench, apply load and measure deflection	Less than 0.005" deflection	DV
3	Upright Failure	Run car through maximum loading conditions	No permanent deformation	DV
4	A-Arm Failure	Run car through maximum loading conditions, measure stresses	No permanent deformation	DV
5	A-Arm Lifting	Lift car by A-arms, measure stresses	No permanent deformation	DV
6	Rocker Stiffness	Apply torsion load to rockers and measure deflection	Less than 0.005" deflection	DV
7	Rocker Failure	Fix shock mount, load push rod mount until failure, measure maximum load	No permanent deformation	DV
8	Suspension tab failure	Apply shearing load to suspension bolt until failure, measure maximum load	Able to sustain 1500lb load	DV
9	Push Rod Failure	Apply compressive load to push rod until failure	Able to sustain 1000lb load	DV
10	Anti-Roll Bar Stiffness	Torsion test anti-roll bar	Twist rate of XX $\pm 10\%$	DV
11	Half shaft failure	Load half shaft in torsion and measure stresses	Able to sustain XX ft-lb torque	DV
12	Suspension Travel	Move wheels through maximum range of motion	At least 1" of travel in both bounce and jounce	PV
15	Tilt Table	Mount vehicle with driver on tilt table, increase tilt angle	Able to maintain 60° tilt without losing tire contact	PV
16	Braking Test	Apply strong braking force while traveling straight	Able to lock all four wheels in a straight line	PV
17	Maximum Braking	Test maximum deceleration of each suspension system	At least 1g of deceleration	PV
18	Acceleration Test	75m acceleration run for each suspension system	At least 0.7g acceleration	PV
19	Skid-pad Test	Run car on FSAE spec skidpad	At least 0.9g lateral acceleration	PV
20	Autocross test	Run car on competition style course	Completion of course	PV

CENTER

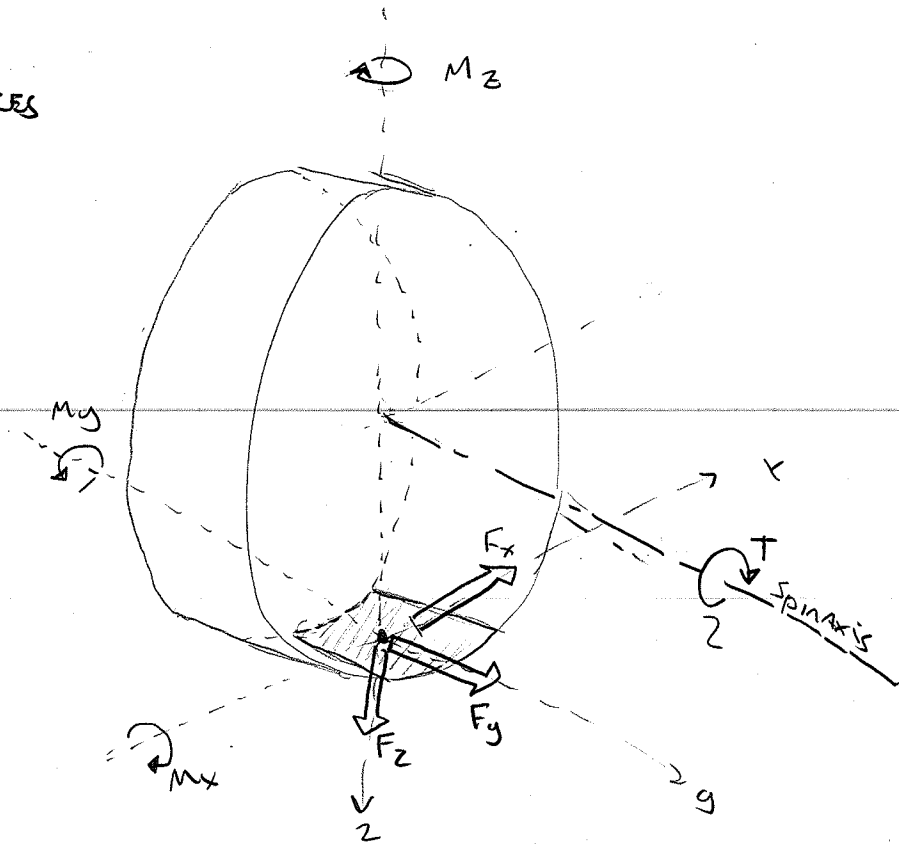
APPENDIX H

DEVELOPMENT OF SUSPENSION QUASI-STATIC
EQUILIBRIUM EQUATIONS USED TO SOLVE
FOR AXIAL SUSPENSION FORCES

- ASSUME 2-FORCE MEMBERS AND
DEFINING SUSPENSION GEOMETRY

DEVELOPMENT OF SUSPENSION QUASI-STATIC EQUILIBRIUM EQNS:

TIRE FORCES



F_x = TRACTIVE FORCE

F_y = LATERAL FORCE

F_z = NORMAL FORCE

M_z = Aligning Moment = $F_y \cdot (\text{TOTAL TRAIL})$

M_x = OVERTURNING MOMENT = $F_x \cdot (\text{DISTANCE FROM WHEEL CENTER PLANE?})$

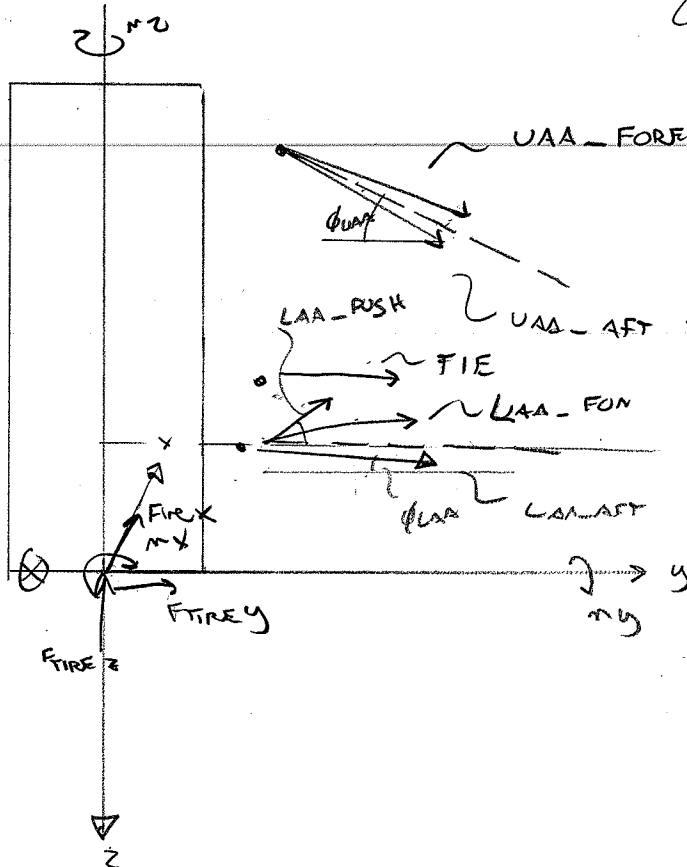
M_y = Rolling Resistance Moment.

T = Torque About spin axis @ TIRES.

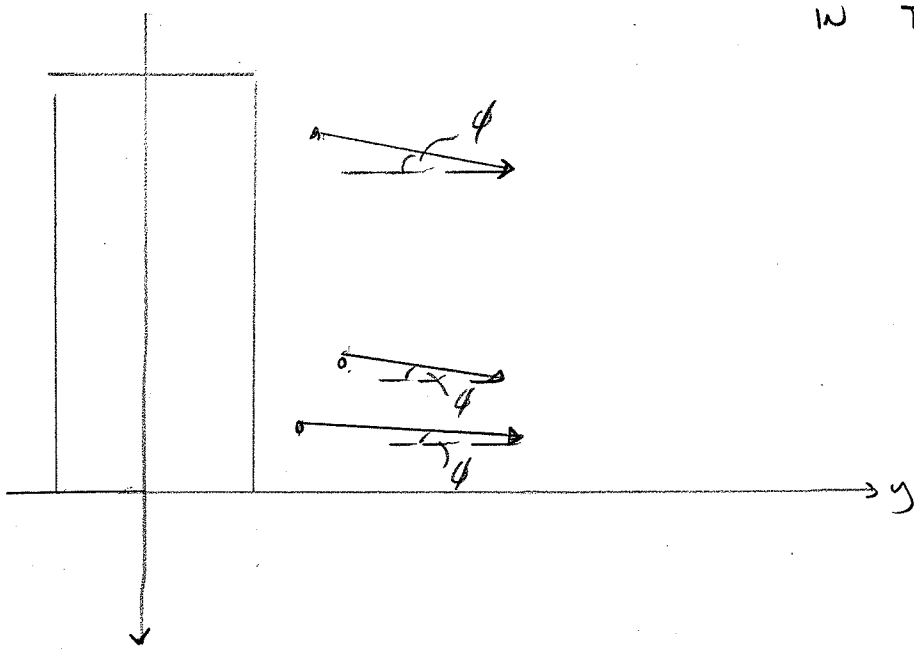
FBD OF 2 FORCE-MEMBER SUSPENSION FORCES

FRONT VIEW

6 FORCES! 6 UNKNOWN
6 EQUATIONS!



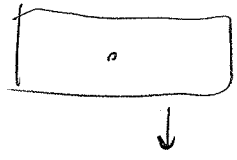
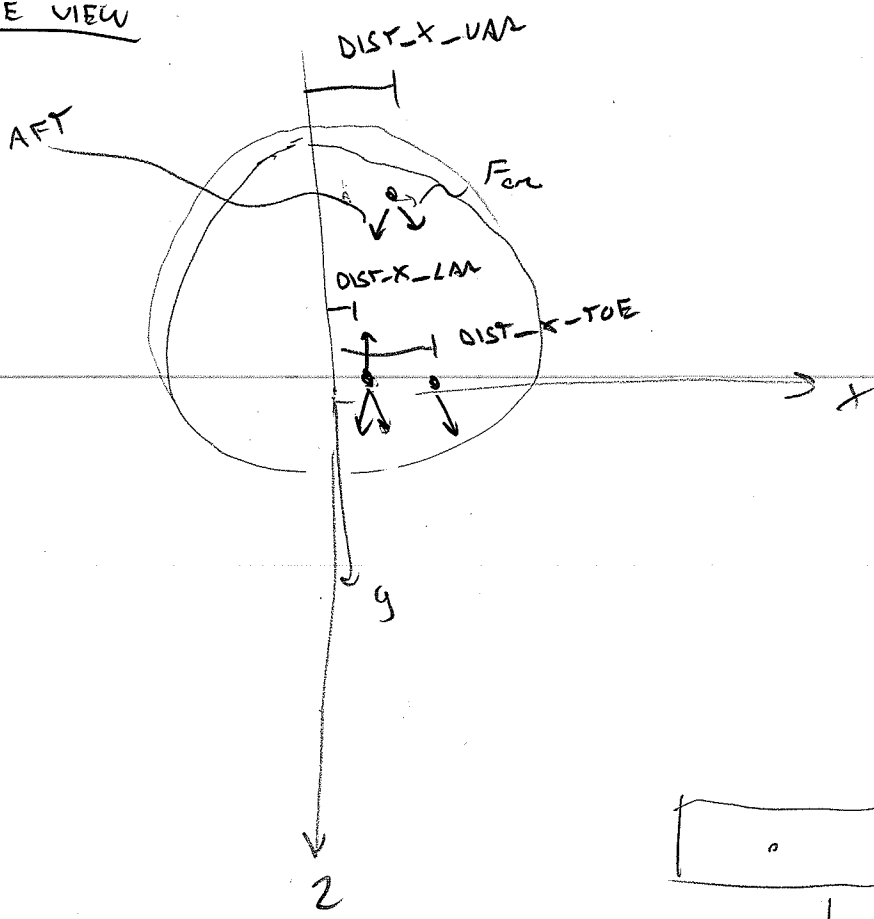
Simplified TO



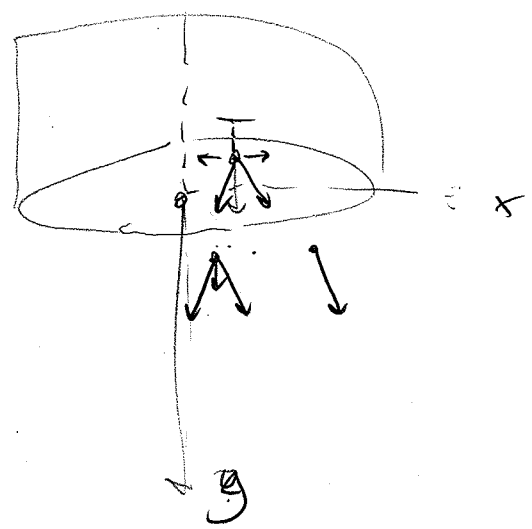
- Assume PUSH ROD IN h-plane OF LOWER A-ARM.
- Assume ALL T-C JOINTS IN TENSION!

FBD (CONTINUED)

SIDE VIEW

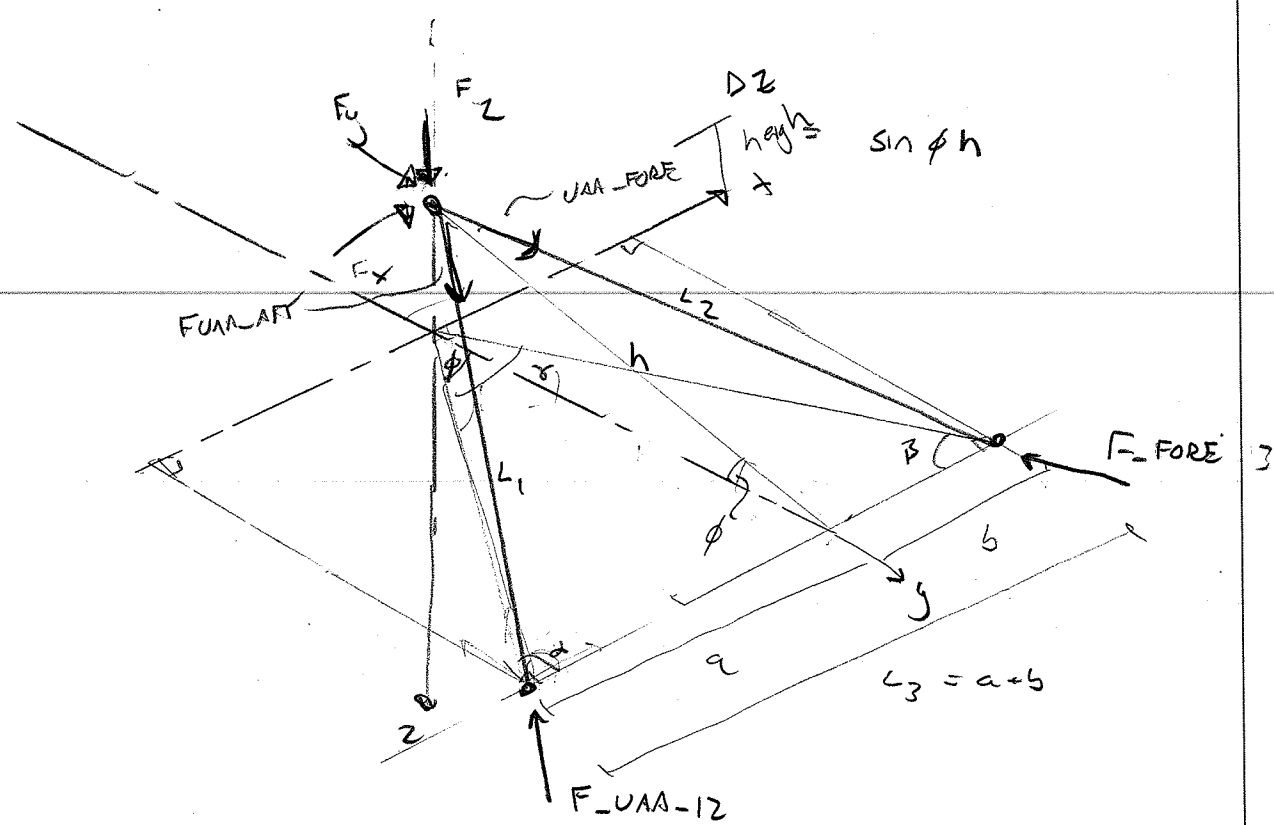


TOP VIEW



42-381 50 SHEETS EYE-EASE®, 5 SQUARES
 42-382 100 SHEETS EYE-EASE®, 5 SQUARES
 42-389 200 SHEETS EYE-EASE®, 5 SQUARES
National Brand

3-D UPPER A-ARM 2-FORCE MEMBER Geometry CONSTRAINTS



$$\sum F_x = 0$$

$$F_x + F_{UAA-12} (\cos \alpha) (\cos \phi) - (F_{UAA-13}) (\cos \beta) (\cos \phi) = 0$$

$$\sum F_y = 0$$

$$F_y - F_{UAA-12} (\sin \alpha) (\cos \phi) - F_{UAA-13} (\sin \beta) (\cos \phi) = 0$$

$$\sum F_z = 0$$

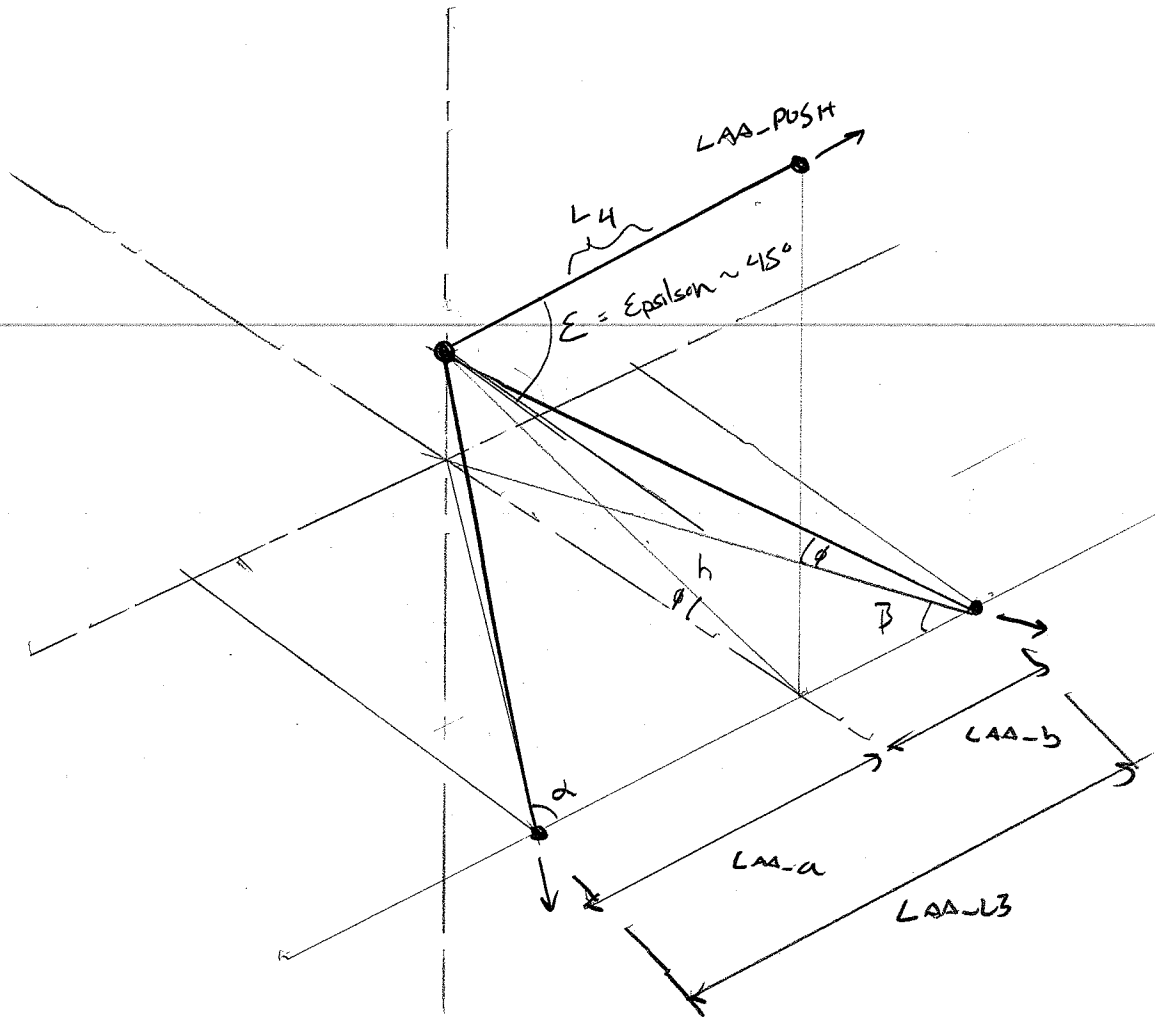
$$F_z - F_{UAA-12} (\sin \phi) - F_{UAA-13} (\sin \phi) = 0$$

$$\sum M_x = 0$$

$$0 = F_y (\sin \phi) (h) - F_{UAA-12} (\sin \phi) (\cos \phi) (h) - F_{UAA-13} (\sin \phi) (\cos \phi) (h)$$

These equations NOT use explicitly,

3-D LOWER A-ARM 2 FORCE MEMBER CONSTRAINT



- * ASSUME LAA-PUSH IS ALL IN Y-DIRECTION!
- Similarly to upper A-arm DEVELOPMENT.

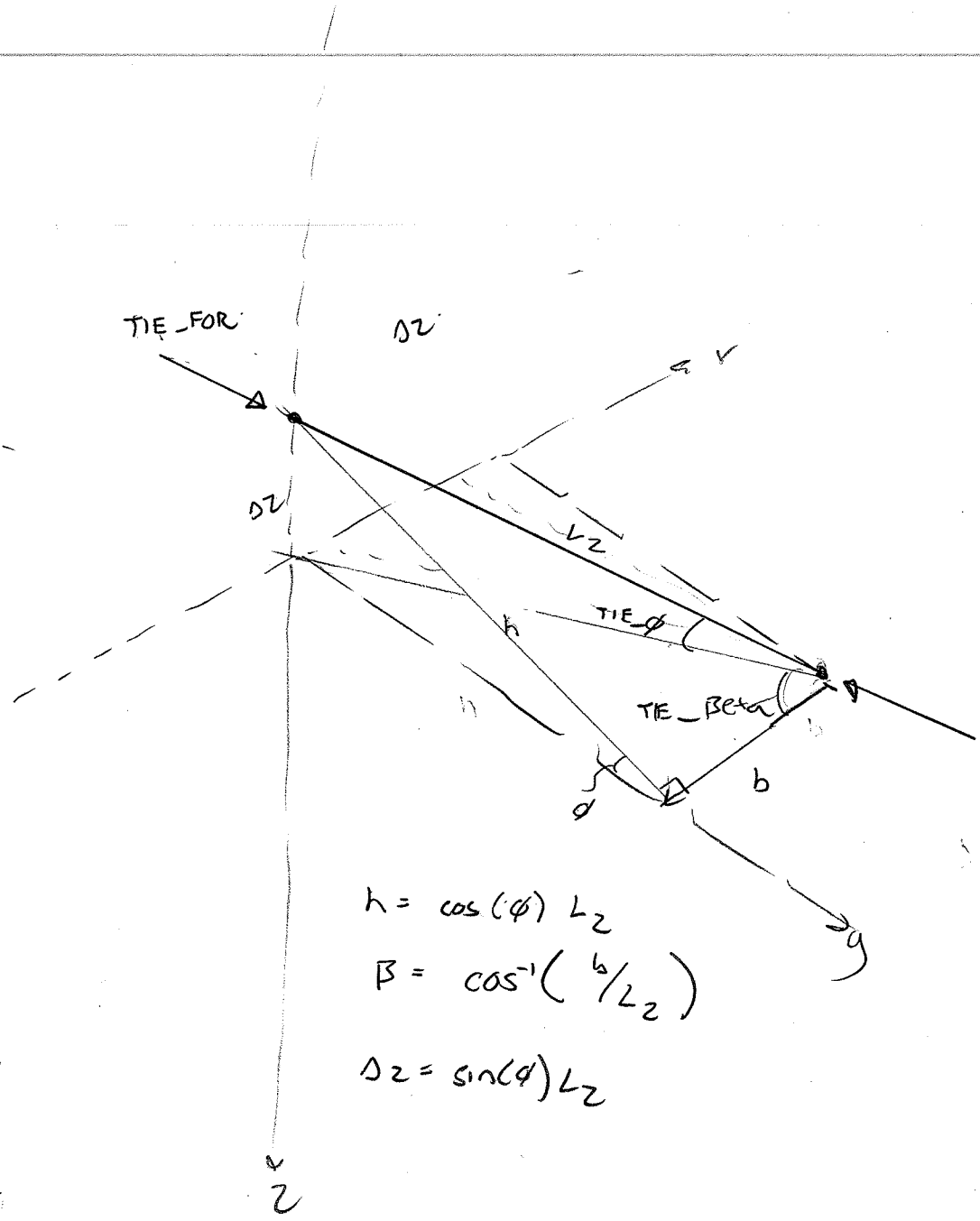
ϕ = inclination angle with horizontal plane.

L_4 = push rod length.

E = push rod inclination angle from horizontal.

3-D TIE-ROD 2 FORCE MEMBER CONSTRAINT

42-381 50 SHEETS EYE/EASE® - 5 SQUARES
42-382 100 SHEETS EYE/EASE® - 5 SQUARES
42-389 200 SHEETS EYE/EASE® - 5 SQUARES
National Brand

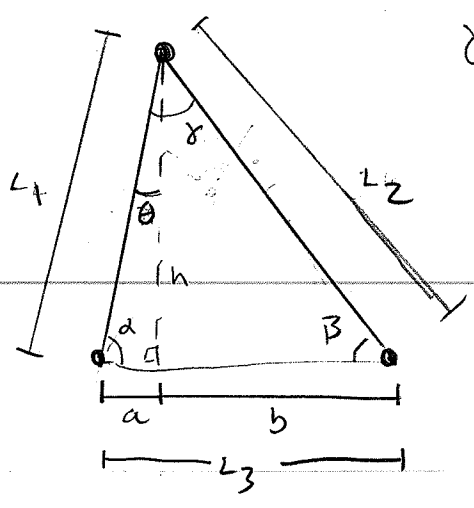


$$h = \cos(\phi) L_2$$

$$\beta = \cos^{-1}\left(\frac{b}{L_2}\right)$$

$$\Delta z = \sin(\phi) L_2$$

A-ARM Trigonometry DEVELOPMENT



$$\gamma = \cos^{-1} \left(\frac{L_2^2 + L_1^2 - L_3^2}{2(L_1)(L_2)} \right)$$

$$h = \sin \alpha (L_1)$$

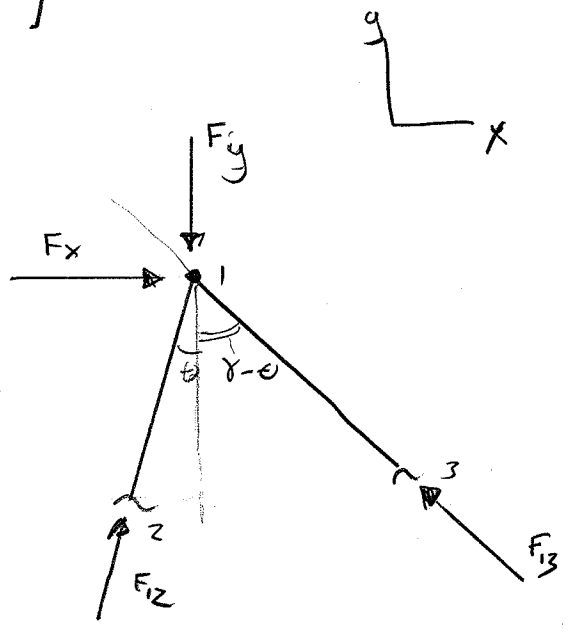
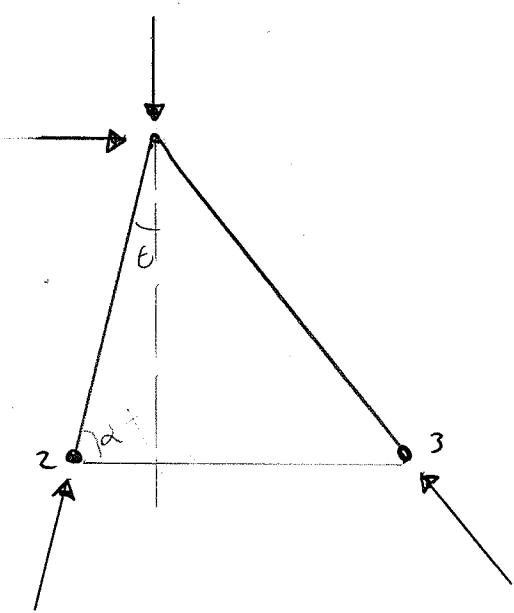
$$\gamma = \cos^{-1} \left[\frac{L_3^2 - L_1^2 - L_2^2}{(-2)(L_1)(L_2)} \right]$$

$$L_2^2 = L_1^2 + L_3^2 - 2(L_1)(L_3)\cos(\alpha)$$

$$\alpha = \cos^{-1} \left[\frac{L_2^2 - L_1^2 - L_3^2}{(-2)(L_1)(L_3)} \right]$$

$$\beta = \cos^{-1} \left[\frac{L_1^2 - L_2^2 - L_3^2}{(-2)(L_2)(L_3)} \right]$$

$$\theta = 90 - \alpha$$



$$\sum F_x = 0$$

$$F_2 \sin \theta + F_3 \sin(\gamma - \theta) = F_x$$

$$\sum F_y = 0$$

$$F_2 \cos \theta + F_3 \cos(\gamma - \theta) = F_y$$

$$\frac{F_x}{F_y} = \frac{F_2 \sin \theta + F_3 \sin(\gamma - \theta)}{F_2 \cos \theta + F_3 \cos(\gamma - \theta)}$$

EQUATIONS OF STATIC EQUILIBRIUM!

$\sum F_y = 0$

$$\begin{aligned}
 & F_{TIRE_y} + (UAA-FOR)(\cos(UAA-\phi))(\sin(UAA-\beta)) \dots \\
 & \dots + (UAA-AFT)(\cos(UAA-\phi))(\sin(UAA-\alpha)) \dots \\
 & \dots + (TIE-FOR)(\cos(TIE-\phi))(\sin(TIE-\beta)) \dots \\
 & \dots + (LAA-FOR)(\cos(LAA-\phi))(\sin(LAA-\beta)) \dots \\
 & \dots + (LAA-AFT)(\cos(LAA-\phi))(\sin(LAA-\alpha)) \dots \\
 & \dots + (LAA-PUSH)(\cos(LAA-\epsilon)) = 0 \quad (1)
 \end{aligned}$$

$\sum F_x = 0$

$$\begin{aligned}
 & F_{TIRE_x} + (UAA-FOR)(\cos(UAA-\phi))(\cos(UAA-\beta)) \dots \\
 & \dots + (UAA-AFT)(\cos(UAA-\phi))(\cos(UAA-\alpha)) \dots \\
 & \dots + (TIE-FOR)(\cos(TIE-\phi))(\cos(TIE-\beta)) \dots \\
 & \dots + (LAA-FOR)(\cos(LAA-\phi))(\cos(LAA-\beta)) \dots \\
 & \dots + (LAA-AFT)(\cos(LAA-\phi))(\cos(LAA-\alpha)) = 0 \quad (2)
 \end{aligned}$$

$\sum F_z = 0$

$$\begin{aligned}
 & F_{TIRE_z} + (UAA-FOR)(\sin(UAA-\phi)) \dots \\
 & \dots + (UAA-AFT)(\sin(UAA-\phi)) \dots \\
 & \dots + (TIE-FOR)(\sin(TIE-\phi)) \dots \\
 & \dots + (LAA-FOR)(\sin(LAA-\phi)) \dots \\
 & \dots + (LAA-AFT)(\sin(LAA-\phi)) \dots \\
 & \dots + (LAA-PUSH)(\sin(LAA-\epsilon)) = 0 \quad (3)
 \end{aligned}$$

42-381 50 SHEETS EYE-EASE® - 5 SQUARES
 42-382 100 SHEETS EYE-EASE® - 5 SQUARES
 42-389 200 SHEETS EYE-EASE® - 5 SQUARES
 National Brand

$$\sum M_{X \text{ AXIS}} = 0$$

$$\begin{aligned}
 M_{TIRE X} &+ (UAA_FORE)(\cos(UAA_phi))(\sin(UAA_beta))(DIST_Z - UAA) \dots \\
 &+ (UAA_FORE)(\sin(UAA_phi))(DIST_Y - UAA) \dots \\
 &+ (UAA_AFT)(\cos(UAA_phi))(\sin(UAA_alpha))(DIST_Z - UAA) \dots \\
 &+ (UAA_AFT)(\sin(UAA_phi))(DIST_Y - UAA) \dots \\
 &+ (TIE_FORE)(\cos(TIE_phi))(\sin(TIE_beta))(DIST_Z - TIE) \dots \\
 &+ (TIE_FORE)(\sin(TIE_phi))(DIST_Y - TIE) \dots \\
 &+ (LAA_FORE)(\cos(LAA_phi))(\sin(LAA_beta))(DIST_Z - LAA) \dots \\
 &+ (LAA_FORE)(\sin(LAA_phi))(DIST_Y - LAA) \dots \\
 &+ (LAA_AFT)(\cos(LAA_phi))(\sin(LAA_alpha))(DIST_Z - LAA) \dots \\
 &+ (LAA_AFT)(\sin(LAA_phi))(DIST_Y - LAA) \dots \\
 &+ (LAA_PUSH)(\cos(LAA_epsilon))(DIST_Z - LAA) \dots \\
 &- (LAA_PUSH)(\sin(LAA_epsilon))(DIST_Y - LAA) \dots = 0 \quad (4)
 \end{aligned}$$

$$\sum M_{y \text{ axis}} = 0$$

$$\begin{aligned}
 M_y - T &= (UAA - FORE)(\cos(UAA - \phi))(\cos(UAA - \text{beta}))(\text{DIST}_Z - UAA) \dots \\
 &\dots - (UAA - FORE)(\sin(UAA - \phi))(\text{DIST}_X - UAA) \dots \\
 &\dots + (UAA - AFT)(\cos(UAA - \phi))(\cos(UAA - \text{alpha}))(\text{DIST}_Z - UAA) \dots \\
 &\dots - (UAA - AFT)(\sin(UAA - \phi))(\text{DIST}_X - UAA) \dots \\
 &\dots - (TIE - FORE)(\cos(TIE - \phi))(\cos(TIE - \text{beta}))(\text{DIST}_Z - TIE) \dots \\
 &\dots - (TIE - FORE)(\sin(TIE - \phi))(\text{DIST}_X - TIE) \dots \\
 &\dots - (LAA - FORE)(\cos(LAA - \phi))(\cos(LAA - \text{beta}))(\text{DIST}_Z - LAA) \dots \\
 &\dots - (LAA - FORE)(\sin(LAA - \phi))(\text{DIST}_X - LAA) \dots \\
 &\dots + (LAA - AFT)(\cos(LAA - \phi))(\cos(LAA - \text{alpha}))(\text{DIST}_Z - LAA) \dots \\
 &\dots - (LAA - AFT)(\sin(LAA - \phi))(\text{DIST}_X - LAA) \dots \\
 &\dots + (LAA - PUSH)(\sin(LAA - \text{EPSILON}))(\text{DIST}_X - LAA) \dots = 0 \quad (5)
 \end{aligned}$$

End!

$$\sum M_z = 0$$

$$\begin{aligned}
 M_z = & (UAA_FORE)(\cos(UAA_phi))(\cos(UAA_beta))(DIST_Y_UAA) \dots \\
 & + (UAA_FORE)(\cos(UAA_phi))(\sin(UAA_beta))(DIST_X_UAA) \dots \\
 & + (UAA_AFT)(\cos(UAA_phi))(\cos(UAA_alpha))(DIST_Y_UAA) \dots \\
 & + (UAA_AFT)(\cos(UAA_phi))(\sin(UAA_alpha))(DIST_X_UAA) \dots \\
 & - (TIE_FORE)(\cos(TIE_phi))(\cos(TIE_beta))(DIST_Y_TIE) \dots \\
 & + (TIE_FORE)(\cos(TIE_phi))(\sin(TIE_beta))(DIST_X_TIE) \dots \\
 & - (LAA_FORE)(\cos(LAA_phi))(\cos(LAA_beta))(DIST_Y_LAA) \dots \\
 & + (LAA_FORE)(\cos(LAA_phi))(\sin(LAA_beta))(DIST_X_LAA) \dots \\
 & + (LAA_AFT)(\cos(LAA_phi))(\cos(LAA_alpha))(DIST_Y_LAA) \dots \\
 & + (LAA_AFT)(\cos(LAA_phi))(\sin(LAA_alpha))(DIST_X_LAA) \dots \\
 & + (LAA_PUSH)(\cos(LAA_EPSILON))(DIST_X_LAA) \dots \quad (6)
 \end{aligned}$$

6 EQUATIONS . . .

6 UNKNOWN . . .

- SOLVE FOR:
- (1) UAA-FORE
 - (2) UAA-AFT
 - (3) TIE-FORE
 - (4) LAA-FORE
 - (5) LAA-AFT
 - (6) LAA-PUSH

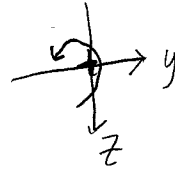
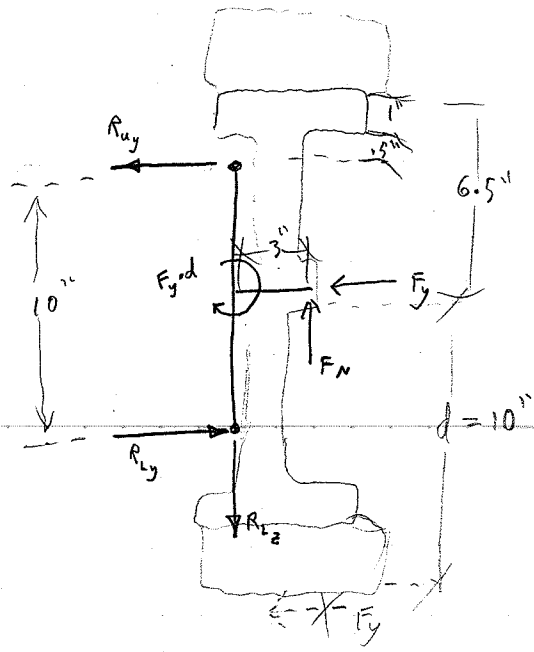
20 EQUATIONS

$$A \cdot X = b$$

$$X = \text{inv}(A) \cdot b$$

• THESE FORCES ARE AXIAL IN MEMBERS, USE DEFLATED SUSPENSION GEOMETRY TO CONVERT BACK TO X, Y, Z FORCES AT BOTH UPRIGHT AND CHASSIS PICKUP POINTS.

Loading for outside Rear

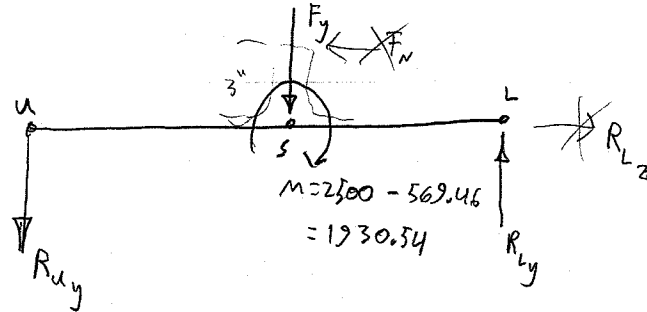


$$F_y = 250 \text{ lbf}$$

$$F_N = 189.82 \text{ lbf}$$

$$F_y \cdot d = 2500 \text{ in}\cdot\text{lb}$$

$$F_N(3") = 569.46 \text{ in}\cdot\text{lb}$$



$$R_{Lz} = F_N$$

$$\sum M_L = 0$$

$$R_{uy}(10") + \underbrace{F_y(5")}_{250 \text{ lbf}} - 1930.54 \text{ in}\cdot\text{lb} = 0$$

$$R_{uy} = \frac{1930.54 \text{ in}\cdot\text{lb} - 250(5)}{10}$$

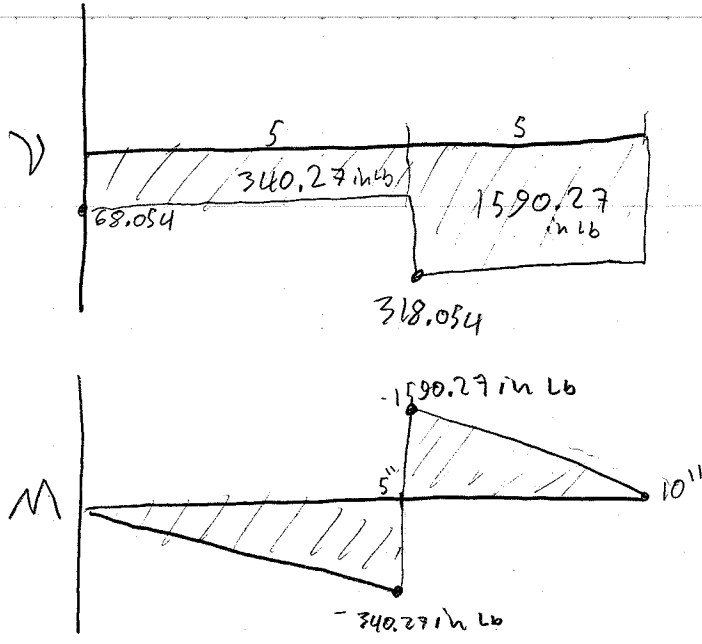
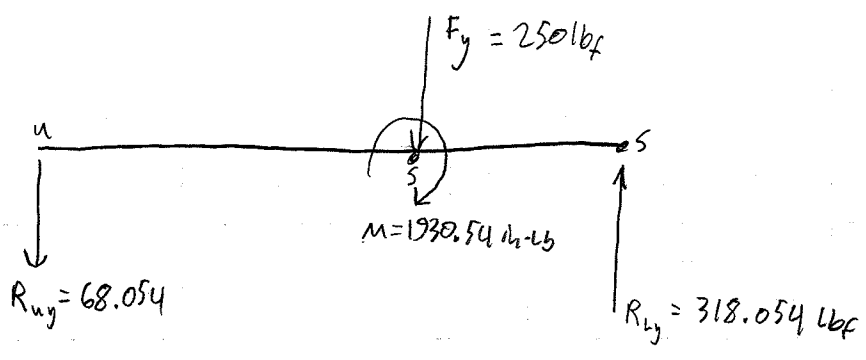
$$R_{uy} = 68.054 \text{ lbf}$$

$$\sum F_y = 0$$

$$R_{Ly} - F_y - R_{uy} = 0$$

$$R_{Ly} = 250 + 68.054$$

$$R_{Ly} = 318.054 \text{ lbf}$$



• max moment occurs at center of upright